

R/V Mirai Cruise Report

MR22-06C (MR22-1toh)



Arctic Ocean, Bering Sea, and North Pacific Ocean
/2 August - 29 September, 2022



Japan Agency for Marine - Earth
Science and Technology (JAMSTEC)

KOTO SUGIMOTO (C)

Contents

1. Cruise Summary	4
1.1. Objectives	4
1.2. Overview	4
1.3. Basic information	8
1.4. Cruise tracks	9
1.5. List of participants	10
2. Meteorology	13
2.1. C-band weather radar	13
2.2. Surface Meteorological Observations	16
2.3. Ceilometer	26
2.4. Tropospheric gas and particles observation	29
2.4.1. Atmospheric surface observation for trace gas and aerosols	29
2.4.2. Precipitation sampling	37
2.5. Lidar observation	39
2.6. Greenhouse gases observation	41
2.7. Isotope analysis of water vapor	45
2.8. Mercury observation	49
3. Physical Oceanography	51
3.1. CTD casts and water sampling	51
3.2. XCTD	60
3.3. Shipboard ADCP	63
3.4. Wave Buoys	67
3.5. Microwave wave gauge	70
3.6. Network camera	72
3.7. Radar	74
3.7.1. Ice radar	74
3.7.2. Wave-Ice radar	76
3.8. Sea ice observation from drones	79
3.9. Moorings	81
3.9.1. Barrow Canyon Moorings	81
3.9.2. RAS and SUNA	85
3.9.3. Sea ice profile and wave height	87
3.9.4. Sediment trap	89
3.10. Salinity	98

4. Biogeochemical Oceanography	103
4.1. Dissolved Oxygen	103
4.2. Nutrients	107
4.3. Dissolved Inorganic Carbon	141
4.3.1. Bottled-water analysis	141
4.3.2. Underway DIC	144
4.4. Total alkalinity	146
4.5. Chlorophyll <i>a</i>	149
4.6. ^{18}O	153
4.7. Iodine-129	155
4.8. Uranium-236	157
4.9. Polycyclic Aromatic Hydrocarbons (PAHs)	159
4.10. Radiocesium	161
4.11. Radium isotopes	163
4.12. Underway surface water monitoring	165
4.12.1. Basic biogeochemical analyses	165
4.12.2. Discrete samplings	171
4.12.3. Continuous silicate determination from the surface water pump system	173
4.13. Continuous measurement of $p\text{CO}_2$ and $p\text{CH}_4$	178
4.14. Trace metal clean seawater sampling	181
4.15. Zooplankton	190
4.16. Phytoplankton	195
4.17. Environmental DNA	197
4.18. Microplastic	204
5. Under-the-Ice Drone Trials	208
6. Geology	215
6.1. Sediment core sampling	215
6.2. Porewater sampling	293
6.3. Sea bottom topography measurements	299
6.4. Sea surface gravity measurements	303
6.5. Surface magnetic field measurement	305
7. Notice on using	307

Front cover illustration by Koto Sugimoto, Kobe University

Last updated on 12th Jun, 2023

1. Cruise Summary

1.1. Objectives

The Arctic Ocean is the area with the fastest rate of global oceanic warming in the world. The detailed research of the Research Vessel (R/V) Mirai along with other icebreaking vessels, satellite observation and numerical modeling have documented the impact of inflow of the Pacific origin water. We have observed sea ice decrease and marine ecosystem changes associated with Pacific origin waters bringing heat, nutrients, fresh water into the Arctic. Its impact is getting greater and more widely spread into the entire Arctic. This cruise aimed to develop the dataset that could allow for a synoptic view of the totality of hydrographic and ecosystem changes taking place in the Arctic Ocean and facilitate advancing model development to predict the future state of the Arctic. In addition to observation of present Arctic environments, sediment records were observed to understand differences between the present environmental changes and past warming events in the Arctic Ocean. This cruise contributed to Synoptic Arctic Survey (SAS) and Distributed Biological Observatory (DBO) that are multi ship international research programs.

1.2. Overview

We conducted the Arctic Ocean cruise from 12 August to 29 September 2022 using the Research Vessel (R/V) Mirai (Figure 1.2-1). We left Shimizu on 12 August and arrived in Dutch Harbor on 21 August. Then, we passed through the Bering Strait toward the north on 24 August and carried out the Arctic Ocean survey for 25 days. On 17 September, we passed through the Bering Strait southward and came back to Shimizu on 29 September. This cruise was supported by the project of Arctic Challenge for Sustainability II (ArCS II), which was funded by the Ministry of Education, Culture, Sports, Science and Technology of Japan (MEXT).

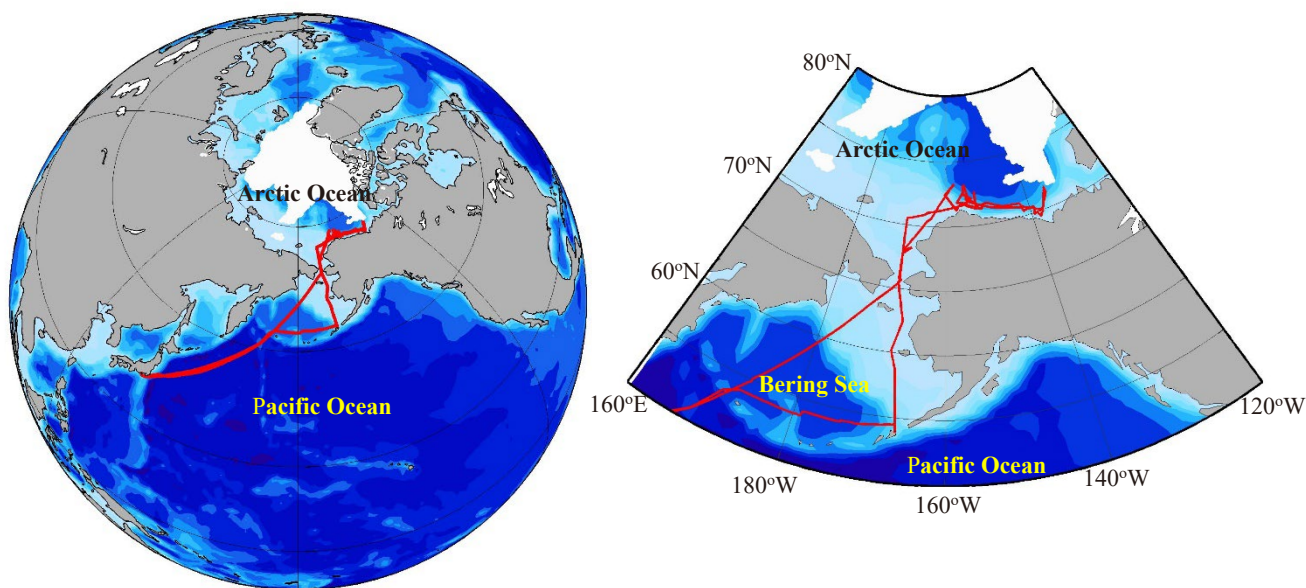


Figure 1.2-1. Cruise tracks (red lines), Sea Ice Concentration (SIC) on 15 September 2022.

According to the report from National Snow and Ice Data Center (NSIDC), the Arctic sea ice appears to have reached its seasonal minimum extent of 4.67 million square kilometers on 18 September 2022, tying for tenth lowest in the nearly 44-year satellite record, with 2018 and 2017. This was 1.28 million square kilometers above the satellite-era record minimum extent of 3.39 million square kilometers, which occurred on September 17, 2012. It is also 1.55 million square kilometers below the 1981 to 2010 average minimum extent.

The research areas included the EEZ and the territorial sea of the USA and the EEZ of Canada (Figure 1.2-2). We conducted hydrographic, paleoenvironmental and biogeochemical surveys, including plankton, microplastic, and bottom sediment samplings from the Chukchi Sea and the Beaufort Sea to marginal ice zones of the Canada Basin. The observational activities consisted of CTD/water samplings, XCTD, wave and surface drifting buoy deployments, zooplankton net samplings, sediment samplings, microplastic samplings, ship-board ocean current and surface water monitoring, meteorological measurements and samplings, aerosol observations, trials of an in-water drone, satellite observations, doppler radar, sea ice radar, sea bottom topography, gravity, and magnetic field measurements, and mooring and sediment trap recoveries and deployments.

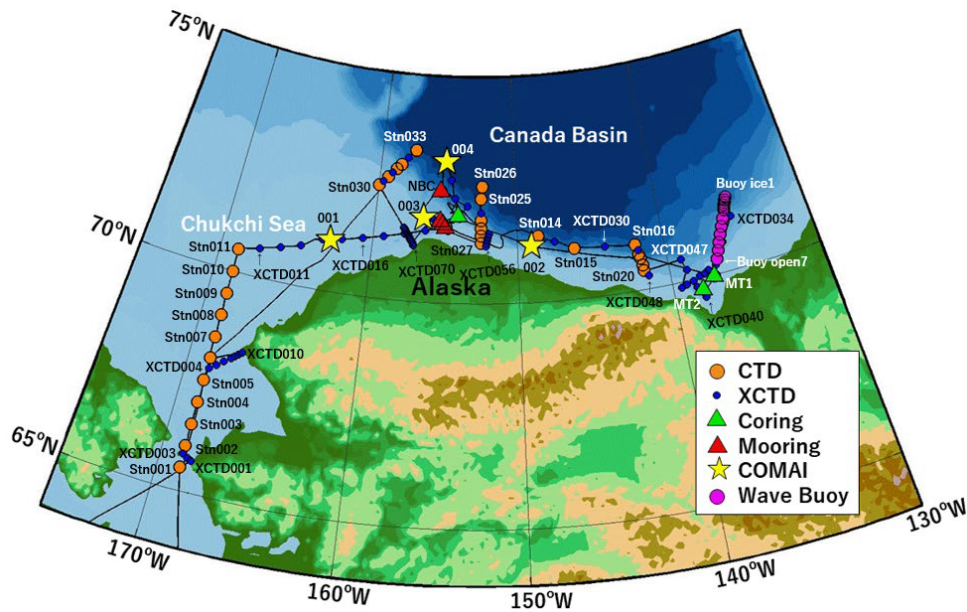


Figure 1.2-2. Close research area for the Chukchi Sea and the Bering Sea. Orange dots indicate stations where we conducted observations using Conductivity-Temperature-Depth (CTD) sensors with water sampling bottles and plankton nets and sediment core sampling (see Chapters 3 and 4). Red triangles (BCC, BCE, BCW and NBC¹) represent mooring sites (see 3.9 for details). Blue dots reveal where we collected hydrographic data using eXpendable CTD (XCTD) sensor (see 3.2 for the details). Yellow stars are COMAI-under ice drones test survey sites (see Chapter 5). Green triangles represent sediment core sampling sites (see Chapter 6 for the details). Magenta dots indicate wave buoy deployment sites (see 3.4 for the details). We also carried out intensive oceanographic surveys under an international collaboration (Distributed Biological Observatory) off Pt. Hope (DBO3), across the Barrow Canyon (DBO5) and Beaufort slope (DBO6).

¹ Abbreviations represent the places of mooring arrays and sediment traps; Barrow Canyon - Center (BCC), Barrow Canyon - East (BCE), Barrow Canyon - West (BCW) and North of Barrow Canyon (NBC).

In this cruise, we had 115 oceanographic stations (34 CTD and 81 XCTD stations) including 33 water sampling sites, 19 Neuston net sites, 17 NORPAC net sites, 10 clean seawater sampling sites, 9 Asyura sediment sampling sites, 15 sites for drifting buoy launches, 4 sites for recoveries and deployments of hydrographic and sediment trap moorings (see Chapters 3 and 4). We also conducted 1 piston core, 8 gravity cores, 8 box cores and 8 multiple core samplings at 4 geological stations (see Chapter 6). The trial of an in-water drone, which is designed for oceanographic observation including under sea ice was performed at 4 stations (see Chapter 5). Continuous meteorological and oceanographic observations/samplings were carried out along the cruise tracks.



Photo 1.2-1: Commemorative photograph for the participants of R/V Mirai Arctic Ocean cruise in 2022 (taken by T. Kinase).

These missions were successfully completed thanks to great efforts made by the captain, ice pilot, officers, crews, and all the participants in this cruise (Photo 1.2-1). And we would like to express our sincere appreciation to the United States Department of State and the Alaska Fisheries Science Center of the NOAA National Marine Fisheries Service of the Department of Commerce of the United States for allowing us to conduct observations in the areas under their jurisdictions. We also would like to express our sincere appreciation to the Government of Canada, including the Fisheries and Oceans Canada, and the Aurora Research Institute and the Environmental Impact Screening Committee for allowing us to conduct observations in the areas under their jurisdictions. We would like to express our sincere appreciation to Alaska Eskimo Whaling Commission in USA, Yukon Scientists and

explorers, Wildlife Management Advisory Council North Slope, Fisheries Joint Management Committee in Canada. Based on the data obtained in this cruise, we will be able to shed light on the Arctic change and its controlling factors and will contribute to the global climate change studies.

This cruise included the following 11 studies:

- On board research themes

- Representative of the Science Party [Affiliation]: Amane Fujiwara [JAMSTEC]
- Title of proposal: ArCS II: Arctic Challenge for Sustainability II
- Representative of the Science Party [Affiliation]: Motoyo Itoh [JAMSTEC]
- Title of proposal: Observational study of the Arctic environmental changes: Pacific-Arctic interaction, biogeochemical transport, mixing and marine ecosystem
- Representative of the Science Party [Affiliation]: Hiroshi Yoshida [JAMSTEC]
- Title of proposal: Research on sea ice observation technology for the purpose of understanding environmental changes in the Arctic ocean
- Representative of the Science Party [Affiliation]: Fumikazu Taketani [JAMSTEC]
- Title of proposal: Ship-borne observations of trace gases/aerosols over the Arctic
- Representative of the Science Party [Affiliation]: Ryota Nakajima [JAMSTEC]
- Title of proposal: Distribution and abundance of microplastics in the Arctic Ocean
- Representative of the Science Party [Affiliation]: Takuji Waseda [The University of Tokyo/JAMSTEC]
- Title of proposal: Observation of air-sea-wave-ice interaction in the Marginal Ice Zone
- Representative of the Science Party [Affiliation]: Akihide Kasai [Hokkaido University]
- Title of proposal: Analysis of Arctic fish communities using environmental DNA
- Representative of the Science Party [Affiliation]: Masanobu Yamamoto [Hokkaido University]
- Title of proposal: Holocene Arctic Palaeoclimatology and Paleoceanography Investigation
- Representative of the Science Party [Affiliation]: Michiyo Yamamoto-Kawai [Tokyo University of Marine Science and Technology]
- Title of proposal: Study on nutrient transport by Summer Pacific Water

- Studies not on board

- Representative of the Science Party [Affiliation]: Yasunori Tohjima [Hokkaido University]
- Title of proposal: Ship-board observations of atmospheric greenhouse gases and related species in the Arctic ocean and the western North Pacific
- Representative of the Science Party [Affiliation]: Hotaek Park [JAMSTEC]
- Title of proposal: Observation of water vapor isotope in the Arctic

1.3. Basic information

Name of vessel	R/V Mirai
L x B x D	118.02 m x 19.0 m x 10.5 m
Gross Tonnage	8,706 tons
Call Sign	JNSR
Cruise code	MR22-06C (MR22-Itoh)
Undertaking institute	Japan Agency for Marine-Earth Science and Technology (JAMSTEC)
Chief scientist	Motoyo Itoh Japan Agency for Marine-Earth Science and Technology (JAMSTEC)
Cruise periods	12 August 2022 – 29 September 2022 First entry into the EEZ of Canada: 1 September 2022 Final departure from the EEZ of Canada: 5 September 2022 First entry into the EEZ of USA: 17 August 2022 Departure from the EEZ of USA: 1 September 2022 Second entry into the EEZ of USA: 5 September 2022 Final departure from the EEZ of USA: 22 September 2022
Port call	21 August 2022, Dutch Harbor (Embarkation of the ice pilot and three scientists) 29 September 2022, Shimizu (arrival in port)
Research areas	The Arctic Ocean, Bering Sea and North Pacific Ocean

1.4. Cruise tracks

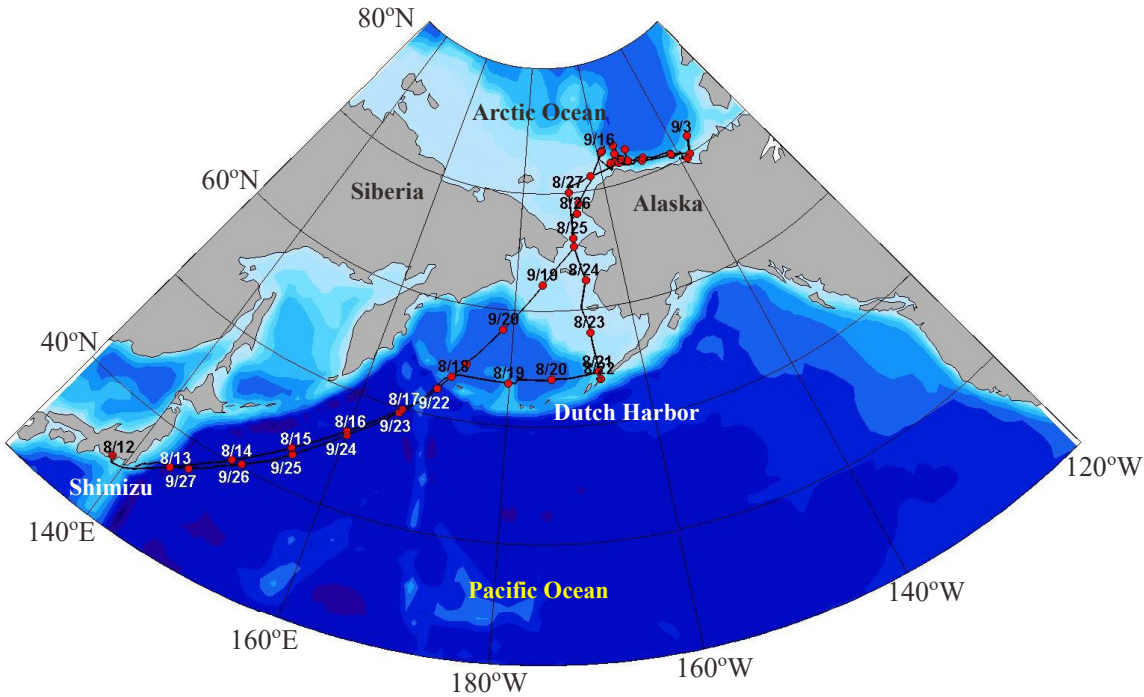


Figure 1.4-1. Map of the entire cruise track. The red dots indicate the noon positions (UTC).

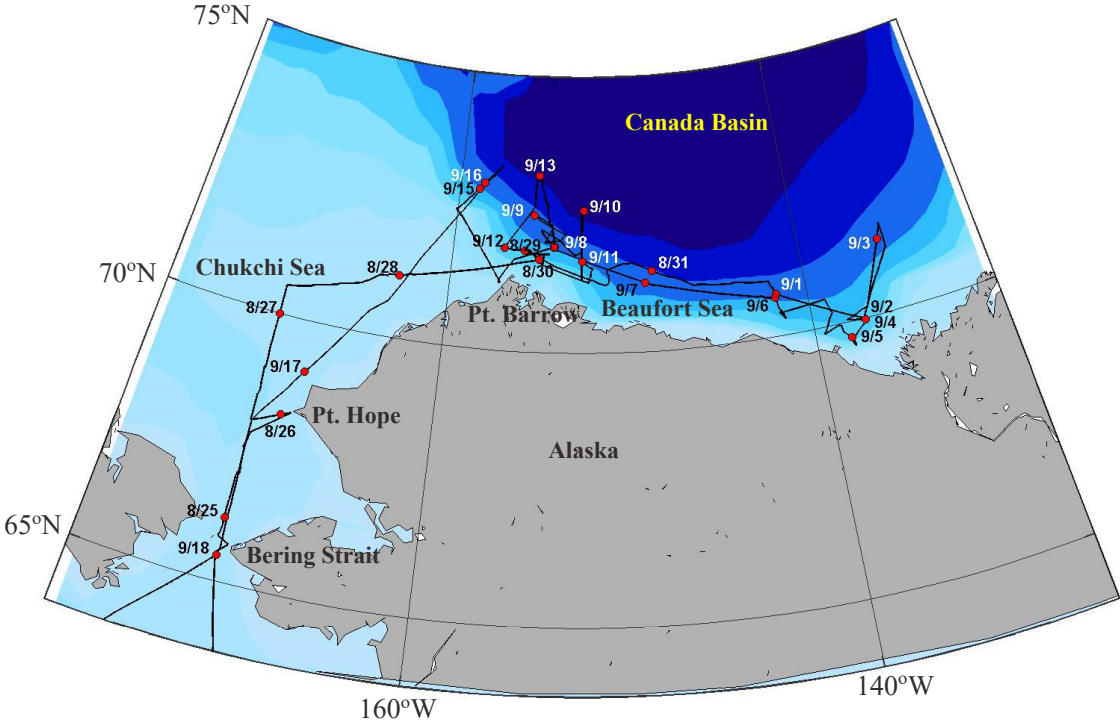


Figure 1.4-2. Detailed cruise tracks for the Chukchi Sea and the Beaufort Sea. The red dots indicate the noon positions (UTC).

1.5. List of participants

Table 1.5-1: List of participants of MR22-06C.

No.	Name	Organization	Position
1	Motoyo Kitamura (Itoh)	Japan Agency for Marine-Earth Science and Technology (JAMSTEC)	Research Scientist
2	Jonaotaro Onodera	Japan Agency for Marine-Earth Science and Technology (JAMSTEC)	Senior Research Scientist
3	Mariko Hatta	Japan Agency for Marine-Earth Science and Technology (JAMSTEC)	Research Scientist
4	Takahito Ikenoue	Japan Agency for Marine-Earth Science and Technology (JAMSTEC)	Research Scientist
5	Takeshi Kinase	Japan Agency for Marine-Earth Science and Technology (JAMSTEC)	Post-Doctoral Researcher
6	Hiroshi Yoshida	Japan Agency for Marine-Earth Science and Technology (JAMSTEC)	Principal Researcher
7	Kiyotaka Tanaka	Japan Agency for Marine-Earth Science and Technology (JAMSTEC)	Senior Research Technician
8	Makoto Sugesawa	Japan Agency for Marine-Earth Science and Technology (JAMSTEC)	Research Assistant
9	Michiyo Yamamoto Kawai	Tokyo University of Marine Science and Technology	Associate Professor
10	Tomotaka Katsuno	Graduate School of Frontier Sciences, The University of Tokyo	Graduate Student
11	Makoto Ozaki	Graduate School of Fisheries Sciences, Hokkaido University	Graduate Student
12	Masanobu Yamamoto	Faculty of Environmental Earth Science, Hokkaido University	Professor
13	Shoma Uchida	Graduate School of Environmental Earth Science, Hokkaido University	Graduate Student
14	Minoru Kobayashi	Graduate School of Environmental Earth Science, Hokkaido University	Graduate Student
15	Koji Seike	National Institute of Advanced Industrial Science and Technology	Senior Research Scientist
16	Leonid Polyak	Faculty of Environmental Earth Science, Hokkaido University	Guest Professor

17	Laura Gemery	United States Geological Survey	Research Scientist
18	Youngjin Joe	Korea Polar Research Institute	Ph.D. student
19	Koto Sugimoto	Kobe University	Graduate Student
20	Haruka Tsujimoto	Tokyo University of Marine Science and Technology	Graduate Student
21	Minami Ishihara	Graduate School of Fisheries Sciences, Hokkaido University	Graduate Student
22	Kazuho Yoshida	Nippon Marine Enterprises, Ltd.	Technical Staff
23	Ryo Kimura	Nippon Marine Enterprises, Ltd.	Technical Staff
24	Satomi Ogawa	Nippon Marine Enterprises, Ltd.	Technical Staff
25	Fumine Okada	Nippon Marine Enterprises, Ltd.	Technical Staff
26	Rei Ito	Marine Works Japan Ltd.	Technical Staff
27	Masahiro Orui	Marine Works Japan Ltd.	Technical Staff
28	Katsunori Sagishima	Marine Works Japan Ltd.	Technical Staff
29	Hiroki Ushiromura	Marine Works Japan Ltd.	Technical Staff
30	Yuko Miyoshi	Marine Works Japan Ltd.	Technical Staff
31	Nagisa Fujiki	Marine Works Japan Ltd.	Technical Staff
32	Aine Yoda	Marine Works Japan Ltd.	Technical Staff
33	Erii Irie	Marine Works Japan Ltd.	Technical Staff
34	Shiori Ariga	Marine Works Japan Ltd.	Technical Staff
35	Riho Fujioka	Marine Works Japan Ltd.	Technical Staff
36	Yuta Oda	Marine Works Japan Ltd.	Technical Staff
37	Shintaro Amikura	Marine Works Japan Ltd.	Technical Staff
38	Yohei Katayama	Marine Works Japan Ltd.	Technical Staff

39	Kazuma Takahashi	Marine Works Japan Ltd.	Technical Staff
40	Yoshiki Kido	Marine Works Japan Ltd.	Technical Staff
41	Yuta Shinomiya	Marine Works Japan Ltd.	Technical Staff
42	David Snider	Martech Polar Consulting Ltd.	Ice Pilot

2. Meteorology

2.1. C-band weather radar

(1) Personnel

Fumikazu Taketani	(JAMSTEC)	(not on board)
Masaki Katsumata	(JAMSTEC)	(not on board)
Kazuho Yoshida	(NME: Nippon Marine Enterprises, Ltd.)	
Satomi Ogawa	(NME)	
Fumine Okada	(NME)	
Ryo Kimura	(NME)	
Yoichi Inoue	(MIRAI crew)	

(2) Objectives

The objective of weather radar observations is to investigate the structures and evolutions of precipitating systems over the high-latitude region including the Arctic Ocean.

(3) Instrumentation and methods

(a) Radar specifications

The C-band weather radar on board the R/V Mirai was used. Basic specifications of the radar are as follows:

Frequency:	5370 MHz (C-band)
Polarimetry:	Horizontal and vertical (simultaneously transmitted and received)
Transmitter:	Solid-state transmitter
Pulse Configuration:	Using pulse-compression
Output Power:	6 kW (H) + 6 kW (V)
Antenna Diameter:	4 meters
Beam Width:	1.0 degrees
Inertial Navigation Unit:	PHINS (IXBLUE S.A.S)

(b) Available radar variables

Radar variables, which were converted from the power and phase of the backscattered signal at vertically- and horizontally-polarized channels, were as follows:

Radar reflectivity:	Z
Doppler velocity:	V_r
Spectrum width of Doppler velocity:	SW
Differential reflectivity:	Z_{DR}
Differential propagation phase:	Φ_{DP}
Specific differential phase:	K_{DP}
Co-polar correlation coefficients:	ρ_{HV}

(c) Operation methodology

The antenna was controlled to point the commanded ground-relative direction, by controlling the azimuth and elevation to cancel the ship attitude (roll, pitch and yaw) detected by the laser gyro. The Doppler velocity was also corrected by subtracting the ship movement in beam direction.

For the maintenance, internal signals of the radar were checked and calibrated at the beginning and the end of the cruise. Meanwhile, the following parameters were checked daily; (1) frequency, (2) mean output power, (3) pulse width, and (4) PRF (Pulse Repetition Frequency).

During the cruise, the radar was operated as in Table 2.1-1. A dual PRF mode was used for a volume scan. For RHI (Range Height Indicator) and surveillance PPI (Plan Position Indicator) scans, a single PRF mode was used.

(4) Preliminary results

The C-band weather radar observations were conducted through the cruise, except in the area where the operations were prohibited by Japanese license and the period of calling at Dutch Harbor. The observation periods are:

03:00UTC, 13 Aug. 2022 to 16:00UTC 20 Aug. 2022

17:00UTC, 22 Aug. 2022 to 07:48UTC 27 Sep. 2022

The obtained data will be analyzed after the cruise.

(5) Data archive

These data obtained in this cruise will be submitted to the Data Management Group of JAMSTEC, and will be opened to the public via “Data Research System for Whole Cruise Information in JAMSTEC (DARWIN)” in JAMSTEC web site.

<<http://www.godac.jamstec.go.jp/darwin/e>>

Table 2.1-1: Scan modes of C-band weather radar

	Surveillance PPI Scan	Volume Scan					RHI Scan
Repeated Cycle (min.)	30	6					6
Times in One Cycle	1	1					3
PRF(s) (Hz)	400	dual PRF (ray alternative)					1250
		667	833	938	1250	1333	
Azimuth (deg)	Full Circle					Option	
Bin Spacing (m)	150						
Max. Range (km)	300	150	100	60	100		
Elevation Angle(s) (deg.)	0.5	0.5	1.0, 1.8, 2.6, 3.4, 4.2, 5.1, 6.2, 7.6, 9.7, 12.2, 15.2	18.7, 23.0, 27.9, 33.5, 40.0	0.0 ~ 60.0		

2.2. Surface Meteorological Observations

(1) Personnel

Motoyo Itoh	JAMSTEC	-PI
Kazuho Yoshida	NME (Nippon Marine Enterprises, Ltd.)	
Satomi Ogawa	NME	
Fumine Okada	NME	
Ryo Kimura	NME	
Yoichi Inoue	MIRAI Crew	

(2) Objectives

Surface meteorological parameters are observed as a basic dataset of the meteorology. These parameters provide the temporal variation of the meteorological condition surrounding the ship.

(3) Parameters

- i. MIRAI Surface Meteorological (SMet) system measured parameters are listed in Table 2.2-1.

Table 2.2-1: Parameters of MIRAI SMet system

Parameter	Units	Remarks
1 Latitude	degree	
2 Longitude	degree	
3 Ship's speed	knot	MIRAI log
4 Ship's heading	degree	MIRAI gyro
5 Relative wind speed	m/s	6sec./10min. averaged
6 Relative wind direction	degree	6sec./10min. averaged
7 True wind speed	m/s	6sec./10min. averaged
8 True wind direction	degree	6sec./10min. averaged adjusted to sea surface level
9 Barometric pressure	hPa	6sec. averaged
10 Air temperature (starboard)	degC	6sec. averaged
11 Air temperature (port)	degC	6sec. averaged
12 Dewpoint temperature (starboard)	degC	6sec. averaged
13 Dewpoint temperature (port)	degC	6sec. averaged
14 Relative humidity (starboard)	%	6sec. averaged
15 Relative humidity (port)	%	6sec. averaged
16 Sea surface temperature	degC	6sec. averaged
17 Precipitation intensity (optical rain gauge)	mm/hr	hourly accumulation

18 Precipitation (capacitive rain gauge)	mm/hr	hourly accumulation
19 Downwelling shortwave radiation	W/m ²	6sec. averaged
20 Downwelling infra-red radiation	W/m ²	6sec. averaged
21 Significant wave height (bow)	m	hourly
22 Significant wave height (stern)	m	hourly
23 Significant wave period (bow)	second	hourly
24 Significant wave period (stern)	second	hourly

- ii. Shipboard Oceanographic and Atmospheric Radiation (SOAR) system measured parameters are listed in Table 2.2-2.

Table 2.2-2: Parameters of SOAR system (JamMet)

Parameter	Units	Remarks
1 Latitude	degree	
2 Longitude	degree	
3 SOG	knot	
4 COG	degree	
5 Relative wind speed	m/s	
6 Relative wind direction	degree	
7 Barometric pressure	hPa	
8 Air temperature	degC	
9 Relative humidity	%	
10 Precipitation intensity (optical rain gauge)	mm/hr	
11 Precipitation (capacitive rain gauge)	mm/hr	reset at 50 mm
12 Down welling shortwave radiation	W/m ²	
13 Down welling infra-red radiation	W/m ²	
14 Defuse irradiance	W/m ²	
15 "SeaSnake" raw data	mV	
16 SSST (SeaSnake)	degC	
17 PAR	microE/cm ² /sec	
18 UV 305 nm	microW/cm ² /nm	
19 UV 320 nm	microW/cm ² /nm	
20 UV 340 nm	microW/cm ² /nm	
21 UV 380 nm	microW/cm ² /nm	

(4) Instruments and methods

In this cruise, the two systems for the observation were used.

i. SMet system

Instruments of SMet system are listed in Table 2.2-3. Data were collected and processed by KOAC-7800 weather data processor made by Koshin-Denki, Japan. The dataset consists of 6 seconds averaged data.

Table 2.2-3: Instruments and installation locations of SMet system

Sensors	Type	Manufacturer	Location (altitude from surface)
Anemometer	KS-5900	Koshin Denki, Japan	Foremast (25 m)
Tair/RH with aspirated radiation shield	HMP155 43408 Gill	Vaisala, Finland R.M. Young, U.S.A.	Compass deck (21 m) starboard and port side
Thermometer: SST	RFN2-0	Koshin Denki, Japan	4th deck (-1m, inlet -5m)
Barometer	Model-370	Setra System, U.S.A.	Captain deck (13 m) Weather observation room
Capacitive rain gauge	50202	R. M. Young, U.S.A.	Compass deck (19 m)
Optical rain gauge	ORG- 815DS	Osi, USA	Compass deck (19 m)
Radiometer (short wave)	MS-802	Eko Seiki, Japan	Radar mast (28 m)
Radiometer (long wave)	MS-202	Eko Seiki, Japan	Radar mast (28 m)
Wave height meter	WM-2	Tsurumi-seiki, Japan	Bow (10 m) Stern (8m)

ii. SOAR measurement system

SOAR system designed by BNL (Brookhaven National Laboratory, USA) consists of major five parts.

- a) Analog meteorological data sampling with CR1000 logger manufactured by Campbell Scientific Inc. Canada – wind pressure, and rainfall (by a capacitive rain gauge) measurement.
- b) Digital meteorological data sampling from individual sensors - air temperature, relative humidity and precipitation (by Optical Rain Gauge (ORG)) measurement.
- c) Radiation data sampling with CR1000X logger manufactured by Campbell Scientific Inc. and radiometers with ventilation unit manufactured by Hukseflux Thermal Sensors B.V. Netherlands – short and long wave downward radiation measurement.
- d) Photosynthetically Available Radiation (PAR) sensor manufactured by Biospherical Instruments Inc. (USA) - PAR measurement.
- e) Scientific Computer System (SCS) developed by NOAA (National Oceanic and Atmospheric Administration, USA) - centralized data acquisition and

logging of all data sets.

SCS recorded radiation, air temperature, relative humidity, CR1000 and ORG data. SCS composed Event data (JamMet) from these data and ship's navigation data every 6 seconds. Instruments and their locations are listed in Table 2.2-4.

Table 2.2-4: Instruments and installation locations of SOAR system

Sensors (Meteorological)	Type	Manufacturer	Location (altitude from surface)
Anemometer	05106	R.M. Young, USA	Foremast (25 m)
Barometer	PTB210	VAISALA, Finland	Foremast (23 m)
with pressure port	61002 Gill	R.M. Young, USA	
Rain gauge	50202	R.M. Young, USA	Foremast (24 m)
Tair/RH	HMP155	VAISALA, Finland	Foremast (23 m)
with aspirated radiation shield	43408 Gill	R.M. Young, USA	
Optical rain gauge	ORG-815DR	Osi, USA	Foremast (24 m)

Sensors (Radiation)	Type	Manufacturer	Location (altitude from surface)
Radiometer (short wave)	SR20	Hukseflux Thermal	Foremast (25 m)
with ventilation unit	VU01	Sensors B.V., Netherlands	
Radiometer (long wave)	IR20	Hukseflux Thermal	Foremast (25 m)
with ventilation unit	VU01	Sensors B.V., Netherlands	

Sensor (PAR&UV)	Type	Manufacturer	Location (altitude from surface)
PAR&UV sensor	PUV-510	Biospherical Instrum ents Inc., USA	Navigation deck (18m)

For the quality control as post processing, we checked the following sensors, before and after the cruise.

- i. Young Rain gauge (SMet and SOAR)
Inspect of the linearity of output value from the rain gauge sensor to change input value by adding fixed quantity of test water.
- ii. Barometer (SMet and SOAR)
Comparison with the portable barometer value, PTB220, VAISALA
- iii. Thermometer (air temperature and relative humidity) (SMet and SOAR)

Comparison with the portable thermometer value, HM70, VAISALA

(5) Observation log

12 Aug. 2022 - 29 Sep. 2022

(6) Preliminary results

Figure 2.2-1 shows the time series of the following parameters:

Wind (SOAR)

Air temperature (SMet)

Relative humidity (SMet)

Precipitation (SOAR, CRG)

Short / Long wave radiation (SOAR)

Pressure (SMet)

Sea surface temperature (SMet)

Significant wave height (SMet)

(7) Data archive

These data obtained in this cruise will be submitted to the Data Management Group of JAMSTEC, and will be opened to the public via “Data Research System for Whole Cruise Information in JAMSTEC (DARWIN)” in JAMSTEC web site.

<<http://www.godac.jamstec.go.jp/darwin/e>>

(8) Remarks

i) The following periods, Sea surface temperature of SMet data were available.

07:30UTC 12 Aug. 2022 - 00:35UTC 21 Aug. 2022

02:50UTC 22 Aug. 2022 - 04:00UTC 26 Sep. 2022

ii) The following periods, increasing of SMet capacitive rain gauge data were invalid due to MF/HF radio transmission.

00:20UTC 12 Aug. 2022

04:21UTC 12 Aug. 2022 - 04:27UTC 12 Aug. 2022

05:18UTC 12 Aug. 2022

18:37UTC 20 Aug. 2022 - 18:44UTC 20 Aug. 2022

01:09UTC 11 Sep. 2022

02:26UTC 24 Sep. 2022 - 02:30UTC 24 Sep. 2022

iii) The following period, SMet wind speed/direction were measured by the ultrasonic anemometer on the aftermast.

01:53UTC 10 Sep. 2022 - 02:30UTC 10 Sep. 2022

iv) The following periods, SMet wind speed/direction were measured by the vane anemometer on the foremast.

02:55UTC 10 Sep. 2022 - 13:00UTC 10 Sep. 2022

02:46UTC 12 Sep. 2022 - 05:32UTC 13 Sep. 2022

16:43UTC 14 Sep. 2022 - 03:47UTC 16 Sep. 2022

v) The following periods, SMet wind speed/direction data were invalid due to system maintenance.

01:50UTC 10 Sep. 2022 - 01:53UTC 10 Sep. 2022

02:30UTC 10 Sep. 2022 - 03:47UTC 10 Sep. 2022

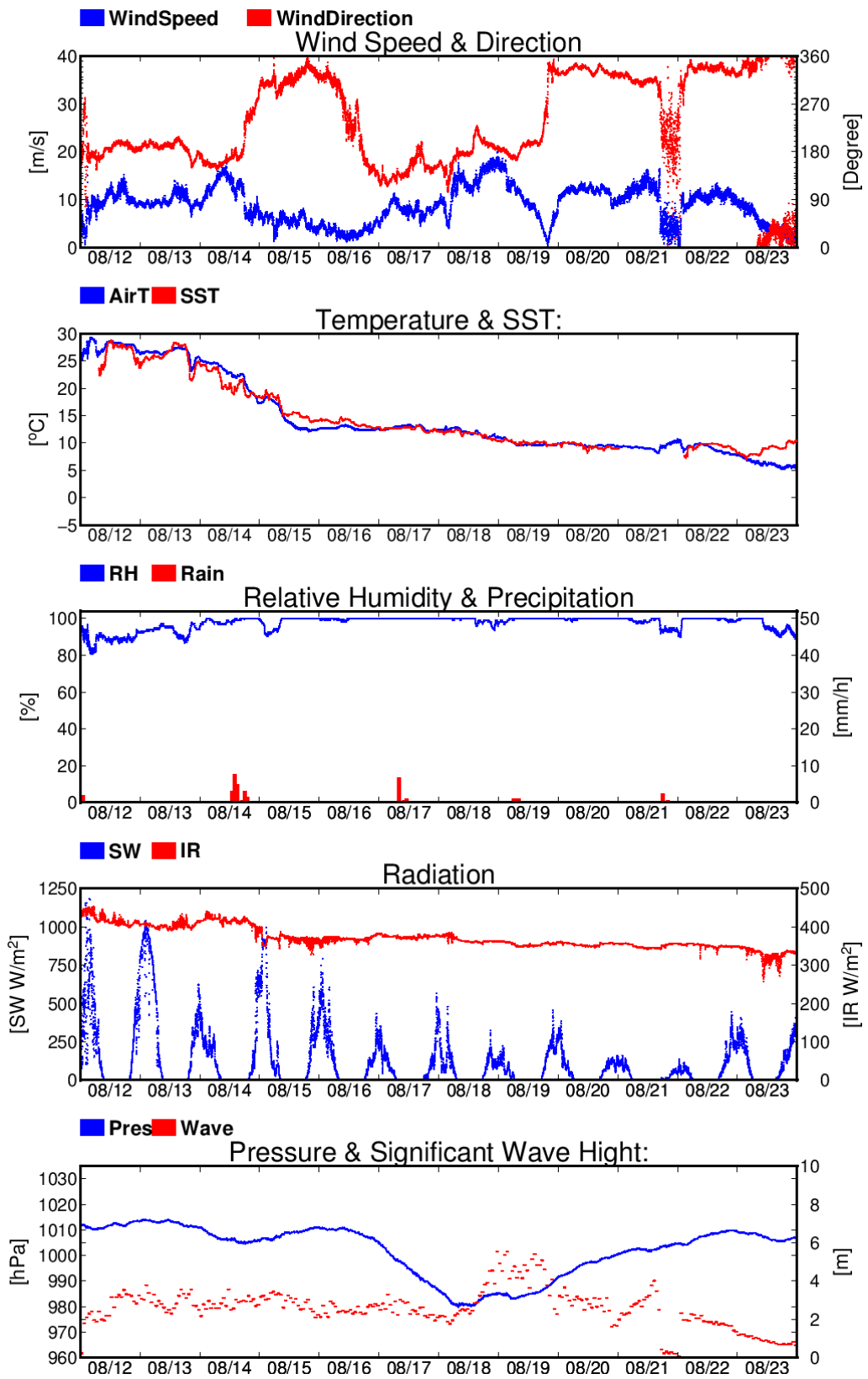


Figure 2.2-1: Time series of surface meteorological parameters during this cruise

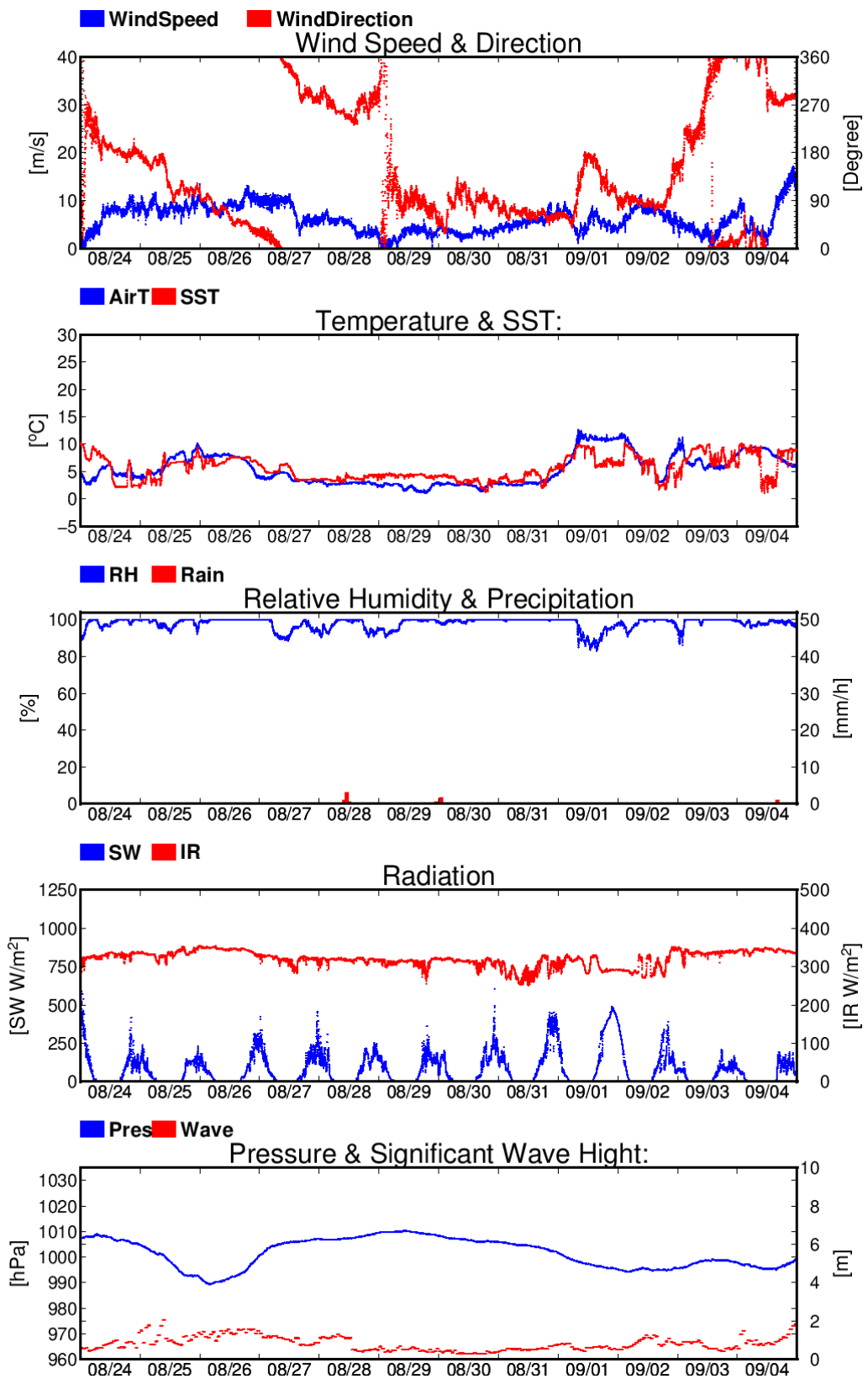


Figure 2.2-1: (Continued)

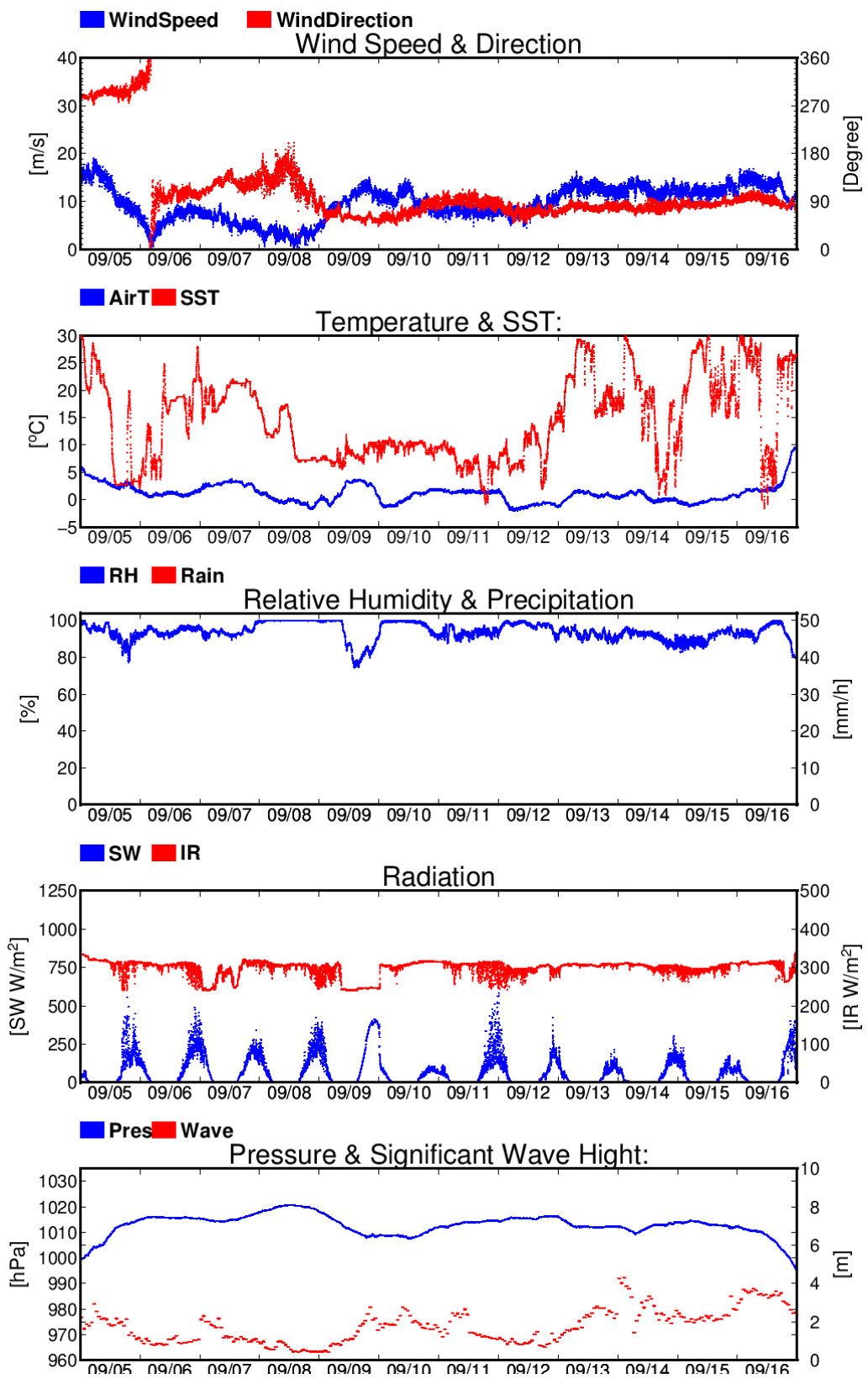


Figure 2.2-1: (Continued)

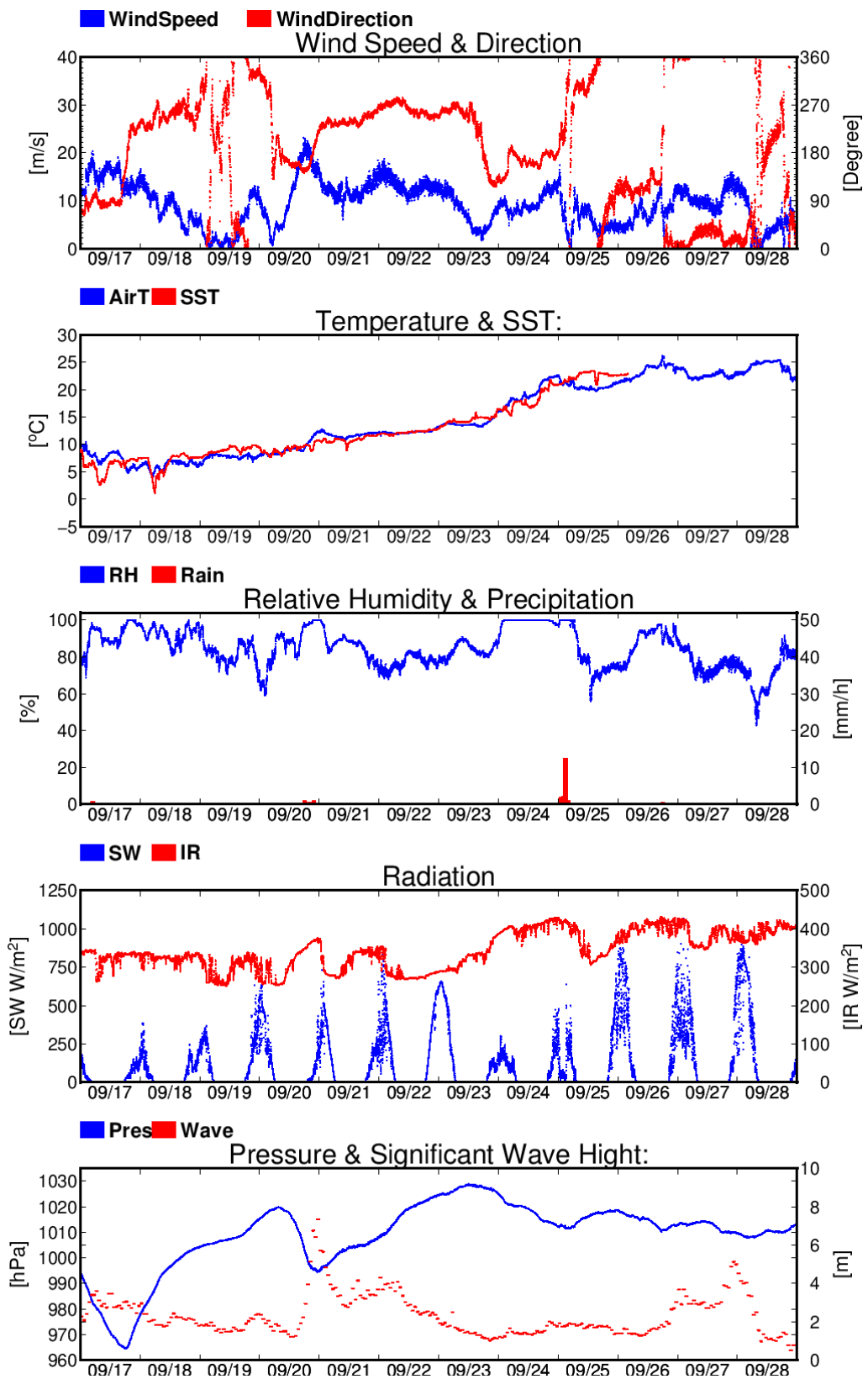


Figure 2.2-1: (Continued)

2.3. Ceilometer

(1) Personnel

Motoyo Itoh	JAMSTEC	-PI
Kazuho Yoshida	NME (Nippon Marine Enterprises, Ltd.)	
Satomi Ogawa	NME	
Fumine Okada	NME	
Ryo Kimura	NME	
Yoichi Inoue	MIRAI Crew	

(2) Objectives

The information of cloud base height and the liquid water amount around cloud base is important to understand the process on formation of the cloud. As one of the methods to measure them, the ceilometer observation was carried out.

(3) Parameters

Cloud base height [m].

Backscatter profile, sensitivity and range normalized at 10 m resolution.

Estimated cloud amount [oktas] and height [m]; Sky Condition Algorithm.

(4) Instruments and methods

Cloud base height and backscatter profile were observed by ceilometer (CL51, VAISALA, Finland). The measurement configurations are shown in Table 2.3-1. On the archive dataset, cloud base height and backscatter profile are recorded at 10 m resolution.

Table 2.3-1: The measurement configurations

Property	Description
Laser source	Indium Gallium Arsenide (InGaAs) Diode
Transmitting center wavelength	910±10 nm at 25 degC
Transmitting average power	19.5 mW
Repetition rate	6.5 kHz
Detector	Silicon Avalanche Photodiode (APD)
Responsibility at 905 nm	65 A/W
Cloud detection range	0 ~ 13 km
Measurement range	0 ~ 15 km
Resolution	10 m in full range
Sampling rate	36 sec.
	Cloudiness in oktas (0 ~ 9)
Sky Condition	0 Sky Clear
	1 Few
	3 Scattered

5-7	Broken
8	Overcast
9	Vertical Visibility

(5) Observation log

12 Aug. 2022 – 28 Sep. 2022

(6) Preliminary results

Figure 2.3-1 shows the time-series of the lowest, second and third cloud base height during the cruise.

(7) Data archive

These data obtained in this cruise will be submitted to the Data Management Group of JAMSTEC, and will be opened to the public via “Data Research System for Whole Cruise Information in JAMSTEC (DARWIN)” in JAMSTEC web site.

<<http://www.godac.jamstec.go.jp/darwin/e>>

(8) Remarks

- i) Window cleaning
 - 19:13UTC 21 Aug. 2022
 - 18:13UTC 04 Sep. 2022
 - 17:02UTC 14 Sep. 2022
 - 06:48UTC 23 Sep. 2022

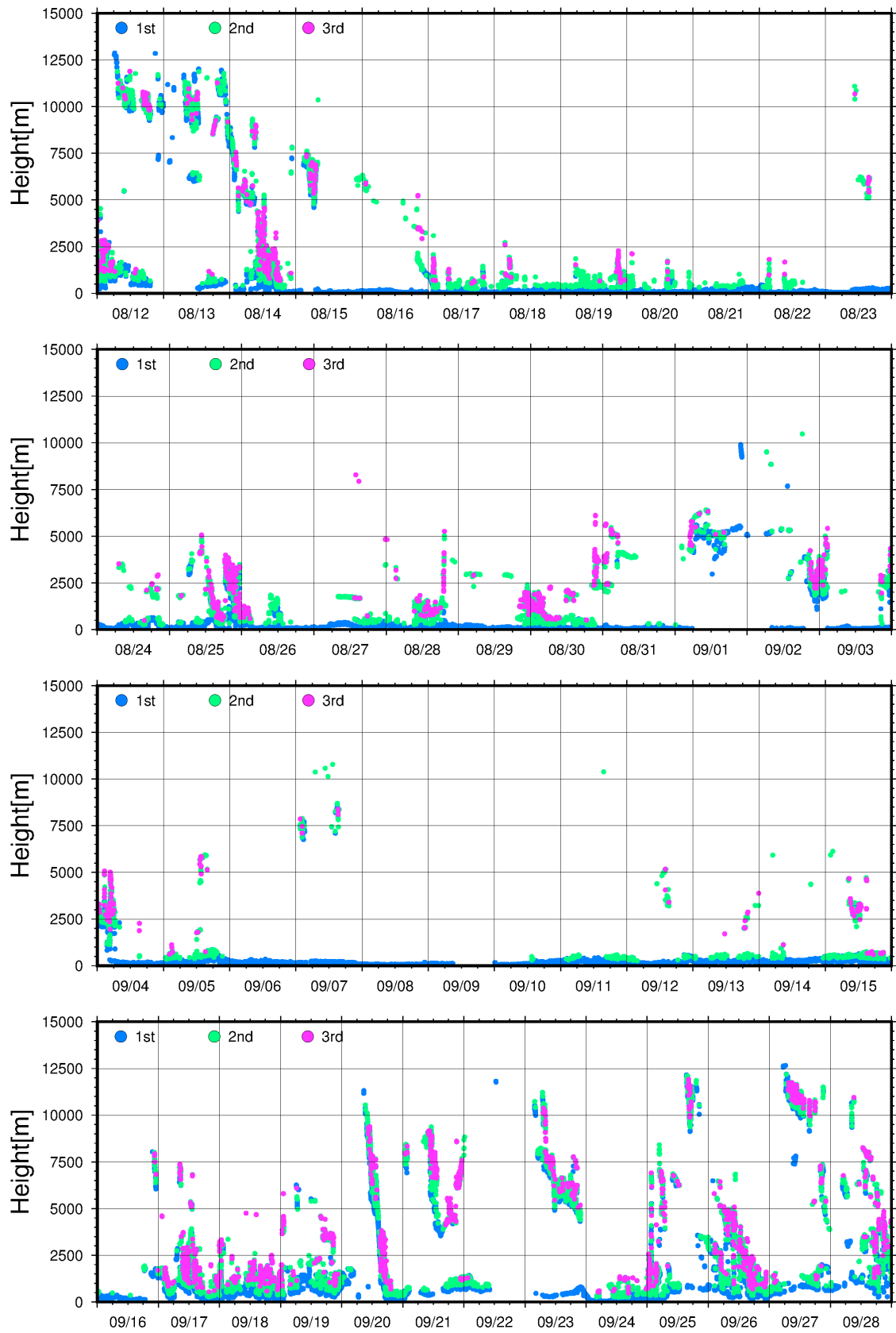


Figure 2.3-1: Time series of cloud base height during this cruise

2.4. Tropospheric gas and particles observation

2.4.1. Atmospheric surface observation for trace gas and aerosols

(1) Personnel

Fumikazu Taketani	JAMSTEC (Principal Investigator)	- not on board
Takeshi Kinase	JAMSTEC	- on board
Masayuki Takigawa	JAMSTEC	- not on board
Yugo Kanaya	JAMSTEC	- not on board
Takuma Miyakawa	JAMSTEC	- not on board
Hisahiro Takashima	JAMSTEC/Fukuoka Univ.	- not on board
Kazuyo Yamaji	JAMSTEC/Kobe Univ.	- not on board
Yutaka Tobo	NIPR*	- not on board
Zhu Chunmao	JAMSTEC	- not on board

*National Institute of Polar Research

(2) Objectives

- To investigate roles of gas and aerosols in the marine atmosphere in relation to climate change
- To investigate processes of biogeochemical cycles between the atmosphere and the ocean.
- To investigate gas and aerosol transports from anthropogenic activities
- To investigate physical and chemical particle states of aerosols
- To investigate contribution of suspended particles to the rain, and snow

(3) Parameters

- Particle size distribution
- Fluorescent particles
- Composition of ambient particles
- Individual particle features of ambient particles
- Hygroscopicity and ice nucleation of ambient particles
- Surface ozone(O₃), and carbon monoxide(CO) mixing ratios

(4) Instruments and methods

(4-1) Online aerosol observations:

(4-1-1) Particle size distribution

The size distribution of aerosol particles was measured by a Scanning Mobility Particle Sizer (SMPS) (Nano Scan model 3910, TSI), and a handheld Optical Particle Counter (OPC) (KR-12A, Rion).

The sample air for SMPS measurements was drawn from the rooftop of the environmental research room through a custom-made concentric tube-type inlet at the sampling rate of 30 L/min for sampling Total Suspended Particulate matters (TSP) (Miyakawa et al., in preparation) to the SMPS. A part of the sample air (~1.15

L/min) was isokinetically extracted and dehumidified using a large diameter Nafion dryer (MD-700, Perma Pure, LLC) to eliminate water vapor and liquid water contents of airborne particles (typical values of Relative Humidity (RH) at the exit of the dryer were lower than ~23 % over the Arctic Ocean), and was subsequently introduced via flow splitters to those instruments installed in the environmental research room. OPC was installed on the compass deck and the sample air was introduced to OPC directly at ambient RH.

(4-1-2) Fluorescent property

Fluorescent properties of aerosol particles were measured by a single particle fluorescence sensor, Waveband Integrated Bioaerosol Sensor (WIBS4) (WIBS-4A, Droplet Measurement Technologies). Two pulsed xenon lamps emitting UV light (280 nm and 370 nm) were used for excitation. Fluorescence emitted from a single particle within 310–400 nm and 420–650 nm wavelength windows was recorded. WIBS4 was installed on the compass deck and the sample air was introduced to WIBS4 directly at ambient RH.

(4-2) Ambient aerosol sampling

Ambient aerosol samplings were carried out by air samplers installed at the compass deck. Ambient particles were collected on the quartz fiber filter (QR-100, ADVANTEC) and a precleaned Whatman Nuclepore track-etched membrane filter (47mm in diameter and 0.2 μm in pore size, Whatman) along the cruise tracks to analyze their composition and ice nuclei ability using a high-volume air sampler (HV-700F, SIBATA) and a handmade air sampler operated at a flow rate of 500L/min and 10L/min, respectively. To avoid collecting particles emitted from the funnel of the own vessel, the sampling period was controlled automatically by using a “wind-direction and speed selection system”.

For analysis by a Transmission Electron Microscope (TEM) and an Environmental Scanning Electron Microscope (ESEM), aerosol particles were collected on the Cu grid with a Formvar thin film (U1007, EM Japan) or a Lacey carbon substrate (U1001, EM Japan) to analyze physical and chemical particle features, mixing states, hygroscopicity, and ice nucleation efficiency for individual aerosol particle. These samples were collected by an automated two-stage impactor (AS-24W, Arios) and a three-stage impactor (MPS-3, California Measurements) operated at a flow rate of 1.0 L/min and 2.0 L/min, respectively. The sampling time length was between 10 and 60 minutes depending on the aerosol concentration. AS-24W usually worked every four hours during the Pacific Ocean and every two hours during the Bering Sea and Arctic Ocean. In addition, AS-24W was operated manually when the aerosol events were detected by online instruments. MPS-3 was operated manually between 1 and 4 times a day.

These sampling logs are listed in Tables 2.4.1-1, 2.4.1-2, 2.4.1-3, and 2.4.1-4. The

samples are going to be analyzed in the laboratory.

(4-3) CO and O₃

Ambient air was continuously sampled on the compass deck and drawn through ~20m long Teflon tubes connected to a Nondispersive Infrared (NDIR) CO analyzer (Model 48i-TLE, Thermo Fisher Scientific) and a UV photometric ozone analyzer (model 205, 2B Technologies), located in the environmental research room. The data will be used for characterizing air mass origins

(5) Station list or Observation log

Table 2.4.1-1: Log of ambient particles sampling on the quartz filter by a high-volume air sampler.

ID	Data collected (Sampling end)				Latitude			Longitude		
	YYYY	MM	DD	hh:mm: (UTC)	Deg.	Min.	N/S	Deg.	Min.	E/W
MR2206C-HV-C/F-1	2022	8	23	0:27	58	3.11	N	167	19.03	W
MR2206C-HV-C/F-2	2022	8	24	17:08	65	30.32	N	168	44.93	W
MR2206C-HV-C/F-3	2022	8	26	20:20	69	30	N	168	45.03	W
MR2206C-HV-C/F-4	2022	8	28	20:02	71	47.9	N	155	19.89	W
MR2206C-HV-C/F-5	2022	8	30	20:14	71	31.85	N	149	1.25	W
MR2206C-HV-C/F-6	2022	9	2	4:04	71	34.9	N	135	17.18	W
MR2206C-HV-C/F-7	2022	9	2	4:55	71	34.9	N	135	17.18	W
MR2206C-HV-C/F-8	2022	9	3	20:20	69	58.52	N	137	14.82	W
MR2206C-HV-C/F-9	2022	9	3	23:57	69	58.52	N	137	14.82	W
MR2206C-HV-C/F-10	2022	9	5	22:50	70	42.13	N	141	46.22	W
MR2206C-HV-C/F-11	2022	9	6	2:44	70	47.07	N	142	51.28	W
MR2206C-HV-C/F-12	2022	9	7	19:13	71	54.6	N	154	9.5	W
MR2206C-HV-C/F-13	2022	9	9	21:50	71	20.86	N	152	30.86	W
MR2206C-HV-C/F-14	2022	9	11	22:29	71	52.13	N	157	0.86	W
MR2206C-HV-C/F-15	2022	9	13	22:34	71	55.46	N	154	6.98	W
MR2206C-HV-C/F-16	2022	9	15	22:16	73	0.39	N	158	30.95	W
MR2206C-HV-C/F-17	2022	9	18	23:03	62	24.94	N	174	53.02	W
MR2206C-HV-C/F-18	2022	9	20	5:05	48	36.54	N	164	2.05	E
MR2206C-HV-C/F-19	2022	9	25	3:51	42	24.67	N	154	4.43	E
MR2206C-HV-C/F-20	2022	9	26	4:02	40	14.62	N	150	9.02	E
MR2206C-HV-C/F-21	2022	9	27	4:30	37	27.16	N	144	49.15	E
MR2206C-HV-C/F-22	2022	9	27	4:50	37	25.62	N	144	43.93	E

Table 2.4.1-2: Log of ambient particles sampling on the nuclepore filter by a handmade air sampler.

ID	Data collected (Sampling end)				Latitude			Longitude		
	YYYY	MM	DD	hh:mm: (UTC)	Deg.	Min.	N/S	Deg.	Min.	E/W
MR2206C-INP-1	2022	8	24	17:08	65	30.32	N	168	44.93	W
MR2206C-INP-2	2022	8	28	20:02	69	30	N	168	45.03	W
MR2206C-INP-3	2022	8	28	20:02	71	47.9	N	155	19.89	W
MR2206C-INP-4	2022	8	30	20:14	71	31.85	N	149	1.25	W
MR2206C-INP-5	2022	9	2	4:32	71	34.9	N	135	17.18	W
MR2206C-INP-6	2022	9	3	20:20	69	58.52	N	137	14.82	W
MR2206C-INP-7	2022	9	3	23:57	69	58.52	N	137	14.82	W
MR2206C-INP-8	2022	9	5	22:50	70	42.13	N	141	46.22	W
MR2206C-INP-9	2022	9	6	2:44	70	47.07	N	142	51.28	W
MR2206C-INP-10	2022	9	7	19:13	71	54.6	N	154	9.5	W
MR2206C-INP-11	2022	9	9	21:50	71	20.86	N	152	30.86	W
MR2206C-INP-12	2022	9	11	22:29	71	52.13	N	157	0.86	W
MR2206C-INP-13	2022	9	13	22:34	71	55.46	N	154	6.98	W
MR2206C-INP-14	2022	9	15	22:16	73	0.39	N	158	30.95	W
MR2206C-INP-15	2022	9	18	23:03	62	24.94	N	174	53.02	W
MR2206C-INP-16	2022	9	23	3:03	48	36.54	N	164	2.05	E
MR2206C-INP-17	2022	9	25	3:51	42	24.67	N	154	4.43	E
MR2206C-INP-18	2022	9	26	4:02	40	14.62	N	150	9.02	E
MR2206C-INP-19	2022	9	27	8:03	37	11.61	N	143	59.67	E
MR2206C-INP-20	2022	9	27	8:30	37	9.84	N	143	54.03	E
MR2206C-INP-21	2022	9	27	9:00	37	7.88	N	143	47.5	E

Table 2.4.1-3: Log of ambient particles sampling on the Cu grid by an AS-24W sampler.

ID	Data collected (Sampling start)				Latitude			Longitude		
	YYYY	MM	DD	hh:mm: (UTC)	Deg.	Min.	N/S	Deg.	Min.	E/W
MR2206C-TEM-1	2022	8	15	4:00	43	58.23	N	155	26.44	E
MR2206C-TEM-2	2022	8	19	0:00	53	43.11	N	179	50.93	E
MR2206C-TEM-3	2022	8	23	4:00	58	44.9	N	167	28.93	W
MR2206C-TEM-4	2022	8	26	4:41	68	12.73	N	168	45.39	W
MR2206C-TEM-5	2022	8	29	4:00	71	40.44	N	154	45.22	W
MR2206C-TEM-6	2022	8	30	20:00	71	35.84	N	149	30.06	W
MR2206C-TEM-7	2022	8	31	20:00	70	57.63	N	141	56.79	W
MR2206C-TEM-8	2022	9	2	8:00	70	55.12	N	135	39.01	W
MR2206C-TEM-9	2022	9	4	16:30	69	43.12	N	138	8.88	W
MR2206C-TEM-10	2022	9	6	6:00	70	53.2	N	144	10.33	W
MR2206C-TEM-11	2022	9	8	19:41	72	28.35	N	155	24.53	W
MR2206C-TEM-12	2022	9	10	20:00	71	29.96	N	152	30.44	W
MR2206C-TEM-13	2022	9	12	10:00	72	38.29	N	155	18.28	W
MR2206C-TEM-14	2022	9	13	20:00	71	55.47	N	154	6.97	W
MR2206C-TEM-15	2022	9	15	20:00	73	16.16	N	157	40.42	W
MR2206C-TEM-16	2022	9	19	0:00	62	17.69	N	175	5.62	W
MR2206C-TEM-17	2022	9	20	10:00	56	36.49	N	175	45.25	W
MR2206C-TEM-18	2022	9	22	10:00	51	11.54	N	168	15.61	E
MR2206C-TEM-19	2022	9	24	20:38	43	24.24	N	155	35.87	E

Table 2.4.1-4: Log of ambient particles sampling on the Cu grid by an MPS-3 sampler.

ID	Data collected (Sampling end)				Latitude			Longitude		
	YYYY	MM	DD	hh:mm: (UTC)	Deg.	Min.	N/S	Deg.	Min.	E/W
MR2206C-ESEM-1	2022	8	15	23:35	46	29.95	N	159	45.24	E
MR2206C-ESEM-2	2022	8	16	20:52	49	21.29	N	164	50.55	E
MR2206C-ESEM-3	2022	8	18	2:31	53	47.99	N	172	9.25	E
MR2206C-ESEM-4	2022	8	23	0:26	57	55.59	N	167	17.48	W
MR2206C-ESEM-5	2022	8	23	23:29	62	29.39	N	167	7.05	W
MR2206C-ESEM-6	2022	8	24	17:53	65	30.23	N	167	45	W
MR2206C-ESEM-7	2022	8	25	2:06	66	29.92	N	168	44.79	W
MR2206C-ESEM-8	2022	8	25	17:26	67	30	N	168	44.89	W
MR2206C-ESEM-9	2022	8	26	6:44	68	12.23	N	167	31.83	W
MR2206C-ESEM-10	2022	8	26	20:53	69	30.55	N	168	45.08	W
MR2206C-ESEM-11	2022	8	27	3:55	70	30.13	N	168	46.08	W
MR2206C-ESEM-12	2022	8	2	22:09	71	8.34	N	162	50.41	W
MR2206C-ESEM-13	2022	8	28	20:50	71	47.9	N	155	19.89	W
MR2206C-ESEM-14	2022	8	29	18:57	71	44.07	N	155	13.73	W
MR2206C-ESEM-15	2022	8	30	6:55	71	19.7	N	152	3.27	W
MR2206C-ESEM-16	2022	8	30	15:13	71	14.72	N	151	23.78	W
MR2206C-ESEM-17	2022	8	30	21:00	71	32.52	N	149	5.75	W
MR2206C-ESEM-18	2022	8	31	4:12	71	9.42	N	146	23.66	W
MR2206C-ESEM-19	2022	9	31	18:09	71	1.03	N	141	58.95	W
MR2206C-ESEM-20	2022	9	1	4:28	70	20.84	N	139	18.46	W
MR2206C-ESEM-21	2022	9	1	16:11	69	50.54	N	137	50.54	W
MR2206C-ESEM-22	2022	9	1	18:36	69	58.51	N	137	14.8	W
MR2206C-ESEM-23	2022	9	2	5:30	70	25.62	N	136	36.24	W
MR2206C-ESEM-24	2022	9	2	17:43	71	35	N	135	12.7	W
MR2206C-ESEM-25	2022	9	3	5:19	70	47.83	N	136	14.43	W
MR2206C-ESEM-26	2022	9	3	20:17	69	58.52	N	137	58.52	W
MR2206C-ESEM-27	2022	9	4	18:51	69	43.15	N	138	8.95	W
MR2206C-ESEM-28	2022	9	5	17:30	70	25.29	N	141	39.78	W
MR2206C-ESEM-29	2022	9	5	18:02	70	25.29	N	141	39.78	W
MR2206C-ESEM-30	2022	9	5	23:26	70	42.06	N	141	46.2	W
MR2206C-ESEM-31	2022	9	6	18:08	71	14.97	N	148	59.67	W
MR2206C-ESEM-32	2022	9	7	19:56	71	54.6	N	154	9.5	W
MR2206C-ESEM-33	2022	9	7	23:16	71	54.6	N	154	9.5	W
MR2206C-ESEM-34	2022	9	8	20:53	72	28.53	N	155	23.97	W
MR2206C-ESEM-35	2022	9	9	4:17	72	20.59	N	154	28.4	W
MR2206C-ESEM-36	2022	9	9	17:40	71	50	N	152	31.07	W
MR2206C-ESEM-37	2022	9	9	22:16	72	19.09	N	152	30.62	W
MR2206C-ESEM-38	2022	9	10	3:04	72	35.47	N	152	24.91	W
MR2206C-ESEM-39	2022	9	10	19:22	71	20.07	N	152	30.32	W
MR2206C-ESEM-40	2022	9	10	23:10	71	39.99	N	152	30.01	W
MR2206C-ESEM-41	2022	9	11	18:25	71	52.02	N	156	59.72	W
MR2206C-ESEM-42	2022	9	11	23:03	71	52.13	N	157	0.86	W
MR2206C-ESEM-43	2022	9	12	5:42	72	39.19	N	155	19.97	W
MR2206C-ESEM-44	2022	9	12	17:45	73	8.7	N	155	0.23	W
MR2206C-ESEM-45	2022	9	12	22:45	73	12.21	N	155	8.3	W
MR2206C-ESEM-46	2022	9	12	23:36	73	12.21	N	155	8.3	W
MR2206C-ESEM-47	2022	9	13	20:07	71	55.49	N	154	6.96	W
MR2206C-ESEM-48	2022	9	13	23:08	71	55.46	N	154	7.08	W
MR2206C-ESEM-49	2022	9	14	19:16	72	30.1	N	159	59.28	W
MR2206C-ESEM-50	2022	9	15	0:33	72	54	N	158	48.15	W
MR2206C-ESEM-51	2022	9	15	18:06	73	20.09	N	157	27.87	W
MR2206C-ESEM-52	2022	9	15	23:00	73	0.23	N	158	30.59	W
MR2206C-ESEM-53	2022	9	18	18:37	63	10.29	N	173	33.3	W
MR2206C-ESEM-54	2022	9	18	23:36	62	24.92	N	174	53.02	W
MR2206C-ESEM-55	2022	9	20	0:34	58	17.16	N	178	18.52	E
MR2206C-ESEM-56	2022	9	20	5:29	57	26.59	N	177	1.58	E
MR2206C-ESEM-57	2022	9	23	7:20	48	41.01	N	164	10.29	E
MR2206C-ESEM-58	2022	9	23	22:04	46	36.7	N	160	38.55	E
MR2206C-ESEM-59	2022	9	25	4:23	46	26.69	N	154	7.39	E
MR2206C-ESEM-60	2022	9	26	4:56	40	10.24	N	149	59.89	E

(6) Preliminary results

Particle production from the sea spray

We observed several coarse particle enhancements during this cruise (Figure 2.4.1-1). These particle enhancements were related to the wind speed (Figure 2.4.1-2), indicating that particle production from sea spray was the dominant process for these coarse particle enhancements. This particle production from sea spray attracted the attention of many researchers because sea spray can be an important source of aerosols in the

Arctic region and strongly affect the Arctic climate via the radiation process and the cloud process. We collected 180 aerosol samples using MPS-3 during this cruise (Figure 2.4.1-3), and these samples will be analyzed by an optical microscope, TEM, and ESEM for their physicochemical particle features and hygroscopic and ice nucleation activities. These analyses are expected to make new knowledge about the microphysical cloud process, especially ice nucleation, and the impact of sea spray on the Arctic climate.

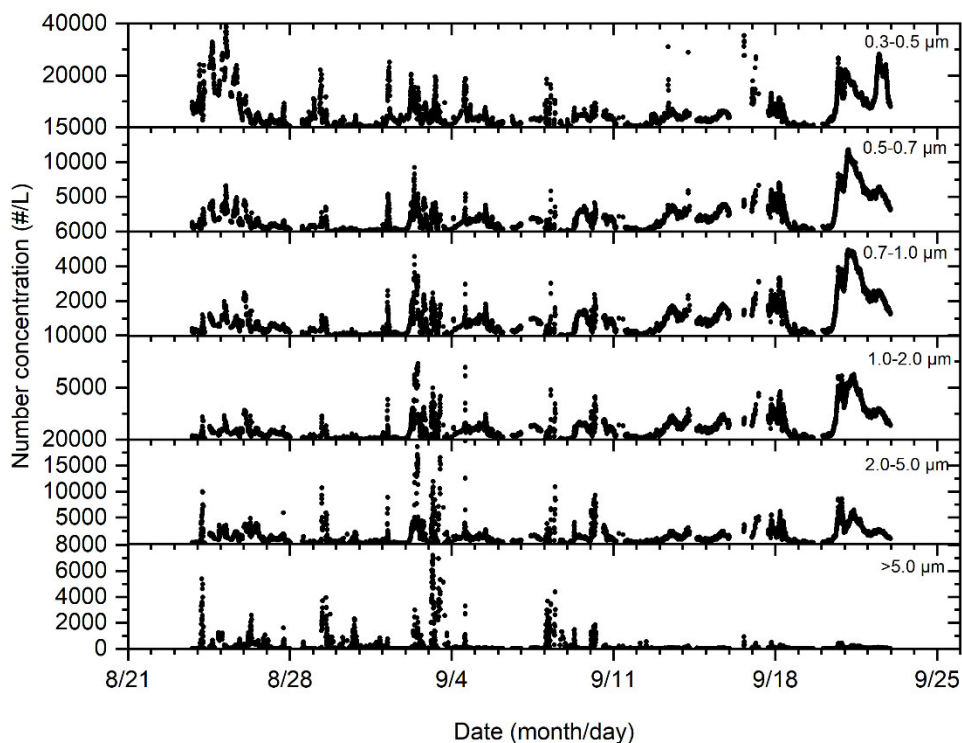


Figure 2.4.1-1: Time series of the OPC observation result. Contaminated data by Mirai exhaust is simply screened but not completely.

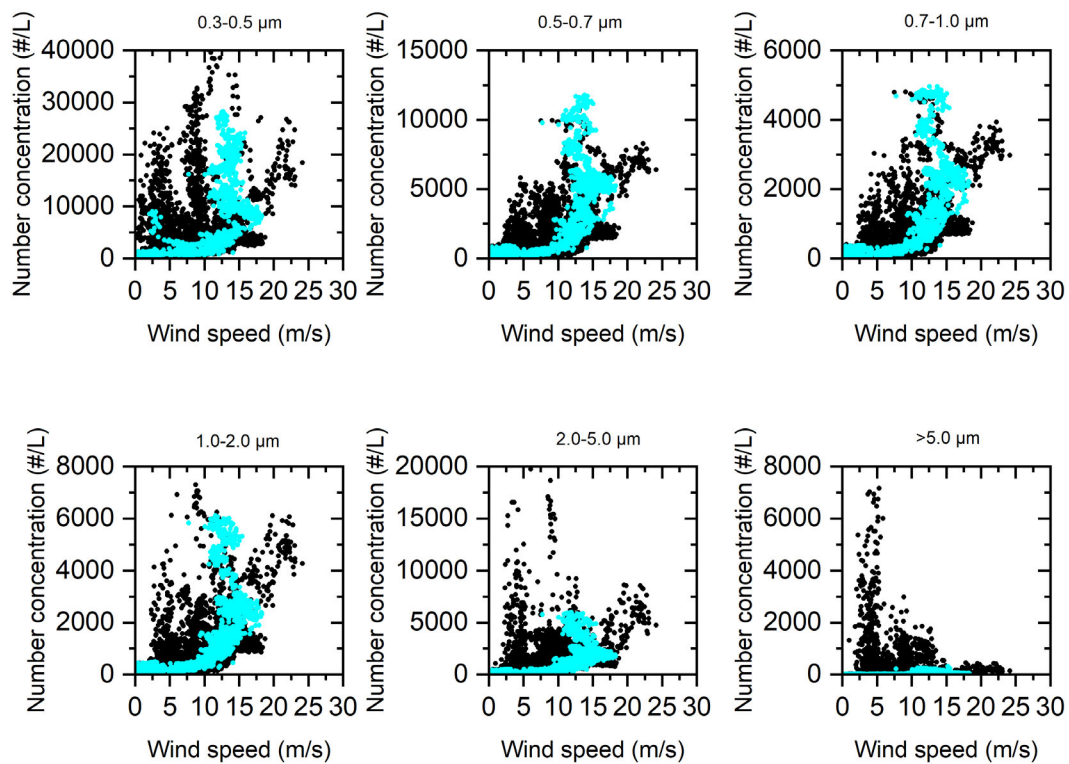


Figure 2.4.1-2: Correlation plots of number concentration of coarse particles and wind speed. The black plot indicates all observation results and the light blue plot indicates the results that RH was below 95 %. Contaminated data by Mirai exhaust is simply screened but not completely.

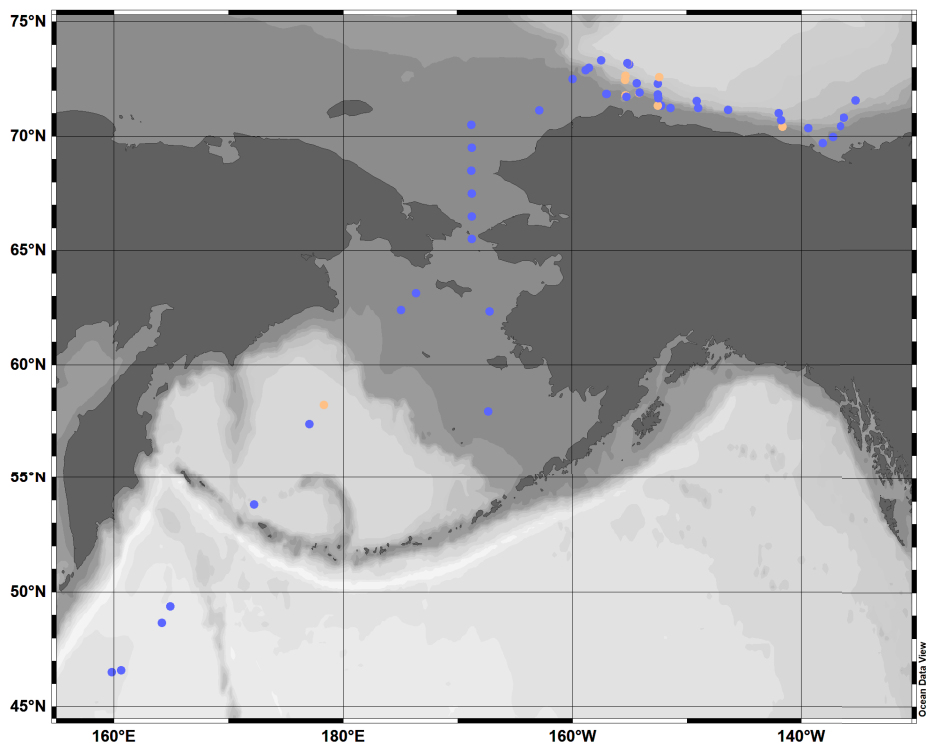


Figure 2.4.1-3: Map of points where ESEM samples were collected. Blue dots indicates the samples which were successfully collected and yellow dots indicates the samples which were possibly contaminated by ship exhaust.

(7) Data archive

These data obtained in this cruise will be submitted to the Data Management Group of JAMSTEC, and will be opened to the public via “Data Research System for Whole Cruise Information in JAMSTEC (DARWIN)” in JAMSTEC web site.

<http://www.godac.jamstec.go.jp/darwin/e>

2.4.2. Precipitation sampling

(1) Personnel

Fumikazu Taketani	JAMSTEC (Principal Investigator)	- not on board
Takeshi Kinase	JAMSTEC	- on board
Hotaek Park	JAMSTEC	- not on board

(2) Objectives

- To investigate contribution of suspended particles to rain and snow
- To investigate isotope ratio of hydrogen and oxygen in rain and snow

(3) Parameters

- Chemical composition of snow and rain
- Isotope ratio of oxygen in rain and snow

(4) Instruments and methods

Snow and rain samples were collected using hand-made rain/snow sampler. These sampling logs are listed in Table 2.4.2-1. To investigate the isotope ratio in rain/snow and interaction between aerosols and rain/snow, these samples are going to be analyzed in laboratory.

(5) Station list and Observation log

Table 2.4.2-1: Log of precipitation sampling.

ID	Data collected (Sampling start)				Latitude			Longitude		
	YYYY	MM	DD	hh:mm: (UTC)	Deg.	Min.	N/S	Deg.	Min.	E/W
MR2206C-RS-1	2022	8	15	23:10	49	30.2	N	165	8.31	E
MR2206C-RS-2	2022	8	16	21:26	53	22.51	N	170	40.13	E
MR2206C-RS-3	2022	8	17	21:26	54	3.25	N	173	50.98	W
MR2206C-RS-4	2022	8	23	22:53	69	0.14	N	168	43.34	W
MR2206C-RS-5	2022	8	26	17:27	71	8.52	N	162	51.17	W
MR2206C-RS-6	2022	8	27	17:05	71	40.3	N	154	59.58	W
MR2206C-RS-7	2022	8	29	18:23	71	34.68	N	149	21.12	W
MR2206C-RS-8	2022	8	30	20:14	71	47.49	N	141	51.4	W
MR2206C-RS-9	2022	9	3	19:47	69	43.15	N	138	8.95	W
MR2206C-RS-10	2022	9	10	2:57	71	39.96	N	152	29.96	W
MR2206C-RS-11	2022	9	10	23:00	71	52.01	N	156	59.76	W
MR2206C-RS-12	2022	9	12	17:38	73	12.22	N	155	11	W
MR2206C-RS-13	2022	9	13	19:34	73	20.18	N	157	27.8	W
MR2206C-RS-14	2022	9	15	19:49	61	41.71	N	176	6.69	W
MR2206C-RS-15	2022	9	20	5:30	48	37.5	N	164	3.95	E

(6) Preliminary results

None.

(7) Data archive

These data obtained in this cruise will be submitted to the Data Management Group of JAMSTEC, and will be opened to the public via “Data Research System for Whole

Cruise Information in JAMSTEC (DARWIN)” in JAMSTEC web site.
<<http://www.godac.jamstec.go.jp/darwin/e>>

2.5. Lidar observation

(1) Personnel

Fumikazu Taketani	JAMSTEC	-not on board
Masaki Katsumata	JAMSTEC	-not on board
Kyoko Taniguchi	JAMSTEC	-not on board
Kazuho Yoshida	NME	-on board
Satomi Ogawa	NME	-on board
Fumine Okada	NME	-on board
Ryo Kimura	NME	-on board

(2) Objectives

The objective of this observation is to capture the vertical distribution of clouds, aerosols, and water vapor in high spatio-temporal resolution.

(3) Parameters

355nm Mie scattering signal

532nm Mie scattering signal

1064nm Mie scattering signal

387nm Raman nitrogen scattering signal (night time only)

408nm Raman water vapor scattering signal (night time only)

607nm Raman nitrogen scattering signal (night time only)

660nm Raman water vapor scattering signal (night time only)

(4) Instruments and methods

The Mirai lidar system transmits a 10-Hz pulse laser in three wavelengths: 1064nm, 532nm, 355nm. For cloud and aerosol observation, the system detects Mie scattering at these wavelengths. The separate detections of polarization components at 532 nm and 355 nm obtain additional characteristics of the targets. The system also detects Raman water vapor signals at 660 nm and 408nm, Raman nitrogen signals at 607 nm and 387nm at nighttime. Based on the signal ratio of Raman water vapor to Raman nitrogen, the system offers water vapor mixing ratio profiles.

(5) Observation log

12 Aug. 2022 to 28 Sep. 2022

(6) Preliminary results

The lidar system observed the lower atmosphere throughout the cruise, except in the EEZs and territorial waters without permission. All data will be reviewed after the cruise to maintain data quality.

(7) Data archive

These data obtained in this cruise will be submitted to the Data Management Group of JAMSTEC, and will be opened to the public via “Data Research System for Whole Cruise Information in JAMSTEC (DARWIN)” in JAMSTEC web site.

<<http://www.godac.jamstec.go.jp/darwin/e>>

2.6. Greenhouse gases observation

(1) Personnel

Yasunori Tohjima	NIES*	-PI, not on board
Shigeyuki Ishidoya	AIST**	-not on board
Hideki Nara	NIES*	-not on board
Takeshi Kinase	JAMSTEC	-on board
Fumikazu Taketani	JAMSTEC	-not on board
Shinji Morimoto	Tohoku Univ.	-not on board
Daisuke Goto	NIPR	-not on board
Prabir Patra	JAMSTEC	-not on board

*National Institute for Environmental Studies

**The National Institute of Advanced Industrial Science and Technology

(2) Objectives

(2-1) Continuous observations of CO₂, CH₄ and CO mixing ratios

The Arctic region is warming about twice as fast as the global average and a huge amount of organic matter is considered to be buried in the permafrost of the Arctic region. Therefore, global warming would potentially enhance emissions of the greenhouse gases including CO₂ and CH₄ from such carbon pools into the atmosphere, which could enhance the global warming due to feedback mechanisms. The recent accelerated increase rate of the atmospheric CH₄ might be attributed to the enhanced emissions from the Arctic region. To detect the changes in the emission strengths of the greenhouse gases and the emission distributions in the Arctic region in the early stage, we conducted continuous observations of the atmospheric CO₂ and CH₄ mixing ratios during this MR22-06C cruise.



Photo 2.6-1: Flask sampling system (left) and continuous measurement system of the atmospheric CO₂, CH₄, and CO (right) based on a Cavity Ring-Down Spectrometer (CRDS) during MR22-06C cruise.

(2-2) Discrete flask sampling

In order to clarify spatial variations and air-sea exchanges of the greenhouse gases at northern high latitude, whole air samples were collected into 40 stainless-steel

flasks on-board R/V MIRAI (MR22-06C). The collected air samples will be analyzed for the mixing ratios of CO₂, O₂, Ar, CH₄, CO, N₂O and SF₆ and the stable isotope ratios of CO₂ and CH₄.

(3) Parameters

(3-1) Continuous observations of CO₂, CH₄ and CO mixing ratios

Mixing ratios of atmospheric CO₂, CH₄, and CO.

(3-2) Discrete flask sampling

Mixing ratios of atmospheric CO₂, O₂ (O₂/N₂ ratio), Ar (Ar/N₂ ratio), CH₄, CO, N₂O and SF₆, $\delta^{13}\text{C}$ and $\delta^{18}\text{O}$ of CO₂, $\delta^{13}\text{C}$ and δD of CH₄.

(4) Instruments and methods

(4-1) Continuous observations of CO₂, CH₄ and CO mixing ratios

Atmospheric CO₂, CH₄, and CO mixing ratios were measured by a Wavelength-Scanned Cavity Ring-Down Spectrometer (WS-CRDS, Picarro, G2401). An air intake, capped with an inverted stainless-steel beaker covered with stainless steel mesh, was placed on the right-side of the upper deck. A diaphragm pump (GAST, MOA-P108) was used to draw in the outside air at a flow rate of ~8L min⁻¹. Water vapor in the sample air was removed to a dew point of about 2°C and about -35°C by passing it through a thermoelectric dehumidifier (KELK, DH-109) and a Nafion dryer (PERMA PURE, PD-50T-24), respectively. Then, the dried sample air was introduced into the WS-CRDS at a flow rate of 100ml min⁻¹. The WS-CRDS were automatically calibrated every 25 hours by introducing 3 standard airs with known CO₂, CH₄ and CO mixing ratios. The analytical precisions for CO₂, CH₄ and CO mixing ratios are about 0.02 ppm, 0.3 ppb and 3 ppb, respectively.

(4-2) Discrete flask sampling

The air sampling equipment consisted of an air intake, a diaphragm pump (GAST MOA), a Stirling cooler (Twinbird) with a water trap, solenoid valves (CKD), a flow meter and a back pressure valve. Ambient air was pumped using the diaphragm pump from an air intake, dried cryogenically and filled into a 1L stainless-steel flask at a pressure of 0.27 MPa.

(5) Station list or Observation log

The continuous observations of CO₂, CH₄ and CO mixing ratios were conducted during the entire cruise. Sampling logs of the discrete flask sampling are listed in Table 2.6-1.

Table 2.6-1: List of logs of the discrete flask sampling.

On board ID	Date Collected				
	YYYY	MM	DD	hh:mm	UTC/JST
MR2205-F001	2022	08	15	21:07	UTC
MR2205-F002	2022	08	16	23:08	UTC
MR2205-F003	2022	08	17	21:53	UTC
MR2205-F004	2022	08	19	4:42	UTC
MR2205-F005	2022	08	20	23:06	UTC
MR2205-F006	2022	08	22	2:01	UTC
MR2205-F007	2022	08	22	20:19	UTC
MR2205-F008	2022	08	23	16:05	UTC
MR2205-F009	2022	08	24	15:30	UTC
MR2205-F010	2022	08	25	14:56	UTC
MR2205-F011	2022	08	26	18:51	UTC
MR2205-F012	2022	08	27	15:44	UTC
MR2205-F013	2022	08	28	17:48	UTC
MR2205-F014	2022	08	29	18:42	UTC
MR2205-F015	2022	08	30	14:43	UTC
MR2205-F016	2022	08	31	17:09	UTC
MR2205-F017	2022	09	01	18:37	UTC
MR2205-F018	2022	09	02	17:14	UTC
MR2205-F019	2022	09	03	19:15	UTC
MR2205-F020	2022	09	04	16:12	UTC
MR2205-F021	2022	09	05	18:55	UTC
MR2205-F022	2022	09	06	15:12	UTC
MR2205-F023	2022	09	07	18:57	UTC
MR2205-F024	2022	09	08	20:02	UTC
MR2205-F025	2022	09	09	18:44	UTC
MR2205-F026	2022	09	10	19:53	UTC
MR2205-F027	2022	09	11	16:30	UTC
MR2205-F028	2022	09	12	17:27	UTC
MR2205-F029	2022	09	13	17:28	UTC
MR2205-F030	2022	09	14	15:40	UTC
MR2205-F031	2022	09	15	19:26	UTC
MR2205-F032	2022	09	17	6:18	UTC
MR2205-F033	2022	09	17	17:13	UTC
MR2205-F034	2022	09	18	16:49	UTC
MR2205-F035	2022	09	20	1:43	UTC
MR2205-F036	2022	09	20	22:30	UTC
MR2205-F037	2022	09	21	19:14	UTC
MR2205-F038	2022	09	22	20:21	UTC
MR2205-F039	2022	09	23	20:53	UTC
MR2205-F040	2022	09	24	20:44	UTC

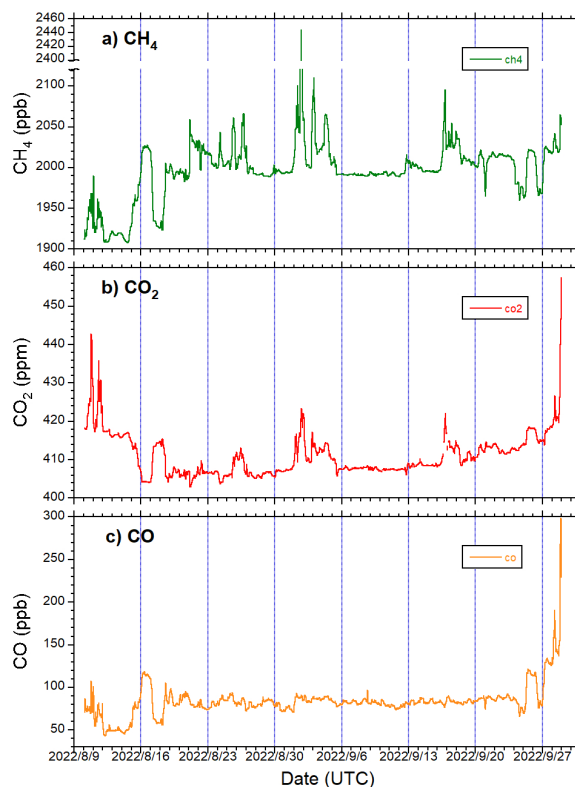


Figure 2.6-1: The time series of the atmospheric (a) CH₄, (b) CO₂, and (c) CO mixing ratios observed during the entire period of MR22-06C cruise.

(6) Preliminary results

The time series of the atmospheric CH₄, CO₂, and CO mixing ratios observed during the entire cruise are shown in Figure 2.6-1.

(7) Data archive

These data obtained in this cruise will be submitted to the Data Management

Group of JAMSTEC, and will be opened to the public via “Data Research System for Whole Cruise Information in JAMSTEC (DARWIN)” in JAMSTEC web site.

<<http://www.godac.jamstec.go.jp/darwin/e>>

2.7. Isotope analysis of water vapor

(1) Personnel

Hotaek Park (JAMSTEC)	Principle investigator	-not on board
-----------------------	------------------------	---------------

(2) Background and objectives

The warming climates lead to a number of changes in the Arctic environmental conditions, represented by the declining Arctic sea-ice and snow cover, permafrost degradation, and longer growing season period. The Arctic sea-ice is continuously going toward the melting direction, since recording the minimum area in 2012. The minimum sea ice extent of this year recorded 4.87 million square kilometers on September, reported by the National Snow and Ice Data Center (NSIDC) at the University of Colorado Boulder. The retreated sea ice decreases albedo, increasing the absorption of solar radiation by the ocean surface, consequently resulting in warmer sea surface and then greater evaporation from the opened warm surface. The interaction between the Arctic Ocean and atmosphere is stronger in autumn and early winter as the sea ice minimally covers the ocean surface. The atmosphere is wetted due to the evaporated water vapor, which has likely a relationship with the terrestrial hydrological cycle as precipitable water through the atmospheric circulation. In reality, observations identified the increase of autumnal precipitation and the resultant increase of snow depth in the northeastern Siberia. The increased snow enhances the insulation effect on permafrost warming during the winter season, as well as is correlated to the increase in spring discharge associated to snowmelt water. The Siberian major rivers indicated the increasing trends for the spring discharge. Furthermore, the snow-induced permafrost warming can increase the melting of ground ice within the permafrost, combining with the warming air temperature, and thus increasing the connectivity of the melted water to the river discharge. Likewise, these linkages suggest the potential impacts of the declining Arctic sea-ice on the terrestrial hydrologic processes.

Up to now, however, observations and models have provided little quantitative information on the declined sea-ice impact on the land water cycle. The linkage of the evaporated water vapor from the opened Arctic sea surface to the terrestrial hydrology is considerably complex over mixing with different source water in the atmosphere. Therefore, we focused on the advantage of stable water isotope to track the source regions along the precipitable water routes. The observation of the isotope of atmospheric water vapor was consecutively conducted until this year since the MR19-03C Arctic cruise of research vessel MIRAI. Simultaneously, an observational network to do sampling of precipitation water at both ocean and land has constructed.

The observed data likely provide important information for the spatial and temporal variability of the isotopic ratios along the cruise route in the opened Arctic Ocean surface and during the precipitation events. However, they have constraints in identifying the implication of the declined sea ice to the

intensified terrestrial water cycle at the global scale. Numerical models are a useful tool to identify the linkage of the declining sea ice and the terrestrial hydrology and at long-term and global scales. Meanwhile, the modeling requires the validation of the simulated results against observations. The combination of numerical model simulation and isotope observation makes it possible to explore the relationship of the declining sea ice and the terrestrial water cycle. This document reports the isotopic properties measured at the cruise of this year.

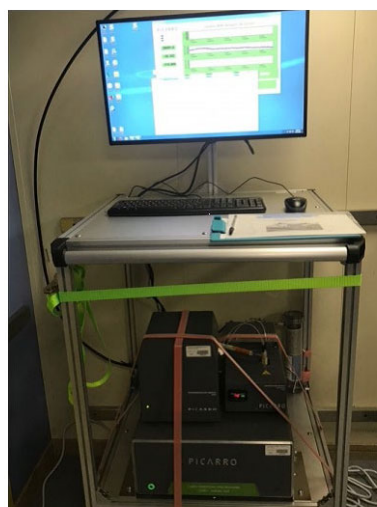


Figure 2.7-1: Isotope spectrometer system.

(3) Parameters

Isotope ratios of oxygen and hydrogen and water vapor concentration

(4) Instruments and method

The isotope of atmosphere water vapor was monitored by a L2130-*i* Isotope and Gas Concentration Analyzer (Picarro, Figure 2.7-1), which simultaneously provides $\delta^{18}\text{O}$ and $\delta^2\text{H}$ for isotopic H_2O with high-precision measurements, including water vapor concentration for the range of 1000 to 50000 ppm with 1–2 Hz measuring frequency. The observed data are archived in the storage of the spectrometer, operated by windows operational system. Two standard liquids, for example with isotopic values of -0.41/-1.59‰ and -31.20/-245.26‰ for $\delta^{18}\text{O}/\delta^2\text{H}$, are individually injected for 15 minutes every 12-hours, in which the derived linear regression equation is used to calibrate the monitored values by the spectrometer.

(5) Preliminary results

The measured isotopic ratios were averaged to hourly time steps, and Figure 2.7-2 exhibits their time-series variability in the Arctic Ocean during the whole cruise period from August 10 to September, 2022, including air and sea surface temperature. Unfortunately, there was a measurement gap during Aug. 23 to Sep. 3. The isotopic ratios generally showed higher values at the initial and end dates of the cruise as the vessel ran relatively warm regions. Then, the ratios tended to decrease and recorded the minimum values on Sep. 5, responding to the cold temperatures at the Arctic Ocean. During the period from Aug. 24 to Sep. 16 when the vessel stayed over the Arctic Ocean, the air temperature recorded 10°C or lower. The sea surface temperature also indicated daily variations consistent with the air temperature, which represents the spatial variability of the sea surface heat condition along the vessel cruising routes across north to south and east to west.

The isotopic ratios of $\delta^{18}\text{O}/\delta^2\text{H}$ significantly correlated with air temperature, as identified for the

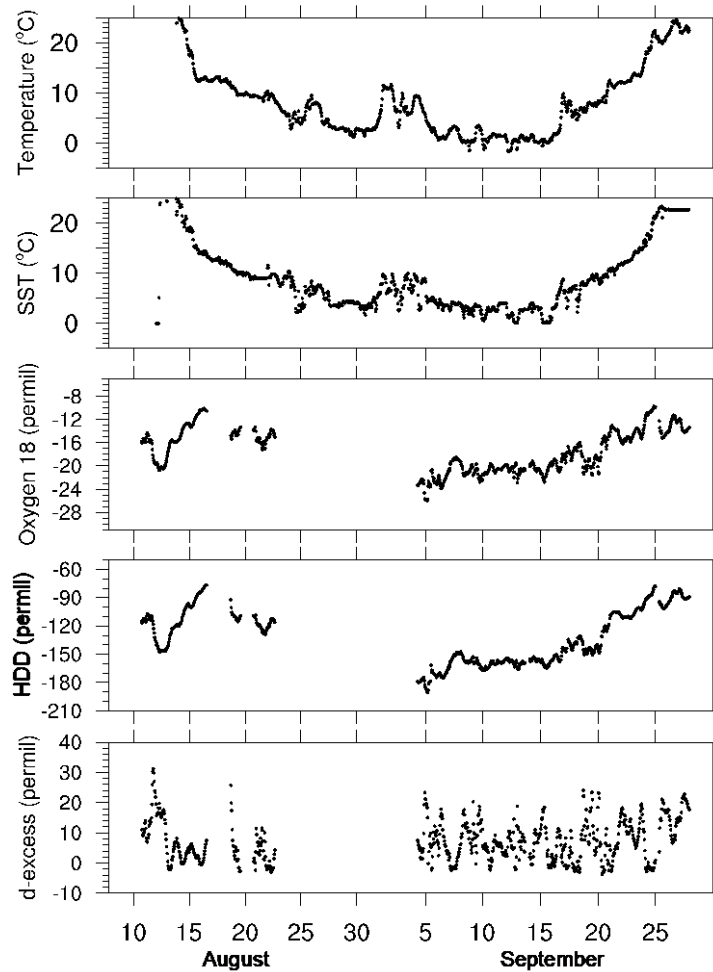


Figure 2.7-2: Time-series variability of averaged hourly air and sea surface temperature and isotopic variables during the MIRAI cruise.

previous three years (i.e., 2019–2021). The isotopic ratios, particularly d-excess ($= -8 \times \delta^{18}\text{O} + \delta^2\text{H}$) that is an index representing humidity and temperature conditions of the evaporated sea surface, displayed the largest diurnal and daily variability relative to $\delta^{18}\text{O}$ and $\delta^2\text{H}$ (Figure 2.7-2). The d-excess was correlated to the difference between sea surface and air temperature, showing larger scattering (Figure 2.7-3). The evaporated water vapor generally records lower $\delta^{18}\text{O}$ value, which results in higher d-excess. The larger difference between sea surface and air temperature is an efficient condition for larger evaporation from the sea surface, in which the d-excess practically indicated higher values. This suggests that the measurements have caught the isotopic ratios of the evaporated water vapor from the warmer ocean surface.

Both oxygen and hydrogen indicated significantly high correlation. Their relationship yielded the slope of 7.7, which is considerably higher than 6.1, 5.9, and 5.0 in 2019, 2020 and 2021, respectively. The slopes distribute within the ranges of 5 and 7 obtained at the northernmost terrestrial sites. However, the slopes derived by the four-year cruise is lower than the value 8 of Global Meteoric Water Line (GMWL), which represent the sensitivity of isotope to air temperature.

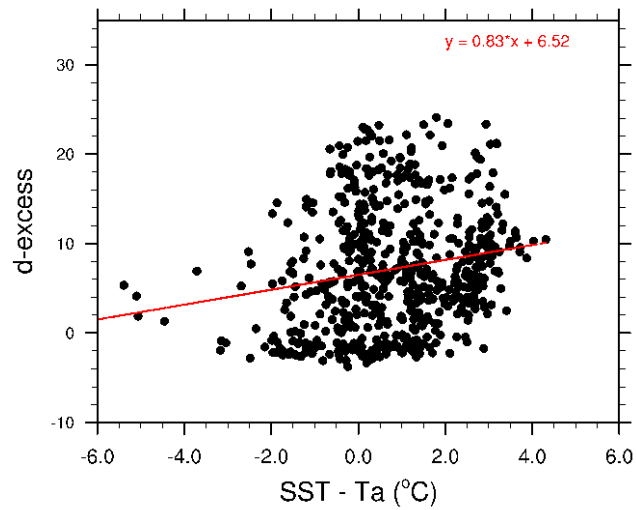


Figure 2.7-3. Relationship of hourly averaged d-excess and difference between sea surface temperature and air temperature.

(6) Data archive

The data obtained in this cruise will be submitted to the Data Management Group of JAMSTEC, and will be opened to the public via “Data Research System for Whole Cruise Information in JAMSTEC (DARWIN)” in JAMSTEC web site. <http://www.godac.jamstec.go.jp/darwin/e>.

2.8. Mercury observation

(1) Personnel

Osamu Nagafuchi	Fukuoka Institute of Technology	-not on board
Masanobu Yamamoto	Hokkaido University (PI)	-on board
Koyomi Nakazawa	Toyama Prefectural University	-not on board
Tetsuo Sueyoshi	JAMSTEC	-not on board

(2) Objectives

Mercury emitted from anthropogenic and natural source around the world continues to be transported to the Arctic environment. However atmospheric mercury concentration levels in the Arctic are generally decreasing. The decreasing trend of atmospheric mercury may be related to a decrease in emissions from regions closer to the Arctic, or to the effects of climate change, or both. However, there were not many observations that have been conducted the long-range transport from East Asia, where high amount of atmospheric mercury has been emitted. Furthermore, observations of atmospheric mercury in the marine boundary layer are rare. The objective of this research is to clarify the characteristics of atmospheric mercury concentration in Arctic area and to understand the dynamics of atmospheric mercury on a global scale, Gaseous Elemental Mercury (GEM) was measured on board during the MR22-06C.

Measurements of mercury concentrations in the Arctic will make an important contribution to assessments of the effectiveness of the Minamata Convention on Mercury.

(3) Parameters

Gaseous Elemental Mercury (GEM)

(4) Instruments and methods

Gaseous Elemental Mercury (GEM) in the atmosphere was measured using the AM-6F (NIPPON INSTRUMENTS CORPORATION), AM-6F is a fully automated, continuous mercury monitor designed to measure GEM from ambient air accurately down to the sub nano-gram per cubic-meter level. The technique used is direct gold amalgamation sampling with a Cold Vapor Atomic Fluorescence Spectrometer (CVAFS).

(5) Observation log

Data from 10 Aug. to 20 Aug. were unreliable due to equipment trouble.

(6) Preliminary results

Measurements of Gaseous Elemental Mercury (GEM) in the marine boundary layer were performed using AM-6F with CVAFS method during this cruise. GEM concentrations varied from 0.56 to 2.02 ng/m³ (n=980); the average value (1.01±0.24 ng/m³) was lower than the background range of the Northern Hemisphere (1.5~1.7ng/m³)

and corresponded to the background concentrations of the Southern Hemisphere (1.1~1.3 ng/m³). However, each sea area had its own characteristics. The average GEM concentrations in the Arctic Sea, the Bering Sea and the Sea of Okhotsk were 0.89 ± 0.12 ng/m³, 1.07 ± 0.13 ng/m³, 1.40 ± 0.27 ng/m³, respectively. Thus, the concentration tended to decrease as one moved toward the northern sea area.

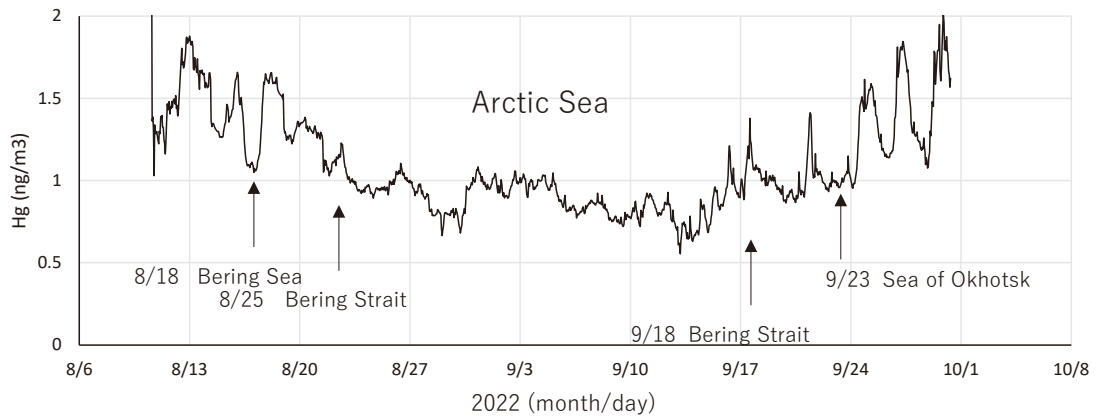


Figure 2.8-1: Daily variation of GEM concentration

(7) Data archive

These data obtained in this cruise will be submitted to the Data Management Group of JAMSTEC, and will be opened to the public via “Data Research System for Whole Cruise Information in JAMSTEC (DARWIN)” in JAMSTEC web site.

<<http://www.godac.jamstec.go.jp/darwin/e>>

3. Physical Oceanography

3.1. CTD casts and water sampling

(1) Personnel

Shigeto Nishino (JAMSTEC) *Principal investigator (not on board)

Motoyo Itoh (JAMSTEC)

Jonaotaro Onodera (JAMSTEC)

Aine Yoda (MWJ: Marine Works Japan Ltd.) *Operation Leader

Rei Ito (MWJ)

Riho Fujioka (MWJ)

Shintaro Amikura (MWJ)

(2) Objectives

Investigation of ocean structures and water characteristics.

(3) Parameters

Temperature (Primary and Secondary), Salinity (Primary and Secondary), Pressure, Dissolved Oxygen, (Primary “RINKO III” and Secondary “SBE43”), Fluorescence, Beam Transmission, Turbidity, Nitrate, Photosynthetically Active Radiation, Altimetric depth and Temperature measured by Deep Ocean Standards Thermometer (SBE35).

(4) Instruments and methods

CTD/Carousel Water Sampling System was used for hydrographic observations and water sampling. Carousel system used in this cruise was a 36-positions Carousel Water Sampler (CWS), and sampling bottles used were 12-liter sampling bottles (Sea-Bird Electronics, Inc.).

The instruments used in this cruise and their specifications are listed below.

Winch and cable

Traction winch system (4.5 tons) (Dynacon, Inc.)

Armored cable ($\phi = 9.53$ mm) (Rochester Wire & Cable)

Compact underwater slip ring swivel (Hanayuu Co., Ltd.)

CTD: SBE911plus CTD system

Deck unit:

SBE11plus (S/N 11P54451-0872, Sea-Bird Electronics, Inc.)

Under water unit:

SBE9plus (S/N: 09P54451-1027, Sea-Bird Electronics, Inc.)

Pressure sensor: Digiquartz pressure sensor (S/N: 117457)

Date of calibration: 09-Jun-2022

Carousel water sampler:

SBE32 (S/N: 3227443-0391, Sea-Bird Electronics, Inc.)

Temperature sensors:

Primary: SBE03F (S/N: 031525, Sea-Bird Electronics, Inc.)

Date of calibration: 19-Jan-2022

Secondary: SBE03F (S/N: 031359, Sea-Bird Electronics, Inc.)

Date of calibration: 19-Jan-2022

Deep ocean standards thermometer: SBE35 (S/N: 0053, Sea-Bird Electronics,
Inc.)

Date of calibration: 31-May-2022

Conductivity sensors:

Primary: SBE04C (S/N: 041206, Sea-Bird Electronics, Inc.)

Date of calibration: 16-Feb-2022

Secondary: SBE04C (S/N: 041203, Sea-Bird Electronics, Inc.)

Date of calibration: 22-Feb-2022

Dissolved oxygen sensors:

Primary: RINKOIII (S/N: 0278_163010BA, JFE Advantech Co., Ltd.)

Date of calibration: 28-May-2021

Secondary: SBE43 (S/N: 430575, Sea-Bird Electronics, Inc.)

Date of calibration: 28-Aug-2021

(001M001 – 012M001)

Secondary: SBE43 (S/N: 432211, Sea-Bird Electronics, Inc.)

Date of calibration: 19-Jun-2019

(013M001 – 034M001)

Transmissometer:

C-Star (S/N CST- 1727DR, WET Labs, Inc.)

Date of calibration: 02-May-2022

Fluorescence sensor:

Chlorophyll Fluorometer (S/N: 3618, Seapoint Sensors, Inc.)

Gain setting: 10X, 0-15 ug/l

Date of calibration: None

Turbidity sensor:

Seapoint Turbidity Meter (S/N: 14953, Seapoint Sensors, Inc.)

Gain setting: 100X, 0-25 FTU

Scale factor: 1.000

Date of calibration: None

Nitrate sensor:

Deep SUNA (S/N: 1613, Satlantic Inc.)

Date of calibration: None

Photosynthetically Active Radiation (PAR) Sensor:

PAR-Log ICSW (S/N: 2180, Sea-Bird Electronics, Inc.)

Date of calibration: 14-Sep-2021

Altimeter:

Benthos PSA-916T (S/N: 1157, Teledyne Benthos, Inc.)

Submersible pump:

Primary: SBE5T (S/N: 055816, Sea-Bird Electronics, Inc.)

Secondary: SBE5T (S/N: 054598, Sea-Bird Electronics, Inc.)

Bottom contact switch: (Sea-Bird Electronics, Inc.)

Configuration files: MR2206C_A.xmlcon

001M001 – 012M001

MR2206C_B.xmlcon

013M001, 018M001 – 025M001, 027M001 – 032M001, 034M001

MR2206C_C.xmlcon

014M001 – 017M001, 026M001, 033M001

Data Collection

CTD was deployed from starboard side of the working deck. CTD raw data were acquired in real time by using Seasave-Win32 (ver.7.26.7.121, Sea-Bird Electronics, Inc.), and stored in the hard disk of the personal computer. Seawater was sampled during the up-cast by sending fire (close) command from the operation PC. At each sampling depth, fire command was sent after waiting for 30 seconds from the winch stop. After closing of water sampling bottle, the underwater unit of CTD/CWS system stayed at the sampling depth at least 5 seconds for measurement of water temperature by SBE 35. For depths where vertical gradient of water properties was expected to be large (e.g. in thermocline), the bottle was exceptionally fired after waiting for 60 seconds from the winch stop to enhance exchanging the water between inside and outside of the bottle.

(5) Problems encountered

At cast 028M001, during 1 min. waiting time before water sampling at SCM, some sensors were shifted, because pumps absorbed jellyfish.

(6) Data processing

The procedure for processing the obtained CTD data is herein described. In these processes, a utility software, SBE Data Processing-Win32 (ver.7.26.7.129) and some original modules were used.

(The process in order)

DATCNV converted the binary raw data into engineering unit data. DATCNV also extracts bottle information where scans were marked with the bottle confirm bit during acquisition. The scan duration to be included in bottle file was set to 4.4 seconds, and the offset was set to 0.0 seconds. The hysteresis correction for the SBE 43 data (voltage) was applied for both profile and bottle information data.

TCORP (original module) corrected the pressure sensitivity of the temperature (SBE3) sensor.

1.714e-008 (degC/dbar) for S/N: 031525

-2.29885054e-007 (degC/dbar) for S/N: 031359

RINKOCOR (original module) corrected the time dependent, pressure induced effect (hysteresis) of the RINKOIII profile data.

RINKOCORROS (original module) corrected the time dependent, pressure induced effect (hysteresis) of the RINKOIII bottle information data by using the hysteresis corrected profile data.

BOTTLESUM created a summary of the bottle data. The data were averaged over 4.4 seconds.

ALIGNCTD aligned parameter data in time, relative to pressure to ensure that all calculations were made using measurements from the same parcel of water. For an SBE 9plus with TC-ducted temperature and conductivity sensors and a 3000-rpm pump, the typical lag of temperature to pressure is 0 second and lag of conductivity relative to temperature is 0.073 seconds. The Deck Unit was programmed to advance conductivity relative to pressure so conductivity alignment in ALIGNCTD was not needed. Dissolved oxygen data are systematically delayed with respect to pressure mainly because of the long time constant of the dissolved oxygen sensor and of an additional delay from the transit time of water in the pumped plumbing line. This delay was compensated by 6 seconds advancing dissolved oxygen sensor (SBE43) output (dissolved oxygen voltage) relative to the temperature data. Delay of the transmissometer data was also compensated by 2 seconds advancing sensor output (voltage) relative to the temperature data. User polynomial 1 was also advanced 1 second.

WILDEDIT marked extreme outliers in the data files. The first pass of WILDEDIT obtained the accurate estimate of the true standard deviation of the data. The data were read in blocks of 1000 scans. Data greater than 10 standard deviations were flagged. The second pass computed a standard deviation over the same 1000 scans excluding the flagged values. Values greater than 20 standard deviations were marked bad. This process was applied to pressure, depth, temperature (primary and secondary), conductivity (primary and secondary), and dissolved oxygen voltage (SBE43).

CELLTM used a recursive filter to remove conductivity cell thermal mass effects from the measured conductivity. Typical values for SBE 9plus with TC duct and 3000 rpm pump which were 0.03 for thermal anomaly amplitude α and 7.0 for the time constant $1/\beta$ were used.

FILTER performed a low-pass filter on pressure and depth with a time constant of 0.15 seconds. In order to produce zero phase lag (no time shift) the filter runs forward first then backward.

WFILTER performed as a median filter to remove spikes in the output voltage of transmissometer voltage, beam transmission data, beam attenuation data, the fluorescence data, nitrate data and turbidity data. A median value was determined by 49 scans of the window. The window length is specified as 73 scans for nitrate data.

SECTIONU (original module of SECTION) selected a time span of data based on scan number in order to reduce a file size. The minimum number was set to be the starting time when the CTD package was beneath the sea-surface after activation of the pump. The maximum number was set to be the end time when the package came up from the surface.

LOOPEDIT marked scans where the CTD was moving less than the minimum velocity of 0.0 m/s (traveling backwards due to ship roll).

DESPIKE (original module) removed spikes of the data. A median and mean absolute deviation was calculated in 1-dbar pressure bins for both down and up cast, excluding the flagged values. Values greater than 4 mean absolute deviations from the median were marked bad for each bin. This process was performed twice for temperature, conductivity and dissolved oxygen (RINKOIII and SBE43) voltage.

DERIVE was used to compute dissolved oxygen (SBE43).

BINAVG averaged the data into 1 dbar pressure bins.

BOTTOMCUT (original module) deleted the deepest pressure bin when the averaged scan number of the deepest bin was smaller than the average scan number of the bin just above.

DERIVE was re-used to calculate salinity, potential temperature, and sigma-theta.

SPLIT was used to split data into down cast and up cast

Remaining spikes in the CTD data were manually eliminated from the 1 dbar averaged data. The data gaps resulting from the elimination were linearly interpolated with a quality flag of 6.

(7) Station list

During the MR22-06C cruise, 34 casts of CTD were carried out. Date, time and locations of the CTD casts are listed in Table 3.1-1.

(8) Preliminary results

During this cruise, we judged presence or absence of noise, spike or shift in the obtained hydro-cast data.

Definitions of these problems

- (1) Noise: Not singly but continuously (mostly from several seconds to several minutes) detected outliers.
- (2) Spike: One-off outlier which is detected after data processing and is oceanographically impossible (e.g. reversal of density). Spike is not caused by a breaking down of sensor. Generally, we can detect spikes in the deep layer (e.g. below the thermocline).
- (3) Shift: Continuous data under trend to collect values deviated from accurate ones. In most cases, the “shift” can be recognized from comparison of profiles between primary and secondary sensors or down and up casts. The “shift” may be caused by absorption of foreign substances into sensors, adhesion of substances on an optical sensor, crack in a part of sensor, characteristics in each sensor, etc.

Detected problems

- 001M001: Conductivity (secondary)
Down 27 dbar: spike
- 002M001: Oxygen (primary)
Down 36, 40 - 44 dbar: spike
- 008M001: Oxygen (primary)
All data: noise
- 009M001: Oxygen (primary)

All data: noise
012M001: Oxygen (primary)
Up 74-52 dbar: noise
015M001: Turbidity
Down 1197-2009 dbar: shift
018M001: Beam Transmission
Up 533 - 390 dbar: noise
Turbidity
Down 519-608 dbar: noise
022M001: Beam Transmission
Up 345-306 dbar: noise
028M001: Temperature, Conductivity, Oxygen (primary)
Up 28 dbar - surface: noise
Temperature, Conductivity (secondary)
Up 30 dbar - surface: noise
034M001: Conductivity (primary)
Down 387 dbar: spike

(9) Data archive

These data obtained in this cruise will be submitted to the Data Management Group of JAMSTEC, and will be opened to the public via “Data Research System for Whole Cruise Information in JAMSTEC (DARWIN)” in JAMSTEC web site.

<<http://www.godac.jamstec.go.jp/darwin/e>>

Table 3.1-1: MR22-06C CTD cast table

MR22-06C CTD cast table													
Stnnbr	Castno	Date(UTC)	Time(UTC)		BottomPosition		Depth (m)	Wire Out (m)	HT Above Bottom (m)	Max Depth	Max Pressure	CTD Filename	Remark
		(mmddyy)	Start	End	Latitude	Longitude							
001	1	082422	17:59	18:18	65-30.34N	168-44.99W	54.8	47.6	4.2	50.5	51.0	001M001	
002	1	082422	22:06	22:26	66-00.12N	168-45.12W	52.9	45.0	4.0	48.5	49.0	002M001	
003	1	082522	01:45	02:03	66-30.21N	168-44.88W	54.5	46.9	4.9	49.5	50.0	003M001	
004	1	082522	04:41	05:01	67-00.16N	168-44.20W	44.9	35.8	4.8	39.6	40.0	004M001	
005	1	082522	17:07	17:25	67-30.00N	168-44.91W	49.8	41.0	5.4	43.6	44.0	005M001	
006	1	082622	02:52	03:09	68-00.22N	168-44.89W	59.1	49.4	4.6	53.5	54.0	006M001	
007	1	082622	06:18	06:36	68-30.11N	168-45.33W	53.4	44.7	4.2	48.5	49.0	007M001	
008	1	082622	17:25	17:42	69-00.20N	168-43.22W	53.0	44.3	4.8	47.5	48.0	008M001	
009	1	082622	20:29	20:43	69-30.01N	168-45.03W	51.6	42.6	4.6	46.5	47.0	009M001	
010	1	082622	23:36	23:49	69-59.97N	168-45.20W	41.0	32.0	4.8	35.6	36.0	010M001	
011	1	082722	03:38	03:58	70-30.02N	168-45.92W	38.8	28.5	4.6	33.7	34.0	011M001	
012	1	082822	14:37	15:02	71-40.48N	154-57.89W	99.0	92.4	4.4	95.0	96.0	012M001	
013	1	082922	18:54	19:52	71-44.09N	155-13.56W	306.0	290.9	10.0	294.7	298.0	013M001	
014	1	083022	22:06	23:58	71-27.26N	148-32.15W	2169.0	2163.5	9.2	2157.4	2191.0	014M001	
015	1	083122	04:38	06:31	71-07.22N	146-06.54W	2123.0	2112.3	9.3	2102.5	2135.0	015M001	
016	1	083122	17:37	19:34	71-01.05N	141-58.96W	2340.0	2330.0	9.0	2324.9	2362.0	016M001	
017	1	083122	21:48	23:30	70-47.35N	141-51.46W	1797.0	1774.7	11.0	1767.2	1793.0	017M001	
018	1	090322	00:06	01:36	71-19.96N	135-30.49W	1324.0	1310.5	9.2	1309.3	1327.0	018M001	
019	1	090422	00:07	00:28	69-58.51N	137-14.72W	58.3	48.7	5.5	51.5	52.0	019M001	
020	1	090522	17:26	17:49	70-25.29N	141-39.88W	79.0	73.1	5.0	76.2	77.0	020M001	
021	1	090522	20:23	21:15	70-32.97N	141-41.95W	470.0	449.8	9.3	450.9	456.0	021M001	
022	1	090522	23:38	00:59	70-42.12N	141-46.43W	1088.0	1082.7	8.9	1080.0	1094.0	022M001	
023	1	090822	20:02	21:51	72-28.56N	155-23.93W	2019.0	2003.7	10.0	1997.5	2028.0	023M001	
024	1	090922	17:12	18:46	71-50.01N	152-31.16W	1297.0	1284.6	10.3	1284.7	1302.0	024M001	
025	1	090922	21:31	22:10	72-19.08N	152-30.58W	2872.0	1003.1	-	1003.1	1016.0	025M001	
026	1	091022	00:05	02:47	72-35.41N	152-24.84W	3628.0	3620.9	9.6	3612.8	3682.0	026M001	
027	1	091022	18:09	18:33	71-19.98N	152-30.09W	61.2	52.0	4.7	56.4	57.0	027M001	
028	1	091022	20:34	20:59	71-30.01N	152-29.99W	107.0	98.5	4.5	102.9	104.0	028M001	
029	1	091022	23:36	00:28	71-40.08N	152-30.06W	313.0	297.7	9.1	301.7	305.0	029M001	
030	1	091422	18:13	18:35	72-30.01N	159-59.49W	48.5	38.6	4.9	42.6	43.0	030M001	
031	1	091422	20:54	21:14	72-42.12N	159-24.21W	84.9	72.4	5.3	77.2	78.0	031M001	
032	1	091522	00:03	00:57	72-54.02N	158-48.34W	397.0	373.6	10.0	377.7	382.0	032M001	
033	1	091522	17:04	19:26	73-20.11N	157-27.91W	3002.0	2992.6	9.0	2985.2	3038.0	033M001	
034	1	091522	22:21	23:52	73-00.33N	158-30.80W	1331.0	1354.6	10.5	1356.4	1375.0	034M001	

3.2. XCTD

(1) Personnel

Motoyo Itoh	JAMSTEC	-PI
Kazuho Yoshida	NME (Nippon Marine Enterprises, Ltd.)	
Satomi Ogawa	NME	
Fumine Okada	NME	
Ryo Kimura	NME	
Yoichi Inoue	MIRAI Crew	

(2) Objectives

To obtain vertical profiles of sea water temperature and salinity (calculated from temperature, pressure (depth), and conductivity).

(3) Parameters

The ranges and accuracies of parameters measured by the XCTD (eXpendable Conductivity, Temperature & Depth profiler) are as follows:

Parameter	Range	Accuracy
Conductivity	0 ~ 60 [mS/cm]	+/- 0.03 [mS/cm]
Temperature	-2 ~ 35 [deg-C]	+/- 0.02 [deg-C]
Depth	0 ~ 1000 [m]	5 [m] or 2 [%] (either of them is major)

(4) Instruments and methods

We observed vertical profiles of sea water temperature and salinity measured by XCTD-1 and XCTD-1N probes manufactured by Tsurumi-Seiki Co. (TSK). The electric signal from the probe was converted by MK-150N (TSK), and was recorded by AL-12B software (Ver.1.6.4, TSK). We launched 81 probes by using the automatic launcher. The XCTD observation log is shown in Table 3.2-1.

(5) Observation log

Table 3.2-1: XCTD observation log

No.	Station No.	Date [YYYY/MM/DD]	Time [hh:mm]	Latitude [deg-min]	Longitude [deg-min]	Depth [m]	SST [deg-C]	SSS [PSU]	Probe S/N
1	XCTD-001	2022/08/24	19:41	65-42.4076N	168-16.0028W	46	7.096	31.099	20111274
2	XCTD-002	2022/08/24	20:15	65-45.2053N	168-29.8780W	56	5.622	31.486	20111278
3	XCTD-003	2022/08/24	20:58	65-49.0761N	168-47.6892W	50	2.178	32.320	20111271
4	XCTD-004	2022/08/25	18:56	67-46.9853N	168-36.1492W	50	5.011	31.501	20111268
5	XCTD-005	2022/08/25	19:49	67-53.8794N	168-14.1404W	58	6.685	31.498	20111269
6	XCTD-006	2022/08/25	20:43	68-00.8221N	167-52.0363W	52	5.576	32.278	20111267
7	XCTD-007	2022/08/25	21:38	68-07.6430N	167-29.8399W	49	7.695	31.203	20111272

8	XCTD-008	2022/08/25	22:05	68-11.0887N	167-18.5297W	48	7.657	31.236	20111270
9	XCTD-009	2022/08/25	22:32	68-14.5134N	167-07.3612W	43	7.716	31.211	20111273
10	XCTD-010	2022/08/25	23:02	68-17.9747N	166-55.9390W	34	9.242	30.919	20111275
11	XCTD-011	2022/08/27	07:41	70-38.1351N	167-25.0048W	51	5.030	31.979	20111282
12	XCTD-012	2022/08/27	10:03	70-46.0283N	166-04.9810W	41	6.204	31.145	20111286
13	XCTD-013	2022/08/27	12:24	70-53.9810N	164-44.9595W	37	5.688	31.092	20111276
14	XCTD-014	2022/08/27	14:58	71-07.0424N	163-25.3318W	45	3.691	30.968	20111285
15	XCTD-015	2022/08/28	01:45	71-11.3622N	162-04.5018W	45	3.635	30.484	20111277
16	XCTD-016	2022/08/28	03:58	71-17.1974N	160-40.0391W	50	3.536	29.335	20111287
17	XCTD-017	2022/08/28	06:14	71-22.9959N	159-15.0292W	53	3.222	28.651	20111288
18	XCTD-018	2022/08/28	08:30	71-28.7823N	157-50.0709W	81	3.390	29.789	20111289
19	XCTD-019	2022/08/28	10:38	71-35.2512N	156-25.0724W	150	4.155	28.847	20111283
20	XCTD-020	2022/08/29	00:28	71-50.0178N	155-51.0440W	90	3.961	28.413	21054552
21	XCTD-021	2022/08/29	00:51	71-48.9947N	155-37.0230W	114	4.005	26.200	21054553
22	XCTD-022	2022/08/29	01:15	71-48.0347N	155-23.0456W	147	4.130	26.234	20111279
23	XCTD-023	2022/08/29	01:28	71-46.0003N	155-17.5165W	196	4.403	26.208	20111281
24	XCTD-024	2022/08/29	01:42	71-43.9974N	155-12.0045W	301	4.533	26.336	20111284
25	XCTD-025	2022/08/29	01:55	71-42.0022N	155-06.4011W	181	3.978	27.936	20111290
26	XCTD-026	2022/08/29	02:09	71-40.0078N	155-01.0766W	106	4.048	28.093	20111280
27	XCTD-027	2022/08/29	02:22	71-38.0054N	154-55.5521W	57	4.317	27.301	21054554
28	XCTD-028	2022/08/29	02:37	71-36.0056N	154-49.0135W	43	4.482	26.759	21054551
29	XCTD-029	2022/08/31	02:00	71-18.8984N	147-26.1547W	2277	3.827	25.129	21054555
30	XCTD-030	2022/08/31	12:32	71-04.6642N	144-01.8121W	1550	4.397	23.311	21054557
31	XCTD-031	2022/08/31	20:29	70-53.2330N	141-51.2301W	2067	5.223	22.515	21054556
32	XCTD-032 (MT1)	2022/09/01	08:10	70-00.1922N	137-18.5237W	61	9.709	13.964	21054558
33	XCTD-033	2022/09/02	06:28	70-39.9864N	136-10.0118W	518	8.574	16.345	21054561
34	XCTD-034	2022/09/02	09:39	71-09.9458N	135-09.4002W	846	6.280	17.629	21054560
35	XCTD-035	2022/09/03	08:42	70-12.0052N	136-59.9872W	47	9.680	14.458	21054559
36	XCTD-036	2022/09/03	09:40	70-08.0114N	137-31.9419W	62	9.693	14.588	21054571
37	XCTD-037	2022/09/03	10:14	70-04.8937N	137-49.9504W	120	9.212	15.502	21054569
38	XCTD-038	2022/09/03	10:51	70-02.9989N	138-10.9530W	209	8.289	18.586	21054572
39	XCTD-039 (MT2)	2022/09/04	06:42	69-43.1021N	138-08.9426W	151	8.809	17.017	21054567
40	XCTD-040	2022/09/04	08:31	69-33.9868N	138-04.1383W	101	9.194	13.997	21054565
41	XCTD-041	2022/09/04	09:09	69-41.0103N	138-12.0189W	134	8.636	17.297	21054568
42	XCTD-042	2022/09/05	02:28	69-49.9381N	138-29.9754W	182	4.882	21.837	21054556
43	XCTD-043	2022/09/05	03:31	69-58.9927N	138-38.5795W	265	5.361	22.037	21054562
44	XCTD-044	2022/09/05	04:24	69-56.0096N	139-05.9598W	157	4.453	22.608	21054570
45	XCTD-045	2022/09/05	05:11	69-52.9880N	139-29.0217W	44	4.223	22.956	21107518
46	XCTD-046	2022/09/05	07:41	70-14.9919N	138-55.0318W	441	4.338	22.800	21054573
47	XCTD-047	2022/09/05	09:19	70-29.9884N	139-09.2447W	867	5.059	20.686	21107517
48	XCTD-048	2022/09/05	18:43	70-18.0068N	141-24.0486W	54	3.728	24.595	21054564
49	XCTD-049 (BC2)	2022/09/07	08:42	71-52.6379N	154-02.7176W	219	4.215	30.982	21054563
50	XCTD-050	2022/09/08	06:59	72-09.0007N	153-28.9779W	2078	2.306	24.849	21107522

51	XCTD-051	2022/09/09	19:42	72-00.0038N	152-30.0666W	1672	2.336	24.486	21107521
52	XCTD-052	2022/09/11	01:52	71-32.2263N	151-56.9187W	562	2.718	26.902	21107526
53	XCTD-053	2022/09/11	02:21	71-28.3319N	152-02.3630W	213	2.633	27.385	21107524
54	XCTD-054	2022/09/11	02:46	71-24.2942N	152-03.4836W	166	2.739	27.278	21107519
55	XCTD-055	2022/09/11	03:14	71-20.4188N	152-07.1445W	69	2.678	27.324	21107528
56	XCTD-056	2022/09/11	03:42	71-16.5586N	152-09.8327W	50	2.415	27.678	21107567
57	XCTD-057	2022/09/11	08:12	71-36.0094N	154-49.0531W	42	3.324	30.281	21107568
58	XCTD-058	2022/09/11	08:26	71-37.9850N	154-55.4697W	56	3.394	30.422	21107566
59	XCTD-059	2022/09/11	08:40	71-39.9818N	155-00.9796W	102	3.507	30.430	21107565
60	XCTD-060	2022/09/11	08:54	71-41.9898N	155-06.5115W	178	3.834	30.685	21107523
61	XCTD-061	2022/09/11	09:07	71-43.9815N	155-11.8514W	296	3.694	30.395	21107525
62	XCTD-062	2022/09/11	09:22	71-45.9869N	155-17.5424W	199	3.898	30.526	21107520
63	XCTD-063	2022/09/11	09:36	71-47.9882N	155-22.9563W	147	3.698	30.140	21107527
64	XCTD-064	2022/09/11	10:00	71-48.9890N	155-36.8862W	116	3.447	29.840	21107570
65	XCTD-065	2022/09/11	10:24	71-49.9870N	155-50.8481W	91	3.692	30.136	21107571
66	XCTD-066	2022/09/12	23:58	73-12.2544N	155-10.3120W	3538	0.033	24.833	21107572
67	XCTD-067	2022/09/13	02:48	72-43.0081N	154-42.0283W	3070	1.026	24.785	21107574
68	XCTD-068	2022/09/13	05:12	72-18.9910N	154-22.4408W	2102	2.420	28.702	21107573
69	XCTD-069	2022/09/14	07:05	71-14.7881N	157-09.9758W	46	1.086	32.208	21107606
70	XCTD-070	2022/09/14	07:21	71-17.2812N	157-14.8786W	56	1.356	32.018	21107575
71	XCTD-071	2022/09/14	07:35	71-19.7866N	157-19.8514W	89	3.141	30.986	21107576
72	XCTD-072	2022/09/14	07:49	71-22.2864N	157-24.8364W	109	3.434	30.900	21107602
73	XCTD-073	2022/09/14	08:04	71-24.7846N	157-29.9310W	122	3.726	31.136	21107569
74	XCTD-074	2022/09/14	08:19	71-27.2867N	157-34.9639W	110	4.381	31.479	21107609
75	XCTD-075	2022/09/14	08:34	71-29.7937N	157-40.0980W	84	4.246	31.420	21107610
76	XCTD-076	2022/09/14	08:48	71-32.1867N	157-45.1377W	72	3.917	31.303	21107607
77	XCTD-077	2022/09/14	09:03	71-34.6943N	157-50.2692W	64	3.766	31.277	21107608
78	XCTD-078	2022/09/14	09:18	71-37.1976N	157-55.4319W	63	3.595	31.170	21107605
79	XCTD-079	2022/09/14	19:40	72-35.9994N	159-42.0989W	57	3.282	30.793	21107604
80	XCTD-080	2022/09/14	22:04	72-47.9832N	159-06.0267W	197	2.516	28.693	21107601
81	XCTD-081	2022/09/15	20:47	73-10.0018N	158-00.0260W	2393	2.086	26.738	21107603

(6) Data archive

These data obtained in this cruise will be submitted to the Data Management Group of JAMSTEC, and will be opened to the public via “Data Research System for Whole Cruise Information in JAMSTEC (DARWIN)” in JAMSTEC web site.

<<http://www.godac.jamstec.go.jp/darwin/e>>

3.3. Shipboard ADCP

(1) Personnel

Motoyo Itoh	JAMSTEC	-PI
Kazuho Yoshida	NME (Nippon Marine Enterprises, Ltd.)	
Satomi Ogawa	NME	
Fumine Okada	NME	
Ryo Kimura	NME	
Yoichi Inoue	MIRAI Crew	

(2) Objectives

To obtain continuous measurement data of the current profile along the ship's track.

(3) Parameters

Upper ocean current velocity: horizontal velocity (u), vertical velocity (v) and depth.

(4) Instruments and methods

Upper ocean current measurements were conducted during this cruise, using the hull-mounted Acoustic Doppler Current Profiler (ADCP) system. For most of its operation, the instrument was configured for water-tracking mode. Bottom-tracking mode, interleaved bottom-ping with water-ping, was made to get the calibration data for evaluating transducer misalignment angle in the shallow water. The system consists of following components;

1. R/V MIRAI has installed the Ocean Surveyor for vessel-mount ADCP (frequency 76.8 kHz; Teledyne RD Instruments, USA). It has a phased-array transducer with single ceramic assembly and creates 4 acoustic beams electronically. We mounted the transducer head rotated to a ship-relative angle of 45 degrees azimuth from the keel.
2. For heading source, we use ship's gyro compass (Tokyo Keiki, Japan), continuously providing heading to the ADCP system directly. Additionally, we have Inertial Navigation Unit (Phins, Ixblue, France) which provide high-precision heading, attitude information, pitch and roll. They are stored in ".N2R" data files with a time stamp.
3. Differential GNSS system (StarPack-D, Fugro, Netherlands) providing precise ship's position.
4. We used VmDas software version 1.50.19(TRDI) for data acquisition.
5. To synchronize time stamp of ping with Computer time, the clock of the logging computer is adjusted to GPS time server by using NTP (Network Time Protocol).

6. Fresh water is charged in the sea chest to prevent bio fouling at transducer face.
7. The sound speed at the transducer does affect the vertical bin mapping and vertical velocity measurement, and that is calculated from temperature, salinity (constant value; 35.0 PSU) and depth (6.5 m; transducer depth) by equation in Medwin (1975).

Data were configured for “8 m” layer intervals starting about 23m below sea surface. Data were recorded every ping as raw ensemble data (.ENR). Additionally, 15 seconds averaged data were recorded as short-term average (.STA). 300 seconds averaged data were long-term average (.LTA), respectively.

Major acquisition parameters for the measurement, Direct Command, are shown in Table 3.3-1.

Table 3.3-1: Major parameters

Bottom-Track Commands	
BP = 001	Pings per Ensemble (almost less than 1,300m depth)
Environmental Sensor Commands	
EA = 04500	Heading Alignment (1/100 deg)
ED = 00065	Transducer Depth (0 - 65535 dm)
EF = +001	Pitch/Roll Divisor/Multiplier (pos/neg) [1/99 - 99]
EH = 00000	Heading (1/100 deg)
ES = 35	Salinity (0-40 pp thousand)
EX = 00000	Coordinate Transform (Xform:Type; Tilts; 3Bm; Map)
EZ = 10200010	Sensor Source (C; D; H; P; R; S; T; U)
	C (1): Sound velocity calculates using ED, ES, ET (temp.)
	D (0): Manual ED
	H (2): External synchro
	P (0), R (0): Manual EP, ER (0 degree)
	S (0): Manual ES
	T (1): Internal transducer sensor
	U (0): Manual EU
EV = 0	Heading Bias (1/100 deg)
Timing Commands	
TE = 00:00:02.00	Time per Ensemble (hrs:min:sec.sec/100)
TP = 00:02.00	Time per Ping (min:sec.sec/100)
Water-Track Commands	
WA = 255	False Target Threshold (Max) (0-255 count)
WC = 120	Low Correlation Threshold (0-255)

WD = 111 100 000	Data Out (V; C; A; PG; St; Vsum; Vsum^2; #G; P0)
WE = 1000	Error Velocity Threshold (0-5000 mm/s)
WF = 0800	Blank After Transmit (cm)
WN = 100	Number of depth cells (1-128)
WP = 00001	Pings per Ensemble (0-16384)
WS = 800	Depth Cell Size (cm)
WV = 0390	Radial Ambiguity Velocity (cm/s)

(5) Observation log

12 Aug. 2022 - 28 Sep. 2022 (UTC)

(6) Preliminary results

Figures 3.3-1 and 3.3-2 show the current velocity of Barrow Canyon line.

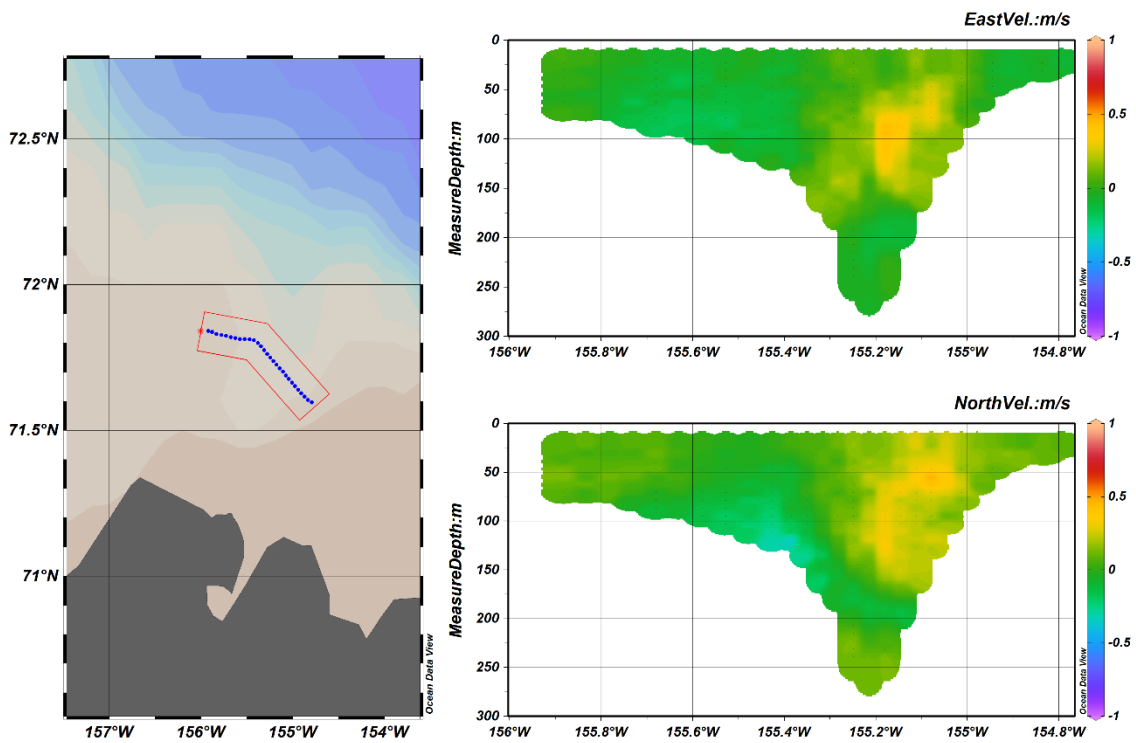


Figure 3.3-1: The current velocity of Barrow Canyon line on 29th August.

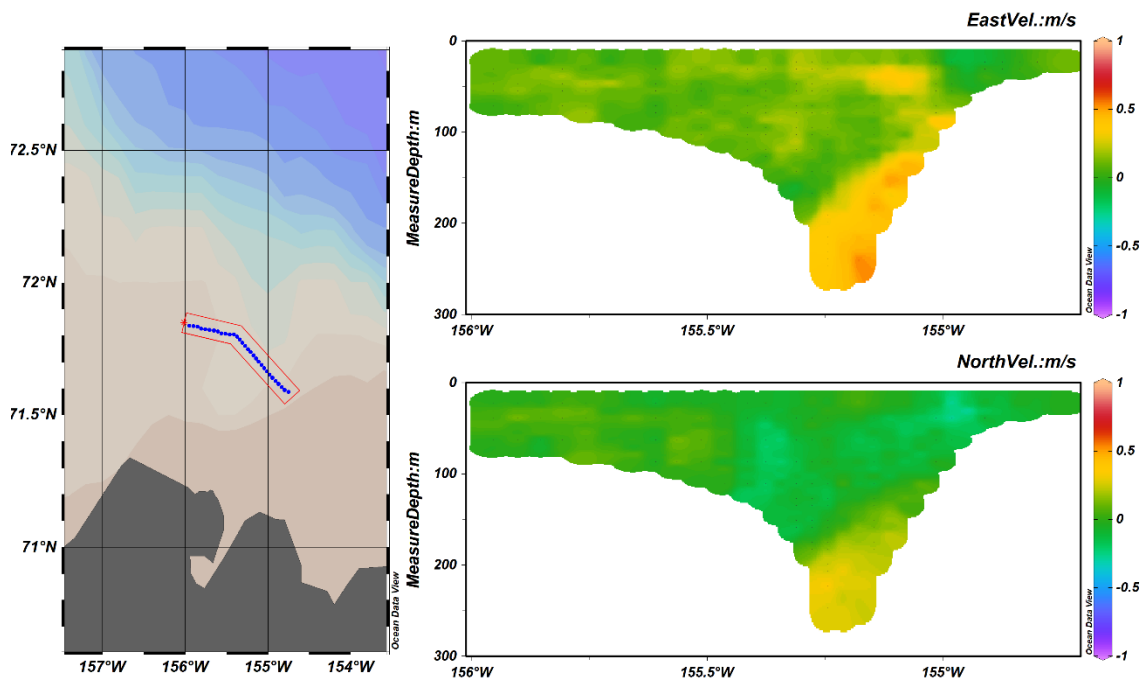


Figure 3.3-2: The current velocity of Barrow Canyon line on 11th September.

(7) Data archive

These data obtained in this cruise will be submitted to the Data Management Group of JAMSTEC, and will be opened to the public via “Data Research System for Whole Cruise Information in JAMSTEC (DARWIN)” in JAMSTEC web site.

< <http://www.godac.jamstec.go.jp/darwin/e> >

3.4. Wave Buoys

(1) Personnel

Takuji Waseda (Principal Investigator, The University of Tokyo/JAMSTEC, not on board)

Tsubasa Kodaira (The University of Tokyo, not on board)

Takehiko Nose (The University of Tokyo, not on board)

Ryosuke Uchiyama (The University of Tokyo, not on board)

Tomotaka Katsuno (The University of Tokyo)

(2) Objectives

Interaction processes between ocean waves and sea ice, which are becoming more important in the Arctic Sea, are not fully understood. To deepen their understandings, two types of drifting wave buoys were deployed near the ice edge to measure the waves in the water near the old sea ice and in the freezing season. One type of buoy is commercial product ‘Spotter’ and the other type of buoy is developed by our research group – ‘FZ’. And 3 FZ buoys were deployed in the Pacific Ocean to test the buoys. Another Spotter buoy was used for tethered measurement, aiming for calibration of other wave measurement instruments.

(3) Parameters

Spotter: The following statistical parameters are calculated and sent via satellite every hour.

Significant wave height, peak wave period, peak wave direction, peak wave directional spread, mean wave period, mean wave direction, mean wave directional spread, sea surface temperature, frequency-directional variance density spectrum, GPS location, wind speed, and wind direction.

In tethered measurement, raw timeseries of 3-dimensional GPS location is also retrieved.

FZ: The following statistical parameters were calculated and sent via satellite every hour.

Board temperature, air pressure, humidity, some configuration datasets, frequency-directional variance density spectrum, and GPS location.

(4) Instruments and methods

Spotter: Spotter buoy was manufactured by Sofar Ocean Technologies. They are battery and solar-powered and have a two-way communication function via Iridium satellite communication. 4 buoys were used. Each serial-number and objective of use are written in Table 3.4-1.

In tethered observations, the buoy was tied to a 1000-meter-long rope and released from

the stern. Then the ship slowly moved away so that the rope would become straight. Then the ship stayed at the location for 0.5~3 hours, keeping distance from the buoy.

FZ: FZ buoys are developed by our research group and their modules are manufactured by Adafruit Industries. They are battery-powered and have Iridium satellite communication. 15 buoys were used. Each serial-number and objective of use are written in Table 3.4-1.

(5) Observation log

Time and locations of wave buoy deployment are listed in Table 3.4-1. Time and locations of wave buoy tethered observation are listed in Table 3.4-2.

Table 3.4-1: Time and locations of wave buoy deployment.

Station #	Deployment time (UTC)	Location		Buoy	
		Longitude	Latitude	FZ ID	Spotter ID
pacific-1	15-08-2022 03:05	40-36.22N	149-48.01E	FZ01, FZ32	-
ice-1	02-09-2022 19:24	71-36.40N	135-11.54W	FZ28	SPOT-1730
ice-2	02-09-2022 19:55	71-32.02N	135-16.66W	FZ29	-
ice-3	02-09-2022 20:15	71-28.98N	135-20.72W	FZ30	-
ice-4	02-09-2022 20:26	71-25.96N	135-24.62W	FZ33	-
ice-5	02-09-2022 20:55	71-22.97N	135-27.55W	FZ35	-
open-1	03-09-2022 01:48	71-20.26N	135-30.73W	FZ36	SPOT-1803
open-2	03-09-2022 02:54	71-09.99N	135-45.72W	FZ37	-
open-3	03-09-2022 03:55	71-00.03N	135-58.60W	FZ38	-
open-4	03-09-2022 04:56	70-50.01N	136-11.78W	FZ39	-
open-5	03-09-2022 05:55	70-40.07N	136-24.51W	FZ40	-
open-6	03-09-2022 06:55	70-30.06N	136-37.14W	FZ41	-
open-7	03-09-2022 07:55	70-20.06N	136-49.96W	FZ02	SPOT-1732
Pacific-2	26-09-2022 02:28	40-19.89N	150-17.49E	FZ31	-

Table 3.4-2: Time and locations of tethered measurement.

Station #	Start time (UTC)	End time (UTC)	Location	
			Longitude	Latitude
cali-1	19-08-2022 22:16	19-08-2022 23:16	54-07.29N	173-46.97E
cali-2	25-09-2022 22:45	26-08-2022 02:02	40-19.71N	150-15.53E

(6) Preliminary results

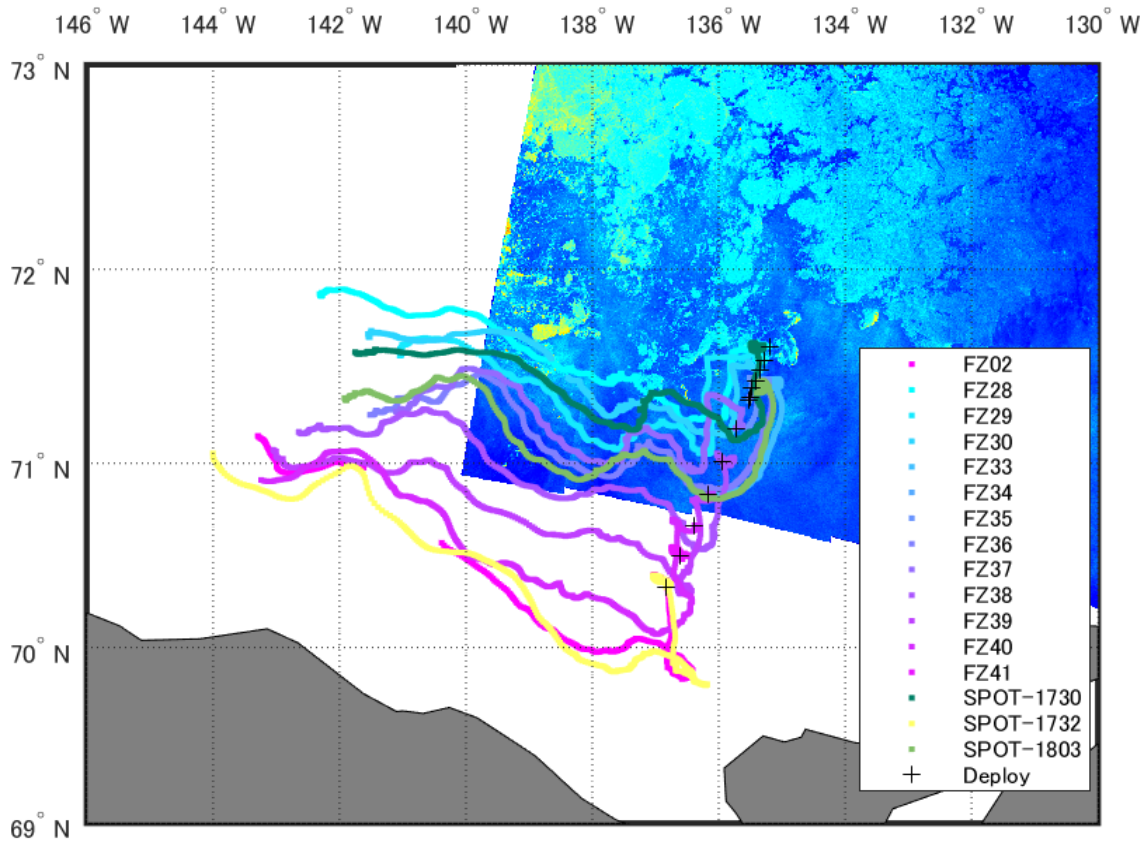


Figure 3.4-1: Map showing trajectories of deployed wave buoys in the Arctic Ocean. Black crosses indicate the locations where the buoys were deployed.

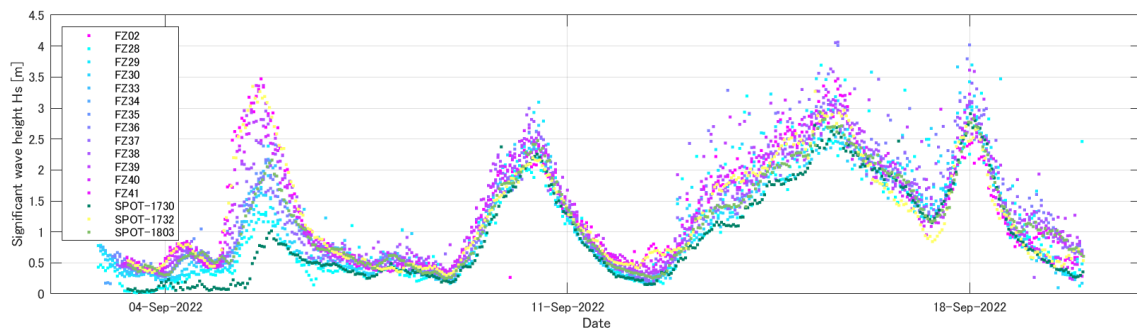


Figure 3.4-2: Timeseries of significant wave height observed by the deployed wave buoys in the Arctic Ocean.

(7) Data archive

These data obtained in this cruise will be submitted to the Data Management Group of JAMSTEC, and will be opened to the public via “Data Research System for Whole Cruise Information in JAMSTEC (DARWIN)” in JAMSTEC web site.

<<http://www.godac.jamstec.go.jp/darwin/e>>

3.5. Microwave wave gauge

(1) Personnel

Takuji Waseda (Principal Investigator, The University of Tokyo/JAMSTEC, not on board)

Tsubasa Kodaira (The University of Tokyo, not on board)

Takehiko Nose (The University of Tokyo, not on board)

Ryosuke Uchiyama (The University of Tokyo, not on board)

Tomotaka Katsuno (The University of Tokyo)

(2) Objectives

Microwave wave gauge was installed at the bow to obtain continuous and detailed wave data at the ship location.

(3) Parameters

Relative speed of the instrument and the water surface, three-component acceleration, and three-component angular velocity.

(4) Instruments and methods

Doppler wave sensor system (SJM-001), produced by Japan Radio Co. Ltd., was installed at the bow (Figure 3.5-1). It was connected to a computer via ethernet, where the data was continuously recorded.



Figure 3.5-1: Microwave wave gauge installed at the bow.

The sensor radiates microwave signal to the water and measures the Doppler shift frequency of the reflected signal. Doppler shift frequency was converted to the relative speed, and then the accelerometer and the gyro sensor data were used to correct for ship motion to obtain the absolute motion of the water surface.

The data was obtained at 10 Hz frequency, and spectral analysis for noise removal was

conducted for every 20 minutes record. Data quality was checked by using the ship heading direction, ship speed, and wind direction.

(5) Station list or Observation log

Data was continuously collected, from 11-08-2022 05:20 to 26-09-2022 07:50 (both in UTC). The data recording software failed between 21-08-2022 00:50 to 21-08-2022 23:10 by software error.

(6) Preliminary results

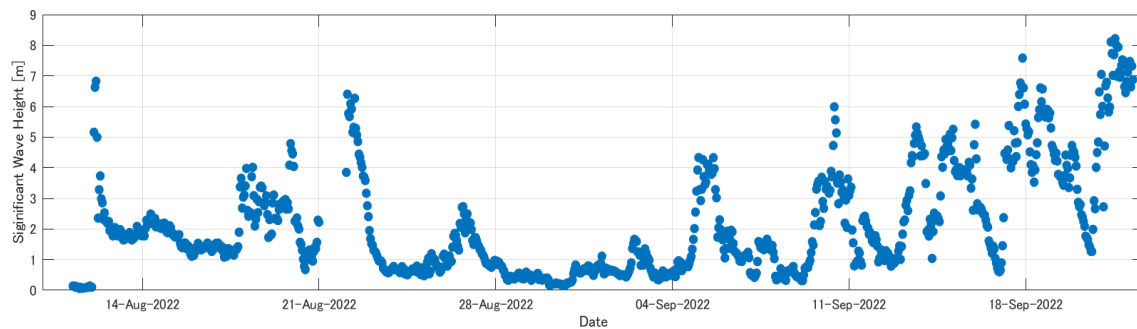


Figure 3.5-2: Time series of the significant wave height up to 20-09-2022.

(7) Data archive

These data obtained in this cruise will be submitted to the Data Management Group of JAMSTEC, and will be opened to the public via “Data Research System for Whole Cruise Information in JAMSTEC (DARWIN)” in JAMSTEC web site.

<<http://www.godac.jamstec.go.jp/darwin/e>>

3.6. Network camera

(1) Personnel

Takuji Waseda (Principal Investigator, The University of Tokyo/JAMSTEC, not on board)

Tsubasa Kodaira (The University of Tokyo, not on board)

Takehiko Nose (The University of Tokyo, not on board)

Ryosuke Uchiyama (The University of Tokyo, not on board)

Tomotaka Katsuno (The University of Tokyo)

(2) Objectives

Network camera is installed to obtain a continuous visual record of waves, sea ice, and sea splay.

(3) Parameters

Camera movie record in the WMV format.

(4) Instruments and methods

Network camera (AXIS M2026-LE Mk II) was installed and recorded the whole footage of the cruise. It was connected to recorders (AXIS S3008, 2TB) placed in the research room of the bridge deck, and the saved movies are backed up to the external HDDs. The installed camera is shown in Figure 3.6-1.



Figure 3.6-1: Installed network camera.

(5) Station list or Observation log

Network camera continuously recorded from 11-08-2022 to 26-09-2022.

(6) Preliminary results

Figure 3.6-2 shows sample images of the network camera.



Figure 3.6-2: A sample images of the network camera.

(7) Data archive

These data obtained in this cruise will be submitted to the Data Management Group of JAMSTEC, and will be opened to the public via “Data Research System for Whole Cruise Information in JAMSTEC (DARWIN)” in JAMSTEC web site.

<<http://www.godac.jamstec.go.jp/darwin/e>>

3.7. Radar

3.7.1. Ice radar

(1) Personnel

Motoyo Itoh	JAMSTEC	-PI
Tomotaka Katsuno	The University of Tokyo	
Kazuho Yoshida	NME (Nippon Marine Enterprises, Ltd.)	
Satomi Ogawa	NME	
Fumine Okada	NME	
Ryo Kimura	NME	
Yoichi Inoue	MIRAI Crew	

(2) Objectives

In the sea ice areas, marine radar provides an important tool for the detection of sea ice and icebergs. It is important to monitor the sea ice daily and produce ice forecasts to assist ship traffic and other marine operations. In order to select route optimally, ice condition prediction technology is necessary, and image information of ice sea radar is used for constructing a route selection algorithm.

(3) Parameters

Capture format: JPEG
Capture interval: 60 seconds
Resolution: 1,024 × 768 pixel
Color tone: 256 gradation

(4) Instruments and methods

R/V MIRAI is equipped with an Ice Navigation Radar, “sigma S6 Ice Navigator (Rutter Inc.)”. The ice navigation radar, the analog signal from the x-band radar is converted by a modular radar interface and displayed as a digital video image (Figure 3.7.1-1). The sea ice radar is equipped with a screen capture function and saves at arbitrary time intervals.

(5) Observation log

23 Aug. 2022 - 17 Sep. 2022

(6) Data archive

These data obtained in this cruise will be submitted to the Data Management Group of JAMSTEC, and will be opened to the public via “Data Research System for Whole Cruise Information in JAMSTEC (DARWIN)” in JAMSTEC web site.

< <http://www.godac.jamstec.go.jp/darwin/e> >

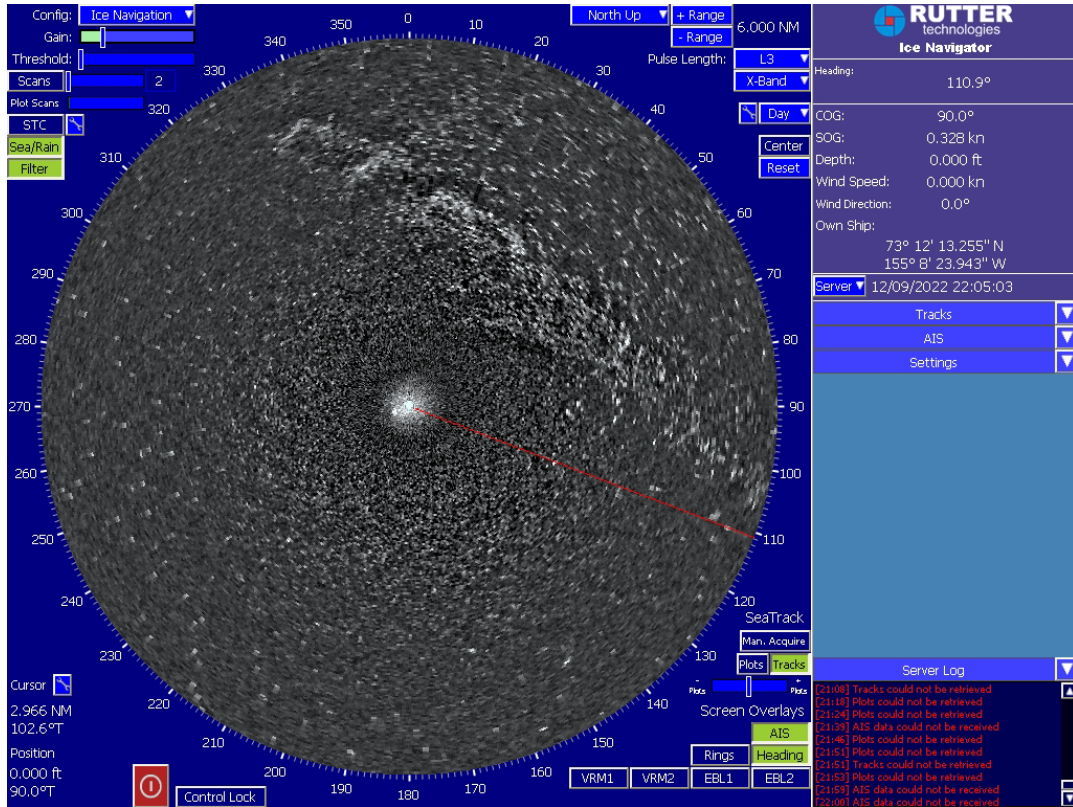


Figure 3.7.1-1: Image of sea ice from Sea ice radar

3.7.2. Wave-Ice radar

(1) Personnel

Takuji Waseda (Principal Investigator, The University of Tokyo/JAMSTEC, not on board)

Takatoshi Matsuzawa (National Maritime Research Institute, not on board)

Kazutaka Tateyama (Kitami Institute of Technology, not on board)

Tsubasa Kodaira (The University of Tokyo, not on board)

Takehiko Nose (The University of Tokyo, not on board)

Wataru Fujimoto (The University of Tokyo, not on board)

Ryosuke Uchiyama (The University of Tokyo, not on board)

Tomotaka Katsuno (The University of Tokyo)

Kazuho Yoshida (Nippon Marine Enterprises, Ltd., NME)

(2) Objectives

The objective of this observation is to collect radar images in the various sea state throughout the expedition. The imagery data can be utilized to conduct following analysis. Calibrate the significant wave height derived from SNR (Signal to Noise Ratio) of the wave-like signal in the radar image by comparing with the buoy data during the buoy deployment. (See 3.4. for the detail.) Compare the wave directional spectra derived from the radar imagery with the buoy. Observe spatial distribution of sea ice in the marginal ice zone.

(3) Parameters

Radar image record in SWP file (raw radar video).

(4) Instruments and methods

Two X-band radars were installed in the radar mast of R/V Mirai. These two radars are horizontally polarized and vertically polarized, respectively. The signal strength of the wave and sea ice from radars is recorded via the radar processing PCs (JRC) and HDD racks installed in the Research Information Center to save these datasets. The PCs has a visualization tool of radar signal image and monitors to visualize radar are also installed in the Research Information Center.

For the calibration of significant wave height derived from the wave analyzing software, the Spotter buoy (Sofar) is used, which is described in 3.4.

(5) Observation log

The radar logging system records the file during the period of entire cruise, except for when the ship is in port at Dutch Harbor and the radar transmit is turned off. In the Marginal Ice Zone (MIZ) and the high wave conditions, the radar system records for 50 minutes every hour. In the other conditions, the radar system records for 20 minutes. The detail is shown in Table 3.7.2-1.

Table 3.7.2-1: Time recording condition of wave ice radar observation.

Start time (UTC)	End time (UTC)	Recording condition	Remarks
12-08-2022 02:31	13-08-2022 00:15	Continuous recording	Stopped by the error
13-08-2022 03:50	19-08-2022 19:48	20min/1h	-
19-08-2022 22:16	19-08-2022 23:16	Continuous recording	Radar calibration
19-08-2022 23:40	21-08-2022 00:53	20min/1h	-
22-08-2022 01:24	28-08-2022 18:56	20min/1h	-
28-08-2022 20:25	28-08-2022 21:47	Continuous recording	Mooring St. BCW21
28-08-2022 22:04	30-08-2022 02:05	20min/1h	-
30-08-2022 03:40	03-09-2022 07:04	50min/1h	MIZ observation
03-09-2022 22:27	04-09-2022 02:21	20min/1h	
04-09-2022 02:21	08-09-2022 04:21	50min/1h	High wave condition
04-09-2022 02:21	09-09-2022 17:00	20min/1h	Stopped by the error
09-09-2022 20:24	12-09-2022 04:30	20min/1h	
12-09-2022 04:30	13-09-2022 02:26	50min/1h	High wave condition
13-09-2022 02:26	15-09-2022 05:26	20min/1h	
15-09-2022 05:26	15-09-2022 21:51	50min/1h	Passing MIZ
15-09-2022 21:51	17-09-2022 03:24	20min/1h	
17-09-2022 03:24	19-09-2022 03:59	50min/1h	High wave condition
19-09-2022 03:59	25-09-2022 19:51	20min/1h	
25-09-2022 19:51	26-09-2022 07:34	Continuous recording	Radar calibration
26-09-2022 07:34	28-09-2022 01:29	20min/1h	

(6) Preliminary results

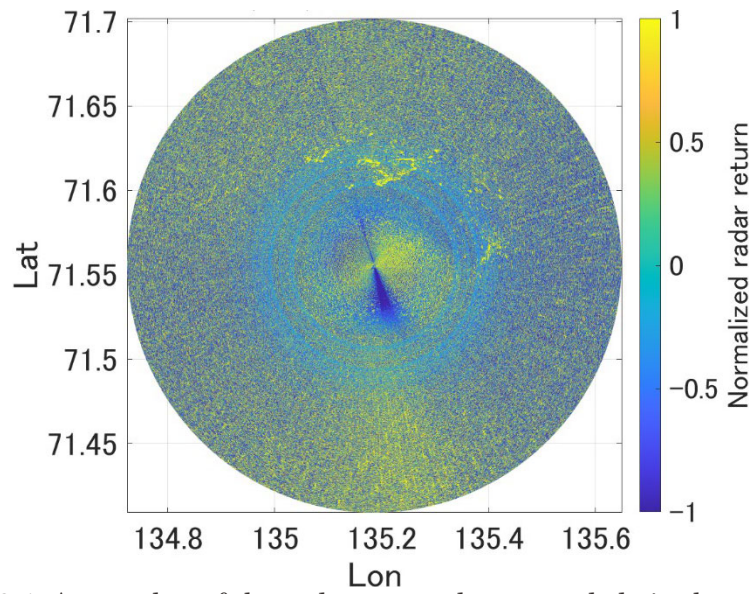


Figure 3.7.2-1: A snapshot of the radar sweep data recorded via the radar processing system on 2nd September 2022 UTC in the Marginal Ice Zone (MIZ) in Arctic Ocean.

(7) Data archive

These data obtained in this cruise will be submitted to the Data Management Group of JAMSTEC, and will be opened to the public via “Data Research System for Whole Cruise Information in JAMSTEC (DARWIN)” in JAMSTEC web site.

<<http://www.godac.jamstec.go.jp/darwin/e>>

3.8. Sea ice observation from drones

(1) Personnel

Takuji Waseda (Principal Investigator, The University of Tokyo/JAMSTEC, not on board)

Tsubasa Kodaira (The University of Tokyo, not on board)

Takehiko Nose (The University of Tokyo, not on board)

Ryosuke Uchiyama (The University of Tokyo, not on board)

Tomotaka Katsuno (The University of Tokyo)

Hiroki Ushiomura (Marine Works Japan Ltd., MWJ)

(2) Objectives

Because we collected sea ice and wave radar data at sea ice edge, its visual image to compare with is fruitful. To achieve these, we flew a flying drone equipped with a high-resolution camera near ice edge. Here, the test flight in the Pacific Ocean is also described.

(3) Parameters

4-K resolution (3840 x 2160) movie data in the mp4 format.

(4) Instruments and methods

The drone that we used was Mavic 2 Pro produced by DJI. The deck above the anti-rolling system was chosen as the take-off/landing place. Before the take-off, IMU calibration was done. After the take-off, the drone flew towards sea ice edge (or floating sea ice) to capture its close-shot movies and flew back to R/V Mirai.

(5) Observation log

Table 3.8-1 below shows the time, location, and target of the flights.

Flight #	Time (UTC)	Location	Target
1	28-08-2022 11:12-11:21	71-08.20N ,162-49.63W	Test flight
2	18-09-2022 03:53-04:09	71-36.40N, 135-11.54W (ice-1)	Ice edge

(6) Preliminary results



Figure 3.8-1: Composited image from movie obtained at flight 2.

(7) Data archive

These data obtained in this cruise will be submitted to the Data Management Group of JAMSTEC, and will be opened to the public via “Data Research System for Whole Cruise Information in JAMSTEC (DARWIN)” in JAMSTEC web site.

<<http://www.godac.jamstec.go.jp/darwin/e>>

3.9. Moorings

Oceanographic moorings continuously measure oceanographic parameters (temperature, salinity, currents, oxygen, chlorophyll, pH, ice thickness) through the year. Three physical oceanographic moorings (BCE-21, BCC-21, BCW-21) in the Barrow Canyon and one sediment trap mooring (NBC-21t) in the northwest of Barrow Canyon are recovered. Three physical oceanographic moorings (BCE-22, BCC-22, BCW-22) are re-deployed in the Barrow Canyon and one sediment trap mooring (NBC-22t) is deployed in the northwest of Barrow Canyon.

3.9.1. Barrow Canyon Moorings

(1) Personnel

Motoyo Itoh (JAMSTEC) Principal Investigator

Hiroki Ushiromura (Marine Works Japan Ltd., MWJ)

as the leader of technical team for mooring operation of MWJ
(Sagishima, K)

Kazuho Yoshida (Nippon Marine Enterprises, Ltd.; NME)

as the leader for SSBL acoustic survey team of NME
(Ogawa, S., Okada, F, and Kimura, R.)

Jonaotaro Onodera (JAMSTEC)

Michiyo Yamamoto-Kawai (Tokyo University of Marine Science and Technology)

Tomotaka Katsuno (The University of Tokyo)

Shigeto Nishino* (JAMSTEC)

Eiji Watanabe* (JAMSTEC)

Takuji Waseda* (The University of Tokyo/JAMSTEC)

Tsubasa Kodaira* (The University of Tokyo)

*: onshore members

(2) Objectives

The objective of mooring measurements in the Barrow Canyon is to monitor the variations of volume, heat and fresh water fluxes of Pacific-origin water through the Barrow Canyon. Barrow Canyon, in the northeast Chukchi Sea, is a major conduit through which the Pacific water enters the Arctic basin. JAMSTEC has conducted subsurface oceanographic mooring observations in the mouth of the Barrow Canyon since 2000.

We recovered three moorings (BCE-21, BCC-21, BCW-21) and re-deployed three similar configuration moorings (BCE-22, BCC-22, BCW-22) in the Barrow Canyon.

(3) Parameters

-Oceanic velocities

-Pressure, Temperature and Conductivity

- Dissolved oxygen
- Chlorophyll-a and turbidity
- Wave height
- Water sampling

(4) Instruments and methods

1) CTD, CT, T, P sensors

- SBE37-SM (Sea-Bird Electronics Inc.)
- A7CT-USB (JFE Advantech)
- DEFI-T (JFE Advantech)
- DEFI-D (JFE Advantech)
- DEFI-CT (JFE Advantech)

2) Current meters

- Workhorse ADCP 300 kHz Sentinel (Teledyne RD Instruments, Inc.)
- Aquadopp Current Meter 2MHz (NORTEK AS)

3) Dissolved oxygen sensor

- AROW-USB (JFE Advantech)

4) Chlorophyll-a and turbidity sensor

- ACLW-USB (JFE Advantech)
- MFL50W-USB (JFE Advantech)

5) Acoustic transponder

- XT-6000, XT6001 (Teledyne Benthos, Inc.)

6) Acoustic releaser

- Model-L, LGC (Nichiyu Giken Kogyo Co., LTD)
- 8242XS (ORE offshore /EdgeTech)
- 865-A (Teledyne Benthos, Inc.)

7) Water sampler

- RAS500 (McLANE)

8) Nitrate sensor

- SUNA (Sea-Bird Electronics Inc.)

9) Wave height and current meter

- Signature500 (NORTEK AS)

(5) Station list

Table 3.9.1-1: Moorings recovered by MR22-06C

Moorings Name	Recovered Time (UTC)	Latitude	Longitude
BCE-21	2022/08/28	71-40.3778°N	154-59.9817°W
BCC-21	2022/08/28	71-44.0519°N	155-09.7849°W
BCW-21	2022/08/29	71-47.7727°N	155-20.7602°W

Table 3.9.1-2: Moorings deployed by MR22-06C

Moorings Name	Deployed Time (UTC)	Latitude	Longitude	Depth (m)
BCE-22	2022/08/30	71-40.3849°N	154-59.9879°W	108
BCC-22	2022/08/29	71-44.0667°N	155-09.8395°W	290
BCW-22	2022/08/29	71-47.7807°N	155-20.8119°W	169

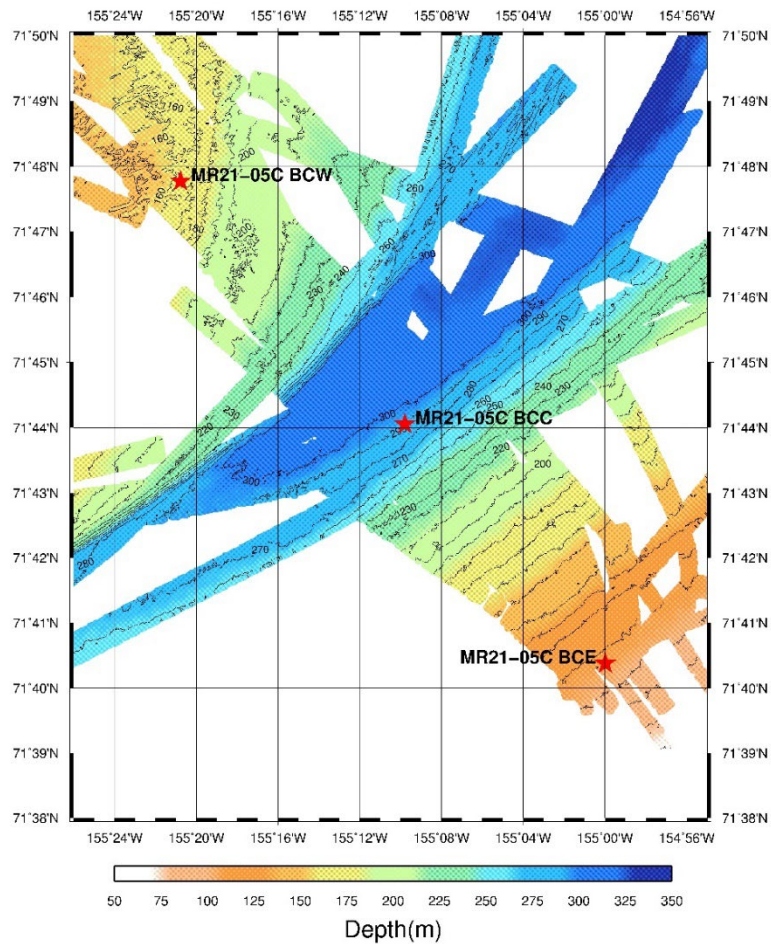


Figure 3.9.1-1: Positions of the moorings (BCE, BCC and BCW).

(7) Data archive

These mooring data will be opened to the public via a web site below.

<http://www.jamstec.go.jp/arctic/data_archive/mooring/mooring_index.html>

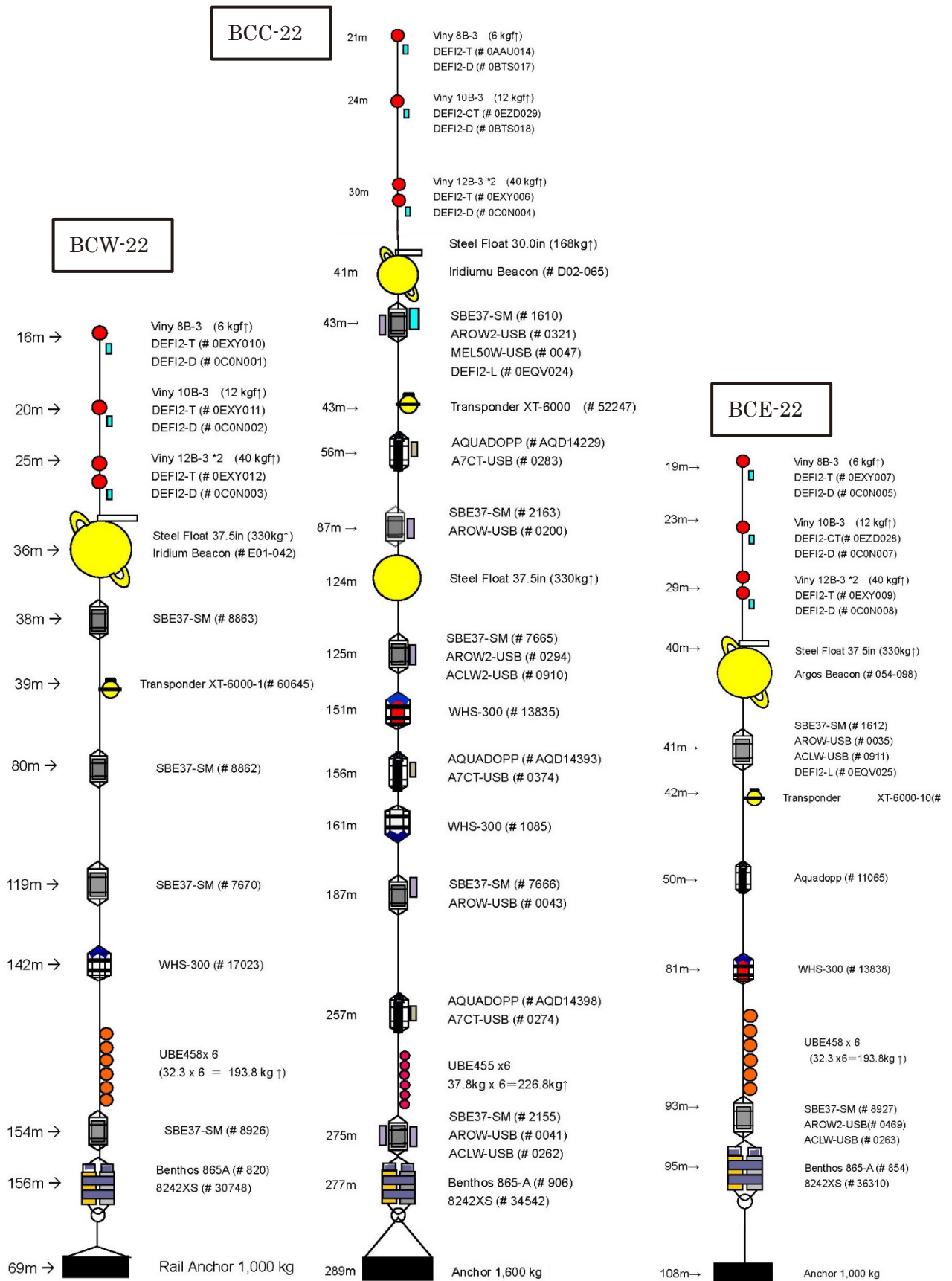


Figure 3.9.1-2: Mooring diagrams.

3.9.2. RAS and SUNA

(1) Personnel

Michiyo Yamamoto-Kawai (Tokyo University of Marine Science and Technology)

-Principal Investigator

Haruka Tsujimoto (Tokyo University of Marine Science and Technology)

(2) Objectives

To observe seasonal changes in chemical properties of Pacific-origin water flowing from the Chukchi Sea to the Canada Basin, an automated water sampler (RAS, McLane Inc.) and a nitrate sensor (SUNA-vs, Sea-Bird Electronics Inc.) were installed on the BCE mooring system at 43 m depth, deployed on 11 September 2021, and recovered on 30 August 2022.

(3) Instruments and methods

The RAS was set to collect 48 of 450 mL seawater samples at 8 days intervals (Table 3.9.2-1). 100 μ L of saturated HgCl₂ was added to each sample bag before the deployment. Sampling tubes between the multi-port valve and sample bags were filled with water made of MQ with NaCO₃ and NaCl to have Dissolved Inorganic Carbon (DIC) and Total Alkalinity (TA) concentrations of \sim 2000 μ M and salinity of \sim 40. This mixture was sub-sampled for later analysis of salinity, DIC, TA and $\delta^{18}\text{O}$ for correction of the tube-water influence on samples.

One sample bag (#11) was empty, and two bags (#14 and #22) contained small volume of sample (\sim 200 mL). Last four bags (#45, 46, 47, 48) were also empty because they were scheduled to collect samples later than the recovery date.

Samples taken by the RAS were analyzed for DIC and nutrients onboard. Remaining samples were transferred into glass bottles for analysis of $\delta^{18}\text{O}$, TA, and salinity on land. List of samples are summarized in Table 3.9.2-2.

SUNA was mounted on the upper frame of the RAS. Before the deployment and after the recovery, the sensor was calibrated using MQ (for FW calibration) and RMNS of KANSO.

Table 3.9.2-1. RAS setting

Instrument	RAS	SUNA
Model No.	RAS-3-48-500	SUNA-v2
Serial No.	ML12905-01	SUNA-06
Sampling start date & time	12 Sept 2021 18:00:00 (UTC)	11 Sept 2021 3:00:00 (UTC)
Sampling schedule	Every 8 days	Every 3 hours
Other information	No filtering for samples	light frame 120 sec, wiper ON

Table 3.9.2-2 List of RAS subsamples

	DIC	Nutrients	TA/ $\delta^{18}\text{O}$ /Salinity		DIC	Nutrients	TA/ $\delta^{18}\text{O}$ /Salinity
#1	○	○	○	#25	○	○	○
#2	○	○	○	#26	○	○	○
#3	○	○	○	#27	○	○	○
#4	○	○	○	#28	○	○	○
#5	○	○	○	#29	○	○	○
#6	○	○	○	#30	○	○	○
#7	○	○	○	#31	○	○	○
#8	○	○	○	#32	○	○	○
#9	○	○	○	#33	○	○	○
#10	○	○	○	#34	○	○	○
#11	—	—	—	#35	○	○	○
#12	○	○	○	#36	○	○	○
#13	○	○	○	#37	○	○	○
#14	—	○	$\delta^{18}\text{O}$ only	#38	○	○	○
#15	○	○	○	#39	○	○	○
#16	○	○	○	#40	○	○	○
#17	○	○	○	#41	○	○	○
#18	○	○	○	#42	○	○	○
#19	○	○	○	#43	○	○	○
#20	○	○	○	#44	○	○	○
#21	○	○	○	#45	—	—	—
#22	—	○	$\delta^{18}\text{O}$ only	#46	—	—	—
#23	○	○	○	#47	—	—	—
#24	○	○	○	#48	—	—	—

(4) Data archive

These data obtained in this cruise will be submitted to the Data Management Group of JAMSTEC, and will be opened to the public via “Data Research System for Whole Cruise Information in JAMSTEC (DARWIN)” in JAMSTEC web site.

<<http://www.godac.jamstec.go.jp/darwin/e>>

3.9.3. Sea ice profile and wave height

(1) Personnel

Takuji Waseda (Principal Investigator, The University of Tokyo/JAMSTEC, not on board)

Tsubasa Kodaira (The University of Tokyo, not on board)

Takehiko Nose (The University of Tokyo, not on board)

Ryosuke Uchiyama (The University of Tokyo, not on board)

Tomotaka Katsuno (The University of Tokyo)

(2) Objectives

Sea ice and wave phenomenon in the Arctic Ocean are not known much. To clarify the fact, the upward ADCP was added to the mooring system. And the top depth beam of ADCP can reach and the flow speed on the sea surface were measured.

(3) Parameters

Water flow direction and speed from the sea surface to the mooring depth (35~40m), and pressure, temperature, roll, pitch, and yaw of ADCP at the mooring depth.

(4) Instruments and methods

The upward Acoustic Doppler Current Profiler (ADCP) is moored on the top of the mooring system on BCW21. The ADCP (Signature 500) is manufactured by the Nortek AS, and additional battery were installed to the frame with floats (Figure 3.9.3-1).

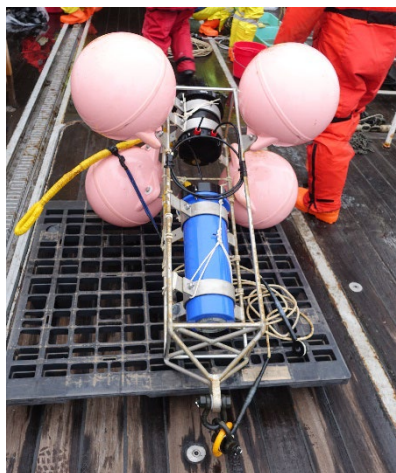


Figure 3.9.3-1: Recovered ADCP on BCW21

(5) Station list

Described in 3.9.1.

(6) Data archive

These data obtained in this cruise will be submitted to the Data Management Group of JAMSTEC, and will be opened to the public via “Data Research System for Whole Cruise Information in JAMSTEC (DARWIN)” in JAMSTEC web site.

<<http://www.godac.jamstec.go.jp/darwin/e>>

3.9.4. Sediment trap

(1) Personnel

Jonaotaro Onodera	JAMSTEC	- Principal Investigator
Motoyo Itoh	JAMSTEC	
Yuichiro Tanaka*	AIST	
Atsushi Suzuki*	AIST	
Katsunori Kimoto*	JAMSTEC	
Eiji Watanabe*	JAMSTEC	
Takuhei Shiozaki*	The University of Tokyo, AORI	
Hiroki Ushiromura	as the leader of technical team for mooring operation of MWJ (Sagishima, K., and Arii, Y.*)	
Kazuho Yoshida	as the leader for SSBL acoustic survey team of NME (Ogawa, S., Kimura, R., and Okada, F.).	

*: onshore members

(2) Objectives

- To understand lateral transportation of shelf materials to basin with physical oceanographic condition from northern off Barrow Canyon to the Chukchi Borderland.
- To monitor hydrographic condition regarding to ocean acidification and warming.
- To investigate biodiversity in the study region.

(3) Parameters

Settling particles, water temperature, salinity, current, ice thickness, dissolved oxygen, CO₂, turbidity, chlorophyll-a, PAR, pH

(4) Instruments and methods

<Instruments>

All instruments on recovered and deployed moorings are listed in Tables 3.9.4-1 and -2. The designs of recovered and deployed mooring are shown in Figures 3.9.4-1, -2, and -3. The all required procedure for export/reimport control at the Shimizu custom was performed by the Suzuyo, Co. Ltd.

<Methods>

Acoustic communication of releasers to be deployed were examined in the Bering Sea (54°03'N 173°46'W, 3638 m water depth) on Aug. 19, 2022. The releasers were mounted on CTD frame, and it was tested at 300 m depth using ship's acoustic

ranging system. The Benthos 865A releaser was successful on the test. The Nichiyu LGC releaser responded to call, but did not for ranging probably due to ship's noise.

For the deployment sensors, log file or photograph of configuration process were taken. Sample cups of sediment trap were filled with filtered sea water taken at 1000 m depth in the southwestern Canada Basin in previous Mirai cruise. The water contains formalin (4v/v%) and Sodium tetraborate decahydrate for pH adjustment (pH ~8.2). The time-series sediment trap was scheduled with 14-days interval from 00:00 of September 10, 2022 to 00:00 of May 20, 2023 (UTC), and then 13-days interval from May 20 to 00:00 of September 1st, 2023. The battery of acoustic releasers is for two-years deployment.

Safety briefing by chief officer was conducted for all related staffs working on stern deck, just before the start of mooring operations. All staffs working on stern deck worn floating jackets, hard hats, safety shoes, and gloves. The "A" frame and capstan winch was applied for the mooring operation on the deck. Just in case, dragging tools, which are composed of hooks, weights, chains, shackles, TRITON wires and ropes, were loaded for mooring recovery.

Recovery operation for NBC21t started from acoustic communication between ship's transducer and the transducer of acoustic releaser. The deployed releaser of Benthos 865A was enabled, and release command was transmitted from 493 m away (horizontal distance). The release was successful, and by the ship's zodiac boat, we went to the drifting top buoy, and connected a rope from stern to the top buoy. The rope was spooled on deck, and the mooring equipment was recovered on deck from the top buoy to acoustic releasers (Table 3.9.4-1).

For deployment, all serial numbers of deploying equipment and connection of all parts were checked just before the deployment and/or during the deployment operation. Mooring deployment started from the throw-in of top buoy into water (Table 3.9.4-2). The ship went forward with slow speed (~1.0knot). Before the dropping sinker, the slow towing of mooring continued until the ship reaches at the planned target position of the mooring. Deepening and vanish of top buoy from sea surface was confirmed, and then reaching of sinker at sea floor was confirmed by ship's acoustic ranging system. The mooring position was determined using SSBL and transducer of Benthos 865A releaser. The water depth was determined by the depth value of the position in MBES (Multi Beam Echo Sounder) topography map (Figure 3.9.4-4). The position, water depth, top depth, and recovery plan (season and ship) of the NBC22t will be noticed to AOOS (Alaska Ocean Observing System) and related persons in the world.

The water sampled at 1000m depth of CTD/R Station 25 is to be used for treatment

of recovered samples and waters for next sediment-trap deployment in 2023.

(5) Tables of sediment trap mooring operation.

Table 3.9.4-1: Recovery of NBC21t on September 8, 2022.

NBC21t	
Coordinates: 72°28.1770'N 155°25.3433'W	
Water depth: 1989 m	
Weather Condition: dense fog	15:00
Air Temp. -0.3°C, Atmospheric Press. 1020.4hPa,	(UTC)
Wind Direction 116°, Wind Speed 1.8 m/s, SST 3.3°C, Wave 0.6 m	
Enable of releaser (Benthos 865A S/N 537)	15:01
(703m away from NBC21t position, relative direction 16.7°)	
Transmission of release command	17:24
(493m away from NBC21t)	
Finding of top buoy at sea surface from bridge	17:25
Connection of ship's rope to top buoy by clue on zodiac	17:37

Recovered Mooring Instruments

Item#	Type	Model	Serial Number	Time
1	Float	MN-IP123	ASL-SFFC-001	17:55
	Ice profiler	IPS-5	51113	
	CT	A7CT2-USB	0310	
	DO	ARO-USB	130	
	Multi-Exciter	MFL50W-USB	20	
	PAR	DEFI2-L	0BKB0023	
	Iridium	iBCN-7	J09-008	
	Beacon	(MMI-513-32000)		
2	LED Flasher	MMF-523-12000	J09-007	18:03
	Transponder	XT6001-17"	47196	
3	Floats	Benthos 17" x4	-	18:04
	CT	SBE37SM	6934	
4	Float	30inch steel	-	18:06
5	CT	SBE37SM	8858	18:14
6	ADCP	WHS-300	15385	18:14
	CT	SBE37SM	8860	
	DO	ARO-USB	135	
7	pH	SPS-14	40306167001	18:18
	Floats	Benthos 17" x5	-	
8	Current, DO, CO2	Seaguard II	1958	18:23
10	Sediment Trap	SMD26S-6000	26S032	18:29
	CT	A7CT-USB	626	
11	Floats	Benthos 17" x5	-	18:47
12	Sediment Trap	SMD26S-6000	26S033	18:57
13	Floats	Benthos 17" x5	-	19:23
	Releaser	Benthos 865A	537	
14	Releaser	Nichiyu LGC	0021	19:23
	End of recovery operation at 72°27.8385'N 155°27.4212'W			

Table 3.9.4-2: Deployment of NBC22t on September 8, 2022.

NBC22t				
Planned Coordinates: 72°28.32' N 155°24.51' W				
Water Depth: 1995 m				
Start of mooring deployment				
(72° 29.4627'N 155° 19.0910'W, 2140 m water depth)				22:43 (UTC)
Weather Condition: fog to cloudy				
Air temp. -0.3°C, Atmospheric pressure 1019.0hPa, Wind direction 83°, Wind speed 4.3 m/s, SST 1.9°C, Current direction 234.7°, Current speed 0.6 knot				
Time of instruments and anchor in water				
Item#	Type	Model	Serial Number	Time
1	Float		ASL-SFFC-01	
	Ice profiler	IPS-5	51123	
	CT	A7CT2-USB	0274	
	DO	ARO-USB	131	
	Multi-Exciter	MFL50W-USB	19	22:46
	PAR	DEFI2-L	0F5I016	
	Iridium Beacon	iBCN-7 (MMI-513-32000)	H01-001	
	LED Flasher	MMF-523-12000	J01-001	
2	Transponder	XT6001	75683	
	Floats	Benthos 17" x4	-	22:48
3	CT	SBE37SM	13677	22:48
4	Float	Steel 30"	-	22:49
5	CT	SBE37SM	13678	22:50
6	ADCP	WH-300 (w/ BT)	1563	22:52
7	CT	SBE37SM	15456	
	DO	ARO-USB	136	22:52
	pH	SPS-14Ti +Battery Unit	390262005	
8	Float	Benthos 17" x5	-	23:00
9	Logger	SeaGuard I	1889	
	└ ADCP	DCS4520IW		
	└ Pressure	4117E		23:04
	└ DO	4330IW		
	└ CO2	CO2		
10	Sediment trap	SMD26S-6000	26S034	
	CT	A7CT-USB	613	
	Turbidity	ACLW-	0261	23:10
	Pressure	DEFI2-D	0C0N009	
11	ADCP	Aquadopp DW	15193	23:11
12	Floats	Benthos 17" x5	-	23:31
13	Sediment trap	SMD26S-6000	26S035	23:42
14	Floats	Benthos 17" x5	-	00:14
15	Releaser	Benthos 865A	537	
	Releaser	Nichiyu LGC	0021	00:14

16	Anchor (72° 28.259'N 155° 24.824'W, 1995 m)	1000kg in air	-	00:32
Confirmation of anchor arrival at sea floor				00:49
Releaser ranging (Item#15)				
	Depth: 1948 m, 1950 m, 1951 m (865A)		537	01:10
	Communication with Nichiyu LGC (no ranging)		0021	01:14
SSBL transponder survey for Benthos 865A				
	Position	72°28.3689'N 155°24.1670'W		
	Water Depth	2004 m (SeaBeam depth of the position)		
	Estimated Top-buoy Depth	50 m		

(6) Preliminary Results

There was no operational trouble during recovery and deployment of the sediment trap moorings. All of sediment trap samples were successfully retrieved (Figure 3.9.4-5). Data from the moored sensors were successfully recovered except for pH sensor. The water depth at NBC22t is 2,004 m, which is ~10m deeper than the planned depth. Estimated top-buoy depth of NBC22t is ~50 m.

(7) Data archive

These data obtained in this cruise will be submitted to the Data Management Group of JAMSTEC, and will be opened to the public via “Data Research System for Whole Cruise Information in JAMSTEC (DARWIN)” in JAMSTEC web site.

<<http://www.godac.jamstec.go.jp/darwin/e>> The calibrated sensor data will also be submitted to the Arctic Data-archive System (ADS). <<https://ads.nipr.ac.jp/>>

NBC21t (Recovery)
 72°28.1770'N 155°25.3433'W

NBC22t (Deployment)
 72°28.3689'N 155°24.1670'W

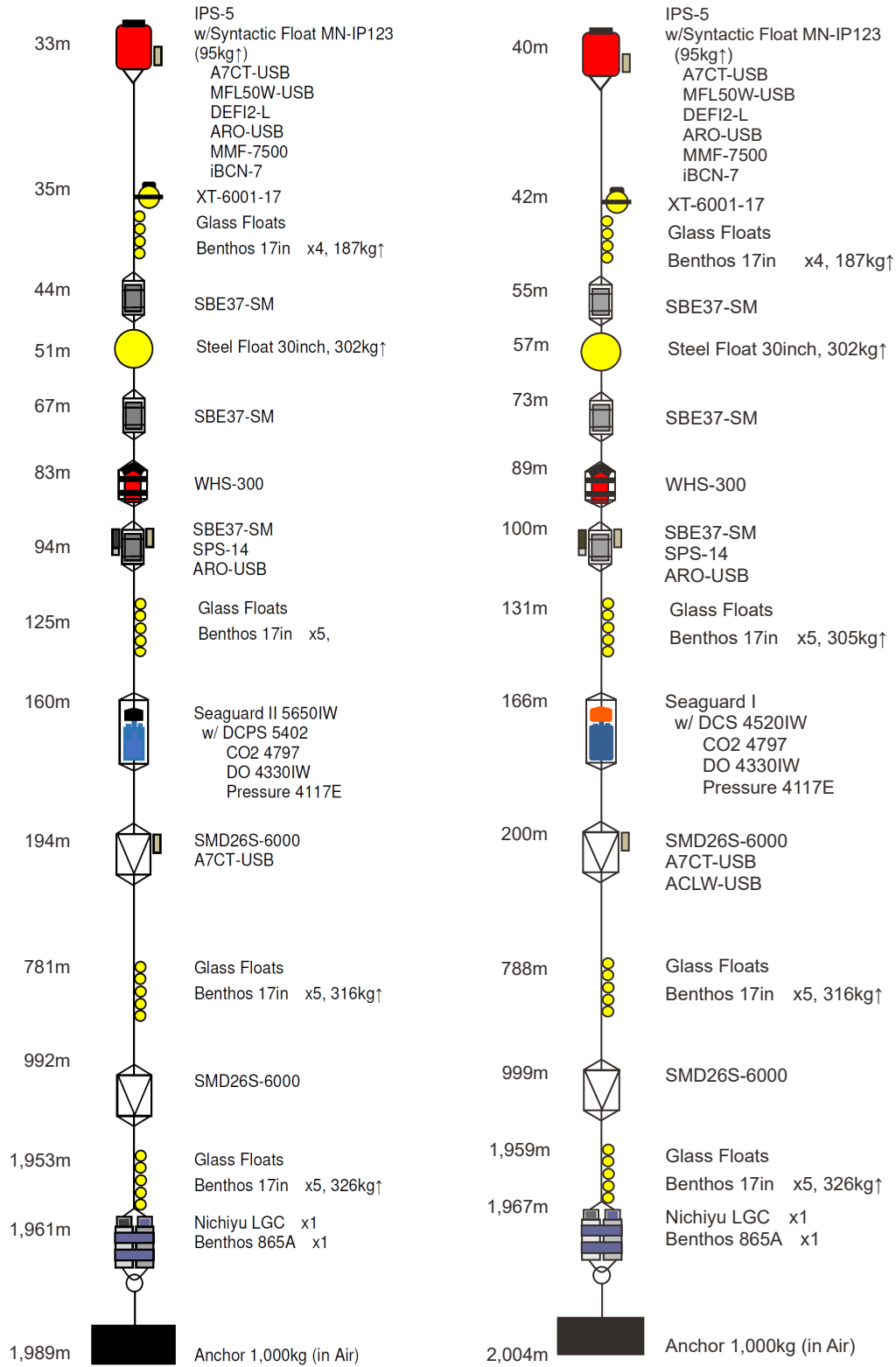


Figure 3.9.4-1. The summary of mooring design for NBC21t and NBC22t.

Recovery

Station NBC21t

72°28.1770'N 155°25.3433'W
1989 m water depth, transponder at 35 m

Aug. 15, 2022



Figure 3.9.4-2: Diagram of the sediment trap mooring NBC21t for recovery.

Deployment

Station NBC22t

72°28.3689'N 155°24.1670'W
2004 m water depth, top 50 m, transponder at 52 m

Sep. 19, 2022
(Final Version)

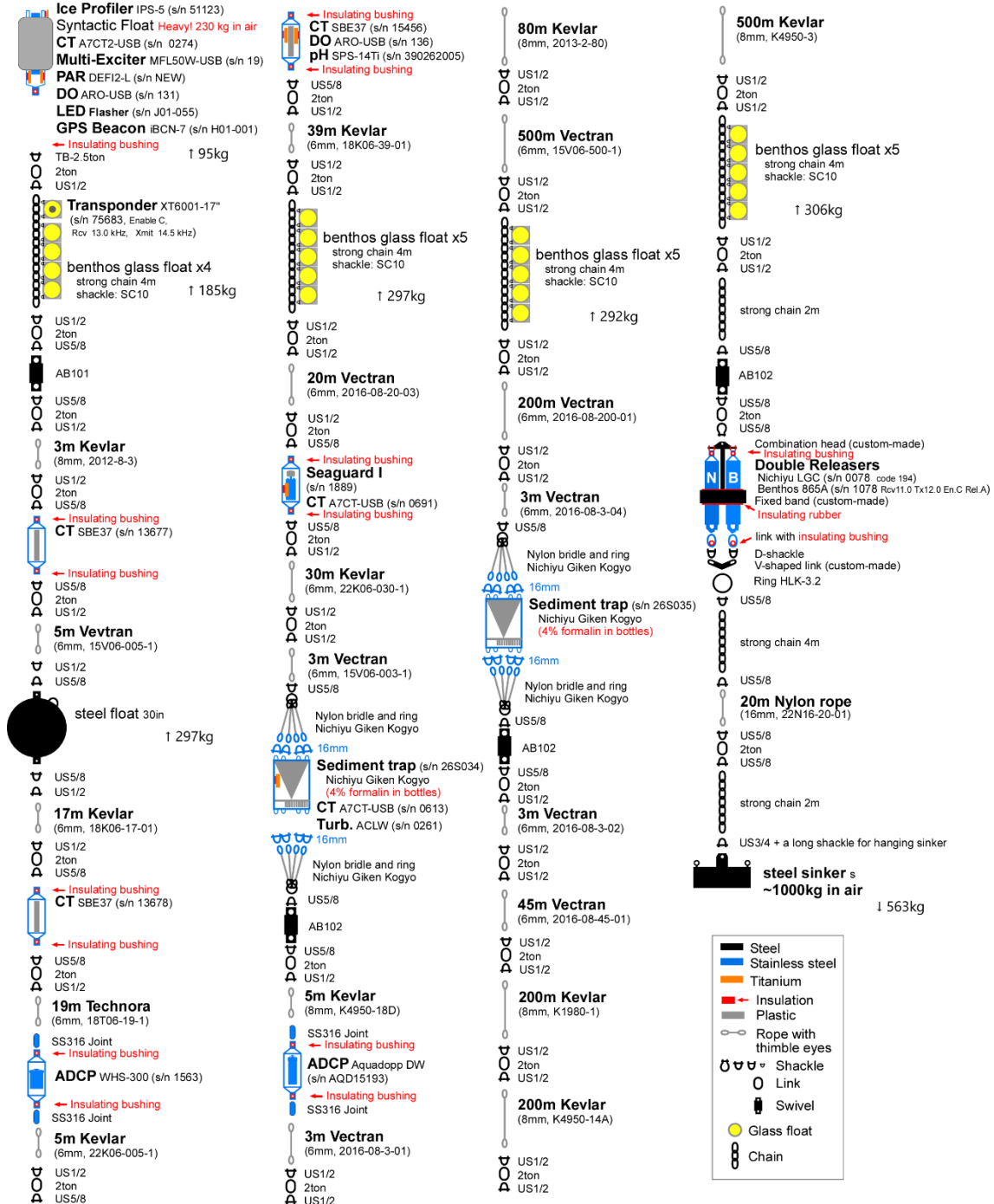


Figure 3.9.4-3: Diagram of the sediment trap mooring NBC22t for deployment.

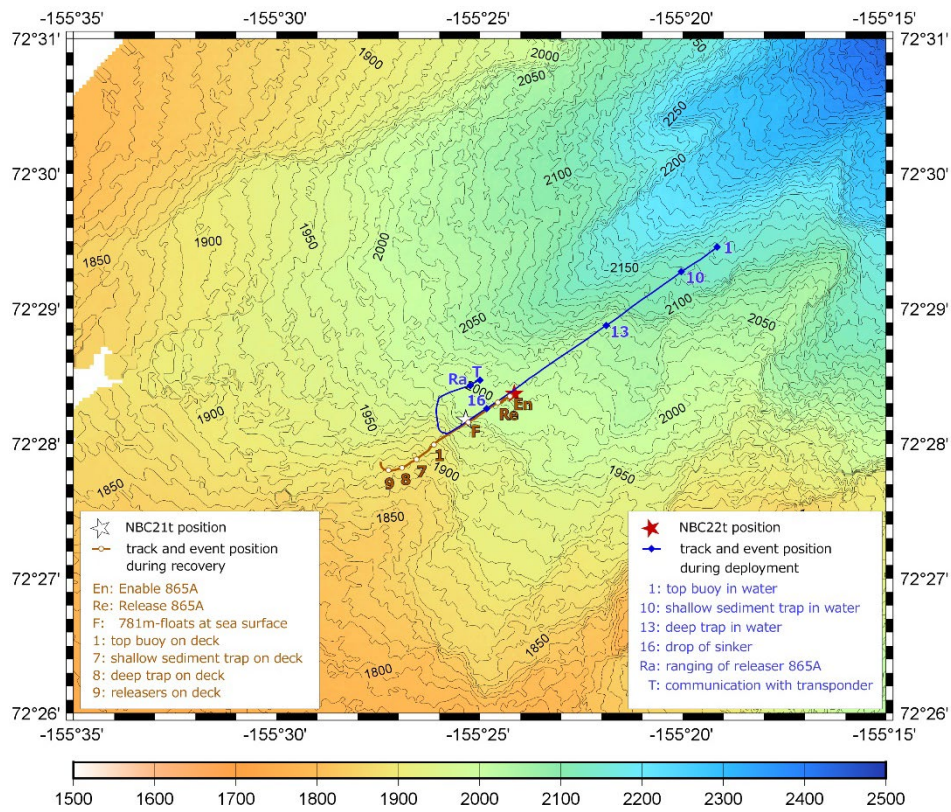


Figure 3.9.4-4: The MBES topography map showing the mooring positions of NBC21t and 22t (star symbol in white and red, respectively) with vessel's track during the turnaround operation. The numbers along ship's track represent the event position of item# in Table 3.9.4-1 and -2.

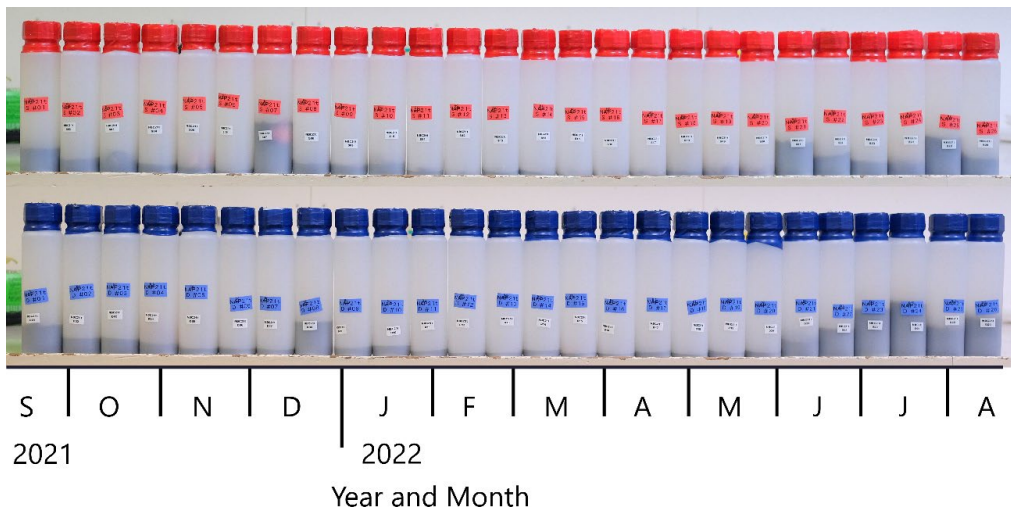


Figure 3.9.4-5. The time-series sample bottles of recovered sediment trap NBC21t. The upper and lower bottles are from shallow (moored at ~200m) and deep (~1000m) sediment traps, respectively.

3. 10. Salinity

(1) Personnel

Shigeto Nishino	(JAMSTEC) - Principal Investigator,	not on board
Motoyo Itoh	(JAMSTEC)	
Rei Ito	(MWJ) -Operation leader	
Katsunori Sagishima	(MWJ)	
Nagisa Fujiki	(MWJ)	
Hiroki Ushiomura	(MWJ)	

(2) Objective

To calibrate the measurements of salinity collected from CTD casts, and to provide the data for bucket sampling and clean CTD casts.

(3) Parameters

Salinity

(4) Instruments and methods

a. Sampling

Seawater samples were collected with 12 Liter water sampling bottles and 12 Liter water clean sampling bottles. A 250ml brown glass bottle with a screw cap was used for collecting the sample water for salinity measurements. Each bottle was rinsed 3 times with the sample water, and was filled with sample water to the bottle shoulder. Each bottle was stored for more than 24 hours in the laboratory before the salinity measurements.

The type and number of samples taken are shown as follows ;

Table 3.10-1. Type and number of samples

Type of Samples	Number of Samples
Samples for CTD	542
Samples for clean bottle	30
Total	572

b. Instruments and Method

The salinity analysis was carried out on R/V MIRAI during the cruise of MR22-06C using the salinometer (Model 8400B “AUTOSAL” ; Guildline Instruments Ltd.: S/N 62556) with an additional peristaltic-type intake pump (Ocean Scientific International, Ltd.). A pair of precision digital thermometers (1502A; FLUKE: S/N B78466 and B81549) were used for monitoring the ambient temperature and the bath temperature of the salinometer.

The specifications of the AUTOSAL salinometer and thermometer are shown as follows ;

Salinometer (Model 8400B “AUTOSAL” ; Guildline Instruments Ltd.)

Measurement Range : 0.005 to 42 (PSU)

Accuracy	: Better than ± 0.002 (PSU) over 24 hours
Maximum Resolution	: Better than ± 0.0002 (PSU) at 35 (PSU)
Thermometer (1502A: FLUKE)	
Measurement Range	: 16 to 30 deg C (Full accuracy)
Resolution	: 0.001 deg C
Accuracy	: 0.006 deg C (@ 0 deg C)

The measurement system was almost the same as Aoyama *et al.* (2002). The salinometer was operated in the air-conditioned ship's laboratory at a bath temperature of 24 deg C. The ambient temperature varied from approximately 22 deg C to 24 deg C, while the bath temperature was very stable and varied within ± 0.002 deg C on rare occasion. The measurement for each sample was done with a double conductivity ratio and defined as the median of 34 readings of the salinometer. (Acquisition of the 34 readings took about 11 seconds when the function dial was turned to the 'read' setting) Data were taken after rinsed 5 times with the sample water. The double conductivity ratio of sample was calculated from average value of two measurements. And it was used to calculate the bottle salinity with the algorithm for the practical salinity scale, 1978 (UNESCO, 1981). In the case of the difference between the double conductivity ratio of these two measurements being greater than or equal to 0.00003, continue to be measured up to 3 times. The difference between the double conductivity ratio of these two measurements being smaller than 0.00002 were selected. The measurement was conducted for about 8 hours per day and the cell was cleaned with neutral detergent after the measurement of the day.

(5) Station list

Table 3.10-2 shows the sampling locations for the salinity analysis in this cruise.

Table 3.10-2 List of sampling locations of the salinity samples collected from CTD

Stnnbr	Castno	Date(UTC) (mmddyy)	Time(UTC)		BottomPosition		Depth (m)
			Start	End	Latitude	Longitude	
001	1	082422	17:59	18:18	65-30.34N	168-44.99W	54.8
002	1	082422	22:06	22:26	66-00.12N	168-45.12W	52.9
003	1	082522	01:45	02:03	66-30.21N	168-44.88W	54.5
004	1	082522	04:41	05:01	67-00.16N	168-44.20W	44.9
005	1	082522	17:07	17:25	67-30.00N	168-44.91W	49.8
006	1	082622	02:52	03:09	68-00.22N	168-44.89W	59.1
007	1	082622	06:18	06:36	68-30.11N	168-45.33W	53.4
008	1	082622	17:25	17:42	69-00.20N	168-43.22W	53.0
009	1	082622	20:29	20:43	69-30.01N	168-45.03W	51.6
010	1	082622	23:36	23:49	69-59.97N	168-45.20W	41.0
011	1	082722	03:38	03:58	70-30.02N	168-45.92W	38.8
012	1	082822	14:37	15:02	71-40.48N	154-57.89W	99.0
013	1	082922	18:54	19:52	71-44.09N	155-13.56W	306.0
014	1	083022	22:06	23:58	71-27.26N	148-32.15W	2169.0
015	1	083122	04:38	06:31	71-07.22N	146-06.54W	2123.0
016	1	083122	17:37	19:34	71-01.05N	141-58.96W	2340.0
017	1	083122	21:48	23:30	70-47.35N	141-51.46W	1797.0
018	1	090322	00:06	01:36	71-19.96N	135-30.49W	1324.0
019	1	090422	00:07	00:28	69-58.51N	137-14.72W	58.3
020	1	090522	17:26	17:49	70-25.29N	141-39.88W	79.0
021	1	090522	20:23	21:15	70-32.97N	141-41.95W	470.0

022	1	090522	23:38	00:59	70-42.12N	141-46.43W	1088.0
023	1	090822	20:02	21:51	72-28.56N	155-23.93W	2019.0
024	1	090922	17:12	18:46	71-50.01N	152-31.16W	1297.0
025	1	090922	21:31	22:10	72-19.08N	152-30.58W	2872.0
026	1	091022	00:05	02:47	72-35.41N	152-24.84W	3628.0
027	1	091022	18:09	18:33	71-19.98N	152-30.09W	61.2
028	1	091022	20:34	20:59	71-30.01N	152-29.99W	107.0
029	1	091022	23:36	00:28	71-40.08N	152-30.06W	313.0
030	1	091422	18:13	18:35	72-30.01N	159-59.49W	48.5
031	1	091422	20:54	21:14	72-42.12N	159-24.21W	84.9
032	1	091522	00:03	00:57	72-54.02N	158-48.34W	397.0
033	1	091522	17:04	19:26	73-20.11N	157-27.91W	3002.0
034	1	091522	22:21	23:52	73-00.33N	158-30.80W	1331.0

(6) Preliminary results

a. Standard Seawater

Standardization control of the salinometer was set to 608 (20th Aug.). The value of STANDBY was 24+5132 ~ 5133 and that of ZERO was 0.0±0000 ~ + 0001. The IAPSO Standard Seawater (SSW) batch P164 was used as the standard for salinity. 42 bottles of P164 were measured.

Figures 3.10-1 and -2 show the time series of the double conductivity ratio of the Standard Seawater batch P164. The average of the double conductivity ratio was 1.99970 and the standard deviation was 0.00001 which is equivalent to 0.0002 in salinity.

The specifications of SSW batch P164 used in this cruise are shown as follows;

Batch : P164
 Conductivity ratio : 0.99970
 Salinity : 34.994
 Use by : 23rd March 2023

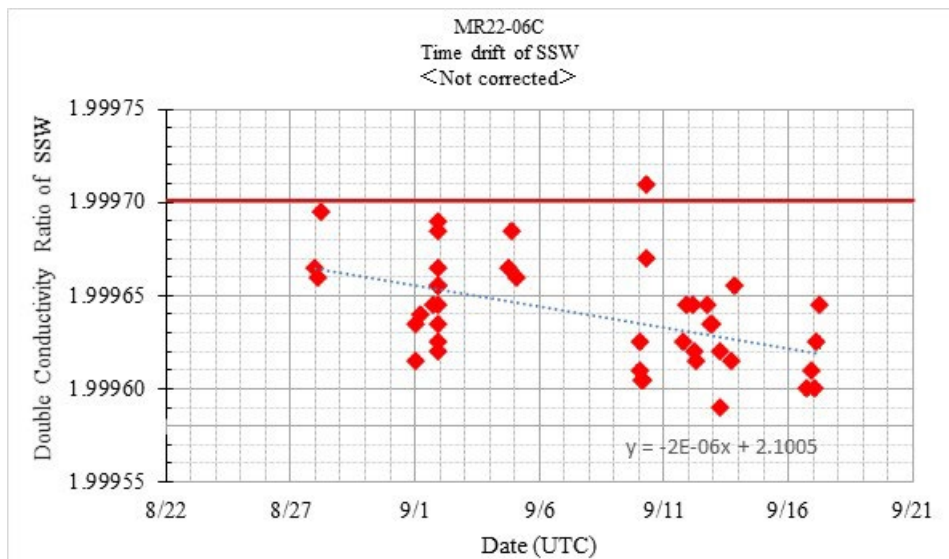


Figure 3.10-1: Time series of double conductivity ratio for the Standard Seawater (before correction)

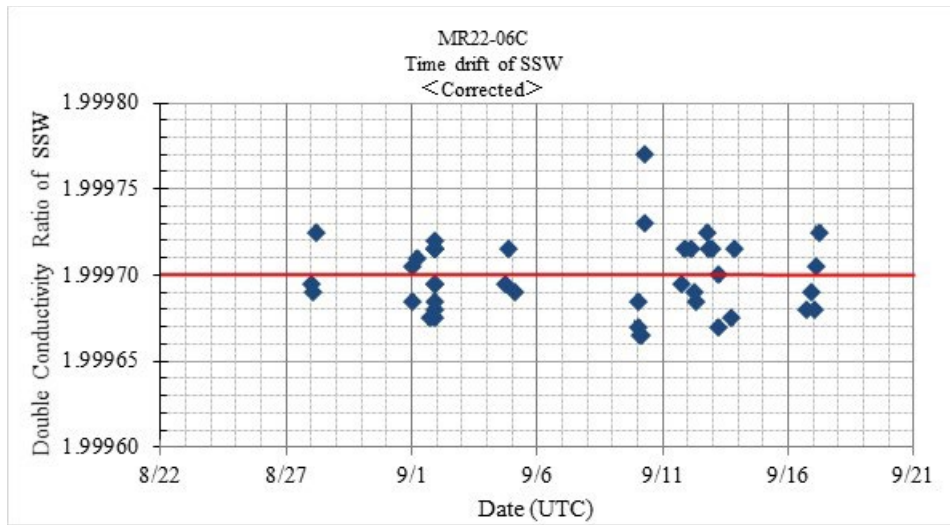


Figure 3.10-2: Time series of double conductivity ratio for the Standard Seawater (after correction)

b. Sub-Standard Seawater

Sub-standard seawater was made from surface sea water filtered by a pore size of 0.2 micrometer and stored in a 20 Liter container made of polyethylene and stirred for at least 24 hours before measuring. It was measured about every 10 samples in order to check for the possible sudden drifts of the salinometer.

c. Replicate Samples

We estimated the precision of this method using 81 pairs of replicate samples taken from the same water sampling bottle. Figure 3.10-3 shows the histogram of the absolute difference between each pair of the replicate samples. The average and the standard deviation of absolute difference among 81 pairs of replicate samples were 0.0012 and 0.0016 in salinity, respectively.

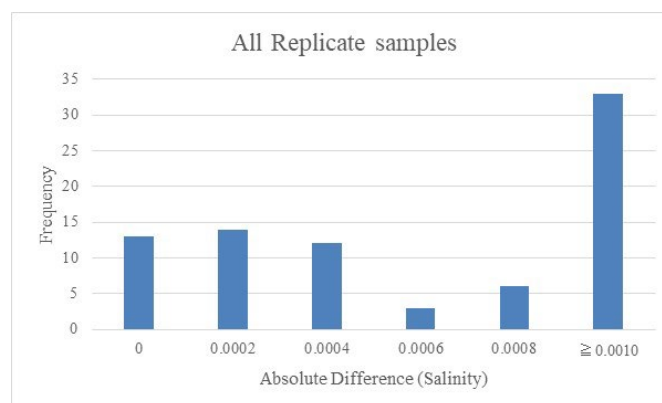


Figure 3.10-3: The histogram of the salinity for the absolute difference of all replicate samples

(7) Data archive

These data obtained in this cruise will be submitted to the Data Management Group of JAMSTEC, and will be opened to the public via “Data Research System for Whole Cruise Information in JAMSTEC (DARWIN)” in JAMSTEC web site.

<<http://www.godac.jamstec.go.jp/darwin/e>>

(8) References

- Aoyama, M., T. Joyce, T. Kawano and Y. Takatsuki : Standard seawater comparison up to P129. Deep-Sea Research, I, Vol. 49, 1103-1114, 2002.
- UNESCO : Tenth report of the Joint Panel on Oceanographic Tables and Standards. UNESCO Tech. Papers in Mar. Sci., 36, 25 pp., 1981.

4. Biogeochemical Oceanography

4.1. Dissolved Oxygen

(1) Personnel

Amane Fujiwara (JAMSTEC): Principal Investigator, not on board

Motoyo Itoh (JAMSTEC)

Katsunori Sagishima (MWJ): Operation Leader

Erii Irie (MWJ)

(2) Objectives

Determination of dissolved oxygen in seawater by Winkler titration.

(3) Parameters

Dissolved Oxygen

(4) Instruments and methods

The following procedure is based on the Winkler method (Dickson, 1996; Culberson, 1991).

a. Instruments

Burette for sodium thiosulfate and potassium iodate;

Automatic piston burette (APB-510, APB-610 and APB-620) manufactured by Kyoto Electronics Manufacturing Co., Ltd. / 10 cm³ of titration vessel

Detector;

Automatic photometric titrator (DOT-15X) manufactured by Kimoto Electric Co., Ltd.

Software;

DOT15X_Terminal Ver. 1.3.1

b. Reagents

Pickling Reagent I:

Manganese(II) chloride solution (3 mol dm⁻³)

Pickling Reagent II:

Sodium hydroxide (8 mol dm⁻³) / Sodium iodide solution (4 mol dm⁻³)

Sulfuric acid solution (5 mol dm⁻³)

Sodium thiosulfate (0.025 mol dm⁻³)

Potassium iodate (0.001667 mol dm⁻³)

c. Sampling

Seawater samples were collected with a Niskin bottle attached to the CTD/Carousel Water Sampling System (CTD system). Seawater for oxygen measurement was

transferred from the bottle to a volume-calibrated flask (ca. 100 cm³), and three times the volume of the flask was overflowed. Temperature was simultaneously measured by a digital thermometer during the overflowing. After transferring the sample, two reagent solutions (Reagent I and II) of 1 cm³ each were added immediately and the stopper was inserted carefully into the flask. The sample flask was then shaken vigorously to mix the contents and to disperse the precipitate finely throughout. After the precipitate has settled at least halfway down the flask, the flask was shaken again vigorously to disperse the precipitate. The sample flasks containing pickled samples were stored in a laboratory until they were titrated.

d. Sample measurement

For over two hours after the re-shaking, the pickled samples were measured on board. Sulfuric acid solution with its volume of 1 cm³ and a magnetic stirrer bar were put into the sample flask and the sample was stirred. The samples were titrated by sodium thiosulfate solution whose morality was determined by potassium iodate solution. Temperature of sodium thiosulfate during titration was recorded by a digital thermometer. Dissolved oxygen concentration ($\mu\text{mol kg}^{-1}$) was calculated by sample temperature during seawater sampling, salinity measured by salinometer, flask volume, and titrated volume of sodium thiosulfate solution without the blank.

e. Standardization and determination of the blank

The concentration of sodium thiosulfate titrant was determined by potassium iodate solution. Pure potassium iodate was dried in an oven at 130 °C, and 1.7835 g of it was dissolved in deionized water and diluted to the final weight of 5 kg in a flask. After 10 cm³ of the standard potassium iodate solution was added to another flask using a volume-calibrated dispenser, 90 cm³ of deionized water, 1 cm³ of sulfuric acid solution, and 1 cm³ of pickling reagent solution II and I were added in order. The amount of titrated volume of sodium thiosulfate for this diluted standard potassium iodate solution (usually 5 times measurements average) gave the morality of sodium thiosulfate titrant.

The oxygen in the pickling reagents I (1 cm³) and II (1 cm³) was assumed to be 7.6×10^{-8} mol (Murray et al., 1968). The blank due to other than oxygen was determined as follows. First, 1 and 2 cm³ of the standard potassium iodate solution were added to each flask using a calibrated dispenser. Then 100 cm³ of deionized water, 1 cm³ of sulfuric acid solution, 1 cm³ of pickling II reagent solution, and the same volume of pickling I reagent solution were added into the flask in order. The blank was determined by the difference between the first (1 cm³ of potassium iodate) titrated volume of the sodium thiosulfate and the second (2 cm³ of potassium iodate) one. The titrations were conducted for 3 times and their average was used as the blank value.

(5) Observation log

a. Standardization and determination of the blank

Table 4.1-1 shows results of the standardization and the blank determination during this cruise.

Table 4.1-1 Results of the standardization and the blank determinations during cruise

Date (yyyy/mm/dd)	Potassium iodate ID	Sodium thiosulfate ID	DOT-15X (No.9)		DOT-15X (No.10)		Stations
			E.P. (cm ³)	Blank (cm ³)	E.P. (cm ³)	Blank (cm ³)	
2022/8/14	K22A09	T-21W	3.963	0.000	3.954	-0.005	
2022/8/17	K22A04	T-21W	3.962	0.000	3.953	-0.004	
2022/8/20	K22A05	T-21W	3.963	0.002	3.957	-0.003	001M001, 002M001, 003M001, 004M001,
2022/8/26	K22A06	T-21W	3.962	0.000	3.957	-0.002	005M001, 006M001, 007M001, 008M001, 009M001, 010M001, 011M001, 012M001, 013M001,
2022/8/31	K22A07	T-21W	3.962	0.001	3.957	-0.005	014M001, 015M001, 016M001, 017M001
2022/9/3	K22A08	T-21W	3.963	0.001	3.958	-0.001	018M001, 019M001, 020M001, 021M001, 022M001
2022/9/10	K22A10	T-21X	3.967	0.000	3.963	-0.004	023M001, 024M001, 026M001, 027M001, 028M001, 029M001
2022/9/14	K22B01	T-21X	3.970	0.002	3.964	-0.002	030M001, 031M001, 032M001, 033M001, 034M001
2022/9/19	K22B11	T-21X	3.969	0.001	3.964	-0.001	
2022/9/23	K22B03	T-21X	-	-	3.964	-0.001	
2022/9/25	K22B04	T-21X	-	-	3.964	0.002	

b. Repeatability of sample measurement

Replicate samples were taken at every CTD casts. The standard deviation of the replicate measurement (Dickson et al., 2007) was $0.13 \mu\text{mol kg}^{-1}$ (n=78).

(6) Data archive

These data obtained in this cruise will be submitted to the Data Management Group (DMG) of JAMSTEC, and will be opened to the public via “Data Research System for Whole Cruise Information in JAMSTEC (DARWIN)” in the JAMSTEC web site.

<<http://www.godac.jamstec.go.jp/darwin/e>>

(7) References

Culbertson, C. H. (1991). *Dissolved Oxygen*. WHP O Publication 91-1.

Dickson, A. G. (1996). Determination of dissolved oxygen in sea water by Winkler titration. In *WOCE Operations Manual*, Part 3.1.3 Operations & Methods, WHP Office Report WHP O 91-1.

Dickson, A. G., Sabine, C. L., & Christian, J. R. (Eds.), (2007). *Guide to best practices for ocean CO₂ measurements, PICES Special Publication 3*. North Pacific Marine Science Organization.

Murray, C. N., Riley, J. P., & Wilson, T. R. S. (1968). The solubility of oxygen in Winkler reagents used for the determination of dissolved oxygen. *Deep Sea Res.*, 15, 237-238.

4.2. Nutrients

(1) Personnel

Michio Aoyama (JAMSTEC/University of Tsukuba): Principal Investigator, not on board

Mariko Hatta (JAMSTEC): Principal Investigator

Yuko Miyoshi (MWJ): Operation Leader

Yuta Oda (MWJ)

Shiori Ariga (MWJ)

(2) Objectives

The objective is to show the present status of the nutrient concentrations during the R/V Mirai MR22-06C cruise (EXPOCODE: 49NZ20220812) in the Arctic Ocean, and then evaluate the comparability of this obtained dataset during this cruise using the certified reference materials of the nutrients in seawater.

(3) Parameters

The parameters are nitrate, nitrite, silicate, phosphate and ammonia in seawater.

(4) Instruments and methods

(4-1) Analytical detail using QuAAtro 39-J systems (BL TEC K.K.)

The analytical platform was replaced from QuAAtro 2-HR to QuAAtro 39 in March 2021. However, since this replacement, the several issues for the QuAAtro 39 system were reported (e.g. unexpected drift issue for the phosphate and the silicate determinations, unusual damage pump cover, see previous cruise report MR21-05C). In July 2022, in order to improve those issues and the analytical precisions, (1) their pumps were replaced from the 13-tube pump (model number: 166+B214-01, BL TEC K.K.) to the 14-tube pump (model number: TRA+B014-02, BL TEC K.K.), and (2) their motor brackets were replaced to the new type that is a stainless model (model number: Motor-Bracket-01-Rev-1 and Motor-Bracket-02-Rev-1, BL TEC K.K.). This modified system is now called “QuAAtro 39-J”.

Nitrate + nitrite and nitrite were analyzed by the following methodology that was modified from the original method of Grasshoff (1976). The flow diagrams were shown in Figure 4.2-1 for nitrate + nitrite and Figure 4.2-2 for nitrite. For the nitrate + nitrite analysis, the samples were mixed with the alkaline buffer (Imidazole) and then the mixture was pushed through a cadmium coil which was coated with a metallic copper. This step was conducted due to reduce from nitrate to nitrite in the sample, which allowed us to determine nitrate + nitrite in the seawater sample. For the nitrite analysis, the sample was mixed with reagents without this reduction step. In the flow system, seawater sample with or without the reduction step was mixed with an acidic

sulfanilamide reagent through a mixing coil to produce a diazonium ion. And then, the mixture was mixed with the N-1-naphthylethylenediamine dihydrochloride (NED) to produce a red azo dye. The azo dye compound was injected into the spectrophotometric detection to monitor the signal at 545 nm. Thus, for the nitrite analysis, sample was determined without passing through the Cd coil. Nitrate was computed by the difference between nitrate+nitrite concentration and nitrite concentration.

The silicate method is analogous to that described for phosphate (see below). The method is essentially that of Grasshoff et al. (1999). The flow diagrams were shown in Figure 4.2-3. Silicomolybdic acid compound was first formed by mixing silicate in the sample with the molybdic acid. The silicomolybdic acid compound was then reduced to silicomolybdous acid, "molybdenum blue," using L-ascorbic acid as the reductant. And then the signal was monitored at 630 nm.

The methodology for the phosphate analysis is a modified procedure of Murphy and Riley (1962). The flow diagrams were shown in Figure 4.2-4. Molybdic acid was added to the seawater sample to form the phosphomolybdic acid compound, and then it was reduced to phosphomolybdous acid compound using L-ascorbic acid as the reductant. And then the signal was monitored at 880 nm.

The ammonia in seawater was determined using the flow diagrams shown in Figure 4.2-5. Sample was mixed with an alkaline solution containing EDTA, which ammonia as gas state was formed from seawater. The ammonia (gas) is absorbed in a sulfuric acid by way of 0.5 µm pore size membrane filter (ADVANTEC PTFE) at the dialyzer attached to the analytical system. And then the ammonia absorbed in sulfuric acid was determined by coupling with phenol and hypochlorite to form indophenols blue, and the signal was determined at 630 nm.

The details of a modification of analytical methods for four parameters, nitrate, nitrite, silicate and phosphate, are also compatible with the methods described in nutrients section in the new GO-SHIP (Global Ocean Ship-based Hydrographic Investigations Program) repeat hydrography nutrients manual (Becker et al., 2019). This manual is a revised version of the GO-SHIP repeat hydrography nutrients manual (Hydes et al., 2010). The analytical method of ammonium is compatible with the determination of ammonia in seawater using a vaporization membrane permeability method (Kimura, 2000).

(4-2) Nitrate + Nitrite reagents

50 % Triton solution

50 mL of Triton™ X-100 (CAS No. 9002-93-1) were mixed with 50 mL of ethanol (99.5 %).

Imidazole (buffer), 0.06 M (0.4 % w/v)

Dissolved 4 g of the imidazole (CAS No. 288-32-4) in 1000 mL ultra-pure water,

and then added 2 mL of the hydrogen chloride (CAS No. 7647-01-0). After mixing, 1 mL of the 50 % triton solution was added.

Sulfanilamide, 0.06 M (1 % w/v) in 1.2 M HCl

Dissolved 10 g of 4-aminobenzenesulfonamide (CAS No. 63-74-1) in 900 mL of ultra-pure water, and then added 100 mL of the hydrogen chloride (CAS No. 7647-01-0). After mixing, 2 mL of the 50 % triton solution was added.

NED, 0.004 M (0.1 % w/v)

Dissolved 1 g of N-(1-naphthalenyl)-1, 2-ethanediamine dihydrochloride (CAS No. 1465-25-4) in 1000 mL of ultra-pure water and then added 10 mL of hydrogen chloride (CAS No. 7647-01-0). After mixing, 1 mL 50 % of the Triton solution was added. This reagent was stored in a dark bottle.

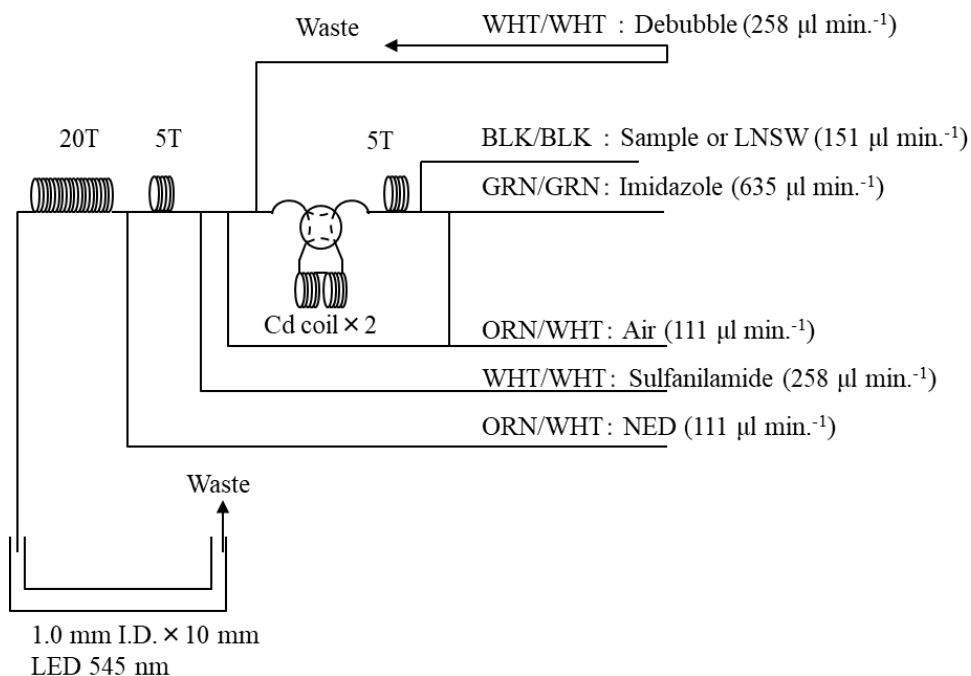


Figure 4.2-1: NO_3+NO_2 (1ch.) flow diagram.

(4-3) Nitrite reagents

50 % Triton solution

50 mL of the Triton™ X-100 (CAS No. 9002-93-1) were mixed with 50 mL ethanol (99.5 %).

Sulfanilamide, 0.06 M (1 % w/v) in 1.2 M HCl

Dissolved 10 g of 4-aminobenzenesulfonamide (CAS No. 63-74-1) in 900 mL of ultra-pure water, and then added 100 mL of hydrogen chloride (CAS No. 7647-01-0). After mixing, 2 mL of the 50 % triton solution were added.

Ascorbic acid, 0.01 M (3 % w/v)

Dissolved 2.5 g of L-ascorbic acid (CAS No. 50-81-7) in 100 mL of ultra-pure water. This reagent was freshly prepared every day.

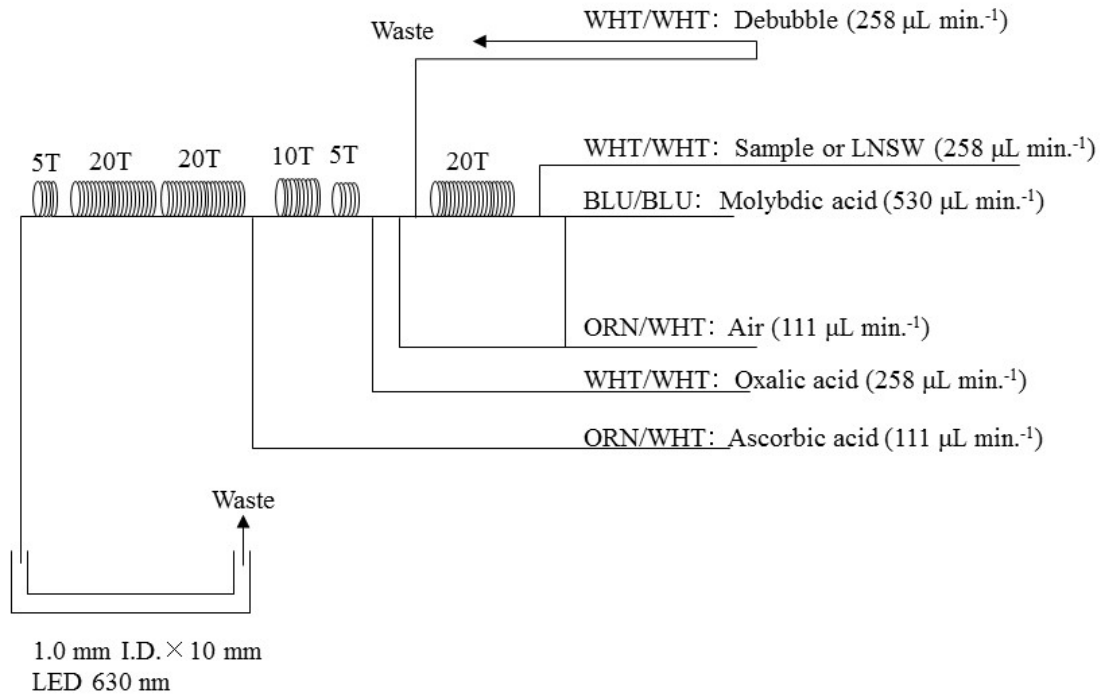


Figure 4.2-3: SiO₂ (3ch.) flow diagram.

(4-5) Phosphate reagents

15 % Sodium dodecyl sulfate solution

75 g of sodium dodecyl sulfate (CAS No. 151-21-3) were mixed with 425 mL of ultra-pure water.

Stock molybdate solution, 0.03 M (0.8 % w/v)

Dissolved 8 g of sodium molybdate dihydrate (CAS No. 10102-40-6) and 0.17 g of antimony potassium tartrate trihydrate (CAS No. 28300-74-5) in 950 mL of ultra-pure water, and then added 50 mL of sulfuric acid (CAS No. 7664-93-9).

PO₄ color reagent

Dissolved 1.2 g of L-ascorbic acid (CAS No. 50-81-7) in 150 mL of the stock molybdate solution. After mixing, 3 mL of the 15 % sodium dodecyl sulfate solution was added. This reagent was freshly prepared before every measurement.

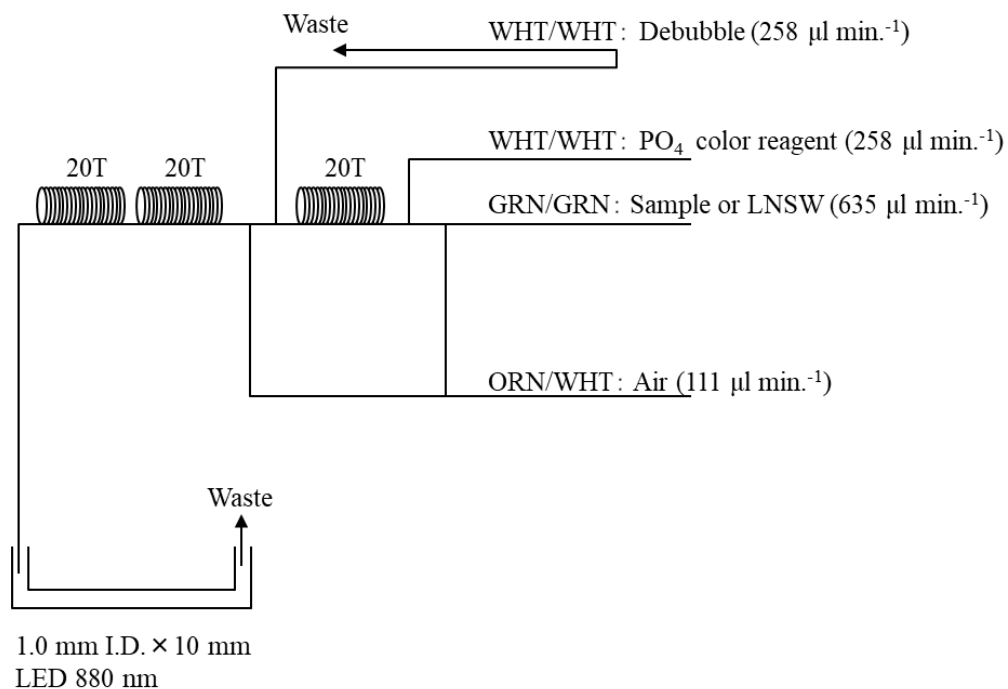


Figure 4.2-4: PO₄ (4ch.) flow diagram.

(4-6) Ammonia reagents

30 % Triton solution

30 mL of a Triton™ X-100 (CAS No. 9002-93-1) were mixed with 70 mL ultra-pure water.

EDTA

Dissolved 41 g of a tetrasodium; 2-[2-[bis(carboxylatomethyl) amino]ethyl-(carboxylatomethyl) amino]acetate; tetrahydrate (CAS No. 13235-36-4) and 2 g of a boric acid (CAS No. 10043-35-3) in 200 mL of ultra-pure water. After mixing, a 1 mL of the 30 % triton solution was added. This reagent is prepared every week.

NaOH liquid

Dissolved 1.5 g of a sodium hydroxide (CAS No. 1310-73-2) and 16 g of a tetrasodium; 2-[2-[bis(carboxylatomethyl) amino]ethyl - (carboxylatomethyl) amino]acetate; tetrahydrate (CAS No. 13235-36-4) in 100 mL of ultra-pure water. This reagent was prepared every week. Note that we reduced the amount of a sodium hydroxide from 5 g to 1.5 g because pH of C standard solutions has been lowered 1 pH unit due to the change of recipe of B standards solution (the detailed of those standard solution, see 7-2-4).

Stock nitroprusside

Dissolved 0.25 g of a sodium nitroferricyanide dihydrate (CAS No. 13755-38-9)

(4-7) Sampling procedures and sample injection

Sampling for the nutrient samples was conducted right after the sampling for other parameters (oxygen, salinity and trace gases). Samples were collected into two new 10 mL polyacrylates vials without any sample drawing tube that usually used for the oxygen samples. Each vial was rinsed three times before filling and then was sealed without any head-space immediately after the collection. The vials were put into a water bath that was adjusted to the ambient temperature at 21.8 ± 0.1 degree Celsius, for more than 30 minutes to keep the constant temperature of samples before measuring. When the transmissometer signal (Xmiss) of the sample was less than 95 % or confirmed the presence of particles in the vial, we basically carried out centrifuging the sample by using a centrifuge (type: CN-820, Hsiang Tai). The conditions of centrifuge were set about 3400 rpm for 2.5 minutes. The treated samples were listed in Table 4.2-1.

No transfer from the vial to another container was made and the vials were placed on an autosampler tray directly. Samples were analyzed within 24 hours after collection.

In order to improve peak shapes, the injection time for the sample and the following wash time have been optimized and now they are 70 seconds and 25 seconds respectively. The optimized time was tested in a shore-based laboratory by BL TEC K.K. and Principal Investigator before this cruise started.

(4-8) Data processing

Raw data from QuAAtro 39-J were treated as follows:

- Checked if there were any baseline shift.
- Checked the shape of each peak and positions of peak values. If necessary, a change was made for the positions of peak values.
- Conducted carry-over correction and baseline drift correction followed by sensitivity correction to apply to the peak height of each sample.
- Conducted baseline correction and sensitivity correction using the linear regression.
- Using the salinity (from determined on the ship) and the laboratory room temperature (20 degrees Celsius), the density of each sample was calculated. The obtained density was used to calculate the final nutrient concentration with the unit of $\mu\text{mol kg}^{-1}$.
- Calibration curves to obtain the nutrients concentrations were assumed second order equations.

(4.9) Summary of nutrients analysis

Total of the 22 runs were conducted to obtain the values for the samples that collected by 33 casts at 33 stations during this cruise. The total number of the seawater samples were 920. For each sample depth, the duplicate of each was corrected. The sampling locations for the nutrients are shown in Figure 4.2-6.

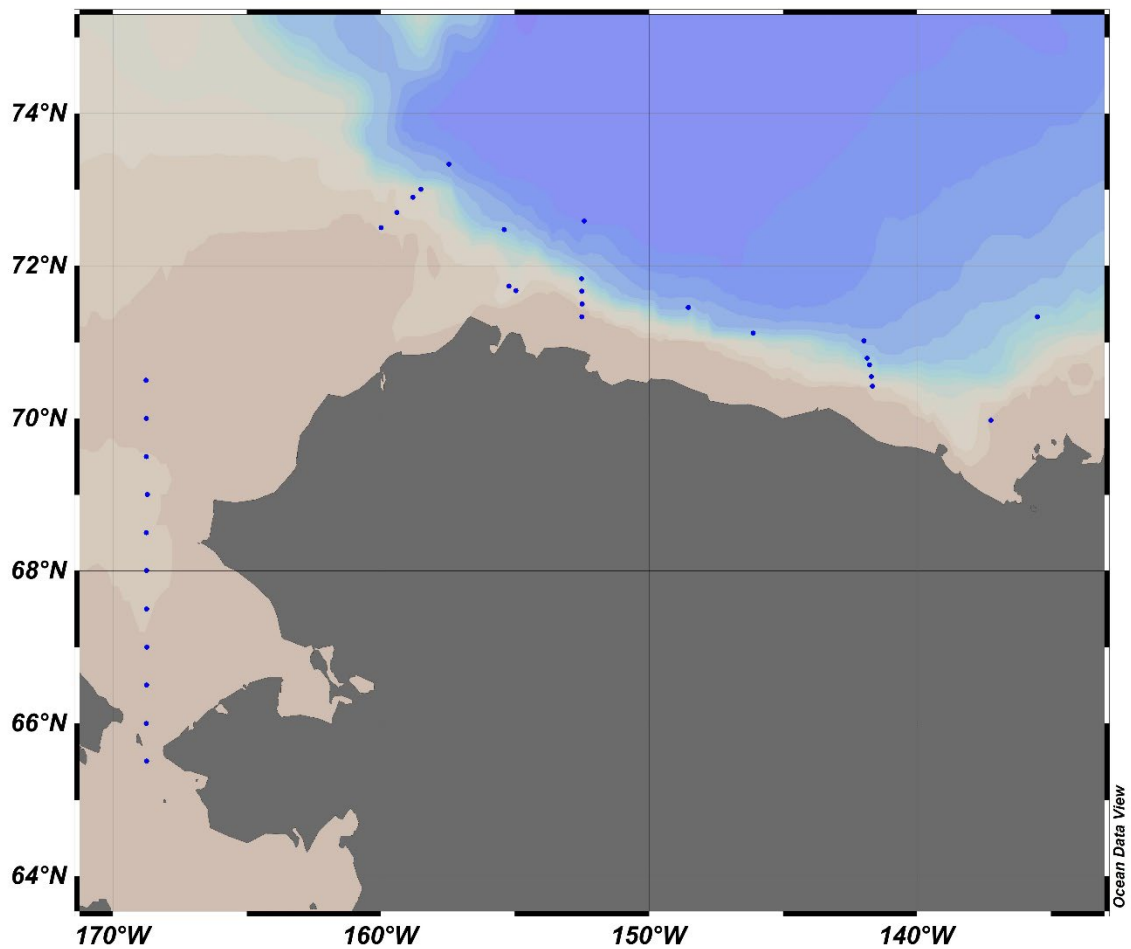


Figure 4.2-6: Sampling positions of nutrients sample.

Table 4.2-1: Centrifuged samples

Station	Cast	Bottle	Depth (dbar)	Trans (%)
1	1	0	0.0	-
1	1	34	5.1	82.0
1	1	33	10.2	82.6
1	1	32	20.4	81.8
1	1	31	30.2	76.0
1	1	35	45.4	72.9
1	1	1	50.7	56.2
2	1	0	0.0	-
2	1	34	5.5	72.9
2	1	33	10.4	74.7
2	1	32	20.3	76.7
2	1	31	30.5	71.7
2	1	35	45.4	63.3
2	1	1	48.6	64.4

Station	Cast	Bottle	Depth (dbar)	Trans (%)
3	1	0	0.0	-
3	1	34	5.1	85.1
3	1	33	10.1	84.3
3	1	35	45.2	77.5
3	1	32	20.1	84.2
3	1	31	30.2	81.9
3	1	1	49.9	69.4
4	1	0	0.0	-
4	1	34	5.4	85.6
4	1	33	10.2	87.6
4	1	35	16.1	87.4
4	1	32	20.2	87.7
4	1	31	30.3	78.8
4	1	1	39.9	73.9

Station	Cast	Bottle	Depth (dbar)	Trans (%)
5	1	0	0.0	-
5	1	34	4.8	90.6
5	1	33	10.0	90.7
5	1	35	16.9	91.0
5	1	32	20.0	92.8
5	1	31	30.4	91.0
5	1	1	44.2	55.5
6	1	0	0.0	-
6	1	34	4.9	84.3
6	1	33	10.2	84.1
6	1	35	14.7	87.0
6	1	32	19.8	93.1
6	1	31	30.1	92.2
6	1	1	53.9	37.7
7	1	0	0.0	-
7	1	34	4.8	84.3
7	1	35	7.8	85.6
7	1	33	10.0	88.3
7	1	32	20.2	94.8
7	1	31	30.4	83.0
7	1	1	48.5	45.7
8	1	0	0.0	-
8	1	34	4.8	89.1
8	1	33	9.5	89.1
8	1	35	12.8	89.1
8	1	32	20.2	89.2
8	1	31	30.4	93.3
8	1	1	47.6	48.4
9	1	0	0.0	-
9	1	34	5.4	92.4
9	1	33	10.3	92.5
9	1	32	20.0	92.6
9	1	31	30.8	94.0
9	1	35	25.4	93.8
9	1	1	46.6	70.5
10	1	0	0.0	-
10	1	34	4.9	92.1
10	1	33	10.3	92.0
10	1	32	20.2	91.4
10	1	31	29.8	90.6
10	1	35	32.7	89.2
10	1	1	36.0	91.8
11	1	0	0.0	-
11	1	34	4.8	90.6
11	1	33	10.2	90.7
11	1	32	20.0	90.8

Station	Cast	Bottle	Depth (dbar)	Trans (%)
11	1	35	24.0	79.8
11	1	31	30.3	77.5
11	1	1	33.6	77.1
12	1	0	0.0	-
12	1	34	5.0	92.3
12	1	33	10.1	92.5
12	1	32	20.0	93.0
12	1	35	22.2	92.9
12	1	31	30.3	96.3
12	1	30	42.9	96.6
12	1	29	50.3	96.6
12	1	28	75.3	88.2
12	1	1	95.7	88.4
13	1	0	0.0	-
13	1	34	5.3	94.1
13	1	35	14.2	94.4
13	1	32	20.2	92.9
13	1	25	175.2	94.4
13	1	24	200.2	90.4
13	1	23	225.4	90.4
13	1	2	250.5	93.0
13	1	1	298.0	89.6
17	1	34	10.1	94.9
17	1	36	11.6	91.7
18	1	35	5.0	93.6
19	1	0	0.0	-
19	1	34	5.0	86.5
19	1	33	10.2	94.1
19	1	32	20.0	90.6
19	1	31	30.5	93.8
19	1	1	52.1	80.3
20	1	30	50.3	94.9
21	1	34	10.0	94.7
22	1	36	12.7	93.7
24	1	9	299.4	94.9
27	1	31	50.1	91.0
27	1	1	56.6	89.8
28	1	30	74.7	93.6
28	1	29	100.5	81.6
28	1	1	103.2	80.7
30	1	33	19.8	93.7
30	1	36	22.7	87.9
31	1	36	42.1	83.7
31	1	30	74.9	82.3
31	1	1	78.0	68.7
32	1	28	125.2	95.0

(5) Station list

The sampling stations were listed as shown in Table 4.2-2.

Table 4.2-2: List of stations

Station	Cast	Date (UTC)	Position*		Depth (m)
		(mmddyy)	Latitude	Longitude	
001	1	082422	65-30.34N	168-44.99W	55
002	1	082422	66-00.13N	168-00.00W	53
003	1	082522	66-30.22N	168-00.00W	55
004	1	082522	67-00.16N	168-44.20W	45
005	1	082522	67-00.41N	168-44.91W	50
006	1	082622	68-00.22N	168-44.90W	59
007	1	082622	68-30.11N	168-45.34W	53
008	1	082622	69-00.21N	168-43.22W	53
009	1	082622	69-30.02N	168-45.04W	52
010	1	082622	69-59.98N	168-45.20W	41
011	1	082722	70-30.03N	168-45.92W	39
012	1	082822	71-40.49N	154-57.89W	99
013	1	082922	71-00.00N	155-00.00W	306
014	1	083022	71-27.27N	148-32.15W	2169
015	1	083122	71-07.22N	146-06.55W	2123
016	1	083122	71-01.05N	141-58.96W	2340
017	1	083122	70-47.35N	141-51.46W	1797
018	1	090322	71-19.97N	135-30.49W	1324
019	1	090422	69-58.52N	137-14.72W	58
020	1	090522	70-25.30N	141-39.88W	79
021	1	090522	70-32.98N	141-41.95W	470
022	1	090622	70-00.00N	141-46.43W	1088
023	1	090822	72-28.57N	155-23.93W	2019
024	1	090922	71-50.01N	152-31.16W	1297
026	1	091022	72-35.41N	152-00.00W	3628
027	1	091022	71-19.99N	152-30.10W	61
028	1	091022	71-30.02N	152-29.99W	107
029	1	091022	71-00.00N	152-30.07W	313
030	1	091422	72-30.01N	159-59.49W	49
031	1	091422	72-00.00N	159-24.22W	85

032	1	091522	72-54.02N	158-48.34W	397
033	1	091522	73-20.12N	157-27.91W	3002
034	1	091522	73-00.34N	158-30.80W	1331

* Position indicates latitude and longitude where CTD reached maximum depth at the cast.

(6) Certified reference material of nutrients in seawater

KANSO Certified Reference Materials (CRMs, Lot: CE, CR, CO, CG) were used to ensure the comparability and traceability of nutrient measurements during this cruise. The details of CRMs are shown below.

Production

KANSO CRMs for inorganic nutrients in seawater were produced by KANSO Co.,Ltd. This CRM has been produced using autoclaved natural seawater based on the quality control system under ISO Guide 34 (JIS Q 0034).

KANSO Co.,Ltd. has been accredited under the Accreditation System of National Institute of Technology and Evaluation (ASNITE) as a CRM producer since 2011. (Accreditation No.: ASNITE 0052 R)

Property value assignment

The certified values were the arithmetic means of the results of 30 bottles from each batch (measured in duplicates) analyzed by both KANSO Co.,Ltd. and Japan Agency for Marine-Earth Science and Technology (JAMSTEC) using the colorimetric method (continuous flow analysis, CFA, method). The salinity of the calibration standards solution to obtain each calibration curve was adjusted to the salinity of the used CRMs within ± 0.5 .

Metrological Traceability

Each certified value of nitrate, nitrite, and phosphate of KANSO CRMs were calibrated using one of Japan Calibration Service System (JCSS) standard solutions for each nitrate ions, nitrite ions, and phosphate ions. JCSS standard solutions were calibrated using the secondary solution of JCSS for each of these ions. The secondary solution of JCSS was calibrated using the specified primary solution produced by Chemicals Evaluation and Research Institute (CERI), Japan. CERI specified primary solutions were calibrated using the National Metrology Institute of Japan (NMIJ) primary standards solution of nitrate ions, nitrite ions and phosphate ions, respectively.

For the certified value of silicate of KANSO CRM was calibrated using a newly established silicon standards solution named “exp96” produced by JAMSTEC and KANSO. This silicon standard solution was produced by a dissolution technique with an

alkaline solution. The mass fraction of Si in the produced solution was calibrated based on NMIJ CRM 3645-a03 Si standard solution by a technology consulting system of National Institute of Advanced Industrial Science and Technology (AIST), and this value is traceable to the International System of Units (SI).

The certified values of nitrate, nitrite, and phosphate of KASNO CRM are thus traceable to the SI through the unbroken chain of calibrations, JCSS, CERI and NMIJ solutions as stated above, each having stated uncertainties. The certified values of silicate of KANSO CRM are traceable to the SI through the unbroken chain of calibrations, NMIJ CRM 3645-a03 Si standard solution, having stated uncertainties.

As stated in the certificate of NMIJ CRMs, each certified value of dissolved silica, nitrate ions, and nitrite ions was determined by more than one method using one of NIST SRM of silicon standard solution and NMIJ primary standards solution of nitrate ions and nitrite ions. The concentration of phosphate ions as stated information value in the certificate was determined NMIJ primary standards solution of phosphate ions. Those values in the certificate of NMIJ CRMs are traceable to the SI.

One of the analytical methods used for certification of NMIJ CRM for nitrate ions, nitrite ions, phosphate ions and dissolved silica was a colorimetric method (continuous mode and batch mode). The colorimetric method is the same as the analytical method (continuous mode only) used for certification of KANSO CRM. For certification of dissolved silica, exclusion chromatography/isotope dilution-inductively coupled plasma mass spectrometry and ion exclusion chromatography with post-column detection were used. For certification of nitrate ions, ion chromatography by direct analysis and ion chromatography after halogen-ion separation were used. For certification of nitrite ions, ion chromatography by direct analysis was used.

NMIJ CRMs were analyzed at the time of certification process for CRM and the results were confirmed within expanded uncertainty stated in the certificate of NMIJ CRMs.

(6-1) CRM for this cruise

22 sets of CRM lots CE, CR, CO, and CG were used, which almost cover a range of nutrients concentrations in the Arctic Ocean.

Each CRM's serial number was randomly selected. The CRM bottles were stored at a room named "BIOCHEMICAL LABORATORY" on the ship, where the temperature was maintained around 20.79 degrees Celsius - 22.87 degrees Celsius.

(6-2) CRM concentration

Nutrients concentrations for the CRM lots CE, CR, CO and CG were shown in Table 4.2-3.

Table 4.2-3: Certified concentration and the uncertainty ($k = 2$) of CRMs.

Unit: $\mu\text{mol kg}^{-1}$					
Lot	Nitrate	Nitrite**	Silicate	Phosphate	Ammonia***
CE*	0.01 ± 0.03	0.031 ± 0.03	0.06 ± 0.09	0.012 ± 0.006	0.689
CR	5.46 ± 0.16	0.97 ± 0.07	14.0 ± 0.3	0.40 ± 0.03	0.95 ± 0.15
CO	15.86 ± 0.15	0.046 ± 0.04	34.72 ± 0.16	1.177 ± 0.014	0.543
CG	23.7 ± 0.2	0.071 ± 0.03	56.4 ± 0.5	1.70 ± 0.02	0.613

*Nitrate, silicate and phosphate values of CRM lot CE are below quantifiable detection limit and shown as only reference values.

** For Nitrite concentration, there is a trend that the value has been increased $0.004 \pm 0.002 \mu\text{mol kg}^{-1}$ per year. Nitrite concentration values for CE, CO, CG were determined on the ship in the beginning of the MR21-04 cruise in July 2021. Since the nitrite value of CR recently reported by KANSO which determined on March 31, 2022, the value was used on this table.

***Ammonia values are all reference value.

Notes: The value of CR was reported by KANSO. The other reported values were determined by MWJ.

(7) Nutrients standards

(7-1) Volumetric laboratory-ware of in-house standards

All volumetric glassware and Polymethylpentene (PMP)-ware used were gravimetrically calibrated. Plastic volumetric flasks were gravimetrically calibrated at the water temperature of use within 0.2 K at around 19.8 degrees Celsius.

(7-1-1) Volumetric flasks

Volumetric flasks of Class quality (Class A) are used because their nominal tolerances are 0.05 % or less over the size ranges likely to be used in this work. Since Class A flasks are made of borosilicate glass, the standard solutions were transferred to plastic bottles as quickly as possible after the solutions were made up to volume and well mixed in order to prevent the excessive dissolution of silicate from the glass. PMP volumetric flasks were gravimetrically calibrated and used only within 4 K of the calibration temperature.

The computation of volume contained by the glass flasks at various temperatures other than the calibration temperatures were conducted by using the coefficient of linear expansion of borosilicate crown glass.

The coefficients of cubical expansion of each glass and PMP volumetric flask was determined by actual measurement in 2022. The coefficients of cubical expansion of glass volumetric flask (IWAKI TE-32 or SHIBATA HARIO) was 0.00000975 to 0.000011 K^{-1} and that of PMP volumetric flask (NALGEN PMP) was 0.00038 to 0.00042 K^{-1} . The

weights obtained in the calibration weightings were corrected for the density of water and air buoyancy.

(7-1-2) Pipettes

All glass pipettes have nominal calibration tolerances of 0.1 % or better. These were gravimetrically calibrated to verify and improve upon this nominal tolerance.

(7-2) Reagents, general considerations

(7-2-1) Specifications

For nitrate standard, “potassium nitrate 99.995 suprapur®” provided by Merck, Batch B1706365, CAS No. 7757-79-1, was used.

For nitrite standard solution, we used a nitrite ion standard solution (NO_2^- 1000) provided by Wako, Lot ESG1055 and DLJ3947, Code. No. 146-06453. This standard solution was certified by Wako using the ion chromatography method. Calibration result is 1004 mg L^{-1} and 1002 mg L^{-1} at 20 degrees Celsius respectively. Expanded uncertainty of calibration ($k=2$) is 0.8 % for the calibration result.

For the silicate standard solution, we used our in-house Si standard solution “exp96” which was produced by alkali fusion technique from 5N SiO_2 powder produced jointly by JAMSTEC and KANSO. The mass fraction of Si in the “exp96” solution was calibrated based on NMIJ CRM 3645-a03 Si standard solution.

For phosphate standard, we used a potassium dihydrogen phosphate anhydrous 99.995 suprapur®” provided by Merck, Batch B1871308, CAS No.: 7778-77-0.

For ammonia standard, ammonium chloride (CRM 3011-a) provided by NMIJ, CAS No. 12125-02-9 was used. The purity of this standard was reported as >99.9 % by the manufacturer. Expanded uncertainty of calibration ($k=2$) was 0.026 %.

(7-2-2) Ultra-pure water

Ultra-pure water (Milli-Q water) freshly drawn was used for the preparation of reagents, standard solutions and for measurements of the reagent and the system blanks.

(7-2-3) Low Nutrients Seawater (LNSW)

Surface water having low nutrient concentration was taken and filtered using $0.20 \mu\text{m}$ pore capsule cartridge filter around 17S and 100E during MR19-04 cruise in February 2020. This water was drained into 20 L cubitainers and stored in a cardboard box.

Nutrients concentrations in LNSW were measured on August 2020. The averaged nutrient concentrations in the LNSW were $0.004 \mu\text{mol L}^{-1}$ for nitrate, $0.001 \mu\text{mol L}^{-1}$ for nitrite, $1.931 \mu\text{mol L}^{-1}$ for silicate, $0.073 \mu\text{mol L}^{-1}$ for phosphate and 0.002

$\mu\text{mol L}^{-1}$ for ammonia. We observed that phosphate concentration values were different for each cardboard box, so we measured the values for each box. The phosphate concentration value in the LNSW we used in this cruise was 0.072 to 0.092 $\mu\text{mol L}^{-1}$. The concentrations of nitrate, nitrite and ammonia were lower than detection limit as stated in chapter (8-5).

(7-2-4) Concentrations of nutrients for A, B, D and C standards

Concentrations of nutrients for A, B, D and C standards were adjusted as shown in Table 4.2-4.

We used JAMSTEC-KANSO in-house Si standard solution for A standard of silicate, which doesn't need to be neutralized by the hydrochloric acid. B standard was diluted from A standard with the following recipes shown in Table 4.2-5. In order to match the salinity and the density of the stock solution (B standard) to the LNSW, during this dilution step, 15.30 g of a sodium chloride powder was dissolved in B standard, and then the final volume was adjusted to 500 mL.

The C standard solution was prepared in the LNSW following the recipes shown in Table 4.2-6. All volumetric laboratory tools were calibrated prior the cruise as stated in chapter (7-1). Then the actual concentration of nutrient in each fresh standard solution was calculated based on the solution temperature, together with the determined factors of volumetric laboratory wares.

The calibration curves for each run were obtained using 4 levels, C-1 (LNSW), C-2, C-3, and C-4 that were diluting using the B standard solution.

The D standard solutions were made to calculate the reduction rate of Cd coil. The D standard was diluted from the A standard solution into the pure water.

Table 4.2-4: Nominal concentrations of nutrients for A, B, D and C standards.

	A	B	D	C-1	C-2	C-3	C-4
NO_3	22500	670	900	LNSW	13	27	40
NO_2	21800	26	870	LNSW	0.5	1.0	1.6
SiO_2	35500	1420		LNSW	30	59	87
PO_4	6000	60		LNSW	1.3	2.5	3.7
NH_4	4000	160		LNSW	3.2	6.4	9.6

Table 4.2-5: B standard recipes. Final volume was 500 mL.

A Std.	
NO ₃	15 mL
NO ₂ *	15 mL
SiO ₂	20 mL
PO ₄	5 mL
NH ₄	20 mL

*NO₂ was D standard solution which was diluted from A standard.

Table 4.2-6: Working calibration standard recipes. Final volume was 500 mL.

C Std.	B Std.
C-2	10 mL
C-3	20 mL
C-4	30 mL

(7-2-5) Renewal of in-house standard solutions

In-house standard solutions as stated in paragraph (7-2-4) were remade by each “renewal time” shown in Tables 4.2-7(a) to (c).

Table 4.2-7(a): Timing of renewal of in-house standards.

NO ₃ , NO ₂ , SiO ₂ , PO ₄ , NH ₄	Renewal time
A-1 Std. (NO ₃)	maximum a month
A-2 Std. (NO ₂)	commercial prepared solution
A-3 Std. (SiO ₂)	JAMSTEC-KANSO Si standard solution
A-4 Std. (PO ₄)	maximum a month
A-5 Std. (NH ₄)	maximum a month
D-1 Std.	maximum 8 days
D-2 Std.	maximum 8 days
B Std.	maximum 8 days
(mixture of A-1, D-2, A-3, A-4 and A-5 std.)	

Table 4.2-7(b): Timing of renewal of working calibration standards.

Working standards	Renewal time
C Std. (diluted from B Std.)	every 24 hours

Table 4.2-7(c): Timing of renewal of in-house standards for reduction estimation.

Reduction estimation	Renewal time
36 μM NO_3 (diluted D-1 Std.)	when C Std. renewed
35 μM NO_2 (diluted D-2 Std.)	when C Std. renewed

(8) Quality control

(8-1) The precision of the nutrient analyses during the cruise

The highest standard solution (C-4) was repeatedly determined every 2 to 14 samples to obtain the analytical precision of the nutrient analyses during this cruise. During each run, the total number of the C-4 determination was 8-13 times depending on the run. Each run, we obtained the analytical precision based on this C-4 results, shown in Figures 4.2-7 to 4.2-11. In this cruise, there were total 22 runs. The analytical precisions were less than 0.2% for nitrate, silicate, and phosphate.

The overall precisions throughout this cruise were calculated based on the analytical precisions obtained from all of the runs, and shown in Table 4.2-8. During this cruise, overall median precisions were 0.14 % for nitrate, 0.22 % for nitrite, 0.13 % for silicate, 0.12 % for phosphate and 0.28 % for ammonia, respectively. The overall median precision for each parameter during this cruise was comparable to the previously published precisions during the R/V Mirai cruises conducted in 2009 - 2022.

Table 4.2-8: Summary of overall precision based on the replicate analyses ($k = 1$)

	Nitrate CV %	Nitrite CV %	Silicate CV %	Phosphate CV %	Ammonia CV %
Median	0.14	0.22	0.13	0.12	0.28
Mean	0.14	0.21	0.13	0.12	0.28
Maximum	0.20	0.31	0.19	0.18	0.41
Minimum	0.03	0.10	0.06	0.06	0.17
N	22	22	22	22	22

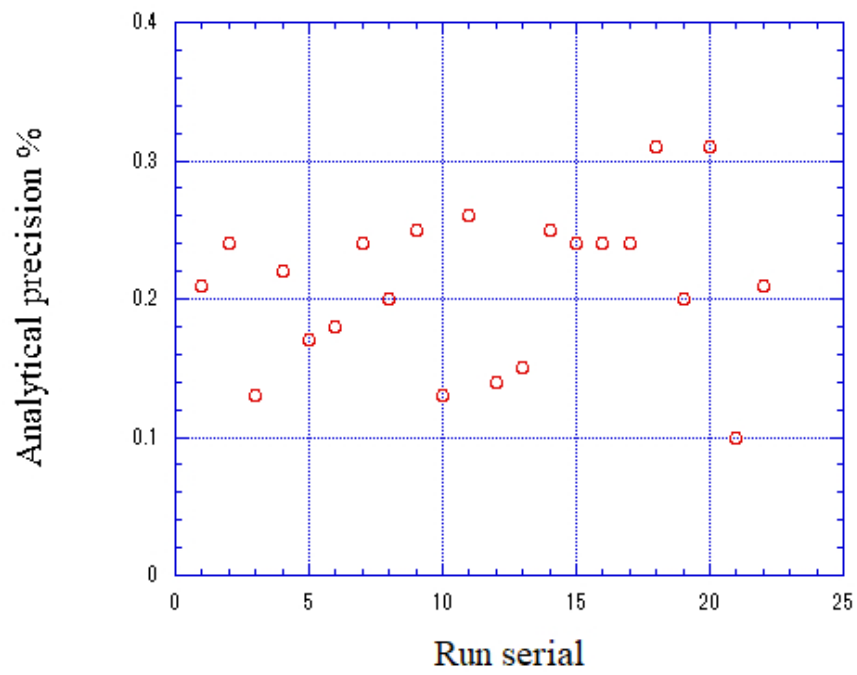


Figure 4.2-7: Time series of precision of nitrate in this cruise.

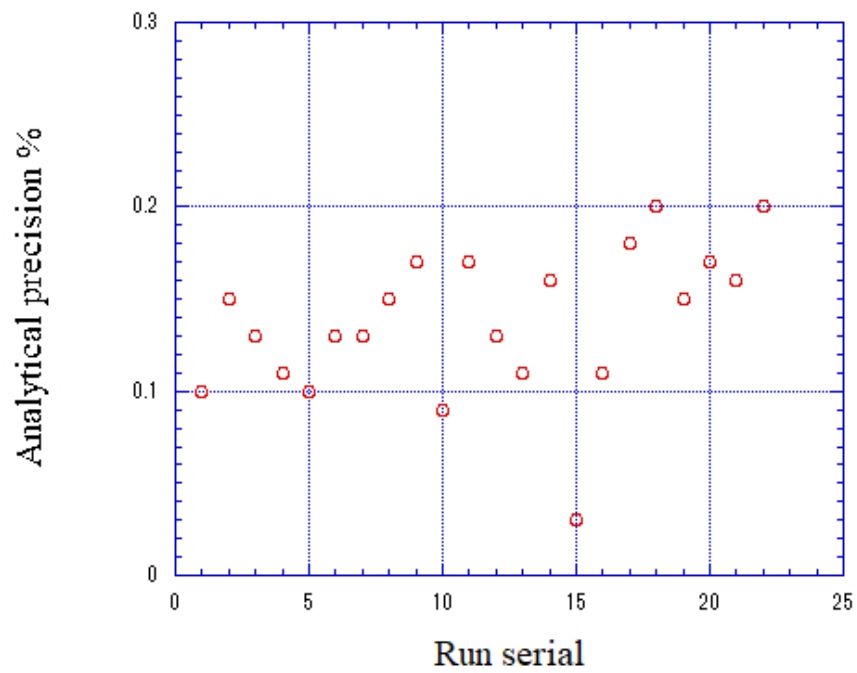


Figure 4.2-8: Same as 4.2-7, but for nitrite.

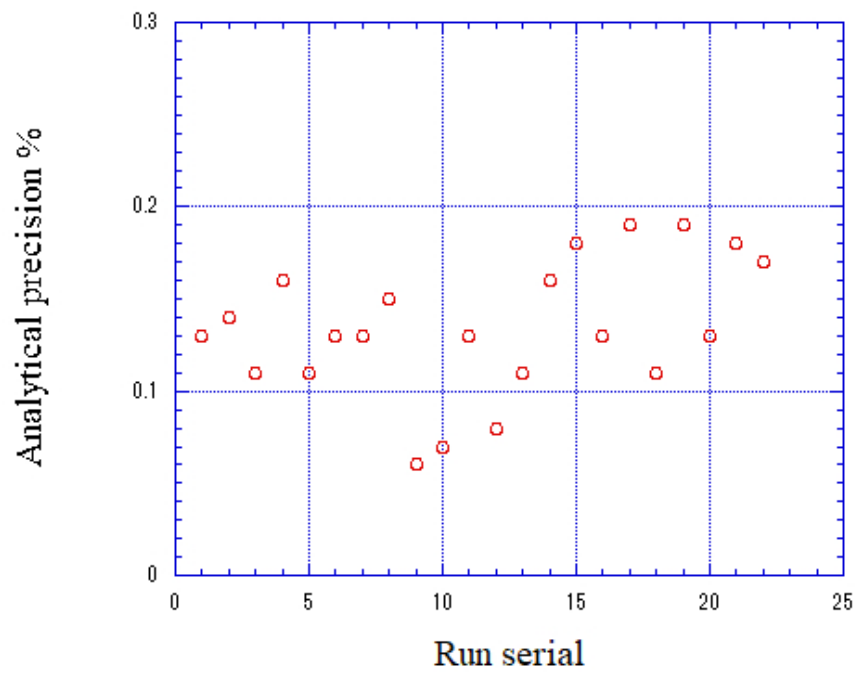


Figure 4.2-9: Same as 4.2-7, but for silicate.

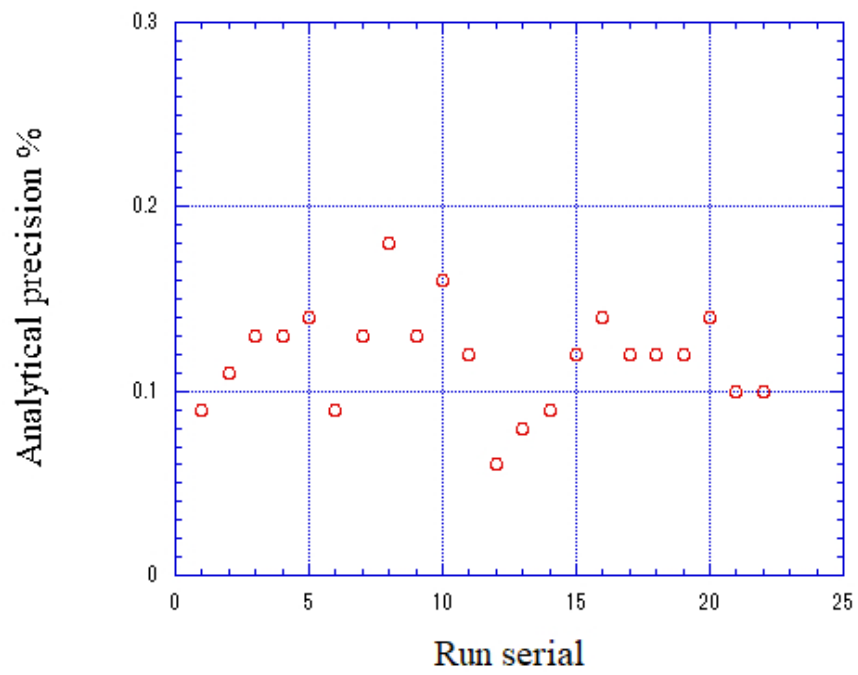


Figure 4.2-10: Same as 4.2-7, but for phosphate.

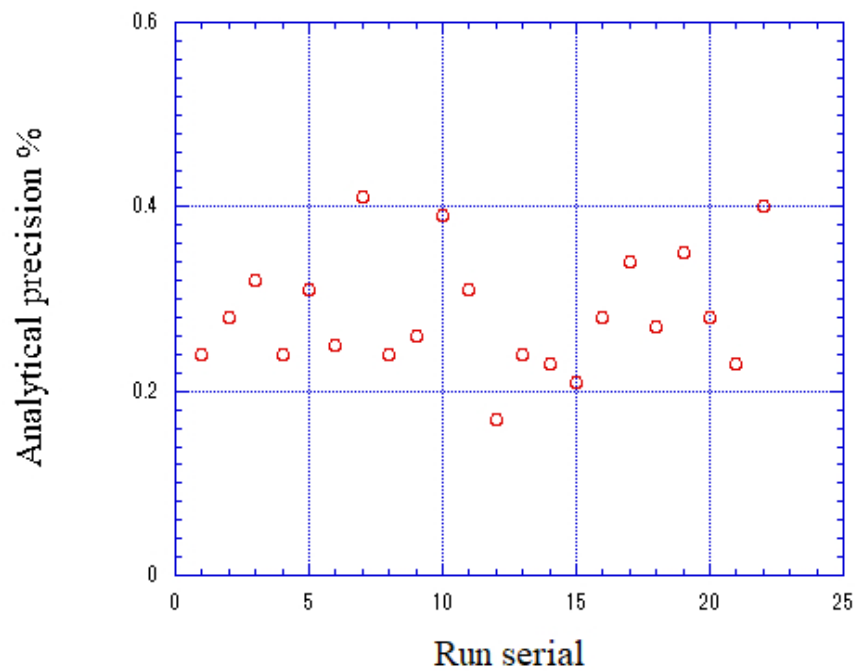


Figure 4.2-11: Same as 4.2-7, but for ammonia.

(8-2) CRM lot. CG measurement during this cruise

CRM lot. CG was measured every run to evaluate the comparability throughout the cruise. The all of the results of lot. CG during this cruise are shown as Figures 4.2-12 to 4.2-16. All of the measured concentrations of CRM lot. CG was within the uncertainty of certified values for nitrate, nitrite, silicate and phosphate. The reported CRM values are shown in Table 4.2-3.

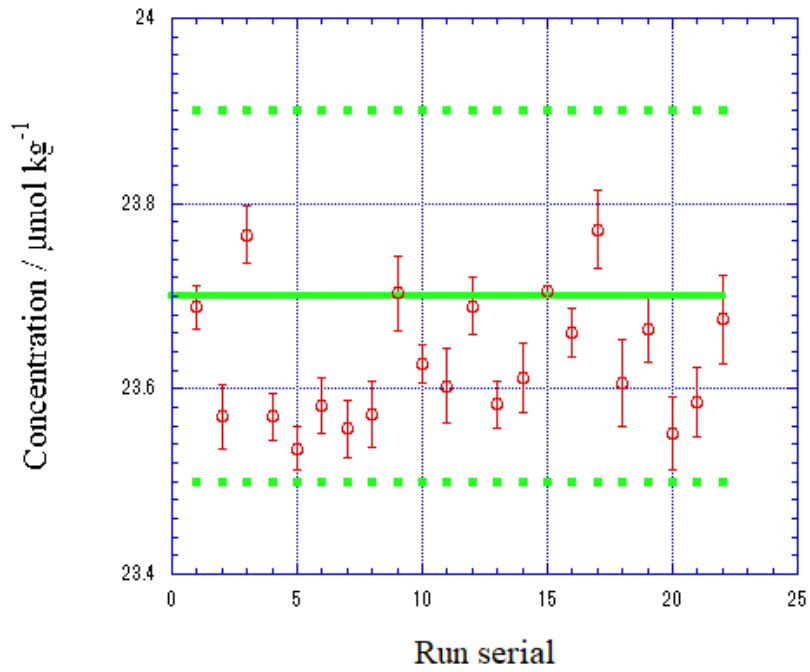


Figure 4.2-12: Time series of CRM-CG of nitrate in this cruise. Solid green line is certified nitrate concentration of CRM and dashed green lines show uncertainty of certified value at $k=2$.

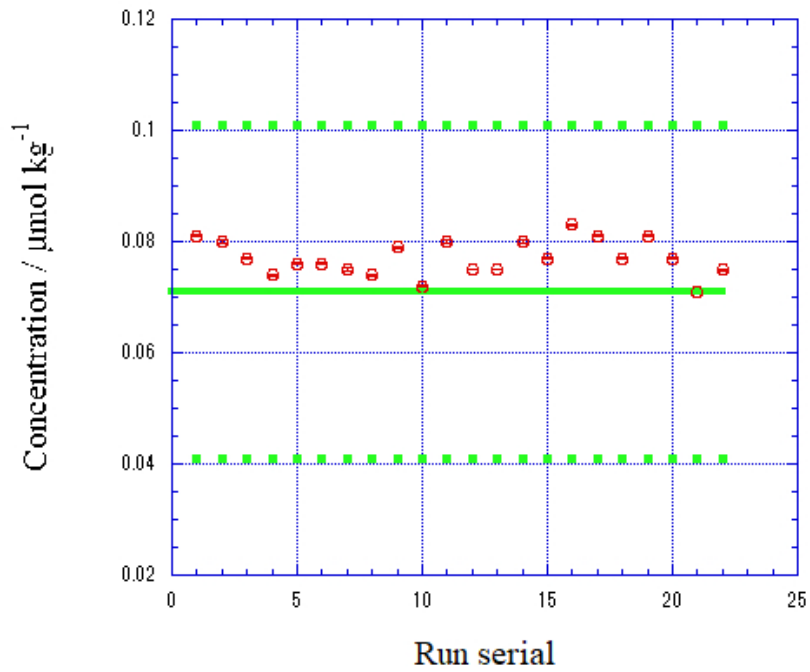


Figure 4.2-13: Same as Figure 4.2-12, but for nitrite.

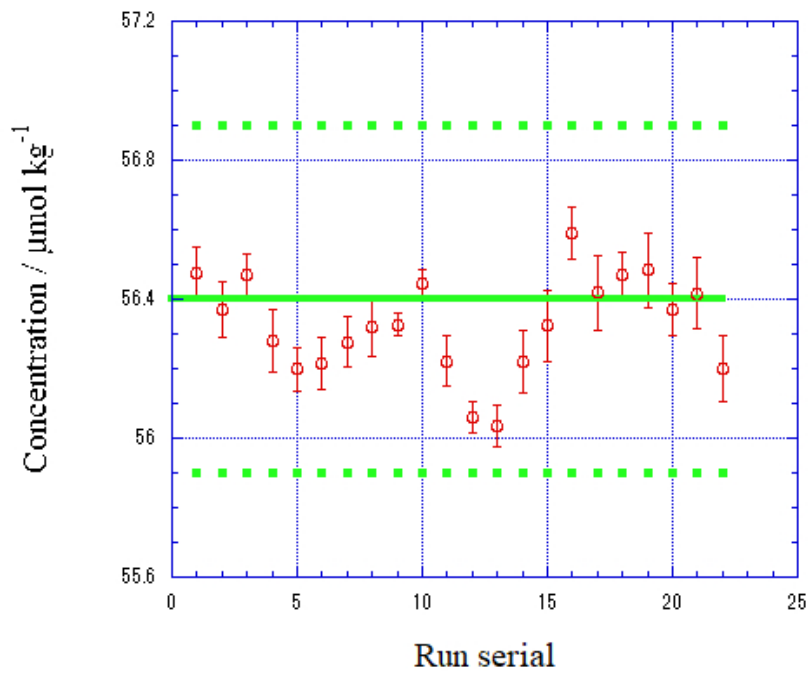


Figure 4.2-14: Same as Figure 4.2-12, but for silicate.

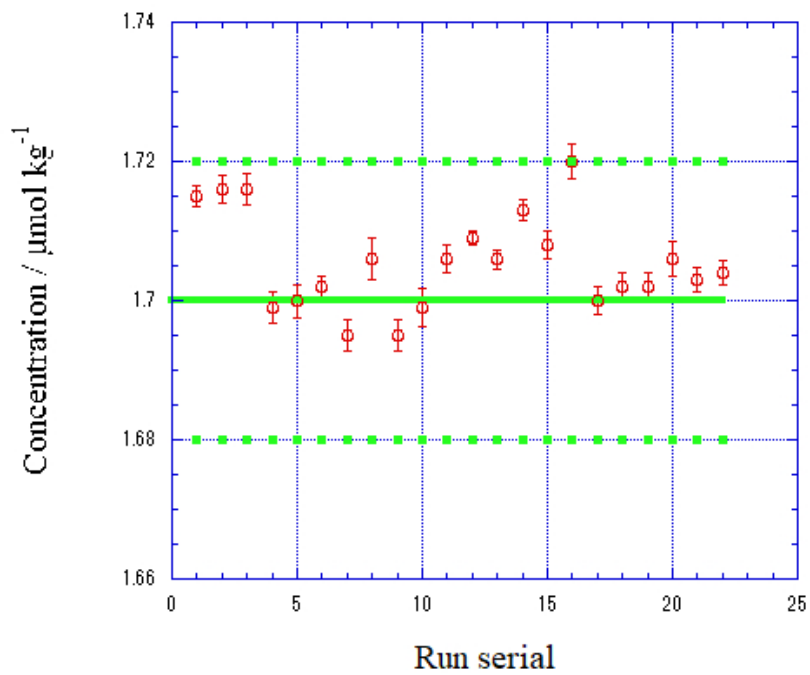


Figure 4.2-15: Same as Figure 4.2-12, but for phosphate.

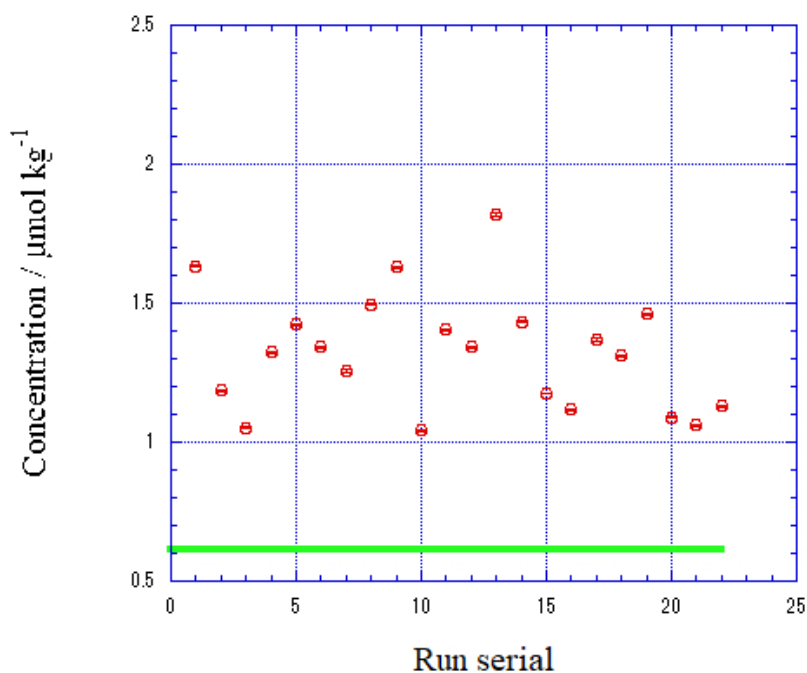


Figure 4.2-16: Time series of CRM-CG of ammonia in this cruise. Solid green line is reference value for ammonia concentration of CRM-CG.

(8-3) Carryover

We also summarized the magnitudes of carryover throughout the cruise. In order to evaluate carryover in each run, we conducted determinations of C-4 followed by determination of LNSW twice. The difference between LNSW-1 and LNSW-2 was obtained and used for this “carryover” evaluation. The Carryover (%) was obtained from the following equation.

$$\text{Carryover (\%)} = (\text{LNSW-1} - \text{LNSW-2}) / (\text{C-4} - \text{LNSW-2}) * 100 (\%)$$

The summary of the carryover (%) is shown in Table 4.2-9 and Figures 4.2-17 to 4.2-21. The results were low % (<0.2 % for nitrate, nitrite and phosphate; <0.3 % for silicate; <1.0 % for ammonia). The low % indicates that there is no significant issue during this cruise.

Table 4.2-9: Summary of carryover throughout this cruise.

	Nitrate %	Nitrite %	Silicate %	Phosphate %	Ammonia %
Median	0.18	0.09	0.24	0.17	0.69
Mean	0.18	0.09	0.23	0.16	0.70
Maximum	0.23	0.20	0.28	0.26	1.03
Minimum	0.14	0.00	0.17	0.00	0.48
N	22	22	22	22	22

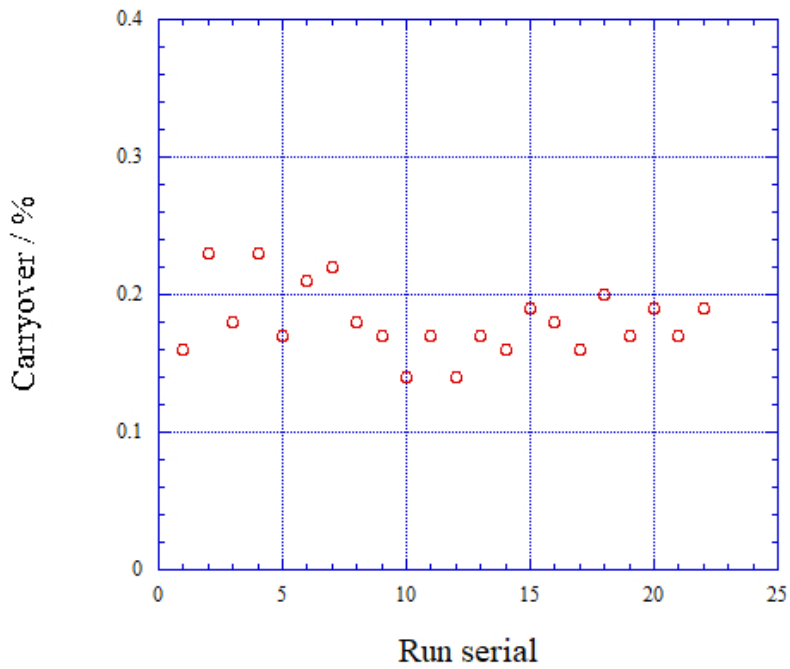


Figure 4.2-17: Time series of carryover of nitrate in MR22-06C.

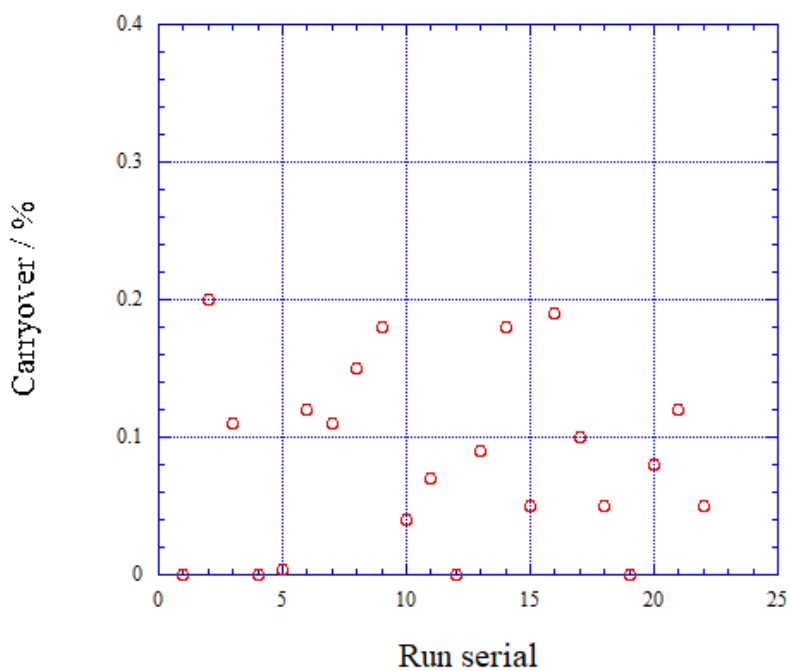


Figure 4.2-18: Same as 4.2-17, but for nitrite.

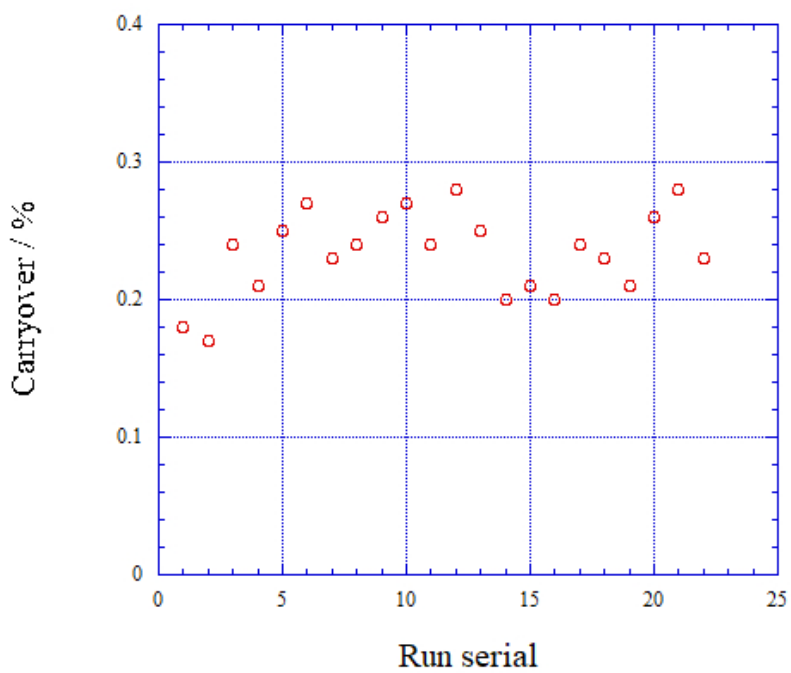


Figure 4.2-19: Same as 4.2-17, but for silicate

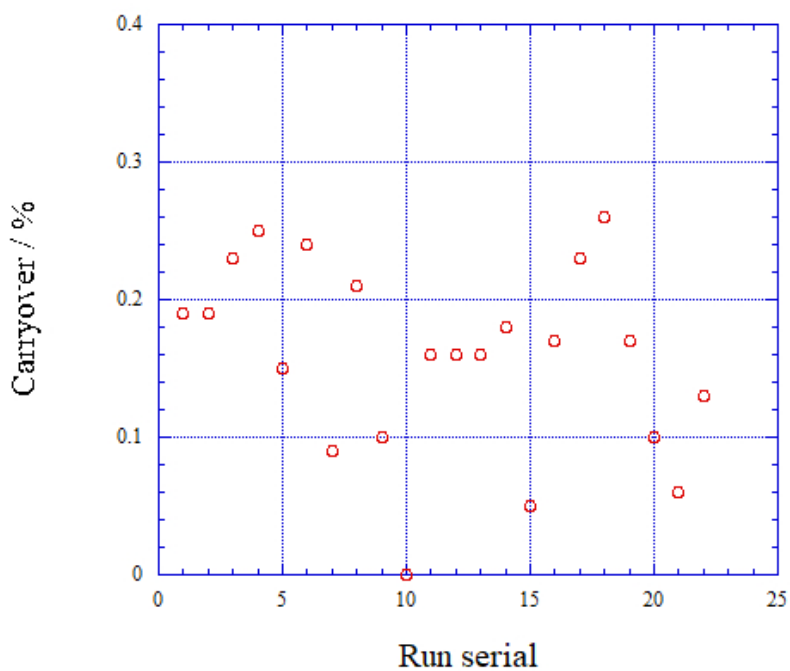


Figure 4.2-20: Same as 4.2-17, but for phosphate.

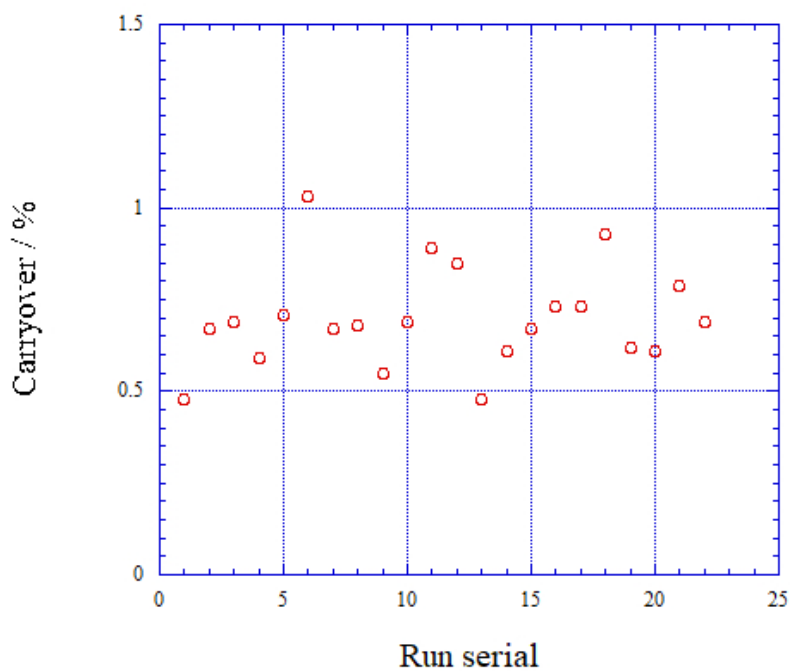


Figure 4.2-21: Same as 4.2-17, but for ammonia.

(8-4) Estimation of uncertainty of nitrate, silicate, phosphate, nitrite and ammonia concentrations

Empirical equations, eq. (1) and (2) to estimate the uncertainty of measurement of silicate and phosphate were obtained based on 22 measurements of 22

sets of CRMs (Table 4.2-3). These empirical equations are as follows, respectively.

Silicate Concentration C_{SiO_2} in $\mu\text{mol kg}^{-1}$:

$$\text{Uncertainty of measurement of silicate (\%)} = 0.24987 + 2.1072 * (1 / C_{SiO_2}) \quad \text{--- (1)}$$

where C_{SiO_2} is silicate concentration of sample.

Phosphate Concentration C_{PO_4} in $\mu\text{mol kg}^{-1}$:

$$\text{Uncertainty of measurement of phosphate (\%)} = 0.068209 + 0.44221 * (1 / C_{PO_4}) \quad \text{--- (2)}$$

where C_{PO_4} is phosphate concentration of sample.

Empirical equations, eq. (3), (4) and (5) to estimate the uncertainty of measurement of nitrate, nitrite and ammonia were obtained based on duplicate measurements of the samples.

Nitrate Concentration C_{NO_3} in $\mu\text{mol kg}^{-1}$:

$$\begin{aligned} \text{Uncertainty of measurement of nitrate (\%)} = \\ 0.11708 + 1.073 * (1 / C_{NO_3}) - 0.00027177 * (1 / C_{NO_3}) * (1 / C_{NO_3}) \end{aligned} \quad \text{--- (3)}$$

where C_{NO_3} is nitrate concentration of sample.

Nitrite Concentration C_{NO_2} in $\mu\text{mol kg}^{-1}$:

$$\begin{aligned} \text{Uncertainty of measurement of nitrite (\%)} = \\ 1.4378 + 0.17252 * (1 / C_{NO_2}) + 0.000047438 * (1 / C_{NO_2}) * (1 / C_{NO_2}) \end{aligned} \quad \text{--- (4)}$$

where C_{NO_2} is nitrite concentration of sample.

Ammonia Concentration C_{NH_4} in $\mu\text{mol kg}^{-1}$:

$$\begin{aligned} \text{Uncertainty of measurement of ammonia (\%)} = \\ 0.086137 + 1.5175 * (1 / C_{NH_4}) - 0.0058232 * (1 / C_{NH_4}) * (1 / C_{NH_4}) \end{aligned} \quad \text{--- (5)}$$

where C_{NH_4} is ammonia concentration of sample.

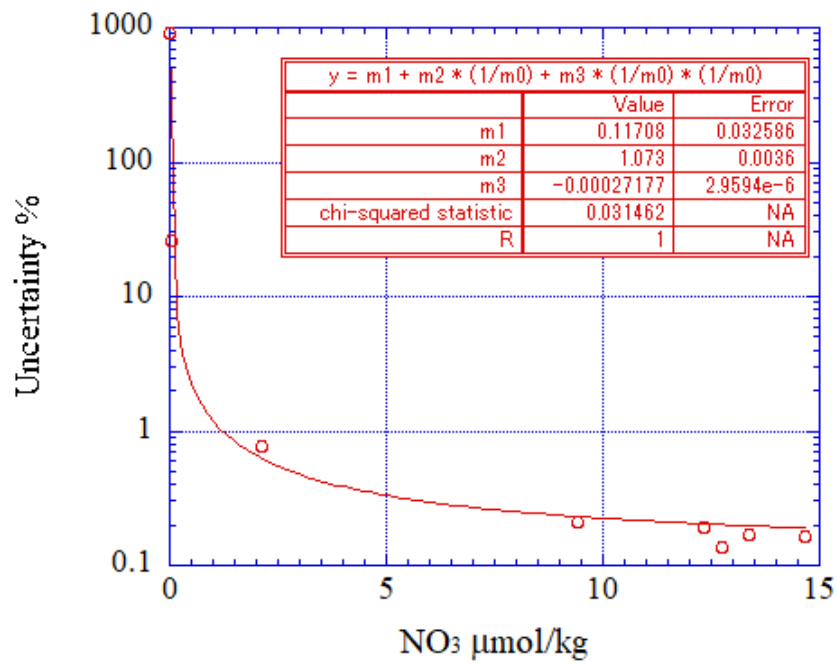


Figure 4.2-22: Estimation of uncertainty for nitrate.

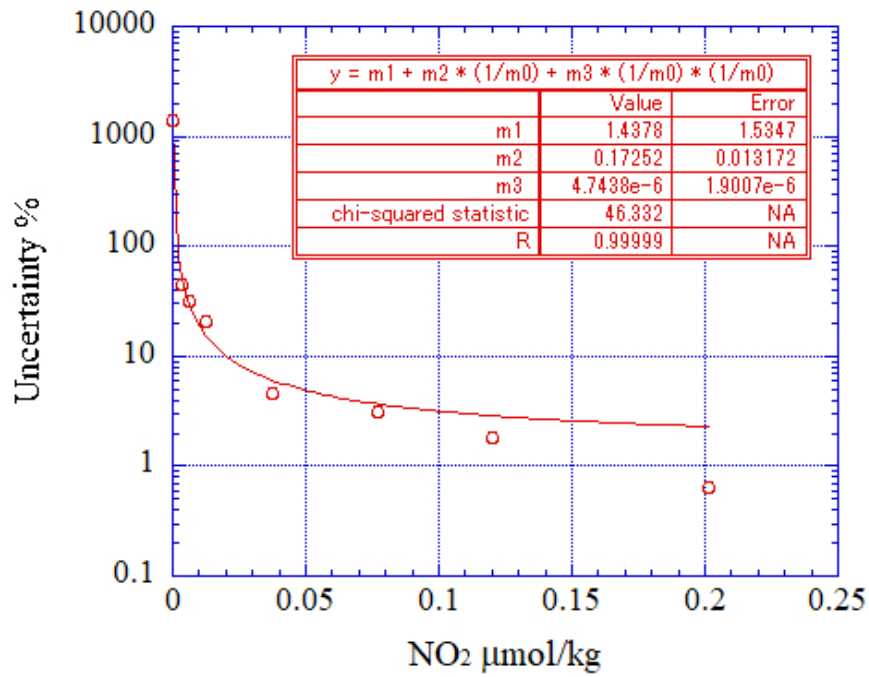


Figure 4.2-23: Estimation of uncertainty for nitrite.

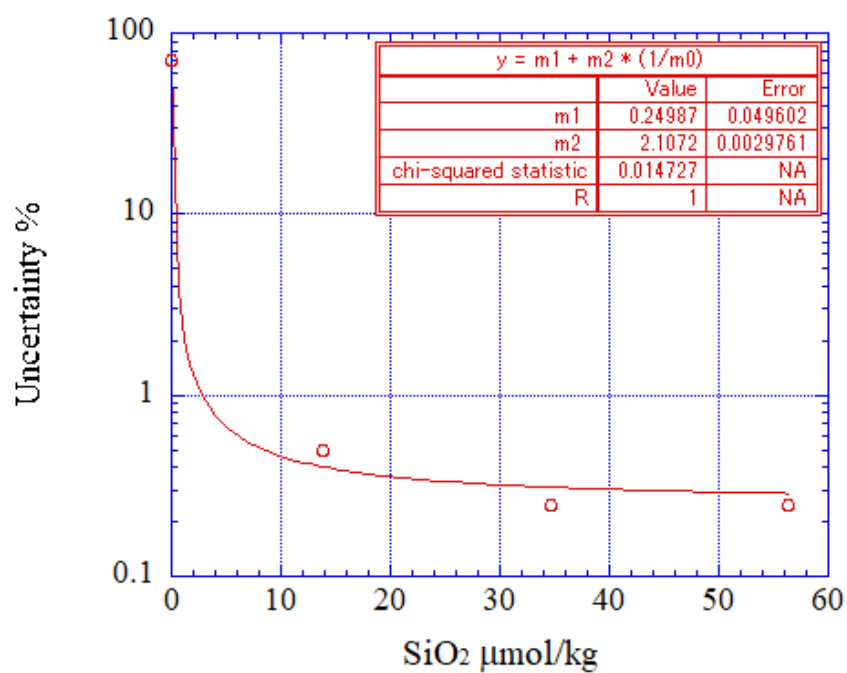


Figure 4.2-24: Estimation of uncertainty for silicate.

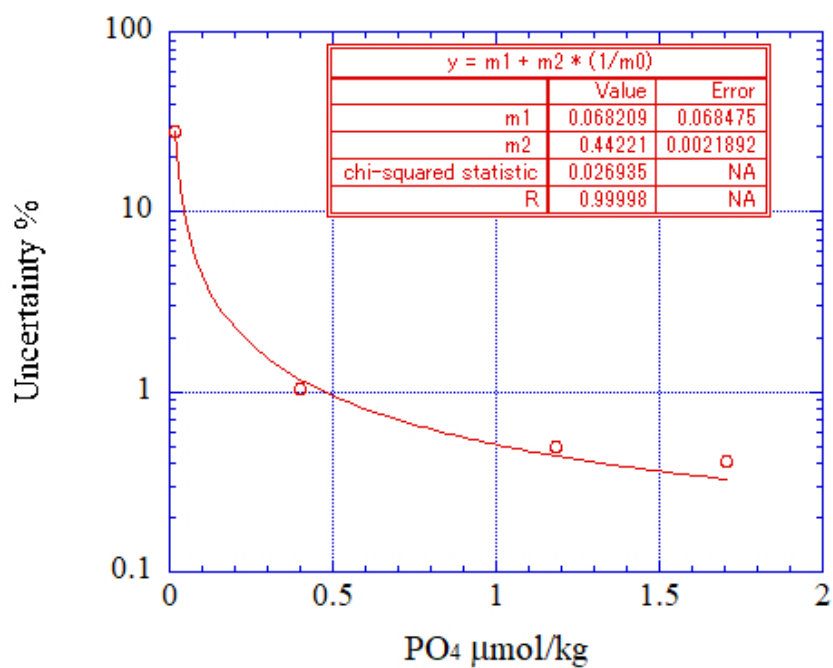


Figure 4.2-25: Estimation of uncertainty for phosphate.

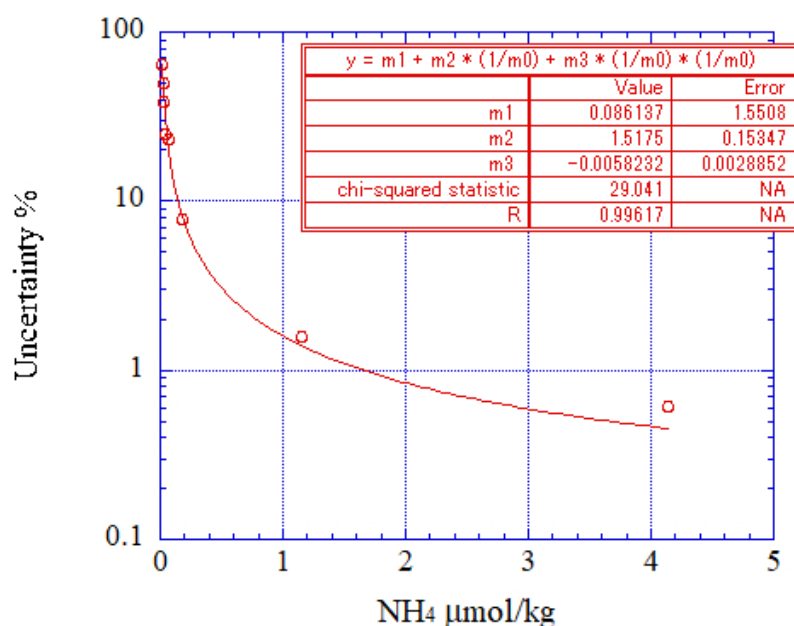


Figure 4.2-26: Estimation of uncertainty for ammonia.

(8-5) Detection limit and quantitative determination of nutrients analyses during the cruise

The LNSW was determined every 2 to 14 samples to obtain detection limit of the nutrient analyses during this cruise. During each run, the total number of the LNSW determination was 6-13 times depending on the run. The detection limit was calculated based on the LNSW results obtained from all the runs by the following equation.

$$\text{Detection limit} = 3 * \text{standard deviation of repeated measurement of LNSW}$$

The summary of detection limit is shown in Table 4.2-10. During this cruise, detection limits were 0.02 $\mu\text{mol kg}^{-1}$ for nitrate, 0.005 $\mu\text{mol kg}^{-1}$ for nitrite, 0.08 $\mu\text{mol kg}^{-1}$ for silicate, 0.010 $\mu\text{mol kg}^{-1}$ for phosphate and 0.03 $\mu\text{mol kg}^{-1}$ for ammonia, respectively.

The quantitative determination of nutrient analyses is the concentration of which uncertainty is 33 % in the empirical equations, eq. (1) to (5) in chapter (8.4). The summary of quantitative determination is shown in Table 4.2-10. During this cruise, the quantitative determination was 0.03 $\mu\text{mol kg}^{-1}$ for nitrate, 0.01 $\mu\text{mol kg}^{-1}$ for nitrite, 0.06 $\mu\text{mol kg}^{-1}$ for silicate, 0.013 $\mu\text{mol kg}^{-1}$ for phosphate and 0.04 $\mu\text{mol kg}^{-1}$ for ammonia, respectively.

Table 4.2-10: Summary of detection limit and quantitative determination.

	Nitrate $\mu\text{mol kg}^{-1}$	Nitrite $\mu\text{mol kg}^{-1}$	Silicate $\mu\text{mol kg}^{-1}$	Phosphate $\mu\text{mol kg}^{-1}$	Ammonia $\mu\text{mol kg}^{-1}$
Detection limit	0.02	0.005	0.08	0.010	0.03
Quantitative determination	0.03	0.01	0.06*	0.013	0.04

* Estimated quantitative determination was within $\pm 1\sigma$ of the calculated detection limit.

(9) Problems and our actions/solutions and remarks

There was no significant issue for this dataset.

In terms of the QuAAtro 39-J, used for the first time during this cruise, the stability of the flow rates and the repeatability have been improved and the data processing was simplified and robust, which reduced our workloads at sea significantly.

(10) List of reagents

List of reagents is shown in Table 4.2-11.

Table 4.2-11: List of reagents in this cruise.

IUPAC name	CAS Number	Formula	Compound Name	Manufacture	Grade
4-Aminobenzenesulfonamide	63-74-1	C ₆ H ₈ N ₂ O ₂ S	Sulfanilamide	FUJIFILM Wako Pure Chemical Corporation	JIS Special Grade
Ammonium chloride	12125-02-9	NH ₄ Cl	Ammonium Chloride	FUJIFILM Wako Pure Chemical Corporation	JIS Special Grade
Antimony potassium tartrate trihydrate	28300-74-5	K ₂ (SbC ₄ H ₂ O ₆) ₂ ·3H ₂ O	Bis[(+)-tartrato]diantimonate(III) Dipotassium Trihydrate	FUJIFILM Wako Pure Chemical Corporation	JIS Special Grade
Boric acid	10043-35-3	H ₃ BO ₃	Boric Acid	FUJIFILM Wako Pure Chemical Corporation	JIS Special Grade
Hydrogen chloride	7647-01-0	HCl	Hydrochloric Acid	FUJIFILM Wako Pure Chemical Corporation	JIS Special Grade
Imidazole	288-32-4	C ₃ H ₄ N ₂	Imidazole	FUJIFILM Wako Pure Chemical Corporation	JIS Special Grade
L-Ascorbic acid	50-81-7	C ₆ H ₈ O ₆	L-Ascorbic Acid	FUJIFILM Wako Pure Chemical Corporation	JIS Special Grade
N-(1-Naphthalenyl)-1,2-ethanediamine, dihydrochloride	1465-25-4	C ₁₂ H ₁₆ Cl ₂ N ₂	N-1-Naphthylethylenediamine Dihydrochloride	FUJIFILM Wako Pure Chemical Corporation	for Nitrogen Oxides Analysis
Oxalic acid	144-62-7	C ₂ H ₂ O ₄	Oxalic Acid	FUJIFILM Wako Pure Chemical Corporation	Wako Special Grade
Phenol	108-95-2	C ₆ H ₆ O	Phenol	FUJIFILM Wako Pure Chemical Corporation	JIS Special Grade
Potassium nitrate	7757-79-1	KNO ₃	Potassium Nitrate	Merck KGaA	Suprapur®
Potassium dihydrogen phosphate	7778-77-0	KH ₂ PO ₄	Potassium dihydrogen phosphate anhydrous	Merck KGaA	Suprapur®
Sodium chloride	7647-14-5	NaCl	Sodium Chloride	FUJIFILM Wako Pure Chemical Corporation	TraceSure®
Sodium citrate dihydrate	6132-04-3	Na ₃ C ₆ H ₅ O ₇ ·2H ₂ O	Trisodium Citrate Dihydrate	FUJIFILM Wako Pure Chemical Corporation	JIS Special Grade
Sodium dodecyl sulfate	151-21-3	C ₁₂ H ₂₅ NaO ₄ S	Sodium Dodecyl Sulfate	FUJIFILM Wako Pure Chemical Corporation	for Biochemistry
Sodium hydroxide	1310-73-2	NaOH	Sodium Hydroxide for Nitrogen Compounds Analysis	FUJIFILM Wako Pure Chemical Corporation	for Nitrogen Analysis
Sodium hypochlorite	7681-52-9	NaClO	Sodium Hypochlorite Solution	Kanto Chemical co., Inc.	Extra pure
Sodium molybdate dihydrate	10102-40-6	Na ₂ MoO ₄ ·2H ₂ O	Disodium Molybdate(VI) Dihydrate	FUJIFILM Wako Pure Chemical Corporation	JIS Special Grade
Sodium nitroferrocyanide dihydrate	13755-38-9	Na ₂ [Fe(CN) ₅ NO]·2H ₂ O	Sodium Pentacyanonitrosylferrate(III) Dihydrate	FUJIFILM Wako Pure Chemical Corporation	JIS Special Grade
Sulfuric acid	7664-93-9	H ₂ SO ₄	Sulfuric Acid	FUJIFILM Wako Pure Chemical Corporation	JIS Special Grade
tetrasodium;2-[2-[bis(carboxylatomethyl)amino]ethyl-(carboxylatomethyl)amino]acetate;tetrahydrate	13235-36-4	C ₁₀ H ₁₂ N ₂ Na ₄ O ₈ ·4H ₂ O	Ethylenediamine-N,N,N',N'-tetraacetic Acid Tetrasodium Salt Tetrahydrate (4NA)	Dojindo Molecular Technologies, Inc.	-
Synonyms: t-Octylphenoxypolyethoxyethanol 4-(1,1,3,3-Tetramethylbutyl)phenyl-polyethylene glycol Polyethylene glycol tert-octylphenyl ether	9002-93-1	(C ₂ H ₄ O) _n C ₁₄ H ₂₂ O	Triton™ X-100	MP Biomedicals, Inc.	-

(11) Data archive

These data obtained in this cruise will be submitted to the Data Management Group of JAMSTEC, and will be opened to the public via “Data Research System for Whole Cruise Information in JAMSTEC (DARWIN)” in JAMSTEC web site.

<<http://www.godac.jamstec.go.jp/darwin/e>>

(12) References

- Susan Becker, Michio Aoyama E. Malcolm S. Woodward, Karel Bakker, Stephen Coverly, Claire Mahaffey, Toste Tanhua, (2019) The precise and accurate determination of dissolved inorganic nutrients in seawater, using Continuous Flow Analysis methods, n: The GO-SHIP Repeat Hydrography Manual: A Collection of Expert Reports and Guidelines. Available online at: <http://www.go-ship.org/HydroMan.html>. DOI: <http://dx.doi.org/10.25607/OBP-555>
- Grasshoff, K. 1976. Automated chemical analysis (Chapter 13) in *Methods of Seawater Analysis*. With contribution by Almgreen T., Dawson R., Ehrhardt M., Fonselius S. H., Josefsson B., Koroleff F., Kremling K. Weinheim, New York: Verlag Chemie.
- Grasshoff, K., Kremling K., Ehrhardt, M. et al. 1999. *Methods of Seawater Analysis*. Third, Completely Revised and Extended Edition. WILEY-VCH Verlag GmbH, D-69469 Weinheim (Federal Republic of Germany).
- Hydes, D.J., Aoyama, M., Aminot, A., Bakker, K., Becker, S., Coverly, S., Daniel, A., Dickson, A.G., Grosso, O., Kerouel, R., Ooijen, J. van, Sato, K., Tanhua, T., Woodward, E.M.S., Zhang, J.Z., 2010. Determination of Dissolved Nutrients (N, P, Si) in Seawater with High Precision and Inter-Comparability Using Gas-Segmented Continuous Flow Analysers, In: *GO-SHIP Repeat Hydrography Manual: A Collection of Expert Reports and Guidelines*. IOCCP Report No. 14, ICPO Publication Series No 134.
- Kimura, 2000. Determination of ammonia in seawater using a vaporization membrane permeability method. 7th auto analyzer Study Group, 39-41.
- Murphy, J., and Riley, J.P. 1962. *Analytica Chimica Acta* 27, 31-36.

4.3. Dissolved Inorganic Carbon

4.3.1. Bottled-water analysis

(1) Personnel

Akihiko Murata	JAMSTEC	Principal Investigator (not on board)
Masahiro Orui	MWJ	Operation Leader
Nagisa Fujiki	MWJ	

(2) Objectives

To clarify vertical distributions of total Dissolved Inorganic Carbon (DIC) in water columns.

(3) Parameters

Total Dissolved Inorganic Carbon (DIC)

(4) Instruments and methods

a. Seawater sampling

Seawater samples were collected by 12 liter sampling bottles mounted on the CTD/Carousel Water Sampling System and a bucket at 33 stations. Seawater was sampled in a 250 mL glass bottle (SHOTT DURAN) that was previously soaked in 5 % alkaline detergent solution at least 3 hours and was cleaned by fresh water for 5 times and Milli-Q ultrapure water for 3 times. A sampling silicone rubber tube with PFA tip was connected to the outlet of Niskin bottle for water sampling. The glass bottles were filled from its bottom gently, without rinsing, and were overflowed by about twice the bottle volume. They were sealed using the polyethylene inner lids with care not to leave any bubbles in the bottle. Immediately after the water sampling on the deck, the glass bottles were carried to the laboratory for the addition of saturated solution of mercury (II) chloride (HgCl_2). Small volume (3 mL) of the sample (1 % of the bottle volume) was removed from the bottle and 100 μL of HgCl_2 was added. Then the samples were sealed by the polyethylene inner lids tightly and stored in a refrigerator at approximately 5 °C. About one hour before the analysis, the samples were taken from refrigerator and put in the water bath kept ~20 °C.

b. Seawater analysis

Measurements of DIC were made with total CO_2 measuring system (Nihon ANS Inc.). The system comprises of seawater dispensing unit, a CO_2 extraction unit, and a coulometer (Model 3000, Nihon ANS Inc.) The seawater dispensing unit has an auto-sampler (10 ports), which dispenses the seawater from a glass bottle to a pipette of nominal 15 mL volume. The pipette was kept at $20.00 \text{ °C} \pm 0.05 \text{ °C}$ by a water jacket, in which water circulated through a thermostatic water bath. The CO_2 dissolved in a seawater sample is extracted in a stripping chamber of the CO_2 extraction unit by adding

10 % phosphoric acid solution. The stripping chamber is made approx. 25 cm long and has a fine frit at the bottom. First, a constant volume of acid is added to the stripping chamber from its bottom by pressurizing an acid bottle with nitrogen gas (99.9999 %). Second, a seawater sample kept in a pipette is introduced to the stripping chamber by the same method. The seawater and phosphoric acid are stirred by the nitrogen bubbles through a fine frit at the bottom of the stripping chamber. The stripped CO₂ is carried to the coulometer through two electric dehumidifiers (kept at 2 °C) and a chemical desiccant (magnesium perchlorate) by the nitrogen gas (flow rate of 140 mL min⁻¹). Measurements of system blank (phosphoric acid blank), 1.5 % CO₂ standard gas in a nitrogen base, and seawater samples (6 samples) were programmed to repeat. The variations of our own made JAMSTEC (batch Q41) and KASNO (batch AW) DIC reference materials were used to correct the signal drift. The values of DIC were set to the certified values of CRM (batch 201) provided by Prof. Dickson, Scripps Institution of Oceanography, Univ. of California.

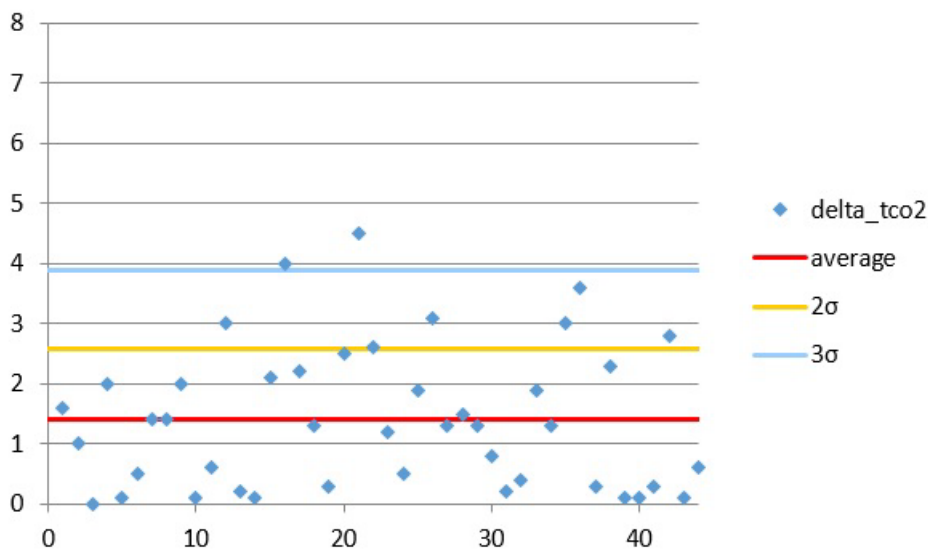


Figure 4.3.1-1: Range control chart of the absolute differences of replicate measurements of DIC carried out during this cruise. The 2 σ and 3 σ indicate the upper control limits of standard deviation (σ) \times 2 and σ \times 3, respectively.

(5) Observation log

Seawater samples were collected at 33 stations.

(6) Preliminary results

A few replicate samples were taken at most of the stations and difference between each pair of analyses was plotted on a range control chart (Figure 4.3.1-1). The repeatability was estimated to be provisionally 1.3 $\mu\text{mol kg}^{-1}$ ($n = 44$).

(7) Data archive

These data obtained in this cruise will be submitted to the Data Management Group of JAMSTEC, and will be opened to the public via “Data Research System for Whole Cruise Information in JAMSTEC (DARWIN)” in JAMSTEC web site.
<http://www.godac.jamstec.go.jp/darwin/e>.

4.3.2. Underway DIC

(1) Personnel

Akihiko Murata	JAMSTEC	Principal Investigator (not on board)
Masahiro Orui	MWJ	Operation Leader
Nagisa Fujiki	MWJ	

(2) Objectives

To elucidate spatial variations of total Dissolved Inorganic Carbon (DIC) concentration in surface seawater.

(3) Parameter

Total Dissolved Inorganic Carbon (DIC)

(4) Instruments and methods

Surface seawater samples for DIC measurement were continuously collected during this cruise. Surface seawater was taken from an intake placed at the approximately 4.5 m below sea surface by a pump, and was filled in a 250 mL glass bottle (SCHOTT DURAN) from the bottom, without rinsing, and overflowed for more than 2 times the amount. Before the analysis, the samples were put in the water bath kept about 20°C for one hour. Measurements of DIC were made with total CO₂ measuring system (Nihon ANS Inc.). The system was comprised of seawater dispensing unit, a CO₂ extraction unit, and a coulometer (Model 3000A, Nihon ANS Inc.). The seawater dispensing unit has an auto-sampler (6 ports), which dispenses the seawater from a glass bottle to a pipette of nominal 15 mL volume. The pipette was kept at 25.00°C ± 0.05 °C by a water jacket, in which water circulated through a thermostatic water bath. The CO₂ dissolved in a seawater sample is extracted in a stripping chamber of the CO₂ extraction unit by adding 10 % phosphoric acid solution. The stripping chamber is made approx. 25 cm long and has a fine frit at the bottom. First, the certain amount of acid is taken to the constant volume tube from an acid bottle and transferred to the stripping chamber from its bottom by nitrogen gas (99.9999 %). Second, a seawater sample kept in a pipette is introduced to the stripping chamber by the same method as that for an acid. The seawater and phosphoric acid are mixed by the nitrogen bubbles through a fine frit at the bottom of the stripping chamber. The stripped CO₂ is carried to the coulometer through two electric dehumidifiers (kept at 2 °C) and a chemical desiccant (Magnesium perchlorate) by the nitrogen gas (flow rate of 140 mL min⁻¹). Measurements of approx. 1.5 % CO₂ standard gas in a nitrogen base, system blank (phosphoric acid blank), and seawater samples (6 samples) were programmed to repeat. Both CO₂ standard gas and blank signals were used to correct the signal drift results from chemical alternation of coulometer solutions. The coulometer solutions were renewed every about 2 days, and JAMSTEC reference

materials (batch Q41) and CRM (batch 201) were measured to correct systematic difference between measurements.

(5) Observation log

The cruise track during underway DIC observation is shown in Figure 4.3.2-1(a).

(6) Results

Temporal variations of DIC in surface water are shown in Figure 4.3.2-1(b), together with those of Sea Surface Temperature: SST (c) and salinity (d).

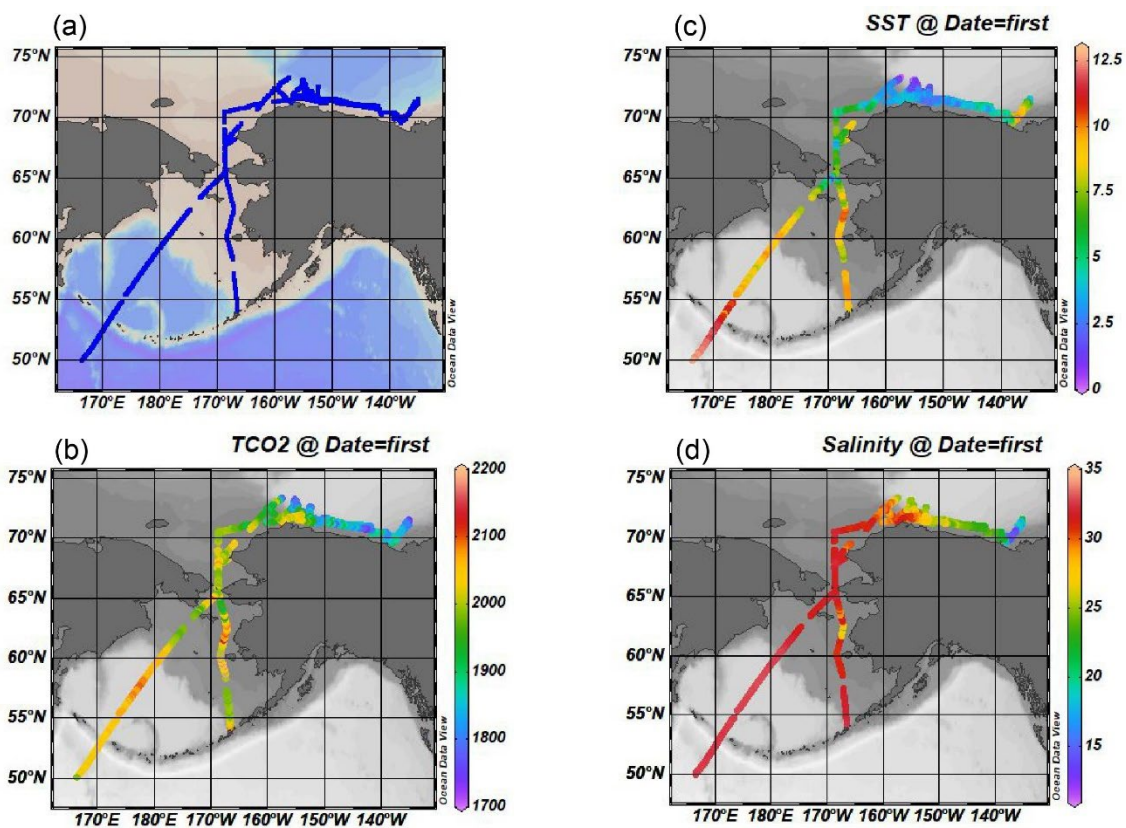


Figure 4.3.2-1: (a) Cruise track for underway DIC measurements in MR22-06C. (b) Distributions of DIC in surface seawater. (c) Same as (b) but for SST. (d) Same as (b) but for salinity.

(7) Date archive

These data obtained in this cruise will be submitted to the Data Management Group (DMG) of JAMSTEC, and will open to the public via “Data Research System for Whole Cruise Information in JAMSTEC (DARWIN)” in JAMSTEC web site. <http://www.godac.jamstec.go.jp/darwin/e>.

4.4. Total Alkalinity

(1) Personnel

Akihiko Murata	JAMSTEC	Principal Investigator (not on board)
Nagisa Fujiki	MWJ	Operation Leader
Masahiro Orui	MWJ	

(2) Objectives

To survey influences of sea ice melting water and river input on carbonate system properties.

(3) Parameters

Total Alkalinity (TA)

(4) Instruments and methods

a. Seawater sampling

Seawater samples were collected by 12 L Niskin bottles mounted on the CTD/Carousel Water Sampling System and a bucket at 33 stations. The seawater from the Niskin bottle was filled into 250 or 100 mL borosilicate glass bottles (SHOTT DURAN) using a sampling silicone rubber tube with PFA tip. The water was filled into the bottle from the bottom smoothly, without rinsing, and overflowed for 2 times bottle volume (20 or 10 seconds). These bottles were pre-washed in advance by soaking in 5 % alkaline detergent for more than 3 hours, and then rinsed 5 times with tap water and 3 times with Milli-Q deionized water. The samples were stored in a refrigerator at approximately 5 °C before the analysis, and were put in the water bath with its temperature of about 25 °C for one hour before analysis.

b. Seawater analysis

TA was measured using a spectrophotometric system (Nihon ANS, Inc.) using a scheme of Yao and Byrne (1998). The calibrated volume of sample seawater was transferred from a sample bottle into the titration cell with its light path length of 4 cm long via dispensing unit. The TA is calculated by measuring two sets of absorbance at three wavelengths (730, 616 and 444) nm with the spectrometer (TM-UV/VIS C10082CAH, HAMAMATSU). One is the absorbance of seawater sample before injecting an acid with indicator solution (bromocresol green sodium) and another is the one after the injection. To mix the acidified-indicator solution with seawater sufficiently, the mixed solution is circulated in a circulation line by a peristaltic pump for 5 minutes. Nitrogen bubbles were introduced into the titration cell for degassing CO₂ from the mixed solution sufficiently. The TA is calculated based on the following equation:

$$TA = (-[H^+]_T V_{SA} + M_A V_A) / V_S,$$

where M_A is the molarity of the acid titrant added to the seawater sample, $[H^+]_T$ is the total excess hydrogen ion concentration in the seawater, and V_S , V_A and V_{SA} are the initial seawater volume, the added acid titrant volume, and the combined seawater plus acid titrant volume, respectively. $[H^+]_T$ is calculated from the measured absorbances based on the following equation (Yao and Byrne, 1998):

$$pH_T = -\log[H^+]_T = 4.2699 + 0.002578(35 - S) + \log((R - 0.00131)/(2.3148 - 0.1299R)) - \log(1 - 0.001005S),$$

where S is the sample salinity, and R is the absorbance ratio calculated as:

$$R = (A_{616} - A_{730}) / (A_{444} - A_{730}),$$

where A_i is the absorbance at wavelength i nm.

(5) Observation log

Seawater samples were collected at 33 stations.

(6) Preliminary results

The repeatability of this system was provisionally $1.5 \mu\text{mol kg}^{-1}$ ($n = 43$), which was calculated from replicate samples. A range control chart of TA measurement is illustrated in Figure 4.4-1.

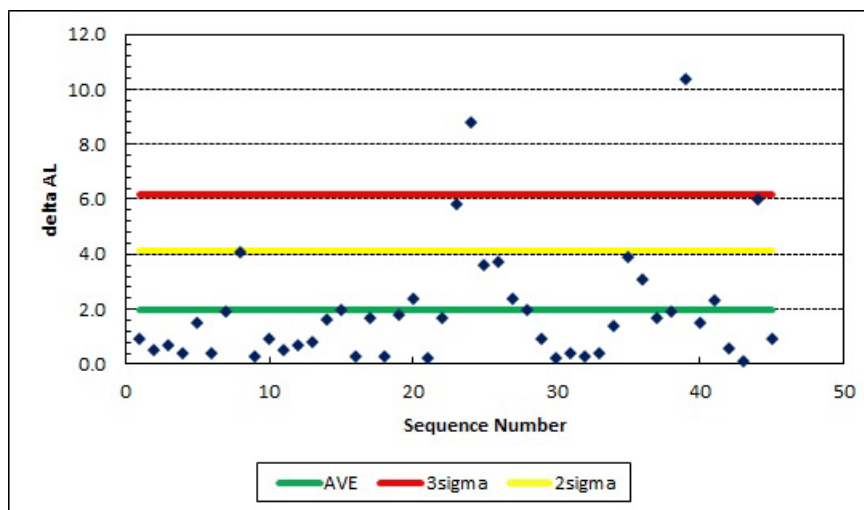


Figure 4.4-1: Range control chart of the absolute differences of replicate measurements of TA. The AVE indicates average. The 2 and 3 sigma indicate the upper control limits of $\sigma \times 2$ and that $\times 3$, respectively.

We usually measure reference materials (KANSO RM, batch AW and JAMSTEC RM, batch Q41) and certified RM (CRM, batch 201) provided by Prof. Dickson of SIO to monitor data quality of TA. If a measuring system works well, the measurements of RMs should show a constant value within a margin of error. In this cruise, however, we observed drifts or shifts of the RMs and CRM measurements, which had been never observed in past cruises. As the variations appeared just after measurements of seawater samples, we suspected contaminations due to water samples. We washed some parts of the measuring system with alkali and acid detergents, and replaced them with new ones. However, we could not resolve the problems completely. We list measurements of TA in the data file, but the data are all tentative. When you use the TA data, please contact to the PI (Akihiko Murata: murataa@jamstec.go.jp).

(7) Date archive

These data obtained in this cruise will be submitted to the Data Management Group (DMG) of JAMSTEC, and will open to the public via “Data Research System for Whole Cruise Information in JAMSTEC (DARWIN)” in JAMSTEC web site.

<http://www.godac.jamstec.go.jp/darwin/e>.

4.5. Chlorophyll *a*

(1) Personnel

Amane Fujiwara (JAMSTEC): Principal Investigator, not on board

Erii Irie (Marine Works Japan Ltd.; MWJ): Operation leader

Katsunori Sagishima (MWJ)

(2) Objectives

Phytoplankton support the base of the marine ecosystem and play important roles in the biogeochemical cycles. To comprehend the distribution of phytoplankton biomass and their size composition, we investigated the vertical and horizontal distributions of total and size-fractionated chlorophyll-*a* concentration in the seawater.

(3) Parameters

Total chlorophyll *a*

Size-fractionated chlorophyll *a*

(4) Instruments and methods

We collected samples for total chlorophyll *a* (chl-*a*) concentration from 7 to 14 depths and size-fractionated chl-*a* from 5 to 7 depths between the surface and 200 m depth including a chl-*a* maximum layer. The chl-*a* maximum layer was determined by an in-water fluorometer (Seapoint Sensors, Inc.) attached to the CTD system. Replicate water samples were taken at chl-*a* maximum depth from the same Niskin bottle to assess the precision of chl-*a* measurements.

Seawater samples for total chl-*a* were vacuum-filtrated (< 0.02 MPa) through the 25mm-diameter ADVANTEC GF-75 filter. Seawater samples for size-fractionated chl-*a* were passed through 20- μ m pore-size nylon filter (47 mm in diameter), 2- μ m pore-size polyester membrane filter (47 mm in diameter), and ADVANTEC GF-75 (25 mm in diameter) under gentle vacuum (< 0.02 MPa).

Each filter sample was immediately soaked in 7 ml of N,N-dimethylformamide (DMF, Wako Pure Chemical Industries Ltd.) in a polypropylene tube (Suzuki and Ishimaru, 1990). The tubes were stored at -20 °C under the dark condition to extract chl-*a* at least for 24 hours. Some tubes were kept at -80°C until the extraction.

Chl-*a* concentrations were measured by a bench-top fluorometer (10-AU, TURNER DESIGNS) following to the method of Welschmeyer (1994). The 10-AU fluorometer was calibrated against a pure chl-*a* (Sigma-Aldrich Co., LLC) prior to the analysis.

(5) Observation Log

The samples for total chl-*a* were collected at 33 sites (Figure 4.5-1) and the samples for size-fractionated chl-*a* were collected at 17 casts in the Arctic Ocean (Figure 4.5-2), respectively.

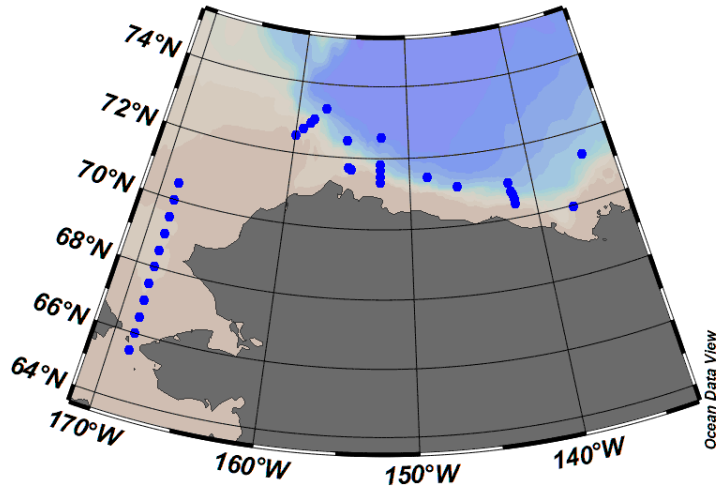


Figure 4.5-1: Sampling positions of total chl-*a*.

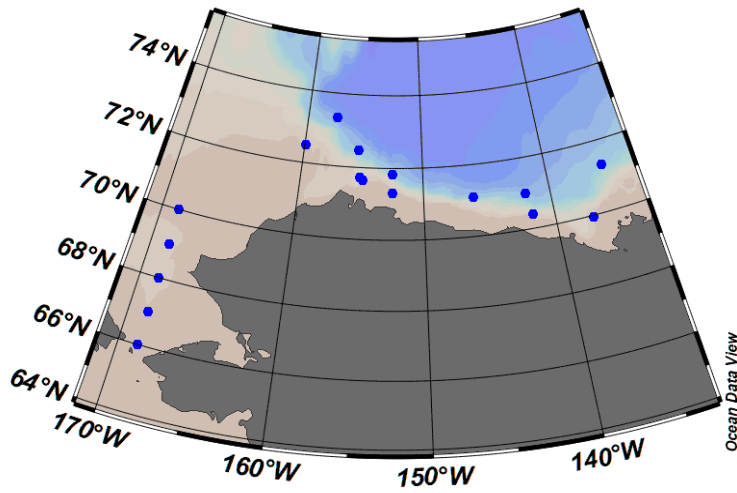


Figure 4.5-2: Sampling positions of size-fractionated chl-*a*.

(6) Preliminary results

The surface distribution of total chl-*a* in the Arctic Ocean are shown in Figure 4.5-3.

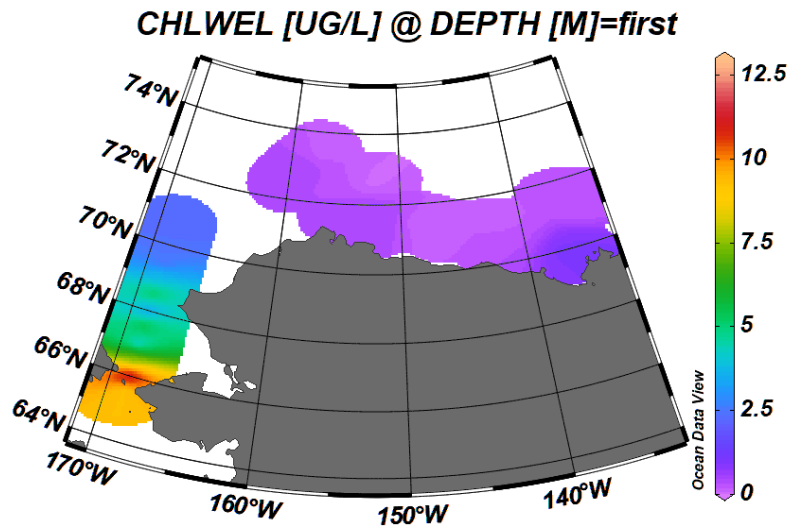


Figure 4.5-3: Surface distribution of total chl-*a*.

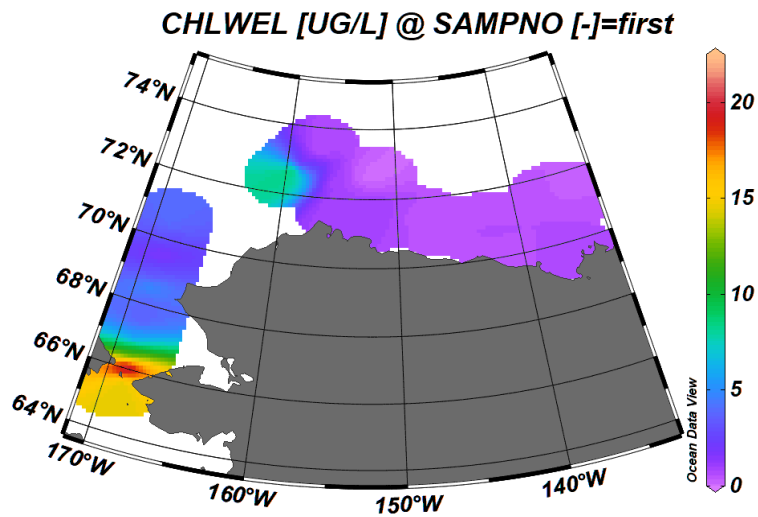


Figure 4.5-4: Distribution of total chl-*a* at the Chl-*a* maximum layer.

At some stations, water samples were collected in replicate at chlorophyll-*a* maximum layer to evaluate the precision of sampling and measurement. The results of the evaluation are shown in Table 4.5-1.

Table 4.5-1: Results of the replicate sample measurements.

Number of replicate sample pairs	Standard deviation (μgL^{-1})	Relative error (%)
33	0.145	3.4

(7) Data archive

The data obtained in this cruise will be submitted to the Data Management Group of JAMSTEC, and will be opened to the public via “Data Research System for Whole Cruise Information in JAMSTEC (DARWIN)” on the JAMSTEC website.

<<http://www.godac.jamstec.go.jp/darwin/e>>

4.6. 18O

(1) Personnel

Michiyo Yamamoto-Kawai Tokyo University of Marine Science and Technology
Mariko Hatta JAMSTEC – Principal investigator
Haruka Tsujimoto Tokyo University of Marine Science and Technology

(2) Objectives

Oxygen isotope of seawater ($\delta^{18}\text{O}$) is a useful tracer to distinguish freshwater sources in seawater between sea ice meltwater and meteoric water. It also provides information about how much sea ice has been formed from seawater (brine content). During the cruise of MR22-06C, seawater samples for analysis of $\delta^{18}\text{O}$ were collected at selected stations and depths. The data will be used to quantify changes in biogeochemical properties (such as nutrients and carbonate parameters) due to dilution by sea ice meltwater, mixing with river runoff, or/and to formation of sea ice.

(3) Parameters

- Oxygen isotopic ratio ($\delta^{18}\text{O}$, $\text{H}_2^{18}\text{O}/\text{H}_2^{16}\text{O}$)

(4) Instruments and methods

Seawater samples were collected from Niskin bottles into glass bottles. Of total 175 samples, 7 were taken in duplicate to check precision of data. Two types of bottles were used: 15·20mL vials sealed without large air bubbles; 50 mL bottles were double-sealed with an inter cap and outer screw cap.

See 4.12.2 for instruments and methods for analysis of $\delta^{18}\text{O}$.

(5) Station list or Observation log

Station	Date (UTC)	Latitude (N)	Longitude (W)	Sampling depth (m)
001	2022/8/24	65.5	168.7	5, 10, 20, 30, 50
002	2022/8/24	66.0	168.8	5, 10, 20, 30, 48
003	2022/8/25	66.5	168.7	5
004	2022/8/25	67.0	168.7	5, 10, 20, 30, 39
005	2022/8/25	67.5	168.7	5, 10, 20, 30, 44
006	2022/8/26	68.0	168.7	5, 10, 20, 30, 53
007	2022/8/26	68.5	168.8	5
008	2022/8/26	69.0	168.7	5, 9, 20, 30, 47
009	2022/8/26	69.5	168.8	5
010	2022/8/26	70.0	168.8	5, 10, 20, 29, 36
011	2022/8/27	70.5	168.8	5

012	2022/8/28	71.7	155.0	22, 5, 10, 20, 30, 42, 50, 75, 95
013	2022/8/29	71.7	155.2	5, 10, 20, 30, 49, 75, 99, 124, 149, 173, 198, 223, 248, 295
014	2022/8/30	71.5	148.5	30, 5, 10, 20, 49
015	2022/8/31	71.1	146.1	5, 10, 20, 30, 50
016	2022/8/31	71.0	142.0	5, 10, 20, 29, 49, 99, 148, 173, 197, 249
017	2022/8/31	70.8	141.9	5, 10, 20, 30, 49, 99, 148, 173, 198, 246
018	2022/9/3	71.3	135.5	5, 10, 20, 30, 49
019	2022/9/4	70.0	137.2	5, 10, 20, 30, 52
020	2022/9/5	70.4	141.7	5, 10, 20, 30, 50, 74, 76
021	2022/9/5	70.5	141.7	6, 10, 20, 30, 50, 99, 148, 198, 247
022	2022/9/6	70.7	141.8	5, 10, 20, 30, 50, 99, 149, 198
023	2022/9/8	72.5	155.4	5, 10, 20, 30, 49
024	2022/9/9	71.8	152.5	5, 10, 20, 30, 50
026	2022/9/10	72.6	152.4	6, 10, 20, 30, 50
027	2022/9/10	71.3	152.5	5, 10, 20, 30, 50, 56
028	2022/9/10	71.5	152.5	5, 10, 20, 30, 49
029	2022/9/10	71.7	152.5	5, 10, 20, 30, 50
030	2022/9/14	72.5	160.0	5, 10, 20, 30, 42
031	2022/9/14	72.7	159.4	5, 10, 20, 30, 50
032	2022/9/15	72.9	158.8	5, 10, 20, 29, 50
033	2022/9/15	73.3	157.5	5, 10, 20, 30, 50
034	2022/9/15	73.0	158.5	6, 10, 19, 30, 50

(6) Data archive

These data obtained in this cruise will be submitted to the Data Management Group of JAMSTEC, and will be opened to the public via “Data Research System for Whole Cruise Information in JAMSTEC (DARWIN)” in JAMSTEC web site. <<http://www.godac.jamstec.go.jp/darwin/e>>

4.7. Iodine-129

(1) Personnel

Yuichiro Kumamoto

Japan Agency for Marine-Earth Science and Technology (Not on board)

(2) Objectives

In order to investigate the water circulation and ventilation process in the Bering Sea and Arctic Ocean, seawater samples were collected for measurements of iodine-129.

(3) Parameters

¹²⁹I

(4) Instruments and methods

Surface seawater samples were collected from continuous pumped-up water from about 4-m depth at 17 stations. We also collected seawater samples vertically from the sea surface to near bottom layer at three stations. The sampling stations are summarized in Table 4.7-1. The seawater sample was collected into a 1-L plastic bottle after two time washing. The total number of the seawater samples is 59.

Iodine-129 in the seawater sample is extracted using solvent extraction with carrier iodine added. The sample is precipitated as silver iodide and ¹²⁹I/¹²⁷I is measured using accelerator mass spectrometry at the MALT (Micro Analysis Laboratory, Tandem accelerator), The University of Tokyo. 5mL aliquot of the sample is measured for ¹²⁷I by ICP-MS.

(5) Station list

Table 4.7-1: Sampling stations for iodine-129 measurement.

No.	Station		Date (UTC)	Time (UTC)	Latitude	Longitude
1	P-1	start	2022/8/17	08:16	50-57.7940N	167-55.7942E
		end	2022/8/17	08:23	50-58.7528N	167-57.5201E
2	P-2	start	2022/8/18	02:35	53-50.8426N	172-21.3444E
		end	2022/8/18	02:41	53-51.2843N	172-23.3738E
3	P-3	start	2022/8/19	06:23	54-04.4174N	178-22.6815W
		end	2022/8/19	06:32	54-04.5311N	178-19.5065W
4	P-4	start	2022/8/22	13:07	55-56.7267N	166-53.1346W
		end	2022/8/22	13:11	55-57.4524N	166-53.3112W
5	P-5	start	2022/8/23	04:48	58-53.3484N	167-34.5779W

		end	2022/8/23	05:06	58-56.4977N	167-36.7108W
6	P-6	start	2022/8/23	18:31	61-25.5749N	167-43.8551W
		end	2022/8/23	18:37	61-26.7291N	167-43.2315W
7	P-7	start	2022/8/24	06:43	63-51.1831N	167-48.7441W
		end	2022/8/24	07:13	63-52.1415N	167-52.1415W
8	P-8	start	2022/8/24	16:25	65-30.4168N	168-45.0550W
		end	2022/8/24	16:50	65-30.0541N	168-44.9712W
9	P-9	start	2022/8/26	16:12	68-59.9148N	168-43.6487W
		end	2022/8/26	16:17	68-59.9460N	168-43.6363W
10	P-10	start	2022/8/27	03:24	70-29.9794N	168-45.5974W
		end	2022/8/27	03:43	70-30.0417N	168-45.9690W
11	P-11	start	2022/8/30	22:08	71-27.2525N	148-32.0680W
		end	2022/8/30	22:33	71-27.2629N	148-32.0922W
12	P-12	start	2022/8/31	23:18	70-47.5981N	141-51.8192W
		end	2022/8/31	23:24	70-47.6197N	141-51.9184W
13	P-13	start	2022/9/2	13:09	71-10.0487N	135-10.2329W
		end	2022/9/2	13:45	71-10.0698N	135-09.7521W
14	P-14	start	2022/9/4	17:13	69-43.1433N	138-08.9350W
		end	2022/9/4	17:43	69-43.1386N	138-08.9209W
15	P-15	start	2022/9/10	04:35	72-35.0545N	152-25.8924W
		end	2022/9/10	05:01	72-35.0393N	152-26.1730W
16	P-16	start	2022/9/18	18:45	63-04.7800N	173-42.8558W
		end	2022/9/18	18:56	63-03.0883N	173-45.8641W
17	P-17	start	2022/9/19	19:25	59-04.3753N	179-32.1651E
		end	2022/9/19	19:48	59-00.4219N	179-26.1967E
18	11	-	2022/8/27	03:40	70-30.03N	168-45.92E
19	14	-	2022/9/19	19:25	59-04.3753N	179-32.1651E
20	26	-	2022/9/19	19:25	59-04.3753N	179-32.1651E

(6) Data archive

These data obtained in this cruise will be submitted to the Data Management Group of JAMSTEC, and will be opened to the public via “Data Research System for Whole Cruise Information in JAMSTEC (DARWIN)” in JAMSTEC web site.

<<http://www.godac.jamstec.go.jp/darwin/e>>

4.8. Uranium-236

(1) Personnel

Yuichiro Kumamoto

Japan Agency for Marine-Earth Science and Technology (Not on board)

(2) Objectives

In order to investigate the water circulation and ventilation process in the Bering Sea and Arctic Ocean, seawater samples were collected for measurements of uranium-236.

(3) Parameters

^{236}U

(4) Instruments and methods

Surface seawater samples were collected from continuous pumped-up water from about 4-m depth at 17 stations. We also collected seawater samples vertically from the sea surface to near bottom layer at three stations. The sampling stations are summarized in Table 4.8-1. The seawater sample was collected into a 5-L plastic container after two-time washing. The total number of the seawater samples is 59.

Uranium-236 in the seawater sample is co-precipitated with Fe hydroxide and purified by UTEVA[®] resin. The purified sample is co-precipitated as uranium oxide with 1.5 mg Fe hydroxide and $^{236}\text{U}/^{238}\text{U}$ is measured using accelerator mass spectrometry at MALT, The University of Tokyo. 5mL aliquot of the sample is measured for ^{238}U by ICP-MS.

(5) Station list

Table 4.8-1: Sampling stations for uranium-236 measurement.

No.	Station		Date (UTC)	Time (UTC)	Latitude	Longitude
1	P-1	start	2022/8/17	08:16	50-57.7940N	167-55.7942E
		end	2022/8/17	08:23	50-58.7528N	167-57.5201E
2	P-2	start	2022/8/18	02:35	53-50.8426N	172-21.3444E
		end	2022/8/18	02:41	53-51.2843N	172-23.3738E
3	P-3	start	2022/8/19	06:23	54-04.4174N	178-22.6815W
		end	2022/8/19	06:32	54-04.5311N	178-19.5065W
4	P-4	start	2022/8/22	13:07	55-56.7267N	166-53.1346W
		end	2022/8/22	13:11	55-57.4524N	166-53.3112W
5	P-5	start	2022/8/23	04:48	58-53.3484N	167-34.5779W
		end	2022/8/23	05:06	58-56.4977N	167-36.7108W
6	P-6	start	2022/8/23	18:31	61-25.5749N	167-43.8551W

		end	2022/8/23	18:37	61-26.7291N	167-43.2315W
7	P-7	start	2022/8/24	06:43	63-51.1831N	167-48.7441W
		end	2022/8/24	07:13	63-52.1415N	167-52.1415W
8	P-8	start	2022/8/24	16:25	65-30.4168N	168-45.0550W
		end	2022/8/24	16:50	65-30.0541N	168-44.9712W
9	P-9	start	2022/8/26	16:12	68-59.9148N	168-43.6487W
		end	2022/8/26	16:17	68-59.9460N	168-43.6363W
10	P-10	start	2022/8/27	03:24	70-29.9794N	168-45.5974W
		end	2022/8/27	03:43	70-30.0417N	168-45.9690W
11	P-11	start	2022/8/30	22:08	71-27.2525N	148-32.0680W
		end	2022/8/30	22:33	71-27.2629N	148-32.0922W
12	P-12	start	2022/8/31	23:18	70-47.5981N	141-51.8192W
		end	2022/8/31	23:24	70-47.6197N	141-51.9184W
13	P-13	start	2022/9/2	13:09	71-10.0487N	135-10.2329W
		end	2022/9/2	13:45	71-10.0698N	135-09.7521W
14	P-14	start	2022/9/4	17:13	69-43.1433N	138-08.9350W
		end	2022/9/4	17:43	69-43.1386N	138-08.9209W
15	P-15	start	2022/9/10	04:35	72-35.0545N	152-25.8924W
		end	2022/9/10	05:01	72-35.0393N	152-26.1730W
16	P-16	start	2022/9/18	18:45	63-04.7800N	173-42.8558W
		end	2022/9/18	18:56	63-03.0883N	173-45.8641W
17	P-17	start	2022/9/19	19:25	59-04.3753N	179-32.1651E
		end	2022/9/19	19:48	59-00.4219N	179-26.1967E
18	11	-	2022/8/27	03:40	70-30.03N	168-45.92E
19	14	-	2022/8/30	22:41	71-27.27N	148-32.15E
20	26	-	2022/9/10	01:01	72-35.41N	152-24.84E

(6) Data archive

These data obtained in this cruise will be submitted to the Data Management Group of JAMSTEC, and will be opened to the public via “Data Research System for Whole Cruise Information in JAMSTEC (DARWIN)” in JAMSTEC web site.

<<http://www.godac.jamstec.go.jp/darwin/e>>

4.9. Polycyclic Aromatic Hydrocarbons (PAHs)

(1) Personnel

Yuichiro Kumamoto

Japan Agency for Marine-Earth Science and Technology (Not on board)

(2) Objectives

Determination of Polycyclic Aromatic Hydrocarbons (PAHs) concentration in surface seawater in the Arctic Ocean and Bering Sea.

(3) Parameters

Polycyclic Aromatic Hydrocarbons (PAHs)

(4) Instruments and methods

Surface seawater samples were collected from continuous pumped-up water from about 4-m depth. The sampling stations are summarized in Table 4.9-1. The total 17 seawater samples for PAHs measurement were collected at 17 stations. The seawater sample was collected into a 10-L stainless container after two-time washing. Just after the water sampling, 300 ml of methanol was added.

Particulate and dissolved phases of 10 L seawater sample are separated by filtration through 0.5 μm glass-fiber filters. Dissolved organic compounds, including PAHs, are concentrated using C18 solid-phase extraction disks. Particulate and dissolved PAHs are respectively extracted from the glass-fiber filters using an ultrasonic method and eluted from the C18 disks with dichloromethane. Dimethyl sulfoxide is added to both extracted solutions, the dichloromethane is evaporated to dryness, and the residue of dimethyl sulfoxide is dissolved in acetonitrile. PAHs in the samples were quantified using the HPLC system with a fluorescence detector.

(5) Station list

Table 4.9-1: Seawater samples collected for PAHs measurement.

No.	Station		Date (UTC)	Time (UTC)	Latitude	Longitude
1	P-1	start	2022/8/17	08:16	50-57.7940N	167-55.7942E
		end	2022/8/17	08:23	50-58.7528N	167-57.5201E
2	P-2	start	2022/8/18	02:35	53-50.8426N	172-21.3444E
		end	2022/8/18	02:41	53-51.2843N	172-23.3738E
3	P-3	start	2022/8/19	06:23	54-04.4174N	178-22.6815W
		end	2022/8/19	06:32	54-04.5311N	178-19.5065W
4	P-4	start	2022/8/22	13:07	55-56.7267N	166-53.1346W
		end	2022/8/22	13:11	55-57.4524N	166-53.3112W

5	P-5	start	2022/8/23	04:48	58-53.3484N	167-34.5779W
		end	2022/8/23	05:06	58-56.4977N	167-36.7108W
6	P-6	start	2022/8/23	18:31	61-25.5749N	167-43.8551W
		end	2022/8/23	18:37	61-26.7291N	167-43.2315W
7	P-7	start	2022/8/24	06:43	63-51.1831N	167-48.7441W
		end	2022/8/24	07:13	63-52.1415N	167-52.1415W
8	P-8	start	2022/8/24	16:25	65-30.4168N	168-45.0550W
		end	2022/8/24	16:50	65-30.0541N	168-44.9712W
9	P-9	start	2022/8/26	16:12	68-59.9148N	168-43.6487W
		end	2022/8/26	16:17	68-59.9460N	168-43.6363W
10	P-10	start	2022/8/27	03:24	70-29.9794N	168-45.5974W
		end	2022/8/27	03:43	70-30.0417N	168-45.9690W
11	P-11	start	2022/8/30	22:08	71-27.2525N	148-32.0680W
		end	2022/8/30	22:33	71-27.2629N	148-32.0922W
12	P-12	start	2022/8/31	23:18	70-47.5981N	141-51.8192W
		end	2022/8/31	23:24	70-47.6197N	141-51.9184W
13	P-13	start	2022/9/2	13:09	71-10.0487N	135-10.2329W
		end	2022/9/2	13:45	71-10.0698N	135-09.7521W
14	P-14	start	2022/9/4	17:13	69-43.1433N	138-08.9350W
		end	2022/9/4	17:43	69-43.1386N	138-08.9209W
15	P-15	start	2022/9/10	04:35	72-35.0545N	152-25.8924W
		end	2022/9/10	05:01	72-35.0393N	152-26.1730W
16	P-16	start	2022/9/18	18:45	63-04.7800N	173-42.8558W
		end	2022/9/18	18:56	63-03.0883N	173-45.8641W
17	P-17	start	2022/9/19	19:25	59-04.3753N	179-32.1651E
		end	2022/9/19	19:48	59-00.4219N	179-26.1967E

(6) Data archive

These data obtained in this cruise will be submitted to the Data Management Group of JAMSTEC, and will be opened to the public via “Data Research System for Whole Cruise Information in JAMSTEC (DARWIN)” in JAMSTEC web site.

<<http://www.godac.jamstec.go.jp/darwin/e>>

4.10. Radiocesium

(1) Personnel

Yuichiro Kumamoto

Japan Agency for Marine-Earth Science and Technology (Not on board)

(2) Objectives

In order to investigate the water circulation and ventilation process in the Bering Sea and Arctic Ocean, seawater samples were collected for measurements of radiocesium.

(3) Parameters

^{137}Cs and ^{134}Cs

(4) Instruments and methods

Surface seawater samples were collected from continuous pumped-up water from about 4-m depth. The sampling stations are summarized in Table 4.10-1. The total 9 seawater samples for radiocesium measurement were collected at 9 stations. The seawater sample was collected into two 20-L plastic containers (40 L each) after two-time washing.

Radiocesium in seawater samples will be concentrated using KNiFC-PAN resin (Eichrom, NC-B200-M, 100-600 μm). A volume of the resin bed is about 5 ml and a flow rate of seawater passing is about 50 ml/min. The radiocesium in the resin will be measured using Ge γ -ray spectrometers.

(5) Station list

Table 4.10-1: Seawater samples collected for radiocesium measurement.

No.	Station		Date (UTC)	Time (UTC)	Latitude	Longitude
1	P-5	start	2022/8/23	04:48	58-53.3484N	167-34.5779W
		end	2022/8/23	05:06	58-56.4977N	167-36.7108W
2	P-7	start	2022/8/24	06:43	63-51.1831N	167-48.7441W
		end	2022/8/24	07:13	63-52.1415N	167-52.1415W
3	P-8	start	2022/8/24	16:25	65-30.4168N	168-45.0550W
		end	2022/8/24	16:50	65-30.0541N	168-44.9712W
4	P-10	start	2022/8/27	03:24	70-29.9794N	168-45.5974W
		end	2022/8/27	03:43	70-30.0417N	168-45.9690W
5	P-11	start	2022/8/30	22:08	71-27.2525N	148-32.0680W
		end	2022/8/30	22:33	71-27.2629N	148-32.0922W
6	P-13	start	2022/9/2	13:09	71-10.0487N	135-10.2329W
		end	2022/9/2	13:45	71-10.0698N	135-09.7521W

7	P-14	start	2022/9/4	17:13	69-43.1433N	138-08.9350W
		end	2022/9/4	17:43	69-43.1386N	138-08.9209W
8	P-15	start	2022/9/10	04:35	72-35.0545N	152-25.8924W
		end	2022/9/10	05:01	72-35.0393N	152-26.1730W
9	P-17	start	2022/9/19	19:25	59-04.3753N	179-32.1651E
		end	2022/9/19	19:48	59-00.4219N	179-26.1967E

(6) Data archive

These data obtained in this cruise will be submitted to the Data Management Group of JAMSTEC, and will be opened to the public via “Data Research System for Whole Cruise Information in JAMSTEC (DARWIN)” in JAMSTEC web site.

<<http://www.godac.jamstec.go.jp/darwin/e>>

4.11. Radium isotopes

(1) Personnel

Yuichiro Kumamoto

Japan Agency for Marine-Earth Science and Technology (Not on board)

(2) Objectives

In order to investigate the water circulation and ventilation process in the Bering Sea and Arctic Ocean, seawater samples were collected for measurements of radium isotopes.

(3) Parameters

^{226}Ra and ^{228}Ra

(4) Instruments and methods

Surface seawater samples were collected from continuous pumped-up water from about 4-m depth. The sampling stations are summarized in Table 4.11-1. The total 9 seawater samples for radium isotopes measurement were collected at 9 stations. The seawater sample was collected into a 20-L plastic container after two-time washing.

In our laboratory on shore, Ra-free Barium carrier and SO_4^{2-} are added to the seawater sample to coprecipitate radium with BaSO_4 . After evaporating to dryness, the BaSO_4 fractions are compressed to disc as a mixture of $\text{Fe}(\text{OH})_3$ and NaCl for gamma-ray spectrometry using Ge-detectors.

(5) Station list

Table 4.11-1: Seawater samples collected for radium isotopes measurement.

No.	Station		Date (UTC)	Time (UTC)	Latitude	Longitude
1	P-5	start	2022/8/23	04:48	58-53.3484N	167-34.5779W
		end	2022/8/23	05:06	58-56.4977N	167-36.7108W
2	P-7	start	2022/8/24	06:43	63-51.1831N	167-48.7441W
		end	2022/8/24	07:13	63-52.1415N	167-52.1415W
3	P-8	start	2022/8/24	16:25	65-30.4168N	168-45.0550W
		end	2022/8/24	16:50	65-30.0541N	168-44.9712W
4	P-10	start	2022/8/27	03:24	70-29.9794N	168-45.5974W
		end	2022/8/27	03:43	70-30.0417N	168-45.9690W
5	P-11	start	2022/8/30	22:08	71-27.2525N	148-32.0680W
		end	2022/8/30	22:33	71-27.2629N	148-32.0922W
6	P-13	start	2022/9/2	13:09	71-10.0487N	135-10.2329W
		end	2022/9/2	13:45	71-10.0698N	135-09.7521W

7	P-14	start	2022/9/4	17:13	69-43.1433N	138-08.9350W
		end	2022/9/4	17:43	69-43.1386N	138-08.9209W
8	P-15	start	2022/9/10	04:35	72-35.0545N	152-25.8924W
		end	2022/9/10	05:01	72-35.0393N	152-26.1730W
9	P-17	start	2022/9/19	19:25	59-04.3753N	179-32.1651E
		end	2022/9/19	19:48	59-00.4219N	179-26.1967E

(6) Data archive

These data obtained in this cruise will be submitted to the Data Management Group of JAMSTEC, and will be opened to the public via “Data Research System for Whole Cruise Information in JAMSTEC (DARWIN)” in JAMSTEC web site.

<<http://www.godac.jamstec.go.jp/darwin/e>>

4.12. Underway surface water monitoring

4.12.1. Basic biogeochemical analyses

(1) Personnel

Amane Fujiwara (JAMSTEC): Principal Investigator (Not on board)

Erii Irie (MWJ) : Operation leader

Katsunori Sagishima (MWJ)

(2) Objectives

Our purpose is to obtain temperature, salinity, dissolved oxygen, fluorescence, turbidity, total dissolved gas pressure and refractive index density data continuously in near-sea surface water.

(3) Parameters

Temperature

Salinity

Dissolved oxygen

Fluorescence

Turbidity

Total dissolved gas pressure

Refractive index density

(4) Instruments and methods

The Continuous Sea Surface Water Monitoring System (Marine Works Japan Ltd.) has seven sensors and automatically measures temperature, salinity, dissolved oxygen, fluorescence, turbidity, total dissolved gas pressure and refractive index density in near-sea surface water every one minute. This system is located in the “sea surface monitoring laboratory” and connected to the shipboard LAN-system. Measured data, time, and location of the ship were stored in a data management PC. Sea water was continuously pumped up to the laboratory from an intake placed at the approximately 4.5 m below the sea surface and flowed into the system through a vinyl-chloride pipe. The flow rate of the surface seawater was adjusted to $10 \text{ dm}^3 \text{ min}^{-1}$.

Instruments

Software

Seamoni Ver.1.2.0.0

Sensors

Specifications of each sensor in this system are listed below.

Temperature and Conductivity sensor

Model:	SBE-45, Sea-Bird Electronics, Inc.
Serial number:	4557820-0319
Measurement range:	Temperature $-5\text{ }^{\circ}\text{C}$ - $+35\text{ }^{\circ}\text{C}$ Conductivity 0 S m^{-1} - 7 S m^{-1}
Initial accuracy:	Temperature $0.002\text{ }^{\circ}\text{C}$ Conductivity 0.0003 S m^{-1}
Typical stability (per month):	Temperature $0.0002\text{ }^{\circ}\text{C}$ Conductivity 0.0003 S m^{-1}
Resolution:	Temperature $0.0001\text{ }^{\circ}\text{C}$ Conductivity 0.00001 S m^{-1}

Bottom of ship thermometer

Model:	SBE 38, Sea-Bird Electronics, Inc.
Serial number:	38-1299
Measurement range:	$-5\text{ }^{\circ}\text{C}$ - $+35\text{ }^{\circ}\text{C}$
Initial accuracy:	$\pm 0.001\text{ }^{\circ}\text{C}$
Typical stability (per 6 month):	$0.001\text{ }^{\circ}\text{C}$
Resolution:	$0.00025\text{ }^{\circ}\text{C}$

Dissolved oxygen sensor

Model:	RINKO II, JFE Advantech Co. Ltd
Serial number:	0035
Measuring range:	0 mg L^{-1} - 20 mg L^{-1}
Resolution:	0.001 mg L^{-1} - 0.004 mg L^{-1} ($25\text{ }^{\circ}\text{C}$)
Accuracy:	Saturation $\pm 2\%$ F.S. (non-linear) (1 atm , $25\text{ }^{\circ}\text{C}$)

Fluorescence & Turbidity sensor

Model:	C3, Turner Designs, Inc.
Serial number:	2300707
Measuring range:	Chlorophyll in vivo $0\text{ }\mu\text{g L}^{-1}$ – $500\text{ }\mu\text{g L}^{-1}$
Minimum Detection Limit:	Chlorophyll in vivo $0.03\text{ }\mu\text{g L}^{-1}$

Measuring range: Turbidity 0 NTU - 1500 NTU
 Minimum Detection Limit: Turbidity 0.05 NTU

Total dissolved gas pressure sensor

Model: HGTD-Pro, Pro- Oceanus Systems Inc
 Serial number: 36-296-10
 Temperature range: -2 °C - 50 °C
 Resolution: 0.0001 %
 Accuracy: 0.01 % (Temperature Compensated)
 Sensor Drift: 0.02 % per year max (0.001 % typical)

Refractive index density

Model: Prototype 1, JAMSTEC (Uchida et al. 2019)
 Serial number: 4D020050 (SI-F80SO [55095])

(5) Observation log

Periods of measurement, maintenance, and problems during this cruise are listed in Table 4.12.1-1.

Table 4.12.1-1: Events list of the Sea surface water monitoring during MR22-06C

System Date [UTC]	System Time [UTC]	Events	Remarks
2022/08/12	09:15	Start data logging	
2022/08/13	04:14-05:04	C3 Maintenance.	-
2022/08/21	00:01	All the measurements stopped.	Pump stopped
2022/08/22	04:04		
2022/08/26	09:48-10:03	Filter Cleaning.	-
2022/09/07	18:19-18:39	Filter Cleaning.	-
2022/09/13	22:34-23:01	Filter Cleaning.	-
2022/09/13	19:55	Piping repair	Air intrusion into piping
2022/09/14	05:12		
2022/09/25	23:00	End data logging	

We took the surface water samples with this system once a day to compare sensor data with bottle data of dissolved oxygen and chlorophyll a. The results are shown in

Figure 4.12.1-1. All the dissolved oxygen samples were analyzed by the Winkler method (see 4.1), and chlorophyll *a* were analyzed by 10-AU manufactured by Turner Designs (see 4.5).

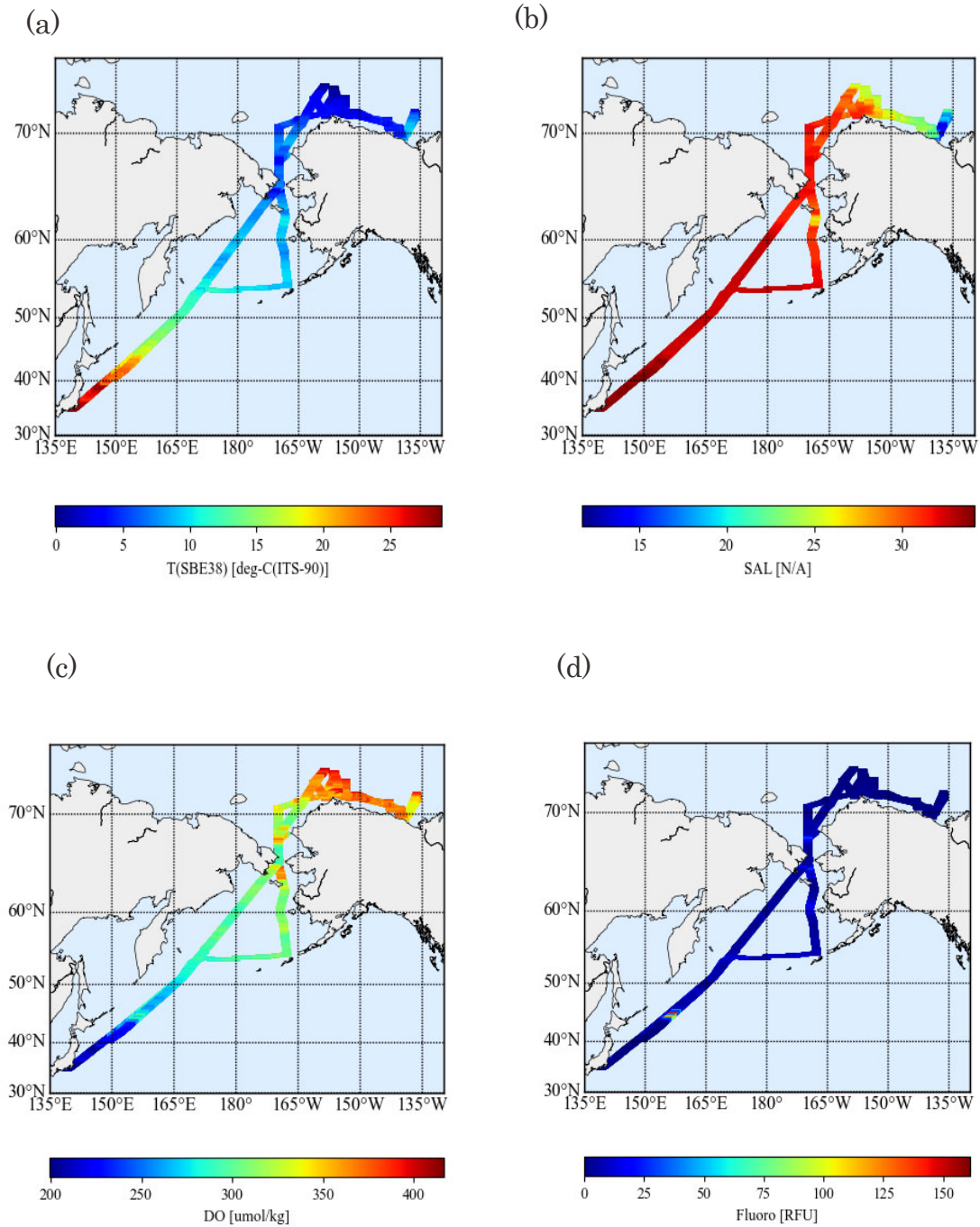


Figure 4.12.1-1: Spatial and temporal distribution of (a) temperature, (b) salinity, (c) dissolved oxygen, and (d) fluorescence in MR22-06C cruise.

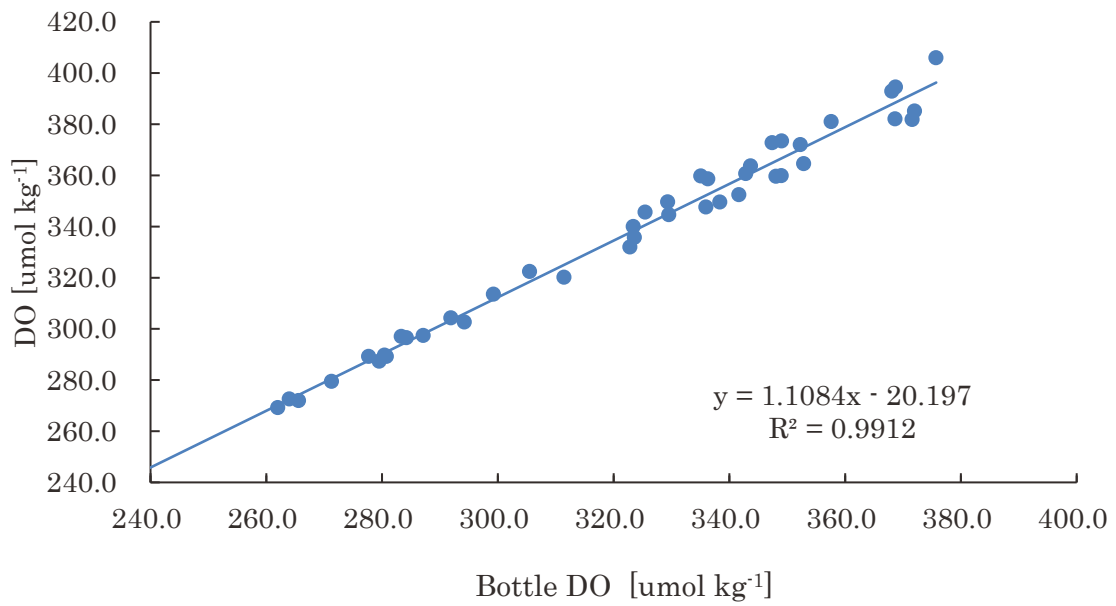


Figure 4.12.1-2: Correlation of dissolved oxygen between sensor data and bottle data.

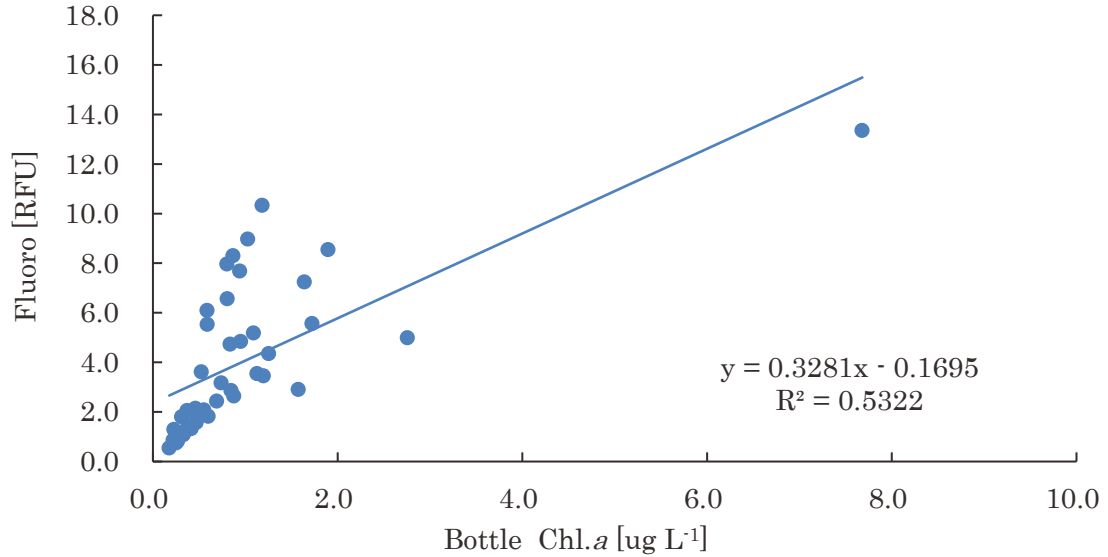


Figure 4.12.1-3: Relationship between the underway measured fluorescence data and bottle sampled Chl-*a* concentration.

(6) Data archive

The data obtained in this cruise will be submitted to the Data Management Group (DMG) of JAMSTEC, and will be opened to the public via “Data Research System for Whole Cruise Information in JAMSTEC (DARWIN)” on the JAMSTEC website.

<<http://www.godac.jamstec.go.jp/darwin/e>>

4.12.2. Discrete samplings

(1) Personnel

Mariko Hatta	JAMSTEC – Principal investigator
Michiyo Yamamoto-Kawai	Tokyo University of Marine Science and Technology
Daiki Nomura	Hokkaido University (Not on board)

(2) Objectives

Meltwater and river water flows into the ocean surface, which greatly affects the chemical composition and biological activities. By clarifying what proportion of seawater/sea ice melt/glacial meltwater/river water is mixed in, we can evaluate how each of them affects the other. For this purpose, we collected the discrete samples for the stable oxygen isotopic ratio of water ($\delta^{18}\text{O}$), nutrients (NO_2 , NO_3 , NH_3 , PO_4 , $\text{Si}(\text{OH})_4$), and total alkalinity analysis.

(3) Parameters

- Oxygen isotopic ratio ($\delta^{18}\text{O}$)
- Nutrient (NO_2 , NO_3 , NH_3 , PO_4 , $\text{Si}(\text{OH})_4$)
- Total alkalinity

(4) Instruments and methods

Nutrient and alkalinity methods and data from MWJ are reported in Chapter 4.2 and Chapter 4.4.

Oxygen isotopic ratio ($\delta^{18}\text{O}$): Discrete samples were collected into glass vials (15-20mL) and sealed well without any additional air bubbles.

Obtained samples will be determined at a shore-based laboratory by a subcontractor. Samples will be determined by an isotope ratio mass spectrometer (Thermo Scientific Delta V Advantage) equipped with an inlet system including an autosampler (NAKANO ELECTRONICS INC.). Samples will be determined together with a reference CO_2 gas ($\delta^{18}\text{O}$ vs VSMOW = 27.88‰, Lot. SKS) and several pre-determined seawaters (DOW3, AGW, SLW4, VSMOW = -0.072, -18.58, -9.62‰, respectively).

The general analytical procedure is as follows:

(1) Pipet 2 mL of the water sample into a dedicated sample bottle (25 mL) and then put them in the equilibrator at a constant temperature (18°C) and then turn on the infiltrator. The twenty-four samples are prepared as a set at the same time.

(2) Open the valve connected to the rotary pump and exhaust the gas phase in the sample bottle.

(3) Close the valve connected to the rotary pump, open the valve connected to the cylinder gas (carbon dioxide gas), and then introduce the equilibrium gas into the sample bottle. The gas introduction step is conducted at the same time for all sample bottles together.

(4) After introducing the specified volume, the individual valves connected to each sample bottle are closed simultaneously.

(5) The sample bottles are placed in a constant temperature bath for 12 hours.

(6) After the equilibration reaction time, the program automatically introduces equilibrated

gas into the mass spectrometer sample introduction container and then measures the stable isotope ratio.

(7) The reference gas and sample gas are determined six times each.

(8) To maintain the precision, the internal standard deviation of the average value of 6 measurements should be 0.05‰ or less. If there is any issue, rerun those samples.

(9) Calculate the oxygen-stable isotope ratio of the sample based on the working standard and the measurement results of the sample.

(5) Station list or Observation log

#	Sampling time	Latitude	Longitude	Depth
1	2022 8 22 3:35 UTC	54 16.16 N	166 37.65 W	4.5
2	2022 8 22 9:24 UTC	55 16.94 N	166 44.17 W	4.5
3	2022 8 22 15:30 UTC	56 22.08 N	167 0.24 W	4.5
4	2022 8 22 21:27 UTC	57 27.41 N	167 12.31 W	4.5
5	2022 8 23 2:45 UTC	58 30.64 N	167 24.73 W	4.5
6	2022 8 23 9:20 UTC	59 41.5 N	168 6.44 W	4.5
7	2022 8 23 15:20 UTC	60 49.31 N	168 3.84 W	4.5
8	2022 8 23 20:39 UTC	61 50.78 N	167 30.66 W	4.5
9	2022 8 24 4:24 UTC	63 23.49 N	167 34.54 W	4.5
10	2022 8 25 19:43 UTC	67 53.07 N	168 16.71 W	4.5
11	2022 8 25 0:11 UTC	66 12.54 N	168 44.82 W	4.5
12	2022 8 25 23:28 UTC	68 16.04 N	167 8.5 W	4.5
13	2022 8 27 8:45 UTC	70 41.69 N	166 48.56 W	4.5
14	2022 8 28 2:22 UTC	71 12.92 N	161 41.67 W	4.5
15	2022 8 28 10:12 UTC	71 33.9 N	156 42.9 W	4.5
16	2022 8 30 16:14 UTC	71 24.1 N	150 59.13 W	4.5
17	2022 9 1 5:05 UTC	70 17.43 N	138 58.33 W	4.5
18	2022 9 1 6:07 UTC	70 11.26 N	138 24.7 W	4.5
19	2022 9 2 3:30 UTC	70 8.25 N	137 5.2 W	4.5
20	2022 9 2 20:25 UTC	71 27.56 N	135 22.58 W	4.5
21	2022 9 8 4:03 UTC	72 8.45 N	154 24.42 W	4.5
22	2022 9 12 21:24 UTC	73 10.15 N	155 4.35 W	4.5

(6) Data archive

These data obtained in this cruise will be submitted to the Data Management Group of JAMSTEC, and will be opened to the public via “Data Research System for Whole Cruise Information in JAMSTEC (DARWIN)” in JAMSTEC web site. <<http://www.godac.jamstec.go.jp/darwin/e>>

4.12.3. Continuous silicate determination from the surface water pump system

(1) Personnel

Mariko Hatta JAMSTEC

(2) Objectives

The goals of this study are following:

- 1) Establish the shipboard system using programmable flow injection system and identify potential trouble and establish the troubleshooting protocol
- 2) Identify the water mass characteristics with Silicate data together with the dataset obtained from the surface water monitoring system

(3) Parameters

- Conductivity, Temperature, Depth, Turbidity, Chlorophyll, DO from a TSG system
- Silicate (SiO₂) data obtained and determined using the programmable flow injection technique
- Nutrient data from the discrete samples obtained from the surface pump system
- Nutrient data at the station from the bucket during the regular rosette sampling cast

The ranges and accuracies of parameters measured by the TSG are shown in the previous section.

Nutrients data from MWJ were reported elsewhere in this cruise report.

(4) Instruments and methods

(4-1) Instrumentation

The instrument, miniSIA-2 (Global FIA, Fox Island, WA, USA), comprises two high precision, synchronously refilling milliGAT pumps, two thermostated holding coils, a 6-port LOV (model COV-MANI-6, constructed from polymethyl methacrylate, Perspex®) furnished with a module for an external flow cell (Figure 4.12.3-1). All tubing connections, downstream from the milliGAT pumps including the holding coils (volume 1000 µL), were made with 0.8 mm I.D. polytetrafluoroethylene (PTFE). The holding coils were thermostated at room temperature for all silicate analysis. The tubing between the carrier stream reservoirs and the milliGAT pump was made from 1.6 mm I.D. PTFE tubing to minimize degassing under reduced pressure at higher aspiration flow rates. A spectrophotometer (Flame, Ocean Insight, Orlando, FL, USA) and a light source were connected to the flow cells by using optical fibers with 500-µm silica cores encased in 0.8 mm I.D. green PEEK tubing. The end of each fiber exposed to the liquid was cemented with epoxy, cut square, and polished. An Ocean Optics Tungsten Halogen (HL-2000, Ocean Insight, Orlando, FL, USA) light source was used. All assay steps were computer-controlled using commercially available software (FloZF, Global FIA, Fox island, WA, USA). The Linear Light Path (LLP) flow cell was purchased from Global FIA. The outlet of the LLP flow cell, was fitted with a 40-psi flow restrictor (GlobalFIA, Fox Island, WA, USA), which, by elevating the pressure within the flow path, efficiently prevented the formation of microbubbles from spontaneous outgassing.

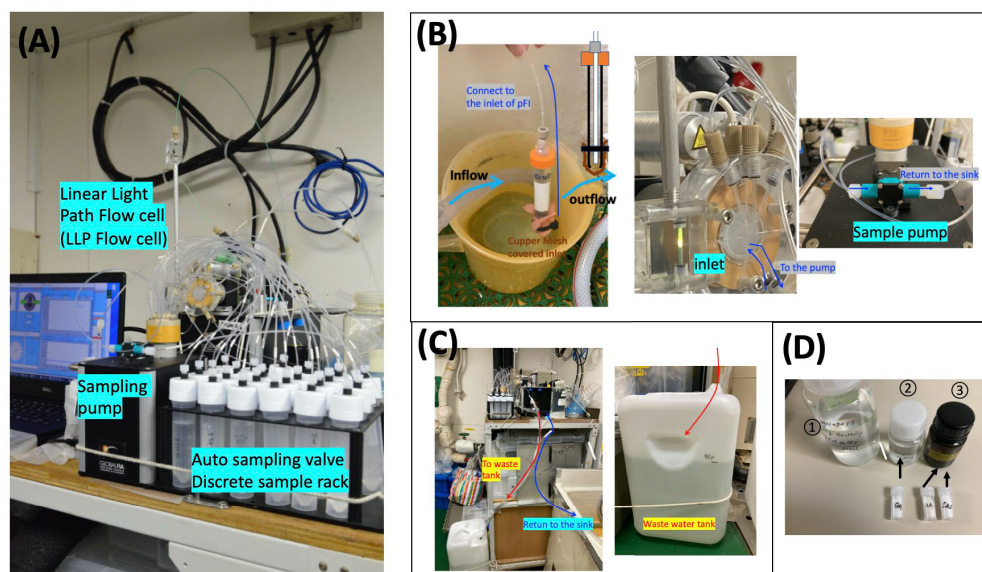


Figure 4.12.3-1: Shipboard analytical system for continuous silicate determination using the programmable flow injection technique (this photo and the set-up are the same as MR21-05C). (A) The mini-SIA2 system and the autosampler. (B) Newly established sampling inlet. (C) The waste water drains system (D) Preparation for the reagents for the Silicate analysis during the cruise.

An inlet of the continuous sampling system was re-built during MR22-05C cruise (Figure 4.12.3-1). The surface water samples were aspirating every ~20 mins using the sample pump for 20 seconds and then homogenized the temperature adjust to the room temperature (25°C) for 20 seconds. After the sample analysis, the flushed surface samples (not mixed with any reagent) were directly returned to the sink. The waste samples/reagents were drained into the waste tank to be stored until the end of the cruise.

(4-2) Analytical methodology

The detailed methodology using programmable flow injection technique was published in Hatta et al., 2021. The details of each reagent and standards were made as follows:

Carrier solution: MilliQ water. Silicate stock standard containing 3.57 mM Si (10 ppm) was prepared by diluting a commercial 1000 ppm Si standard with 0.5 M HCl. This stock solution was further diluted, to obtain working standards (0 to 34 μ M Si) in MilliQ water and sea water (SW). The silica solution had to be neutralized by HCl, because the silica standard is prepared in sodium hydroxide solution (pH12), which must be neutralized to match the pH of MilliQ and SW standard solutions. Using the auto-dilution step, the highest Si standard (34 μ M) was used and diluted with various aspiration volume to obtain the series of the standard solution while the solution was determined.

The acidified molybdate reagent was prepared by dissolving 5 g of ammonium molybdate tetrahydrate crystalline in 500 mL of acidified MilliQ water (2.5 mL of conc. sulfuric acid was added). This solution was stable for 2 months.

The mixed solution of ascorbic acid and SDS solution was prepared by dissolving 3 g of L (+)-

ascorbic acid in 200 mL of MilliQ water, and then 3 g of solid of ultrapure sodium dodecyl sulfate was added into this 3% ascorbic acid solution. Note that it is recommended to prepare this solution 30 min before use, in order to stabilize its reducing strength, as otherwise, the slope of calibration line with freshly prepared reagent will be up to 5% steeper than those obtained later. During the cruise, this solution was prepared one day before and stored in the dark container until it was used.

The oxalic acid solution was prepared by dissolving 2 g of oxalic acid in 100 mL of MilliQ water. The solution was prepared one day before and then stored in a container until it was used.

1M sodium hydroxide solution and 1M EDTA solution were made and used to flush the Holding coil 2 times to avoid any white deposit (calcium oxalate) within the system. This was new protocol established during this cruise.

All of those reagents were top-upped if needed.

Hatta et al., 2021. Programmable flow injection in batch mode: Determination of nutrients in sea water by using a single, salinity independent calibration line, obtained with standards prepared in distilled water, *Talanta*. <https://doi.org/10.1016/j.talanta.2021.122354>.

(5) Station list or Observation log

The surface samples for the continuous determination were collected every 15 mins during the cruise. The location and Si values were shown in Figure 4.12.3-2. Total 1193 samples were determined over 410 hours during this cruise.

(6) Preliminary results

The obtained Si data were shown in Figure 4.13.3-3. The data was taken every 20 mins. The detection limit of this method was <1 μ M (0.3 μ M) during the cruise. The preliminary results of the Si value showed great agreement of the Si value collected at the station while the ship was stopped, and then determined by the shipboard air-segmented classical flow injection method (Figure 4.12.3-2).

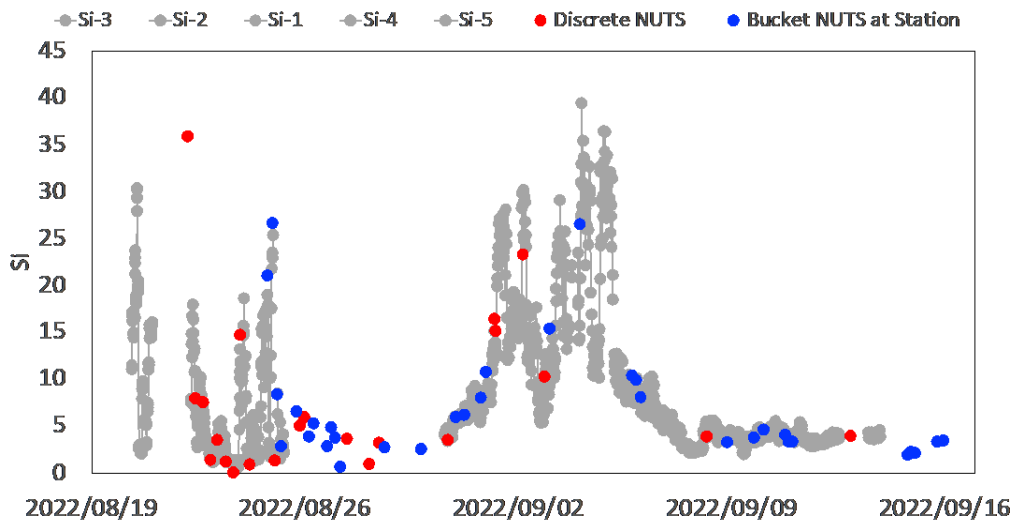


Figure 4.12.3-2: The surface silicate values that determined by pFI method during MR22-06C. The surface Si values from pFI (gray) and Si value determined by MWJ at surface (bucket) and at 5-meter at the regular rosette sampling stations (blue, red, respectively).

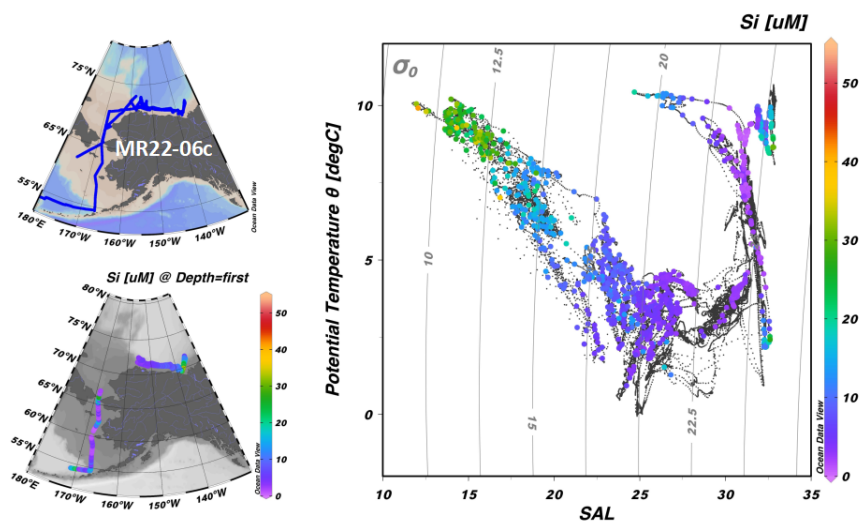


Figure 4.13.3-3: Surface Si values obtained by pFI method plotted with T-S diagram (right panel) and the surface plot (left bottom panel).

The low salinity value indicated that sea-ice melted water have spread in the offshore region (Figure 4.13.3-3), which was very similar to the previous cruise MR21-05C. Those offshore surface Si value were $\sim 4\mu\text{M}$. The wide range of the Si from the Chukchi shelf to the Mackenzie estuary were seen with the significantly high value near the Mackenzie River.

From Dutch Harbor to the Bering strait (Figure 4.13.3-4), the low salinity water with high Si value ($\sim 20\mu\text{M}$) were seen along the Alaskan continent. The salinity values were dropped to 24 psu, suggesting that there was the strong riverine input Yukon River. Strong fluorometer signal suggests that the riverine input transported nutrients from the continent and probably supported the productivity in this area.

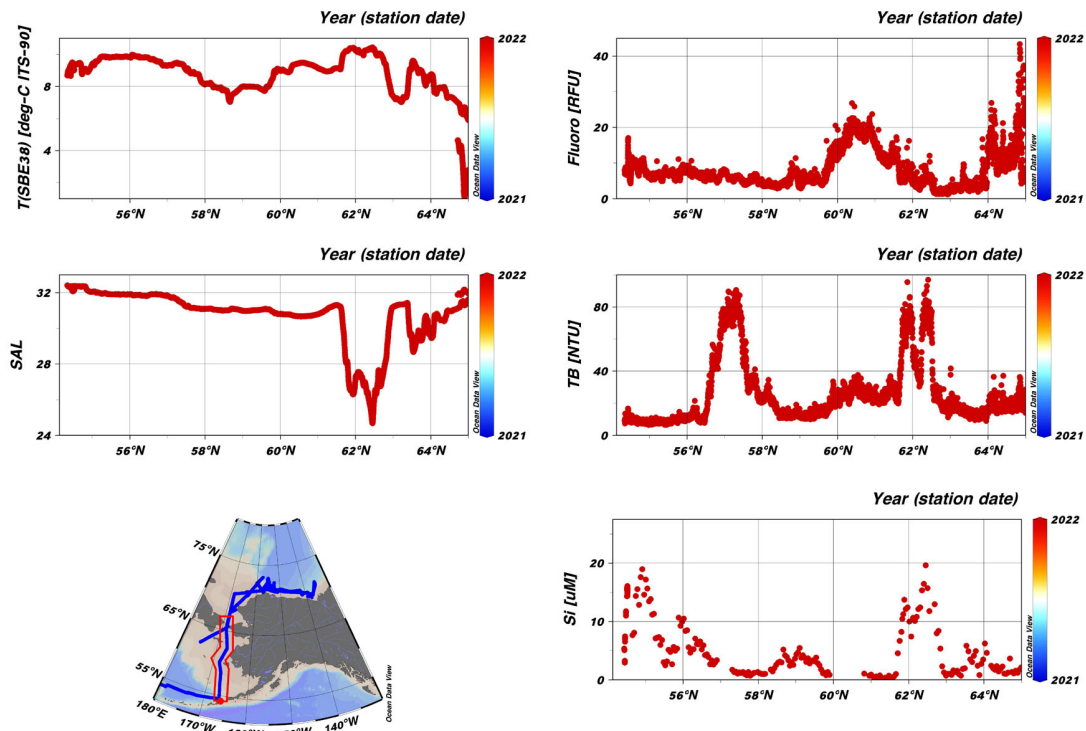


Figure 4.12.3-4: Surface Si with other parameters from TSG data base in the Bering Sea.

(6) Data archive

These data obtained in this cruise will be submitted to the Data Management Group of JAMSTEC, and will be opened to the public via “Data Research System for Whole Cruise Information in JAMSTEC (DARWIN)” in JAMSTEC web site. <<http://www.godac.jamstec.go.jp/darwin/e>>

4.13. Continuous measurement of $p\text{CO}_2$ and $p\text{CH}_4$

(1) Personnel

Akihiko Murata	JAMSTEC	Principal Investigator (not on board)
Masahiro Orui	MWJ	Operation Leader
Nagisa Fujiki	MWJ	
Yuta Oda	MWJ	

(2) Objectives

The purpose is in-situ measurement of concentrations of carbon dioxide (CO_2) and methane (CH_4) in surface seawater.

(3) Parameters

Partial pressures of CO_2 ($p\text{CO}_2$) and CH_4 ($p\text{CH}_4$)

(4) Methods, Apparatus and Performance

Atmospheric and surface seawater CO_2 and CH_4 were measured using an automated system equipped with Off-Axis Integrated-Cavity output Spectroscopy gas analyzer (Off-Axis ICOS; 911-0011, Los Gatos Research) developed on the basis of Cavity Ring-Down Spectroscopy. Standard gases and atmospheric air taken from the bow of the ship (approx. 13 m above the sea level) were also measured. Seawater was taken from an intake placed at the approximately 4.5 m below the sea surface and introduced into the equilibrator at the flow rate of (4 - 5) L min^{-1} by a pump. The equilibrated air was circulated in a closed loop by a pump at flow rate of (0.6 - 0.7) L min^{-1} through two electric cooling units, a starling cooler, and the Off-Axis ICOS.

(5) Preliminary results

Distributions of atmospheric and surface seawater CO_2 are shown in Figure 4.13-1, along with those of sea surface temperature (SST). Those of CH_4 are shown in Figure 4.13-2.

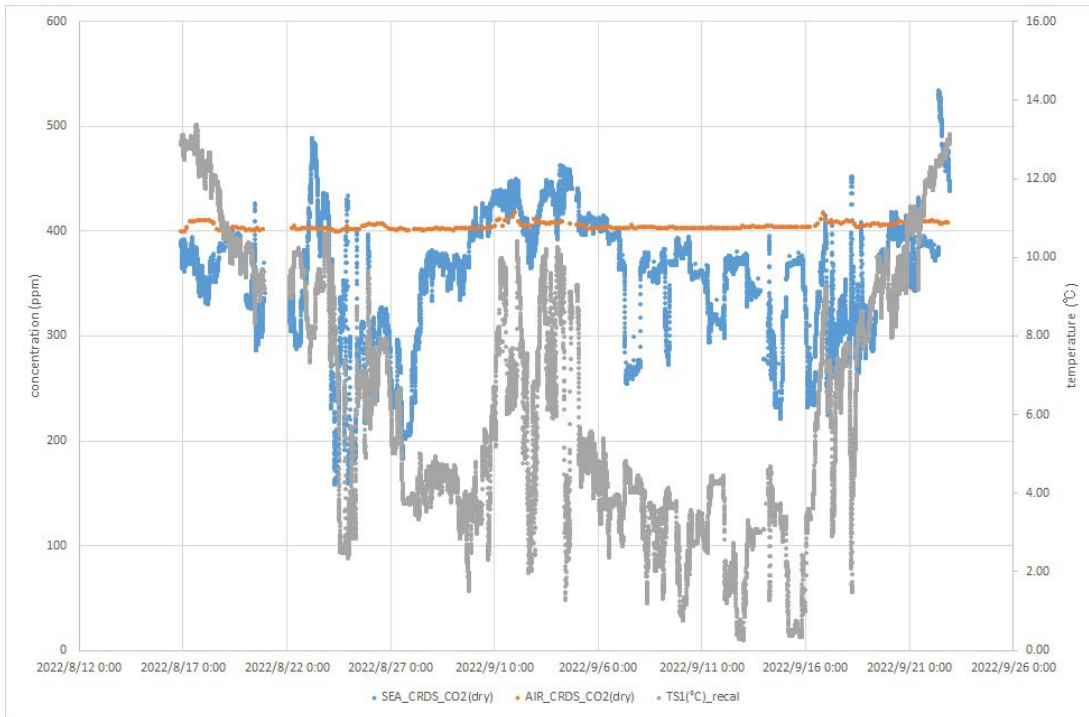


Figure 4.13-1: Distributions of atmospheric (orange), surface seawater CO₂ (blue) and SST (gray) as a function of observation time.

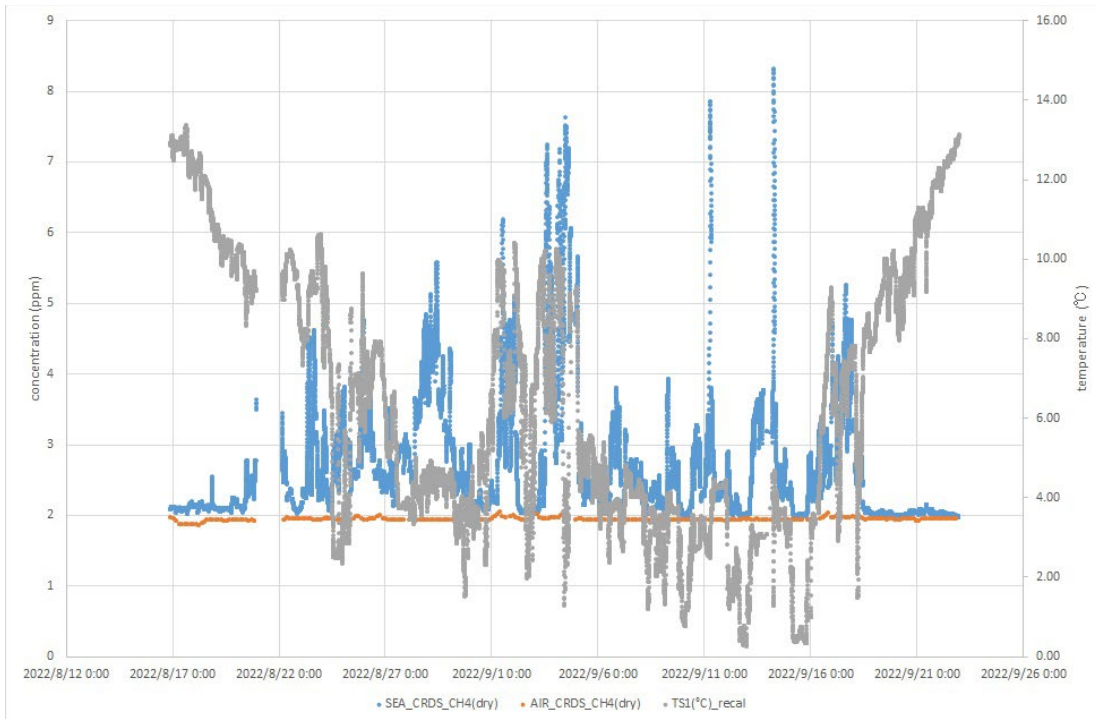


Figure 4.13-2: Distributions of atmospheric (orange), surface seawater CH₄ (blue) and SST (gray) as a function of observation time.

(6) Date archive

These data obtained in this cruise will be submitted to the Data Management Group (DMG) of JAMSTEC, and will open to the public via “Data Research System for Whole Cruise Information in JAMSTEC (DARWIN)” in JAMSTEC web site.

<http://www.godac.jamstec.go.jp/darwin/e>.

4.14. Trace metal clean seawater sampling

(1) Personnel

Mariko Hatta JAMSTEC

(2) Objectives

The goals of this study are following:

- 1) Improve current trace metal clean sampling technique on the R/V Mirai.
- 2) Estimate the potential metal contamination from the Niskin bottle attached to the regular CTD system.
- 3) Collect seawater samples via Niskin-X bottles attached with a Kevlar cable, and characterize the water masses with the trace element concentrations (dissolved iron and Aluminum).
- 4) Collect seawater samples via regular Niskin bottles attached with a rosette sampling unit, and characterize the water masses with Aluminum concentration.

(3) Parameters

- Conductivity, Temperature, Depth, Turbidity, Chlorophyll, DO from a portable RINKO-Profilier
- Depth from a portable depth sensor
- Salinity
- Nutrients (NH₄, NO₃, NO₂, PO₄, SiO₂)
- Dissolved trace metals (Fe, Al etc.)
- Total trace metal (Fe, Al etc.)

The ranges and accuracies of parameters measured by the RINKO-Profilier (ASTD152, S/N:0659) are as follows;

Parameter	Range	Accuracy
Conductivity	0.5 ~ 70 [mS/cm]	+/- 0.01 [mS/cm]
Temperature	-3 ~ 45 [deg-C]	+/- 0.01 [deg-C]
Depth	0 ~ 600 [m]	+/- 0.3 [%] FS
Turbidity	0 ~ 1000 [FTU]	+/- 0.3 [FTU] or +/- 2 [%]
Chlorophyll	0 ~ 400 [ppb]	+/- 1 [%] FS
DO	0 ~ 200 [%]	+/- 2 [%] FS

The calibration data sheet (Date: 2020-07-10):

<u>Parameter.</u>	<u>Actual.</u>	<u>Measured.</u>	<u>Deff.</u>	<u>Accuracy</u>
Temp.[deg-C]	12.655	12.654.	-0.001	+/- 0.008 [deg-C]
Cond. [ms/cm]	40.607	40.607	0.000	+/- 0.008 [mS/cm]
TURB. [FTU]	172.68	172.61	-0.07	+/- 3.11 [FTU]
Chl. [ppb].	75.22.	77.22.	2.00.	+/- 4.00 [ppb]
Depth [MPa].	4.500=447.68 (m)	447.67		-0.01 +/- 2.50 [m]
DO [%].	99.04	98.92.	-0.12.	+/- 1.00 [%]

(4) Instruments and methods

(4-1) Trace metal clean sampling system

The sampling was conducted by each Niskin-X bottle attached to the Kevlar cable directly. The vinyl tape was wound on the Kevlar cable and then each Niskin sampling bottle was attached with stainless pins fitted to the Kevlar cable. This will minimize any damage to the Kevlar cable while the Niskin bottle is mounted. At the bottom of the cable, the 40 kg of the weights (two sets of the 20 kg of weights combined by a rope) and a portable RINKO profiler were attached by a shackle. Weights are to provide negative buoyancy for the Kevlar line. In order to avoid the contamination from the equipment, the deepest Niskin bottles were attached at least 1 meter away from the profiler and weights. The shallowest sampling depths were targeted at the mixed layer depth or deeper than the 10 m, which avoid any contamination from the ship. Individual Teflon-coated Niskin bottles hung manually on a Kevlar cable, this is the standard method used successfully for over three decades (Bruland et al., 1979). Individual Niskin bottles were fitted with an internally recording depth sensor (JFA Advantech). The methods and data used in verifying depth should be documented in the metadata for the cruise. The cable was lowering/rolling up with the speed of less than 0.5 m/sec. Samples were collected at following locations:

<u>Station</u>	<u>Target Depth (m)</u>	<u>Sample</u>	<u>RINKO</u>
2	10,20,30,40	Y	Y
4	10,20,30	Y	Y
5	10,20,35	Y	Y
6	10,20,40	Y	Y
8	10,20,40	Y	Y
10	10,25	Y	Y
15	50,100,200,300,400,500	Y	N
18	20,50,100,150,200,250	Y	N
20	20, 75	Y	N
33	50,100,150,200,300,400	Y	N

(4-2) Niskin-X bottle

In this cruise, Niskin-X, which was Teflon-coated before the cruise started, and then all the O-rings has been replaced with pre-acid washed Viton ones. In the beginning of the MR22-06C, each Niskin bottle was cleaned following the GEOTRACES cookbook protocol. No acid contacted the outside of the bottle, the nylon components in particular.

1. Each bottle was filled with 5% detergent for one day.
2. Rinsed 10x with deionized ultra-high purity water (Milli-Q water) thoroughly until there is no trace of detergent.
3. Each bottle was filled with 0.1M HCl (analytical grade) for two days, and then emptied out through the spigot to rinse these.
4. Rinsed 5x with deionized ultra-high purity water (Milli-Q water).
5. Each bottle was filled with ultra-high purity water (Milli-Q water) for two days.
6. After discarding Milli-Q water from bottles, filled with ultra-high purity water (Milli-Q water) until use.
7. After discarding ultra-high purity water (Milli-Q water) from the Teflon spigot, the bottles were transferred to the clean van and prepared for sampling.

Each Niskin bottles, equipped with a depth sensor (JFE Advantech), were set up inside a clean sampling container van. Each bottle was covered with a plastic bag for top and bottom of the bottles. Teflon-coated messenger was set when needed. Each Niskin bottle was prepared in the clean container, and then transferred to the sampling system, and the plastic bags were removed right before it attached to the Kevlar cable.

During this cruise, there were two sizes of the Niskin bottle used depending on the cast. In generally, 5L Niskin bottles were used on the shelf regions, and 12L Niskin bottles were used at the open ocean.

When the Kevlar cable reached to the target depth, a Teflon coated messenger was released, waited for 1 min (or less, depending on the depth) until the messenger reached the last bottle.

After the cast was over, each bottle was transferred to the clean van for the sampling. Each bottle was transferred by a custom built Niskin bottle cart (updated version). The sampling bottles were carefully rested on the cart and transferred to the van. Secondly personnel (a helper) received the bottle through the large door in the van and transferred and hanged the bottle onto the sampling rack. The sampling rack was also built for this cruise.

(4-3) A clean sampling container van: The clean laboratory “van” is an ISO-sized 20 ft aluminum container built by Silhouette Steel (British Columbia, Canada). This van was

originally designed by US group (Cutter and Bruland, 2012) and then it was modified to adjust for the Japanese research (R/V Shinsei Maru). The van is divided into two rooms, a small anteroom for storage and sample bottle transfers, and a larger, positive pressure clean room for sampling and sample handling. The inner walls are covered in polypropylene sheeting over the standard aluminum walls, and the floor is Altro rolled vinyl with a total of 5 floor drains. The 5' anteroom contains a closet within which is the heating/cooling system (HVAC; two Cruisair 16,000 BTU marine air conditioner units with seawater heat exchange). The doorway between the anteroom and clean room has top to bottom clear vinyl strips to minimize return airflow (i.e., the clean room is positive pressure and at least 14.2 CMS [cubic meters per second] of HEPA-filtered air exits through the vinyl stripped doorway). The end of the clean lab has a counter with sink (ship's water).

This MR22-06C cruise was the second time to use this clean van on this R/V Mirai. This is the research cruise in the Arctic Ocean, which we have to face on several challenges to use this clean van. The van was set up on the port side of the stern on the R/V Mirai. This cooling system has been shut down since the seawater and air temperature in the Arctic Ocean was significantly low and often expected to be below the suitable temperature of the use of this heating/cooling system. Thus, external two oil heaters (upto 1500 W) were setup in this container and kept on 24 hours (set at 26 °C) during the cruise. The room temperature was maintained between ~10 °C while the outside temperature was low as -1 °C. In order to maintain the power supply for this heating system (not to interrupt any other operation inside the clean van), one power cords were directly provided from the ship. In order to avoid any frozen pipes and any spill to freeze the deck, all of the floor drains had been closed during the cruise and no fresh water supply were provided. One drain pipe from the water sink was kept connected, which was ~5-meter length from the drain connector to the side of the ship, coated with a heater cable with a tape. This coating was prevented the pipe from freezing and being clogged with ice.

The clean sampling area was equipped with a stainless steel bottle rack that coated by epoxy paints, holding 6 Niskin-X bottles. This bottle rack was designed by PI, which was used for the first time during this cruise.

(4-4) Sub-sampling in the clean van:

The following samples were drained from each Niskin bottle:

<u>Parameter</u>	<u>Filtered[y/n]</u>	<u>Analysis on the board[y/n]</u>	<u>Stored samples[y/n]</u>
Salinity	n	y	n
Nutrients	y	y	n
Dissolved			
Metal (Fe, Al)	y	n	y
Dissolved REEs	y	n	y

Salinity samples were drained from the bottle directly to each subsampling bottles. Samples for nutrients and dissolved metal were filtered through 0.2 um Acropak filter. Samples for salinity and nutrients were determined on R/V Mirai using each shipboard protocol by MWJ.

Total dissolved metal and dissolved metal samples were stored in pre-cleaned 100mL PFA bottles. Each bottle was cleaned using the GEOTRACES cookbook protocols at the shore-based laboratory.

1. Soaked bottles for one day in an alkaline detergent.
2. Rinsed 10x with ultra-high purity water (MilliQ water) thoroughly until there were no trace of detergent.
3. Soaked in 6 M reagent grade HCl bath for more than one day
4. Rinsed 5x with ultra-high purity water (MilliQ water).
5. Filled with 1M nitric acid (analytical grade) and kept them at 80°C for 5 hours in a heated oven. Each bottle was packed with a plastic bag with milliQ water in case of any spill from each bottle.
6. Rinsed 5x with ultra-high purity water (MilliQ water) in an ISO Class-5 laminar flow hood.
7. Filled bottles with ultra-high purity water (MilliQ water) and kept them at 80°C for 5 hours in a heated oven. Each bottle was packed with a plastic bag with milliQ water in case of any spill from each bottle.
8. Rinsed 5x with ultra-high purity water (MilliQ water) inside an ISO Class-5 laminar flow hood. The bottles were packed in 6 doubled bags until being used.

(4-5) Data:

A portable CTD (RINKO-Profiler): We observed vertical profiles of sea water temperature, salinity, turbidity, chlorophyll, and DO using a RINKO-Profiler, which was manufactured by JFE Advantech Co., Ltd. The profiler was lowered from the broadside with its lowering speed less than 0.5 m/sec. The sensors were collected every 0.1 second interval. We obtained 6 profiles and the observation log is shown in (4-2) in this report.

Salinity: The salinity analysis was carried out on R/V MIRAI during the cruise of MR22-06C using the salinometer. The details of the analysis were reported in Chapter 3.10.

Nutrients: The nutrient analysis was carried out on R/V MIRAI during the cruise of MR22-06C using the QuAAtro 5. The details of the analysis were reported in Chapter 4.2.

(5) Station list or Observation log

Trace metal clean samplings were carried out at the following stations, shown in below table. Total 10 casts were carried out, and in addition to the 20 regular CTD cast samplings, we obtained over 268 unique samples.

#	Sample ID	Year	Month	Day	Time	UTC	Lat	N	Long	W		
1	Stn2-N30-10	2022	08	24	22:44	UTC	66	0.13	N	168	45.1	W
2	Stn2-N11-20	2022	08	24	22:44	UTC	66	0.13	N	168	45.1	W
3	Stn2-N10-30	2022	08	24	22:44	UTC	66	0.13	N	168	45.1	W
4	Stn2-N09-40	2022	08	24	22:44	UTC	66	0.13	N	168	45.1	W
5	Stn4-N09-30	2022	08	25	5:17	UTC	67	0.16	N	168	44.2	W
6	Stn4-N10-20	2022	08	25	5:17	UTC	67	0.16	N	168	44.2	W
7	Stn4-N11-10	2022	08	25	5:17	UTC	67	0.16	N	168	44.2	W
8	Stn5-N9-35	2022	08	25	15:28	UTC	67	30	N	168	44.9	W
9	Stn5-N10-20	2022	08	25	15:28	UTC	67	30	N	168	44.9	W
10	Stn5-N11-10	2022	08	25	15:28	UTC	67	30	N	168	44.9	W
11	Stn6-N9-40	2022	08	26	3:23	UTC	68	0.22	N	168	44.9	W
12	Stn6-N10-20	2022	08	26	3:23	UTC	68	0.22	N	168	44.9	W
13	Stn6-N11-10	2022	08	26	3:23	UTC	68	0.22	N	168	44.9	W
14	Stn8-N9-40	2022	08	26	16:23	UTC	69	0.21	N	168	43.2	W
15	Stn8-N10-20	2022	08	26	16:23	UTC	69	0.21	N	168	43.2	W
16	Stn8-N11-10	2022	08	26	16:23	UTC	69	0.21	N	168	43.2	W
17	Stn10-N9-25	2022	08	27	0:17	UTC	69	59.98	N	168	45.2	W
18	Stn10-N10-10	2022	08	27	0:17	UTC	69	59.98	N	168	45.2	W
19	Stn15-N14-500	2022	08	31	3:00	UTC	71	7.22	N	146	6.55	W
20	Stn15-N16-400	2022	08	31	3:00	UTC	71	7.22	N	146	6.55	W

21	Stn15-N17-300	2022	08	31	3:00	UTC	71	7.22	N	146	6.55	W
22	Stn15-N20-200	2022	08	31	3:00	UTC	71	7.22	N	146	6.55	W
23	Stn15-N29-100	2022	08	31	3:00	UTC	71	7.22	N	146	6.55	W
24	Stn15-N30-50	2022	08	31	3:00	UTC	71	7.22	N	146	6.55	W
25	Stn18-N14-250	2022	09	02	23:00	UTC	71	19.97	N	135	30.5	W
26	Stn18-N16-200	2022	09	02	23:00	UTC	71	19.97	N	135	30.5	W
27	Stn18-N17-150	2022	09	02	23:00	UTC	71	19.97	N	135	30.5	W
28	Stn18-N20-100	2022	09	02	23:00	UTC	71	19.97	N	135	30.5	W
29	Stn18-N29-50	2022	09	02	23:00	UTC	71	19.97	N	135	30.5	W
30	Stn18-N30-20	2022	09	02	23:00	UTC	71	19.97	N	135	30.5	W
31	Stn20-N9-75	2022	09	05	17:00	UTC	70	25.3	N	141	39.9	W
32	Stn20-N11-20	2022	09	05	17:00	UTC	70	25.3	N	141	39.9	W
33	Stn33-N14-400	2022	09	15	15:00	UTC	73	20.12	N	157	27.9	W
34	Stn33-N16-300	2022	09	15	15:00	UTC	73	20.12	N	157	27.9	W
35	Stn33-N17-200	2022	09	15	15:00	UTC	73	20.12	N	157	27.9	W
36	Stn33-N20-150	2022	09	15	15:00	UTC	73	20.12	N	157	27.9	W
37	Stn33-N29-100	2022	09	15	15:00	UTC	73	20.12	N	157	27.9	W
38	Stn33-N30-50	2022	09	15	15:00	UTC	73	20.12	N	157	27.9	W

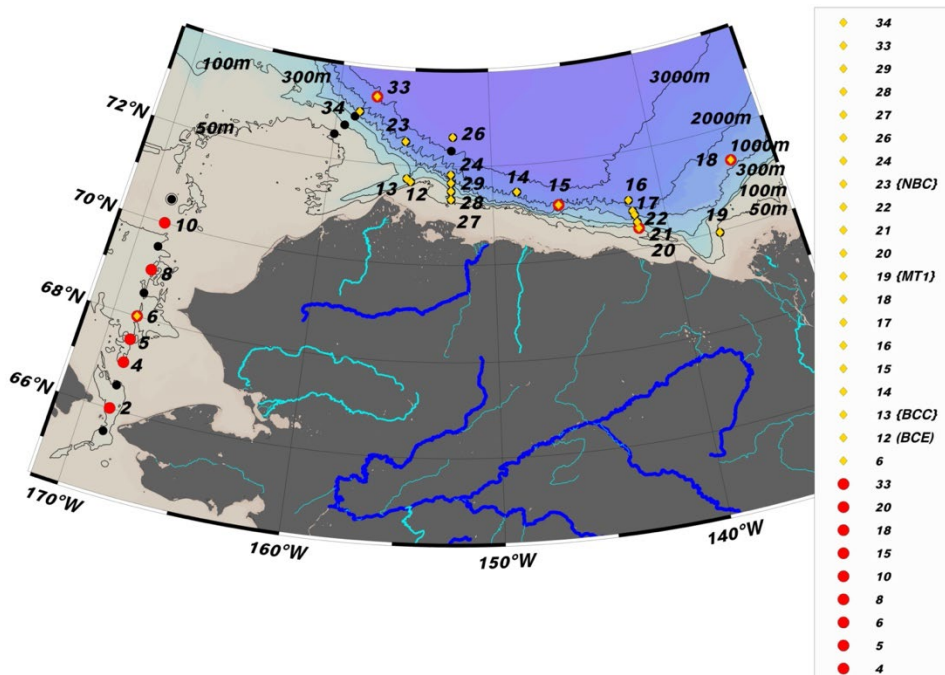


Figure 4.14-1: The sampling locations. Samples indicated by Red circles were obtained by the trace metal cast with X-Niskin. Samples indicated by Yellow circles were obtained by the regular CTD rosette system.

(6) Preliminary results

(6-1) The CTD sensor.

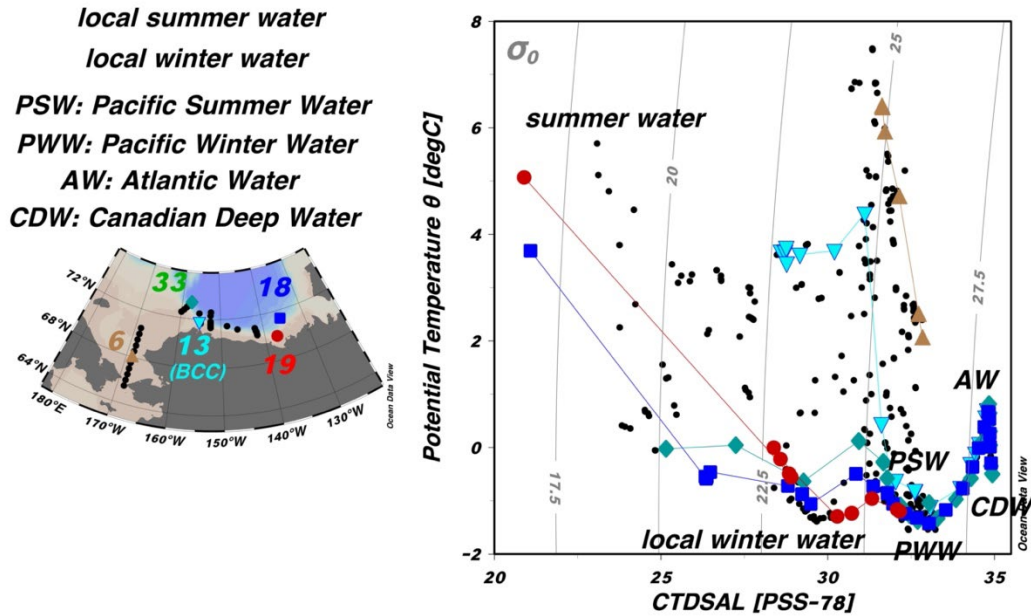


Figure 4.14-2: The water characteristics using T-S diagram. The data are shown from the regular CTD rosette.

The T-S diagram using the regular rosette water system are shown in Figure 4.14-2. In this study area, several water masses were identified; Atlantic Water (AW), Pacific Winter Water (PWW), Pacific Summer Water (PSW), local summer/winter waters, and Canadian Deep Water (CDW). During this cruise, the strong riverine influence was observed near the Mackenzie River.

The strongly turbid elevated water layers were observed along the shelf slope (Stations 14, 15, and 25). Compared with the offshore station (Station 26), the higher turbid waters corresponding with the higher Apparent Oxygen Utility (AOU) and the higher silicate values at each depth. Since the porewater values for the silicate, which could be indicating some events of the turbidity current, which can release porewaters or some materials from the sediments from the shelf slope.

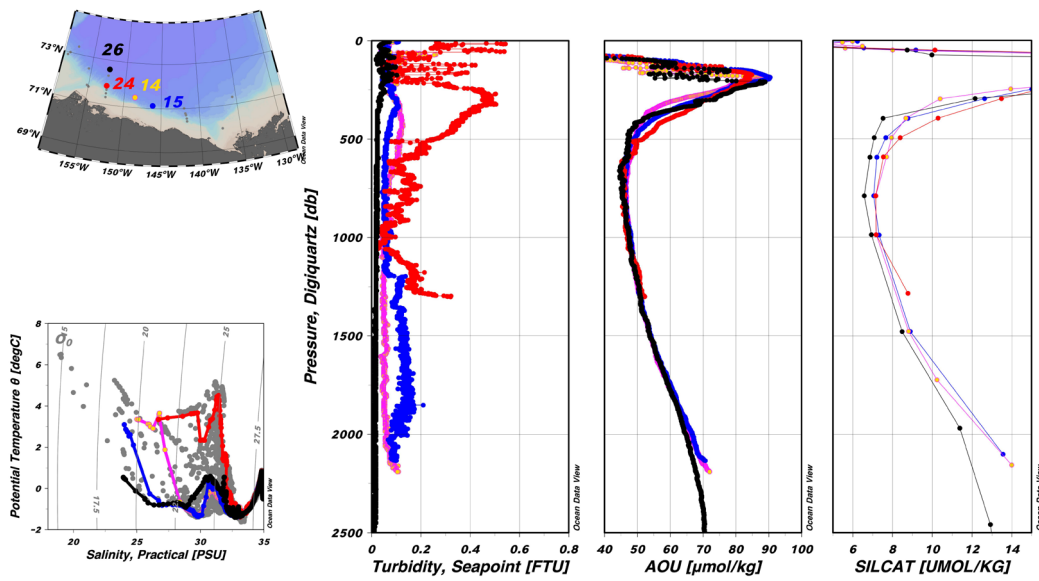


Figure 4.14-3: The vertical profiles of turbidity, AOU, and silicate values at Stations 14, 15, 25, and 26.

(7) Data archive

These data obtained in this cruise will be submitted to the Data Management Group of JAMSTEC, and will be opened to the public via “Data Research System for Whole Cruise Information in JAMSTEC (DARWIN)” in JAMSTEC web site.

<<http://www.godac.jamstec.go.jp/darwin/e>>

4.15. Zooplankton

(1) Personnel

Kohei Matsuno*	Hokkaido Univ.	- Principal Investigator
Katsunori Kimoto*	JAMSTEC	- Principal Investigator
Takuya Itaki*	AIST	- Principal Investigator
Takahito Ikenoue	JAMSTEC	
Jonaotaro Onodera	JAMSTEC	

*: onshore members

(2) Objectives

- To investigate biodiversity and habitat of meso- and micro-zooplanktons
- To analyze shell density of pteropod

(3) Parameters

Assemblages and volume of meso-zooplanktons (mainly Copepod),
Assemblages of micro-zooplanktons (mainly radiolaria)
Shell density of pteropod

(4) Instruments and methods

<Instruments>

Quadruple NORPAC plankton net (supplied by Hokkaido Univ.)
Closing plankton net (JAMSTEC)
Flow-meter (Hokkaido Univ. for Quad. NORPAC, and AIST for closing net)
Depth sensor for closing plankton net (JAMSTEC)

<Methods>

Quadruple NORPAC plankton net was used for vertical towing of 0-150 m depth (or 0 to bottom-7m on shallow shelf region). The obtained samples by Quad NORPAC net are to be shared by three principal investigators (Table 4.15-1). The samples obtained by 335 and 150 μ m mesh were applied to meso-zooplankton studies. The samples of 63 μ m mesh were applied to radiolaria study and investigation of pteropod shell density. Flow-meter was attached except for one of 63 μ m net for pteropod sampling. Towing speed was 0.5 m/s. The towed plankton net was washed from the outside towed nets at the ship's side, and then it was recovered on deck.

The meso-zooplankton samples in cod-end of plankton nets were moved to sample bottle, and were fixed with pH-neutralized formalin (~25mL). The micro-zooplankton

samples in 4L bucket were sieved with 63 μ m mesh, and then remains on the sieve were fixed with ethanol (< ~50mL).

Closing NORPAC net was used for sampling of radiolaria assemblages dwelling different depth ranges. The applied plankton net is new except for metal parts such as ring, meaning that no contamination of radiolaria specimens from previous towing is expected. The mesh size is 63 μ m. The flow-meter (ID: 3355) was attached. A depth sensor (DEFI2-D2XHG, JFE Advantech) was attached outside of the ring, and the towing depth was recorded at 1-second interval. The wire speed was 0.7-1.0 m/s for down, 0.5 m/s for towing, and 0.7-1.0 m/s for recovery after closing. Messenger to close towing net was thrown-in to water without stopping the towing, based on the previous estimation (Table 4.15-2). The sample treatment is the same as NORPAC net samples for the radiolaria study (#3 in Table 4.15-1).

Flow-meter test was not carried out because of limited ship time. No sample analysis was conducted offshore, and all samples were delivered to each principal investigator after this cruise. For safety, a harness was required for washing the net at the ship's side. Sample fixation was conducted in the draft of the wet lab 1 or outside the wet lab.

The sampling in the Canadian water was conducted under the fishery license (License #: S-22/23-4000-IN) for September 1st to 17, 2022. The meso-zooplankton samples obtained in the Canadian water were immediately analyzed after the cruise, and have been reported to the Minister of Fisheries and Oceans Canada due October 16, 2022.

(5) Tables

Table 4.15-1: Summary on the sharing Quad-NORPAC net

Ring #	Mesh Size (μ m)	Flow-meter ID	Cod-end Type	Treatment	Fixation	Principal Investigator
#1	335	3690	Small cup and tube	to sample bottle	pH-neutralized formalin (~25mL)	Kohei Matsuno
#2	150	3998	Small cup and tube	to sample bottle	pH-neutralized formalin (~25mL)	Kohei Matsuno
#3	63	3996	4L bucket	Sieved with 63 μ m mesh	Ethanol (<50mL)	Takuya Itaki

#4	63	N/A	4L bucket	Sieved with 63µm mesh	Ethanol (<50mL)	Katsunori Kimoto
----	----	-----	-----------	--------------------------	-----------------	---------------------

Table 4.15-2: Timing of messenger throw-in for closing net

	Towing Range (m)	Wire out to throw-in messenger (m)	Wire out to start call of the 5-second countdown to throw-in (m)
#1	0-50	N/A (no close)	N/A
#2	50-150	57	59.5
#3	150-300	172	174.5
#4	300-500	345	137.5
#5	500-1000	575	577.5

Table 4.15-3: The list of samples obtained by Quad-NORPAC net

Station	Coordinates	Date (UTC-9)	Time (UTC-9)	Wire out (m)	Wire angle (°)	Mesh size (µm)	Reading of flow-meter	Sample Bottle ¹⁾
1	65°30.04'N 168°44.97'W	Aug. 24	7:51 – 8:00	48	13	335 150 63 63	620 268 170 N/A	N-1 N-2 St. 1S St. 1C
2	66°01.23'N 168°44.42'W	Aug. 24	14:09 – 14:15	46	8	335 150 63 63	420 180 80 N/A	N-3 N-4 St. 2S St. 2C
5	67°29.44'N 168°44.60'W	Aug. 25	6:14 – 6:20	42	5	335 150 63 63	430 378 180 N/A	N-5 N-6 St. 5S St. 5C
8	68°59.89'N 168°43.66'W	Aug. 26	7:10 – 7:16	45	3	335 150 63 63	450 410 255 N/A	N-7 N-8 St. 8S St. 8C
10	70°00.04'N 168°45.29'W	Aug. 26	15:02 – 15:10	34	6	335 150 63 63	432 360 232 N/A	N-9 N-10 St. 10S St. 10C
13	71°46.26'N 155°13.03'W	Aug. 29	11:17 – 11:30	150	5	335 150 63 63	1262 1280 682 N/A	N-11 N-12 St. 13S St. 13C
15	71°07.85'N 146°07.45'W	Aug. 30	22:52 – 23:04	150	2	335 150 63 63	1482 1261 910 N/A	N-13 N-14 St. 15S St. 15C
17	70°47.10'N 141°50.26'W	Aug. 31	12:18 – 12:31	150	7	335 150 63 63	1356 1228 775 N/A	N-15 N-16 St. 17S St. 17C
18	71°19.69'N 135°31.21'W	Sep. 02	13:41 – 13:54	150	3	335 150 63 63	1286 1170 660 N/A	N-17 N-18 St. 18S St. 18C

20	70°25.32'N 141°39.83'W	Sep. 05	7:33 – 7:41	75	7	335 150 63 63	708 428 445 N/A	N-19 N-20 St. 20S St. 20C
24	71°49.97'N 152°30.70'W	Sep. 09	7:41 – 7:54	150	3	335 150 63 63	1570 235 780 N/A	N-21 N-22 St. 24C St. 24S
26	72°35.03'N 152°26.47'W	Sep. 09	20:41 – 20:55	150	4	335 150 63 63	1370 30 795 N/A	N-23 N-24 St. 26S St. 26C
27	71°20.05'N 152°30.21'W	Sep. 10	9:44 – 9:51	53	3	335 150 63 63	605 28 455 N/A	N-25 N-26 St. 27S St. 27C
31	72°41.99'N 159°24.37'W	Sep. 14	11:28 – 11:37	75	5	335 150 63 63	778 45 412 N/A	N-27 N-28 St. 31S St. 31C
32	72°54.19'N 158°49.03'W	Sep. 14	16:09 – 16:21	150	2	335 150 63 63	1395 72 810 N/A	N-29 N-30 St. 32S St. 32C
33	73°20.03'N 157°27.75'W	Sep. 15	7:31 – 7:44	150	6	335 150 63 63	1352 90 775 N/A	N-31 N-32 St. 33S St. 33C
34	73°00.66'N 158°31.72'W	Sep. 15	15:04 – 15:20	150 + 5	15	335 150 63 63	1660 290 1172 N/A	N-33 N-34 St. 34S St. 34C

¹⁾ Sample bottles of N-series for Matsuno, K., S series for Itaki, K., and C series for Kimoto, K.

Table 4.15-4: Samples obtained by the closing plankton net at Station #33 on September 9th, 2022 (UTC-9). The ID of applied flow-meter is 3355.

Coordinate at start	Time (UTC-9)	Sampled Depth (m)	Wire out (m)	Wire out at closing (m) ¹⁾	Wire angle (°)	Flow-meter reading	Remarks
72°34.98'N 152°24.95'W	18:10 – 18:14	0-50	50	N/A	6	378	-
72°35.00'N 152°25.00'W	18:17 – 18:29	50-150	150	50.0	8	454	Failure of sample recovery
72°35.01'N 152°25.24'W	18:31 – no record	50-150	150	50.5	7	373	Failure of sample recovery
72°35.02'N 152°25.36'W	18:44 – no record	50-150	150	50.0	8	450	-
72°35.03'N 152°25.47'W	18:57 – 19:14	150-300	300	150.5	5	777	-

72°35.04'N 152°25.62'W	19:16 – 19:41	300-500	500	301.2	2	978	-
72°35.05'N 152°25.98'W	19:44 – 20:34	500-1000	1000	498.5	2	2420	-

¹⁾ The timing of shock propagation of net closing to sheave and wire on deck.

(6) Preliminary results

The quadruple NORPAC net was conducted at 17 CTD/R stations (Table 4.15-3). The closing plankton net was conducted at Station 33 (Table 4.15-4, Figure 4.15-1).

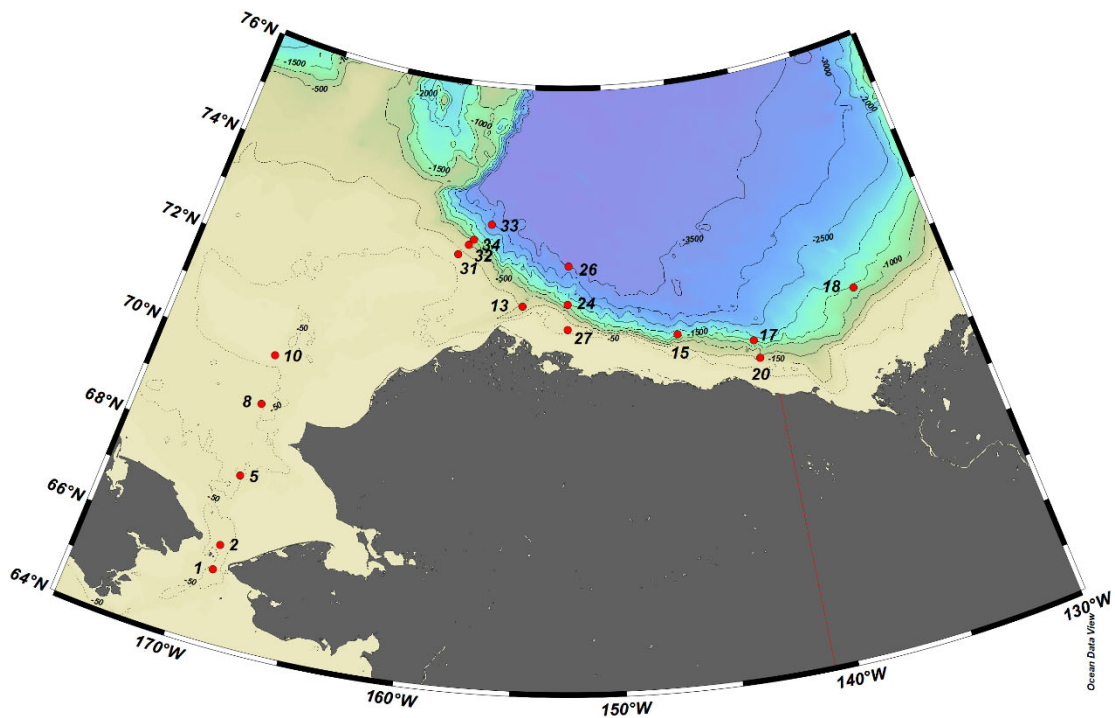


Figure 4.15-1: The map showing sampling position by plankton nets. The number with red symbol is station ID. The closing net was conducted at Station 33 only.

(7) Data archive

These data obtained in this cruise will be submitted to the Data Management Group of JAMSTEC, and will be opened to the public via “Data Research System for Whole Cruise Information in JAMSTEC (DARWIN)” in JAMSTEC web site.

<<http://www.godac.jamstec.go.jp/darwin/e>>

4.16. Phytoplankton

(1) Personnel

Jonaotaro Onodera JAMSTEC - Principal Investigator

(2) Objectives

To investigate biodiversity and habitat of shell-bearing phytoplankton

(3) Parameters

Assemblages and cell abundance of shell-bearing phytoplankton

(4) Instruments and methods

Water samples from sea surface, Subsurface Chlorophyll Maximum (SCM), and bottom-5m on shallow shelf station were obtained at much of CTD/R stations. Sea surface water was taken by a bucket. The SCM and bottom-5m water were taken by CTD/Carousel Water Sampling System. Obtained water samples were filtered by membrane filter with grid (45mm diameter, 0.45 μ m pore size). Filtering water volume was adjusted from 0.3 to 1.0 L because of different particle concentration among samples. The sample filter was desalted by milli Q water, and then it was dried in an oven (40° C). The dried filter in petri dish was packed in zip lock bag, and it was brought to lab on shore. After the cruise, plankton remains on the filter will be observed and counted under scanning electron microscope and light microscope.

(5) Tables

Table 4.16-1: The sample list. The filter ID shown as #**, the filtered water volume (L), the sample depths of SCM and bottom-5m in parenthesis are tabulated.

CTD/R Station	Bucket sample	SCM	Bottom -5m
01	#01: 0.30, #06: 0.10	#02: 0.30, #04: 0.10 (45.0 m)	#03: 0.3, #05: 0.1 (50.2 m)
02	#06: 0.30, #09: 0.10	#07: 0.10 (44.9)	#08: 0.10 (48.1)
03	#10: 0.15	#11: 0.10 (44.7)	#12: 0.10 (49.4)
04	#13: 0.20	#14: 0.10 (16.0)	#15: 0.10 (39.5)
05	#16: 0.30	#17: 0.30 (16.7)	#18: 0.30 (43.8)
06	#19: 0.30	#20: 0.30 (14.6)	#21: 0.30, #22: 0.10 (53.4)
07	#23: 0.30	#24: 0.30 (7.8)	#25: 0.30, #26: 0.10 (48.0)
08	#27: 0.30	#28: 0.30 (12.7)	#29: 0.30 (47.1)
09	#30: 0.40	#31: 0.40 (25.1)	#32: 0.30 (46.1)
10	#33: 0.40	#34: 0.40 (32.3)	#35: 0.30 (35.7)
11	#36: 0.50	#37: 0.40 (23.7)	#38: 0.30 (33.3)
12	#39: 0.40	#40: 0.40 (22.0)	---
13	#41: 0.50	#42: 0.50 (14.1)	---
14	#43: 0.80	#44: 0.80 (29.7)	---
15	#45: 0.98	#46: 1.01 (39.6)	---
16	#47: 0.94	#48: 1.10 (42.8)	---
17	#49: 0.92	#50: 0.95 (11.5)	---

18	#51: 1.00	#52: 1.00 (57.7)	---
19	#53: 0.40	#54: 0.50 (10.1)	#55: 0.50 (51.6)
20	#56: 1.02	#57: 0.89 (6.5)	#58: 0.99 (76.3)
21	#59: 1.00	#60: 1.00 (8.3)	---
23	#61: 1.00	#62: 1.00 (32.8)	---
24	#63: 1.00	#64: 0.98 (24.9)	---
26	#65: 1.01	#66: 0.99 (49.7)	---
27	#67: 1.00	#68: 1.02 (61.0)	---
28	#69: 0.98	#70: 1.00 (29.1)	---
29	#71: 0.98	#72: 1.00 (24.9)	---
30	#73: 1.00	#74: 0.80 (22.5)	#75: 0.80 (42.4)
31	#76: 1.00	#77: 0.50 (41.6)	#78: 0.75 (77.2)
32	#79: 1.00	#80: 1.00 (32.7)	---
33	#81: 1.00	#82: 1.00 (49.9)	---
34	#83: 1.01	#84: 1.00 (37.8)	---

(6) Preliminary results

The total of 84 samples was taken from 32 CTD/R stations (Table 4.16-1, Figure 4.16-1).

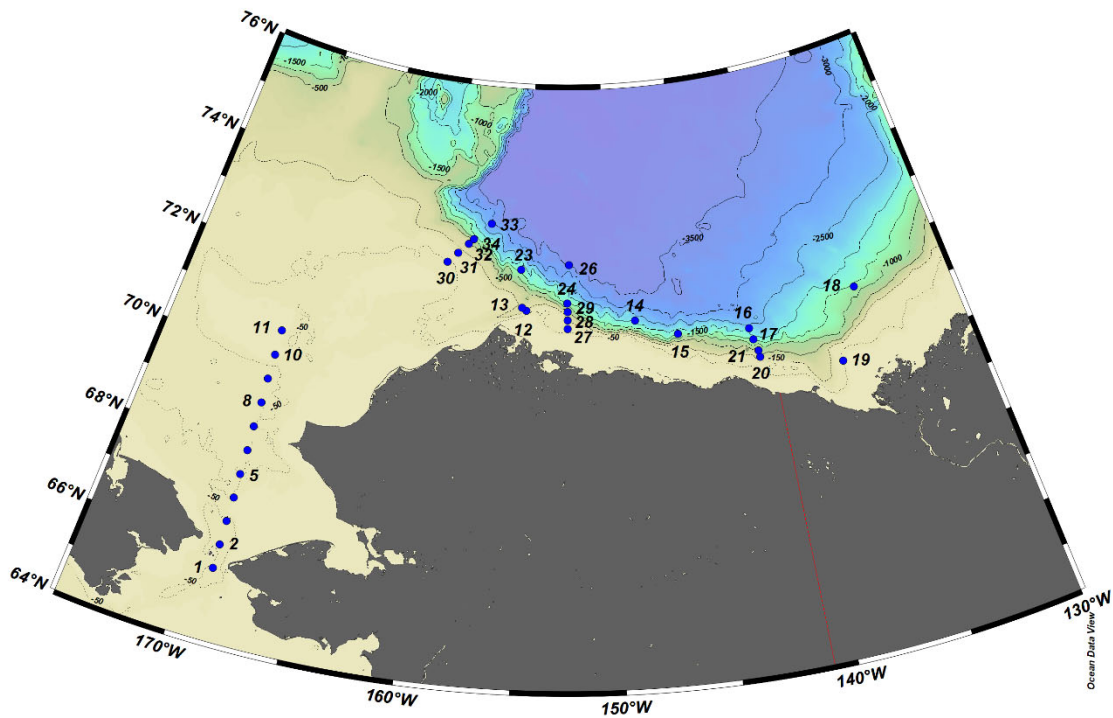


Figure 4.16-1: The map showing sampled position. The number is station ID.

(7) Data archive

These data obtained in this cruise will be submitted to the Data Management Group of JAMSTEC, and will be opened to the public via “Data Research System for Whole Cruise Information in JAMSTEC (DARWIN)” in JAMSTEC web site.

<<http://www.godac.jamstec.go.jp/darwin/e>>

4.17. Environmental DNA

(1) Personnel

Akihide Kasai	Hokkaido University	- Principal Investigator (not on board)
Makoto Ozaki	Hokkaido University	
Tatsuya Kawakami	Hokkaido University	- not on board
Hirromichi Ueno	Hokkaido University	- not on board

(2) Objectives

Ongoing global climate change can induce drastic changes in the Arctic ecosystem. Because many organisms that live in the Arctic rely on sea ice as their suitable habitat, a rapid decrease of sea ice would affect the biodiversity, abundance, distribution, and food web structure of Arctic marine species. Increasing freshwater input to the Arctic Ocean associated with increased river flows and melting glaciers would also drive an ecological change by altering ocean circulation and nutrient transport, especially in the coastal environment. However, tracking such ecological changes is a challenging issue due to a lack of baseline data and difficulty in the continuous survey in the Arctic.

Analyzing the environmental DNA (eDNA) of macro-organisms is a promising approach to revealing the response of the Arctic ecosystem to recent global climate change. In the recent cruises, we successfully demonstrated the usefulness of eDNA for understanding the hidden link between fish community structure and oceanographic environments. On the other hand, the results also suggested that further optimization of the sampling protocol is still required to improve the detection probability of fish eDNA.

In this cruise, we collected eDNA samples to accomplish the aims listed below.

- To obtain a comprehensive view of fish diversity across the shelf of the Chukchi Sea and the Beaufort Sea.
- To clarify the spatial distribution of common fish species in the Arctic region corresponding to the oceanographic environment.
- To clarify the size fraction of particles containing fish eDNA and to testify to the efficiency of pre-filtration for optimizing sampling effort.

(3) Parameters

Environmental DNA

(4) Instruments and methods

(4-1) eDNA collection for detecting fish diversity

Surface seawater continuously pumped up from about 5 m depth for the underway sea-surface monitoring was routinely collected through the cruise. Basically, the collection was performed twice a day, around sunrise and sunset. Seawater was also collected using 12 L Niskin bottles mounted on the CTD/Carousel Water Sampling System at 21 stations from multiple depths, including the bottom layer. When the CTD observation was conducted, pumped seawater was concurrently collected as surface water.

A total of 20 L of water samples was collected in four 5 L plastic tanks at each water collection, except the water collected by CTD at sites having > 100m bottom depth (a total of 10 L each). The 5 L of each water sample was filtered through 0.45 µm pore size cartridge filters (Sterivex™ HV, Millipore, Billerica, MA, USA) in four replicates using a peristaltic tubing pump (Masterflex 07528-10, Cole-Parmer, IL, USA) at a flow rate of 100 mL/min. After filtration, the filters were filled with 2.0 mL of RNA-later and then stored at -20 °C.

Accordingly, eDNA samples were obtained from 67 sites (Table 4.17-1).

All sampling equipment and working space were decontaminated using bleach solution before use, and new nitrile gloves were worn at each water sampling to minimize cross-contamination. Further, 500 mL of Milli-Q water was also filtered as a negative control about once every 2–3 days to check for cross-contamination during the filtration process.

(4-2) Particle size fractionation

Sequential filtration was performed to obtain size fractionated eDNA samples at twelve sites to determine an optimal porosity of filter for collecting fish eDNA. At each site, 5L of pumped surface seawater was sequentially filtered through three filters of decreasing pore size; a Minisart syringe filter (5 µm pore size; Sartorius, Göttingen, Germany), a Sterivex™ HV (0.45 µm pore size; Millipore, Billerica, MA, USA), and a Sterivex™ GV (0.22 µm pore size; Millipore, Billerica, MA, USA). Filtration was conducted in two steps. A Minisart filter and a Sterivex-HV were directly connected via luer locks and used for the first filtration. Filtered seawater was retrieved in a sterilized 5L plastic tank and subsequently filtered using Sterivex-GV.

Water collection, filtration, and preservation were conducted in the same manner as (4-1) except for the preservation of the Minisart filters. The Minisart filters were stored at –80 °C without any preservation buffer after filtration because it does not have enough capacity to retain buffer solution.

Four technical replicates were created at every site.

(4-3) Efficiency of pre-filtration

The efficiency of pre-filtration was evaluated in terms of filtration rate and volume of seawater that can be processed per filter. This test was conducted at six sites. In each test, a maximum of 20 L of pumped seawater was filtered using a Sterivex-HV filter connected with a Minisart (5 µm pore size), which was used as a pre-filter. The Minisart was replaced with a new one when clogging became severe and then the filtration was continued. Filtered seawater was retrieved in four sterilized 5L plastic tanks. Seawater in each tank was subsequently filtered using a Sterivex-GV.

After finishing the filtration, the mean filtration rate (mL/min) and the total volume of filtered water (L) were recorded. Water collection, filtration, and preservation methods were the same as (4-2).

(4-4) eDNA collection from seawater just above the bottom sediments

Seawater just above the bottom sediments was collected at St. 05 and BC2-2 from the sediment core sample obtained using a multiple corer system (Asyura) (Table 4.17-2). The detailed operation was described in 4.18 and 6.1. The water was sequentially filtered using 5 µm pore size filters and a 0.45 µm pore size filter, using a peristaltic tubing pump at a flow rate of 100 mL/min.

(5) Station list

Table 4.17-1: List of sampling sites for eDNA collection from pumped-up surface seawater and seawater collected using Niskin samplers attached to a CTD.

Site (CTD Station)	Date (UTC)	Latitude (N)	Longitude (E)	Bottom depth (m)	Sampling depth (m)
NP01	12-Aug	34.76	140.07	2659	5
NP02	13-Aug	36.97	143.87	6412	5
NP03	13-Aug	38.29	145.94	5290	5
NP04	14-Aug	40.06	148.84	5462	5
NP05	14-Aug	41.41	151.16	5238	5
NP06	15-Aug	43.32	154.38	5444	5
NP07	15-Aug	44.66	156.60	5247	5
NP08	16-Aug	46.28	159.36	5254	5
NP09	16-Aug	47.72	161.91	5591	5
NP10	17-Aug	49.38	164.90	5452	5
NP11	17-Aug	50.89	167.80	2540	5
NP12	17-Aug	53.27	170.44	1819	5
BS01	17-Aug	53.35	174.16	3920	5
BS02	18-Aug	54.07	181.65	3817	5
BS03	19-Aug	54.04	185.89	3667	5
BS04	19-Aug	54.13	188.06	3183	5
BS05	20-Aug	54.41	192.09	1004	5
BS06	21-Aug	54.40	193.42	588	5
BS07	22-Aug	56.74	192.91	90.5	5
BS08	22-Aug	58.89	192.42	42.3	5
BS09	23-Aug	61.23	192.16	27.6	5
BS10	23-Aug	61.91	192.53	25.6	5
BS11	23-Aug	63.48	192.38	32.3	5
BS12 (St01)	24-Aug	65.51	191.25	54.9	5, 50
AO01 (St03)	24-Aug	66.50	193.25	53.1	5, 50
AO02 (St05)	25-Aug	67.50	191.25	49.7	5, 44

AO03 (St07)	25-Aug	68.50	191.25	54	5, 48
AO04 (St09)	26-Aug	69.50	191.24	52.2	5, 46
AO05 (St11)	26-Aug	70.50	191.24	38.9	5, 33
AO06 (St12)	28-Aug	71.67	205.03	99	5, 95
AO07 (St13)	29-Aug	71.73	204.77	305.5	5, 100, 295
AO08 (St14)	30-Aug	71.45	211.47	2170	5, 50, 100, 500, 2157
AO09 (St15)	30-Aug	71.12	213.89	2111	5, 50, 150, 500, 2102
AO10 (St16)	31-Aug	71.02	218.02	2335	5, 50, 150, 500, 2325
AO11	31-Aug	70.26	221.18	470	5
AO12 (MT1)	1-Sep	69.98	222.76	57	5
AO13 (St18)	2-Sep	71.33	224.48	1327	5, 50, 150, 500, 1310
AO14 (St19, MT1-2)	3-Sep	69.98	222.75	58.5	52
AO15 (MT2)	4-Sep	69.72	221.85	152	5
AO16 (St20)	5-Sep	70.42	218.34	80	5, 76
AO17 (COMAI Test2)	6-Sep	71.25	211.02	965	5
AO18	6-Sep	71.59	208.34	1044	5
AO19 (BC2)	7-Sep	71.91	205.84	216	5
AO20 (St23, NBC)	8-Sep	72.47	204.59	1999	5, 50, 150, 500, 1997
AO21 (St24)	9-Sep	71.83	207.48	1303	5, 50, 150, 500, 1285
AO22 (St26)	9-Sep	72.59	207.59	3626	5, 50, 150, 500, 3616
AO23 (St27)	10-Sep	71.33	207.50	60.6	5, 56
AO24 (COMAI Test3)	11-Sep	71.87	202.99	69.3	5
AO25 (COMAI Test4)	12-Sep	73.17	204.94	3605	5
AO26 (BC2-2)	13-Sep	71.92	205.88	274	5
AO27 (St30)	14-Sep	72.50	200.01	48.3	5, 43
AO28 (St32)	14-Sep	72.90	201.20	397	5, 50, 150, 300, 378
AO29 (St33)	15-Sep	73.34	202.53	3000	5, 50, 150, 500, 2985
AO30	15-Sep	72.12	199.49	40.2	5

AO31	16-Sep	70.22	195.47	40.6	5
AO32	16-Sep	68.35	191.87	52.6	5
BS13	17-Sep	65.60	191.39	52	5
BS14	17-Sep	64.93	190.14	49.8	5
BS15	18-Sep	62.77	185.76	74.2	5
BS16	18-Sep	61.35	183.32	114	5
BS17	19-Sep	58.81	179.14	3699	5
BS18	19-Sep	57.10	176.49	3816	5
BS19	20-Sep	55.12	173.50	3886	5
BS20	20-Sep	54.21	172.36	3902	5
NP13	22-Sep	52.20	169.62	5030	5
NP14	23-Sep	48.50	163.85	5827	5
NP15	25-Sep	42.58	154.36	5299	5

Table 4.17-2: List of stations where particle size fractionation, test of pre-filtration, and eDNA collection from Asyura samples was performed.

Purpose	Site	Date (UTC)	Latitude (N)	Longitude (E)	Bottom depth (m)
Particle size fractionation	NP02	13-Aug	36.97	143.87	6412
	NP06	15-Aug	43.32	154.38	5444
	NP10	17-Aug	49.38	164.90	5452
	BS05	20-Aug	54.41	192.09	1004
	BS09	23-Aug	61.23	192.16	27.6
	AO12	1-Sep	69.98	222.76	57
	AO19	7-Sep	71.91	205.84	216
	AO24	11-Sep	71.87	202.99	69.3
	AO31	16-Sep	70.22	195.47	40.6
	AO32	16-Sep	68.35	191.87	52.6
	BS13	17-Sep	65.60	191.39	52
	BS20	20-Sep	54.21	172.36	3902
	Pre-filtration test	AO15	4-Sep	69.72	221.85

	AO17	6-Sep	71.25	211.02	965
	AO25	12-Sep	73.17	204.94	3605
	BS17	19-Sep	58.81	179.14	3699
	NP13	22-Sep	52.20	169.62	5030
	NP15	25-Sep	42.58	154.36	5299
eDNA collection from seawater just above the bottom sediments	AO02	25-Aug	67.50	191.25	49.7
	AO26	13-Sep	71.92	205.88	274

(6) Preliminary results

During the cruise, eDNA samples from surface water were obtained from 67 sites across the North Pacific Ocean (15 sites), the Bering Sea (20 sites), and the Arctic Ocean (32 sites) (Figure 4.17-1). eDNA samples from the bottom layer or water column were also collected at 21 sites using Niskin samplers (Figure 4.17-1). These samples will be the subject of metabarcoding analysis to clarify the species composition of fishes and their regional differences. Quantitative PCR (qPCR) will also be used for species-specific detection of eDNA of common Arctic fishes (e.g., salmon, cods, and flatfishes) to track their distribution and to estimate their abundance.

The particle size fractionation and pre-filtration test (Figure 4.17-2) will provide valuable information to standardize the eDNA sampling method in the Arctic region. eDNA from the water just above the bottom sediments will also be analyzed to find their potential as an eDNA source. Integrating the results and oceanographic conditions observed in this cruise will contribute to clarifying how the environmental change influences the Arctic ecosystem.

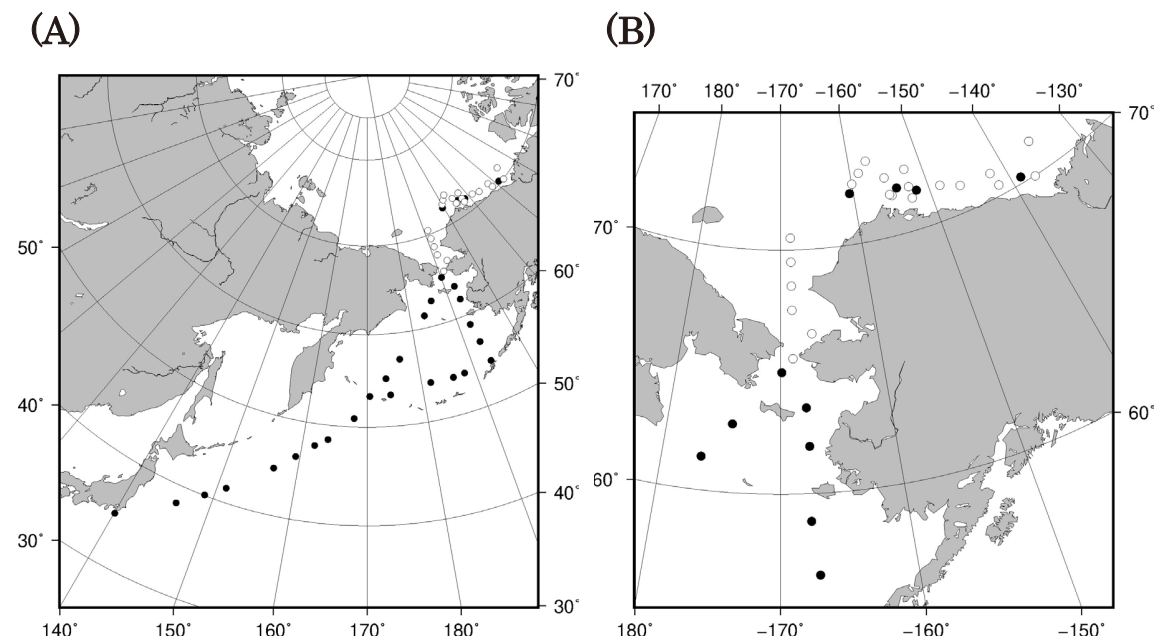


Figure 4.17-1: Map showing the sites where eDNA samples were collected from pumped-

up surface water (filled circles) and both pumped-up surface water and seawater collected using Niskin samplers (open circles). (A) Locations of the sampling sites during the whole cruise. (B) Locations of the sampling sites in the Arctic region.

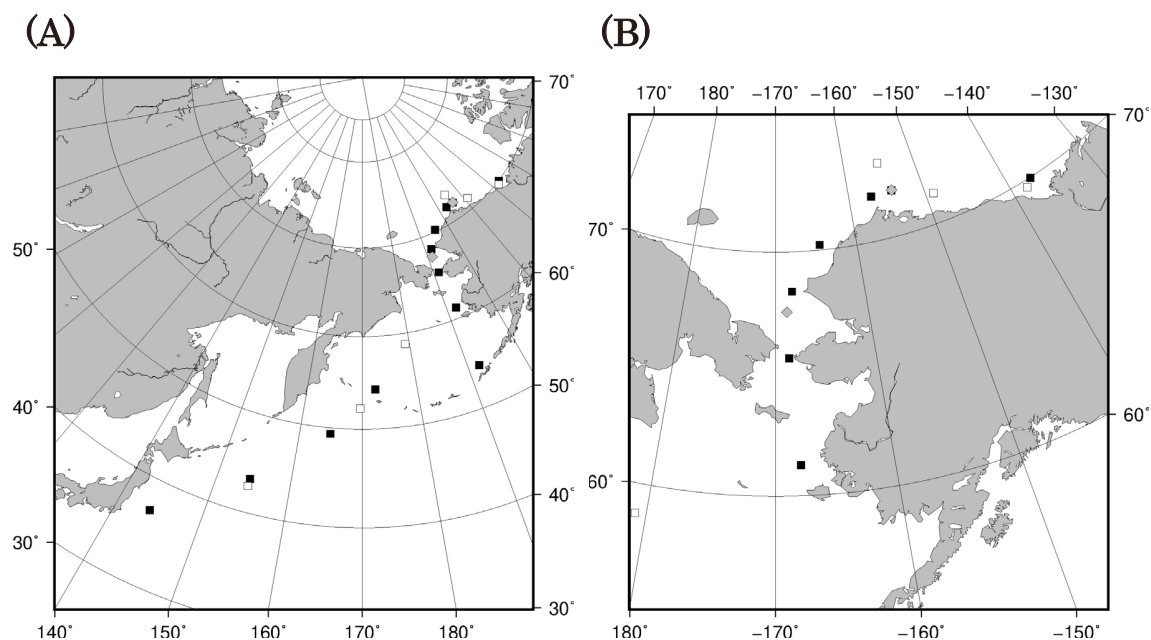


Figure 4.17-2: Map showing the sites where additional experimental filtrations were conducted. (A) Locations of the sites where the size fraction test was performed (filled squares). (B) Locations of the sites where the pre-filter test was performed (open squares), and seawater just above the bottom sediments (gray diamonds) were collected for eDNA sampling.

(7) Data archive

The data obtained in this cruise will be submitted to the Data Management Group of JAMSTEC, and will be opened to the public via “Data Research System for Whole Cruise Information in JAMSTEC (DARWIN)” on JAMSTEC website.

<<http://www.godac.jamstec.go.jp/darwin/e>>

4.18. Microplastic

(1) Personnel

Ryota Nakajima (JAMSTEC): Principal investigator (not on board)

Takahito Ikenoue (JAMSTEC): Acting principal investigator (on board)

Koto Sugimoto (Kobe University/JAMSTEC) (on board)

Eswara Venkatesaperumal Ramasamy (Mahatma Gandhi University) (not on board)

Shambanagouda Marigoudar (National Centre for Coastal Research) (not on board)

(2) Objectives

The distribution of microplastic in the open ocean of the Arctic Ocean is largely undocumented. Substantial numbers of studies on microplastics have been reported in the Pacific and Atlantic Oceans, yet very few data are available in the polar oceans. In the present study, we conducted microplastic surveys along the cruise tracks to fill gaps in the Arctic Ocean.

(3) Parameters

Microplastics (>333 μm)

Size fractionated microplastics (>300 μm , 50-300 μm , and 10-50 μm)

Depth (m)

(4) Instruments and methods

(4-1) *Neuston net sampling for surface microplastic analysis*

Floating microplastic samples were collected at 19 stations using a neuston net with a square mouth opening of 75 cm height and 100 cm width, equipped a 333 μm mesh opening net with a 100 μm mesh net at the cod end. The net was released from the ship's starboard side using a crane and towed for 20 min at a speed of 1–2 kn in the upper 0.4 m of the sea surface. A single sample was collected at Station 13. Duplicate samples were collected at each of the remaining 18 stations by repeating the net towing. A flow meter was installed at the net mouth to estimate the volume of water filtered during each tow. The collected samples were fixed with 5% formalin and stored at room temperature until analysis. Time and position of the neuston net sampling are shown in Table 4.18-1.

(4-2) *Seawater sampling from multiple depths for microplastic analysis*

36 L of seawater samples were collected in each of three layers according to the difference in water mass by Niskin bottles attached to a CTD rosette water sampling system (see 3.1. CTD casts and water sampling for the detailed sampling time and position). Seawater samples were fractionated and filtered to >300 μm , 50-300 μm , and 10-50 μm using filtration pumps in a clean booth. 100% cotton lab coats without plastic fibers were worn during the filtration process. Time and position of the seawater sampling from multiple depths are shown in Table 4.18-2.

(4-3) *Sea floor sediment sampling for microplastic analysis*

A multiple corer system (Asyura) equipped with three aluminum tubes was used to collect microplastics in the sea floor sediment. The aluminum tube is 60 cm length and 7.4 cm inner diameter. At the beginning of multiple corer system going down, the speed of wire out was set to be 0.5 m s⁻¹. Wire out was stopped at a depth about 10 m above the seafloor and the corer system was left stand for 1 minute to reduce any pendulum motion of the system. After the multiple corer system was stabilized, the wire was stored out at a speed of 0.5 m s⁻¹ with carefully watching a tension meter. After confirmation of the multiple corer system touching the bottom, the wire continued out till bowing. The rewinding of the wire was started at a dead slow speed (0.3 m s⁻¹), and then winch wire was wound up at 0.5 m s⁻¹. Two of the three cores were used for microplastic analysis and one for paleoenvironmental analysis (See 6. Geology for the treatment of the core for paleoenvironmental analysis). In the laboratory, 100% cotton lab coats without plastic fibers were worn. Surface sediment (top ca. 5 cm of sediment core) were taken from the sediment core samples at 1 cm intervals and stored in a freezer until analysis. Time and position of the sea floor sediment sampling are shown in Table 4.18-3.

Microplastic samples will be subjected to enumeration and identification of plastic types using a microscope and FT-IR. The distribution, density and concentration of microplastic in this study will be compared with the previous reports in the Arctic Ocean.

(5) Station list

Table 4.18-1: Time and position of the neuston net sampling.

Table 4.18-2: Sampling depths of the seawater samples.

Table 4.18-3: Time and position of the sea floor sediment sampling.

(6) Data archive

These data obtained in this cruise will be submitted to the Data Management Group of JAMSTEC, and will be opened to the public via “Data Research System for Whole Cruise Information in JAMSTEC (DARWIN)” in JAMSTEC web site.

<<http://www.godac.jamstec.go.jp/darwin/e>>

Table 4.18-1: Time and position of the neuston net sampling.

Station No.	Cast No.	Date (UTC)	Start time (UTC)	End time (UTC)	Start Latitude	Start Longitude	End Latitude	End Longitude
1	Cast1	2022/8/24	15:43	16:03	65-30.7450N	168-45.0171W	65-30.5967N	168-45.0317W
	Cast2	2022/8/24	16:17	16:39	65-30.4742N	168-45.0716W	65-30.2984N	168-45.0125W
4	Cast1	2022/8/25	6:25	6:45	67-01.4083N	168-40.2548W	67-01.1355N	168-39.2615W
	Cast2	2022/8/25	6:55	7:15	67-00.9488N	168-38.7071W	67-00.6794N	168-37.5928W
5	Cast1	2022/8/25	14:10	14:30	67-30.0436N	168-47.0421W	67-29.7656N	168-46.0818W
	Cast2	2022/8/25	14:40	15:00	67-29.6836N	168-45.7536W	67-29.4557N	168-44.7701W
7	Cast1	2022/8/26	7:23	7:43	68-30.8377N	168-44.9570W	68-31.2241N	168-43.8801W
	Cast2	2022/8/26	7:54	8:14	68-31.4473N	168-43.3021W	68-31.8739N	168-42.2145W
8	Cast1	2022/8/26	15:08	15:28	68-59.5338N	168-46.9022W	68-59.6833N	168-45.6775W
	Cast2	2022/8/26	15:39	15:59	68-59.7283N	168-45.1665W	68-59.8886N	168-43.7634W
11	Cast1	2022/8/27	4:17	4:37	70-30.4027N	168-45.9824W	70-30.8365N	168-45.7969W
	Cast2	2022/8/27	4:47	5:07	70-31.1530N	168-45.7035W	70-31.5894N	168-45.7035W
13 (BCE)	Cast1	2022/8/30	1:31	1:51	71-40.2336N	154-58.8837W	71-39.8114N	154-58.0773W
15	Cast1	2022/8/31	8:16	8:36	71-07.9860N	146-06.8917W	71-08.1204N	146-05.6657W
	Cast2	2022/8/31	8:45	9:05	71-08.2002N	146-04.8942W	71-08.3316N	146-03.6174W
16	Cast1	2022/8/31	16:06	16:26	71-00.8693N	142-01.4752W	71-00.9130N	142-00.4512W
	Cast2	2022/8/31	16:33	16:53	71-00.9310N	141-59.9872W	71-00.9783N	141-59.0063W
18	Cast1	2022/9/2	21:34	21:54	71-20.0901N	135-34.9658W	71-19.9410N	135-33.6298W
	Cast2	2022/9/2	22:06	22:26	71-19.8442N	135-32.7219W	71-19.6862N	135-31.2800W
19 (MT1)	Cast1	2022/9/4	0:42	1:02	69-58.4133N	137-14.3900W	69-58.1891N	137-13.5257W
	Cast2	2022/9/4	1:08	1:28	69-58.0623N	137-13.0370W	69-57.8049N	137-12.1757W
20	Cast1	2022/9/5	15:09	15:29	70-24.6779N	141-37.2577W	70-24.9548N	141-38.1848W
	Cast2	2022/9/5	15:39	15:59	70-25.0356N	141-38.4605W	70-25.3214N	141-39.4215W
22	Cast1	2022/9/5	22:16	22:36	70-41.2449N	141-44.0693W	70-41.6899N	141-45.1911W
	Cast2	2022/9/5	22:46	23:06	70-41.8639N	141-45.6446W	70-42.3049N	141-46.8084W
24	Cast1	2022/9/9	15:40	16:00	71-49.8469N	152-32.5432W	71-49.8804N	152-31.7466W
	Cast2	2022/9/9	16:12	16:32	71-49.9078N	152-31.4316W	71-49.9513N	152-30.6937W
26	Cast1	2022/9/10	6:12	6:32	72-34.5802N	152-27.8249W	72-34.1175N	152-28.7568W
	Cast2	2022/9/10	6:42	7:02	72-33.8277N	152-29.2250W	72-33.3262N	152-29.9181W
27	Cast1	2022/9/10	17:03	17:23	71-19.8209N	152-32.8980W	71-19.8493N	152-31.7813W
	Cast2	2022/9/10	17:34	17:54	71-19.8769N	152-31.1291W	71-19.9541N	152-30.0487W
30	Cast1	2022/9/14	17:06	17:26	72-30.0032N	160-02.7633W	72-29.9799N	160-00.8724W
	Cast2	2022/9/14	17:36	17:56	72-29.9810N	160-00.6405W	72-29.9841N	159-59.2339W
32	Cast1	2022/9/14	22:54	23:14	72-54.1195N	158-51.9305W	72-54.0710N	158-50.4862W
	Cast2	2022/9/14	23:24	23:44	72-54.0496N	158-49.6481W	72-53.9764N	158-48.1880W
33	Cast1	2022/9/15	14:42	15:02	73-20.0820N	157-30.6654W	73-20.0345N	157-29.2574W
	Cast2	2022/9/15	15:12	15:32	73-20.0586N	157-29.2674W	72-19.9978N	157-27.8972W

Table 4.18-2: Sampling depths of the seawater samples.

Station No.	Sampling depths (m)
1	10, 25, 50
4	10, 25, 39
5	10, 25, 44
8	9, 25, 47
12 (BCE)	10, 40, 95
13 (BCC)	10, 69, 198
15	10, 69, 296
16	10, 69, 296
18	10, 25, 69
19	10, 25, 52
20	10, 25, 76
23	10, 69, 296
24	10, 69, 296
26	10, 70, 295
27	10, 25, 56
30	10, 25, 42
32	10, 69, 297
33	10, 69, 296

Table 4.18-3: Time and position of the sea floor sediment sampling.

Station No.	Date (UTC)	Time (UTC)	Latitude	Longitude	Sea floor depth (m)	Remarks
1	2022/8/24	17:35	65-30.89N	168-44.87W	54	No sample
4	2022/8/25	06:06	67-01.48N	168-41.15W	44	HandA: 0-5 cm, HandB: 0-5 cm
5	2022/8/25	15:59	67-29.55N	168-44.30W	49	HandA: 0-5 cm, HandB: 0-4 cm
7	2022/8/26	07:05	68-30.54N	168-45.65W	53	HandA: 0-5 cm, HandB: 0-5 cm
8	2022/8/26	17:08	69-00.09N	168-43.43W	53	HandA: 0-5 cm, HandB: 0-5 cm
11	2022/8/27	03:18	70-29.97N	168-45.39W	38	HandA: 0-4 cm, HandB: No sample
20	2022/9/5	16:57	70-25.29N	141-39.81W	79	HandA: 0-5 cm, HandB: 0-5 cm
27	2022/9/10	19:01	71-20.08N	152-30.39W	61	HandA: 0-5 cm, HandB: 0-5 cm
30	2022/9/14	18:50	72-30.11N	159-59.32W	48	HandA: 0-5 cm, HandB: 0-5 cm

5. Under-the-Ice Drone Trials

(1) Personnel

Shojiro Ishibashi (JAMSTEC) – System Integrator (Not on board)
Kiyotaka Tanaka (JAMSTEC) – Operation Leader and System Engineer
Yosaku Maeda (JAMSTEC) – (Not on board)
Hiroshi Matsumoto (JAMSTEC) – (Not on board)
Makoto Sugawara (JAMSTEC) – System Engineer and Operator
Ryo Kimura (Nippon Marine Enterprises, Ltd.; NME) – Operator
Mariko Hatta (JAMSTEC) – Operator
Tomotaka Katsuno (The University of Tokyo) – Engineer and Operator
Kazuho Yoshida (NME) – Operator
Fumine Okada (NME) – Operator
Satomi Ogawa (NME) – Operator
Hiroshi Yoshida (JAMSTEC) – Adviser

(2) Objectives

The under-the-ice drone named COMAI (Figure 5-1) is a middle size Autonomous Underwater Vehicle (AUV) for observations under the sea ice in the Arctic. The drone autonomously cruise and observe environment under the ice in coverage area of 15 km. A completion of fully autonomous operation under ice is more complex than operation in open sea because of two big breakthrough items. One is positioning and the other is emergency recovery. In high latitude area, vertical magnetic field component of the Earth becomes great larger than horizontal one and $\omega \cos \lambda$ becomes small, where ω and λ are angular speed of Earth and latitude, respectively. These changes cause errors of navigation system. In this second trial we focus on evaluations of the navigation system. Observations of ice bottom is also targeted because we wrote in the last cruise report of MIRAI (MR21-05C), “we intend to carry out under ice surveys with the drone fixed bugs in FY2022.” Test items are followings:

- 1) evaluation of the navigation system in high longitude area,
- 2) acoustic homer performance check,
- 3) cruising tests using acoustic remote control mode and autonomous control mode, and
- 4) observation under the ice.

All tests were performed with a safety tether because recovery functions are not yet evaluated in this test.



Figure 5-1: A recovery scene of COMAI.

(3) Parameters

None

(4) Instruments and methods

COMAI is a platform of observation sensors for under the ice area. It autonomously cruises and surveys under the ice without a tether cable. Specifications of the drone is listed in Table 5-1. The maximum cruising range is about 30 km or endurance is about 16 hours (at cruising speed of 1 kt). The drone utilizes a hybrid navigation system consisting of a MEMS inertial measurement unit, a magnetic compass and a Doppler velocity log. The navigation system block diagram is shown in Figure 5-2. COMAI has four operation modes: 1) an Untethered Remotely Operated Vehicle mode (UROV), 2) an Acoustical ROV mode (AROV), 3) a Radio wave ROV mode (RROV), and 4) an Autonomous Underwater Vehicle (AUV) mode. In the AUV mode, three cruising patterns (heading-depth control, way-point control, and way-line control) are selectable. It has a special cruising mode named “escape mode” in addition to them. The mode automatically controls the drone to return to a preprogrammed position after completion of an autonomous mission. This enables the drone to escape from ice covered area to open sea area. If one of the navigation device is down, the drone automatically changes the control mode to a heading-depth control with an acoustical super short baseline navigation toward an acoustical light house pre-deployed as shown in Figure 5-3.

COMAI consists of major three parts: a vehicle body, a ship-side console, and an acoustical system. Its body is made from aluminum and covered with an FRP fairing cover. The ship-side console provides a graphical user interface of the drone system for operation and maintenance. The acoustical system consists of an acoustical communication modem/ locator and an acoustical pinger for the acoustical lighthouse.

Table 5-1: Specifications of COMAI.

Items	Specifications	Remarks
Size	2.3 x 0.6 x 0.7 m	
Weight	330 kg	in air
Depth rating	300 m	
Cruising speed	2 kt	3 kt max.
Cruising range	30 km	
Power	Li-ion battery (5.7 kWh)	
Actuators	Horizontal thrusters (100 W) x 2 Vertical thruster (100 W) x 1 Rudders	
Scientific payloads	CTD (conductivity, temperature, depth) sensor Turbidity and chlorophyll meter Snap shot camera Multi beam sonar	installed on top side installed on top side

COMAI is equipped with scientific sensors: a CTD sensor (miniCTD, Valeport), a turbidity and chlorophyll meter (ECO FLNTU, WET Labs), a snap shot camera (2592 x 1944 pixels, F2.2) with LED strobe lights, and a 260 kHz multi beam sonar (837B Delta T, IMAGENEX). The camera and the multi beam sonar are mounted on the top side of the body for ice bottom observations. All data obtained are automatically logged in the drone internal memory and a hard disk of the personal computer of the ship-side console (when ROV mode).

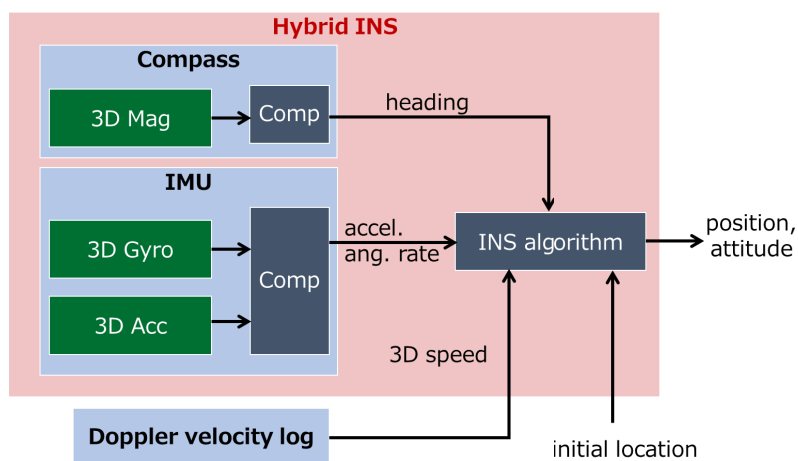


Figure 5-2: Block diagram of the hybrid navigation system.

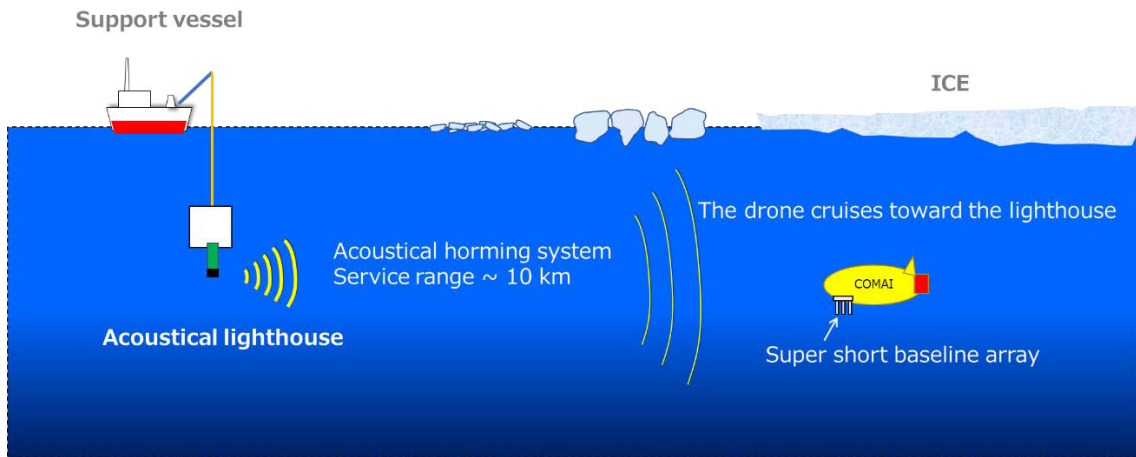


Figure 5-3: A working image of the heading-depth control with the acoustical super short baseline navigation in the escape mode.

(5) Test log

Station No.	Position		Date	Time(Local)		Water depth	Test No.	Test item	Descriptions
	Lat.	Lon.		Start	End				
none	71.138733N	162.839294W	27-Aug-22	7:56	16:01	46 m	Test-1	Test # 1	Navigation test
none	71.25016N	148.995621W	06-Sep-22	7:50	15:48	230 m	Test-2	Test # 2 &Test # 1	Acoustic homer test Navigation test
none	71.866707N	156.99646W	11-Sep-22	8:00	15:47	70 m	Test-3	Test # 3	Acoustical remote control & AUV test
none	73.168623N	155.062865W	12-Sep-22	8:07	13:56	3610 m	Test-4	Test # 4	Observation under sea ice

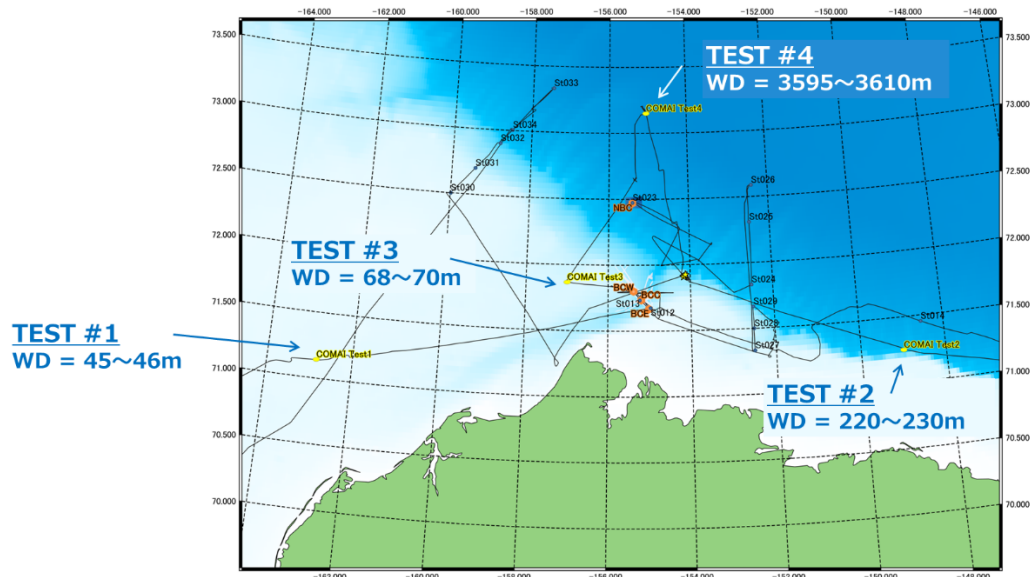


Figure 5-4: Test points.

(6) Preliminary results

Figure 5-5 shows tracks of COMAI measured with the hybrid navigation system (closed circle) and with the USBL: Ultra Short Base Line (open circle) in the test #1. The former completely differs from the latter. In this test bottom tracking of the DVL (Doppler Velocity Log) was invalid because of the deep sea area. This would make error in the navigation but it would not become so large. We need to evaluate cause of the difference urgently because it is very important to ensure accuracy of navigation system.

Position measured with hybrid navigation system

- It could not detect forces of sea current.
(潮流が検知できていません)
- Large position error.
(大きな位置計測誤差が出ています)

Position measured with USBL

It measures relative position 「みらい」との相対位置を計測

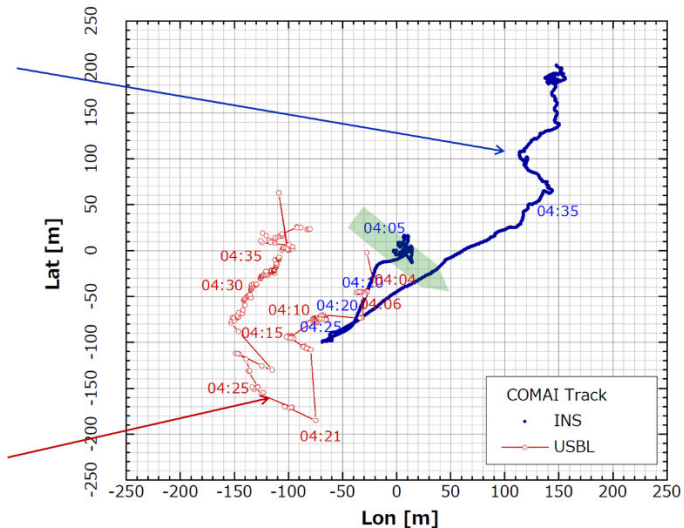


Figure 5-5: The drone tracks measured by the GPS and INS (Inertial Navigation System) in the test #1.

Last year we suffered from azimuth errors caused by magnetic field around the R/V Mirai. In this tests, we see compass dancing around in circle many times at points distant from the ship. These do not result from magnetic field made by the ship. Figure 5-6 shows time trends of heading of and depth of COMAI in the test #4. When the drone is near the surface (depths = 0 ~ 10 m), heading measured turns round and round. The test area was high latitude area where the ratio of magnetic field of vertical to horizontal component became about ten. In this situation north direction measured is easily switched with small change of roll or pitch angle. When the drone goes under 10 m deep, effect of waves to body of the drone disappeared and then heading become stable. From this results, we recognize that magnetic compass is not suitable for highly accurate navigation in high latitude area.

In test #4 COMAI successfully dived below a large piece of sea ice. The drone cruised toward 200 degree from the ship (see Figure 5-5). A total cruising distance is more than 200 m along the ice edge. COMAI was controlled with the heading-depth pattern of the AUV mode with target depth of 50 m. Figure 5-7 illustrates vertical profiles of temperature and salinity around the ice. XCTD data measured near point of the test are also plotted. We estimate the thickness of the ice using difference between depth of the drone and vertical distance measured by the DVL as shown in Figure 5-8. Grey parts

means data are invalid. The ice thickness of 7 ~14 m is estimated. We obtained snapshots and multi-beam image of the ice bottom. These data are under analysis but ice size is already estimated as about 100 m.

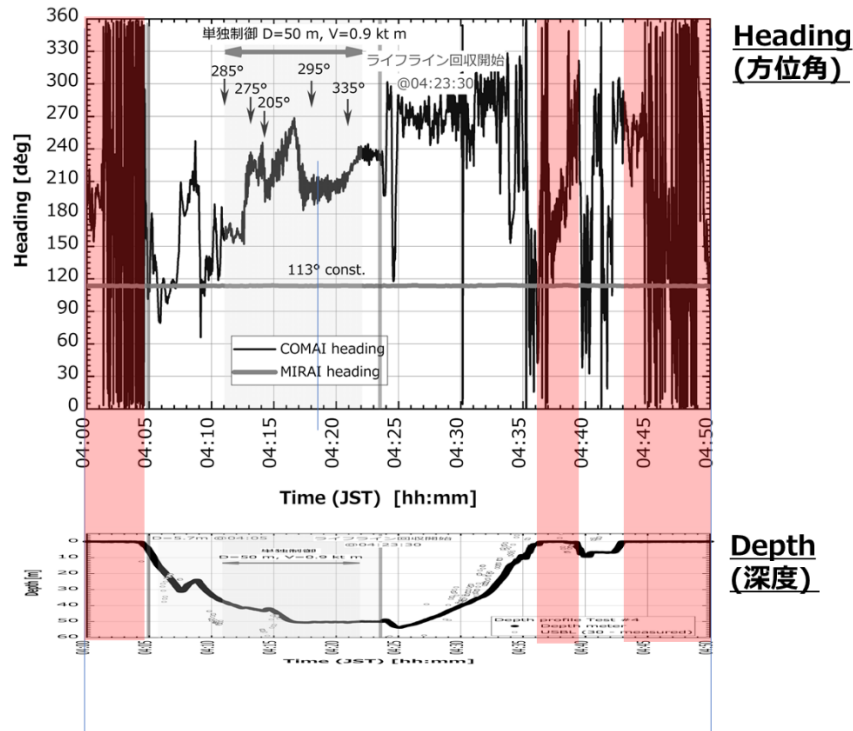


Figure 5-6: Time trends of heading and depth in the test #4. Red areas show the period of heading turn round and round.

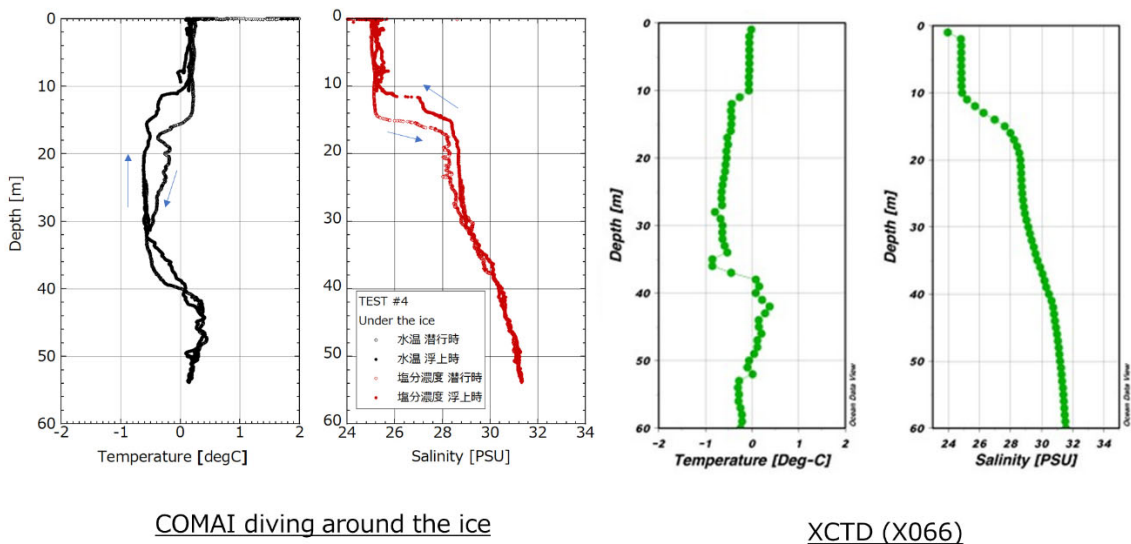


Figure 5-7: Vertical trends temperature and salinity. Left data obtained with COMAI and right obtained with an XCT at near point.

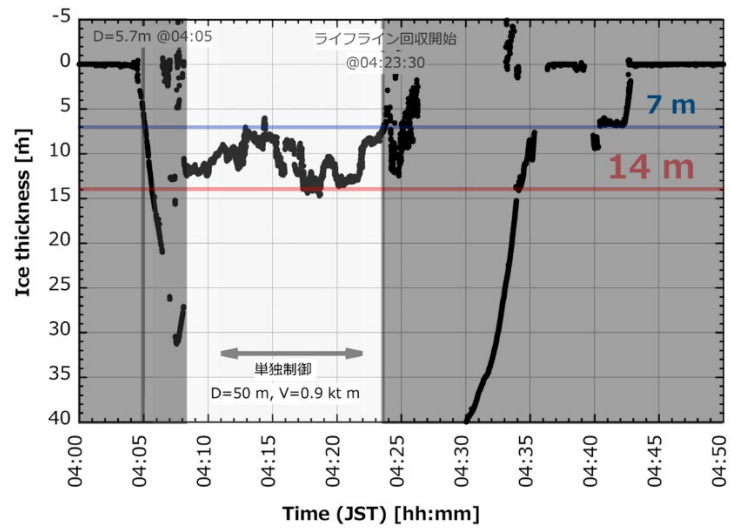


Figure 5-8: Ice thickness estimated from difference between depth and distance from the drone.

6. Geology

6.1 Sediment core sampling

(1) Personnel

Masanobu Yamamoto (Hokkaido University): Principal Investigator

Koji Seike (National Institute of Advanced Industrial Science and Technology)

Leonid Polyak (Hokkaido University)

Laura Gemery (United States Geological Survey)

Youngjin Joe (Korea Polar Research Institute)

Shoma Uchida (Hokkaido University)

Minoru Kobayashi (Hokkaido University)

Kazuma Takahashi (Marine Works Japan)

Yohei Katayama (Marine Works Japan)

Yoshiki Kido (Marine Works Japan)

Yuta Shinomiya (Marine Works Japan)

Kazuho Yoshida (NME)

Jonaotaro Onodera (JAMSTEC)

(2) Objectives

The Arctic Ocean and terrestrial environment have recently been reported to be changing drastically, but it is unclear whether these changes are similar to natural variations in the past or how sudden and large the changes are compared to natural variations. In this study, we plan to 1) analyze sediment cores collected off the mouth of the Mackenzie River to reconstruct changes in the Mackenzie River inflow to the Arctic Ocean, permafrost thawing in the catchment area, summer sea ice cover, primary productivity, and biological communities over the past 2000 years, 2) analyze sediment cores collected off Barrow in the Alaskan margin to reconstruct changes in the Bering Strait inflow to the Arctic Ocean, the strength of the Beaufort gyre circulation, summer sea ice cover, primary productivity, and biological communities over the past 2000 years and 3) generate the detailed record of environmental change covering the preindustrial period without anthropogenic influence. Based on this information over a wide range of marine and terrestrial environments, the ongoing drastic changes in the Arctic environment will be quantitatively placed within the past 2000 years, and the elements of environmental change closely related to anthropogenic changes will be identified. High-resolution records of the ocean and terrestrial environments that can be compared with observation records will enable us to reinterpret observation data accumulated by the Arctic research communities. It is expected to dramatically improve our understanding of environmental changes in the Arctic region.

(3) Parameters

Site Survey

Geophysical seafloor surveys were performed in the areas selected for coring, including two sites in the Mackenzie Trough (MT) and two sites in the Barrow Canyon (BC) area (Table 6.1-1; Figure 6.1-1). Survey was performed by Kazuho Yoshida and the NME team, Leonid Polyak, Youngjin Joe, and Masanobu Yamamoto on September 01, 04, 07, and 12. The survey included the Multi-Beam Echo-Sounder (MBES) seafloor mapping, and attendant high-resolution Sub-Bottom Profiling (SBP) performed at a slow cruising speed of ~3 knots for better quality results. The survey strategy capitalized on the comparable MBES and SBP data and sediment cores collected from the R/V Araon in 2013 (ARA04-B&C).

A SeaBeam 3012 MBES collected swath bathymetry with wide beam angles ranging from 120 (60° to -60°) to 140 (70° to -70°) degrees. The MBES data were processed onboard using the Caris HIPS software. The resolution of the processed images has 20-m and 75-m grids in the Mackenzie Trough and Barrow Canyon, respectively, depending on the water depth of survey areas. The mapped swath bathymetry was superimposed on the International Bathymetric Chart of the Arctic Ocean (IBCAO v. 4; Jakobsson et al., 2020) with QGIS software. High-resolution CHIRP Sub-Bottom Profiling (SBP) data were obtained by Bathymetry 2010 Sub-bottom profiler with the frequency set to 3.5 kHz with the ping rates of 1.33 to 2.08 Hz.

Table 6.1-1: Information on geophysical survey data acquisition.

Site	SBP line no.	Length (km)	MBES (km ²)	Site	SBP line no.	Length (km)	MBES (km ²)
MT1	Line 1	4.4	3.9	BC2	Line 1	6.2	31.5
	Line 2a	3.1			Line 2	6.0	
	Line 2b	3.1			Line 3	3.1	
	Line 3	3.3			Line 4	5.8	
	Line 4a	3.4			Line 5	5.2	
	Line 4b	3.4			Line 6	3.0	
	Line 5	3.4		BC2-2	Line 7	5.2	
	Line C1	0.5			Line 8	5.7	
	Line C2	0.5		Total length (km)	72.5	Total Area (km ²)	
MT2	Line 2	5.2	11.0				

The survey objectives included:

- Selecting sites for coring
- Collecting background information for the study areas
- Addressing attendant scientific problems, where applicable

Gravity Corer (GC)

The gravity corer system consists of a weight, a 5 m- or 7 m-long stainless steel barrel with an acryl liner tube, and a pilot core sampler (Figure 6.1-1). The Inner Diameter (I.D.) of the steel barrel is 120 mm; the acryl liner tube is 114 mm, respectively. We used a small multiple corer (“Asyura”) of approximately 100 kg weight for a pilot core sampler. The total weight of the system is about 750 kg.

Piston Corer (PC)

The piston corer system consists of a weight, a 15 m-long aluminum barrel with polycarbonate liner tube, and a pilot core sampler (Figure 6.1-1). The Inner Diameter (I.D.) of the aluminum barrel is 80 mm; polycarbonate liner tube is 74 mm, respectively. We used an Asyura corer for a pilot core sampler. The total weight of the system is approximately 1.4 t.

Multiple Corer (MC)

A multiple-core sampler was used for retrieving the surface sediment (Figure 6.1-1). This core sampler consists of a main body of 640 kg-weight and eight sub-core samplers (I.D. 74mm and length of 60cm) equipped with a set of transparent polycarbonate liners.

Long Asyura corer

A long Asyura corer sampler was used for retrieving the surface sediment (Figure 6.1-1). This core sampler consists of a main body and three sub-core samplers (I.D. 82 mm and length 80cm) equipped with transparent polycarbonate liner tubes. This sampler was designed to retrieve longer surface sediments than the conventional Asyura corer. It worked properly at station 5 when it was used as a single corer but failed at the MT1 site due to unknown reasons when it was used as a pilot corer.

Box Corer (BC)

A box corer was used for retrieving the surface sediment (Figure 6.1-1). This core sampler consists of a main body of 330 kg weight and a metal box sampler (40 cm x 40 cm x 50 cm height). The memory CTD Rinkoprofiler (ASTD102-ALC-R02, JFE Advantech Co., Ltd., Japan) was attached to measure environmental variables of the water column in the sampling station, such as water temperature, salinity, chlorophyll concentration, and turbidity. Seafloor

photographs were taken by an underwater camera attached to the box corer.



Figure 6.1-1: Corers.

(4) Instruments and methods

CCR measurements

After splitting each section of cores into working and archive halves, and the Core Color Reflectance (CCR), the value calculated for the spectral reflectance from 400 to 700 nm in wavelengths using the Konica Minolta CM-700d, was measured from the archive halves.

Calibrations include zero calibration and white calibration before the measurement of core samples. Zero calibration is carried out in the air. White calibration is carried out using the white calibration piece (CM-700d standard accessories) without clear polyethylene wrap. The color of the split sediment (archive half core) was measured every 1 cm through transparent polyethylene film.

We used the LAB system that is visualized as a cylindrical coordinate system in which the cylinder's axis is the lightness variable L^* , ranging from 0% to 100%, and the radii are the chromaticity variables a^* and b^* . Variable a^* is the green (negative) to the red (positive) axis, and variable b^* is the blue (negative) to the yellow (positive) axis.

MSCL measurements

A GEOTEK Multi-Sensor Core Logger (MSCL) has five sensors, which are Gamma-Ray Attenuation (GRA), P-Wave Velocity (PWV), Magnetic Susceptibility (MS), Non-Contact Resistivity (NCR), and Natural Gamma Ray Radiation (NGR). These were measured on split-core sections using the onboard MSCL. Measurement every 1 cm (NGR was measured every 20 cm).

GRA was measured by a gamma-ray source and detector. These are vertically mounted across the core on a sensor stand that aligns them with the center of the core. A narrow gamma-ray beam is emitted by Cesium-137 (^{137}Cs) with energies at 0.662 MeV. Also, the gamma-ray photon is collimated through 5 mm diameter in a rotating shutter at the front of the housing

of ^{137}Cs . The photon passes through the core and is detected on the other side. The detector comprises a scintillator (a 2" diameter and 2" thick NaI crystal).

GRA calibration assumes a two-phase system model for sediments, where the two phases are the minerals and the interstitial water. Aluminum has an attenuation coefficient similar to common minerals and is used as the mineral phase standard. Pure water is used as the interstitial-water phase standard. The standard consists of a telescoping aluminum rod (six elements of varying thickness) mounted in a piece of core liner and half-filled with ultrapure water. GRA was measured with 10 seconds of counting.

PWV was measured by a pulse transmitter and an oil-filled Acoustic Rolling Contact (ARC) transducer vertically mounted on the center sensor stand with a gamma system. The transmitter touches a split core surface and produces a short pulse. The P-Wave propagates through the core and is detected by the transducer. Then the velocity of the P-Wave through the core and the P-Wave pulse frequency were measured.

MS was measured using two Bartington loop sensors; one of those has an internal diameter of 100 mm and is used for the multiple and Asyura cores. The other loop sensor has an inner diameter of 140 mm and is used for the gravity core. An oscillator circuit in the sensor produces a low intensity (approx. 80 A/m RMS) non-saturating, alternating magnetic field (0.565 kHz). MS was measured for 1 second.

NCR was measured with an NCR sensor installed under the rail in MSCL. NCR sensor has a transmitter coil which creates a high-frequency magnetic field through a core. The magnetic field induces electrical currents in the core which are inversely proportional to the resistivity. A calibration curve for NCR is made by using the relationship between electrical current and resistivity of five NCR pieces with different concentrations of NaCl solution (0.35, 1.75, 3.5, 17.5, and 35 g/L). NCR was measured for 5 seconds.

NGR was measured with three scintillation detectors attached to a central lead cube. Radiated gamma-ray from a core is recorded as a spectrum by a multi-channel analyzer. The analyzer divides the gamma ray into 1024 channels according to the energy level (the energy range is 0-3000 keV). NGR was measured with 120 seconds of counting.

Core Photographs

After splitting each section of cores into working and archive halves, sectional photographs of working were taken using a digital camera.

Microscopic observation

Box cores were sectioned in 1-cm subsamples, bagged, refrigerated, and frozen when shipboard work was complete. Each box core was evaluated for microfossil composition based on planktic, benthic and agglutinated foraminifera, and ostracodes. Box core sediment samples

were wet sieved using a hand-held shower faucet with tap water through a stainless-steel, 63 micron (μm) sieve. Wet sediment weight per 1-cm aliquot averaged $\sim 250\text{-}350\text{g}$. The $>63\ \mu\text{m}$ fractions were removed from the sieve using Milli-Q water to filter paper and oven dried at 40°C . The dry residues were evaluated for Mollusca and microfossil presence and abundance.

(5) Station list

We retrieved a piston, ten gravity, eight pilot Asyura, four box, and four multiple cores at geologically targeted MT1, MT2, BC2, and BC2-2 sites. In addition, we retrieved a long Asyura core at Station 5 as a test. A hand of the Asyura cores from Stations 5, 7, 8, and 11 for the microplastic study (See Chapter 4.18) was offered for the descriptions of lithology, color, and physical properties. The locations of cores are summarized in Figure 6.1-2 and Table 6.1-2. Stratigraphic columns of obtained cores from the MT1, MT2, BC2, and BC2-2 sites are shown in Figure 6.1-3.

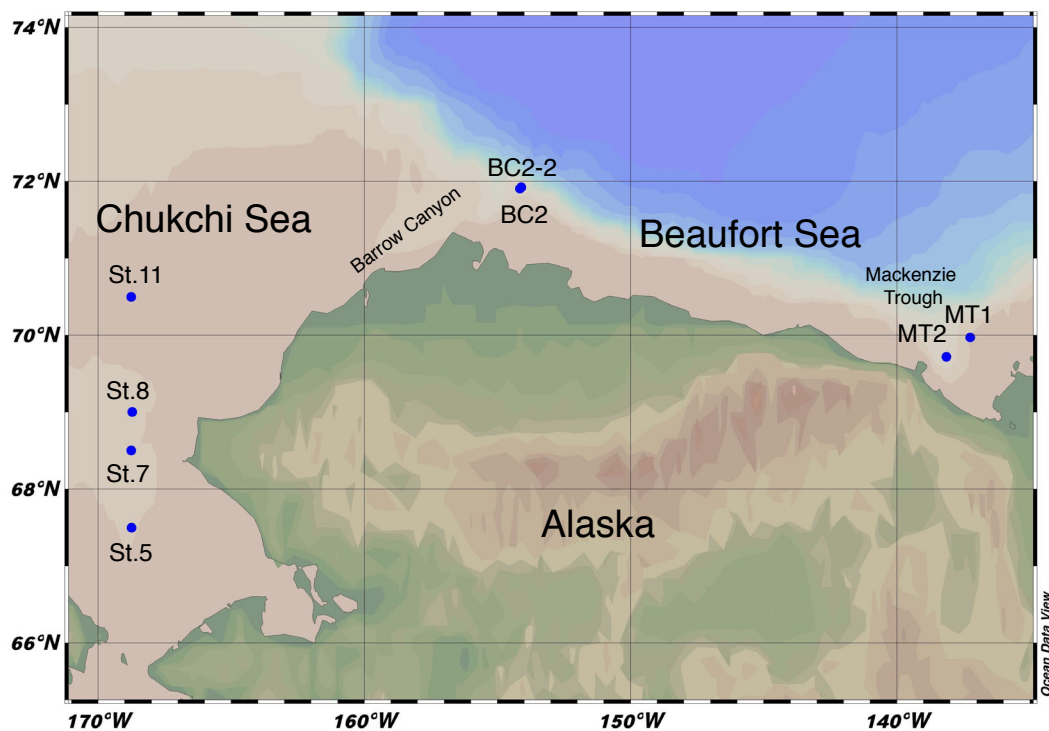


Figure 6.1-2: Location of coring sites.

Table 6.1-2: Core information

Shipboard ID	Core name	Site name	Year	Month	Day	Time (UTC)	Latitude (degree)	Longitude (degree)	Water depth (m)	Core length (cm)	Section
MR22-06C St.5 Sediment	MR22-06C St.5 Sediment	St. 5	2022	08	25	16:00:56	67.4927	-168.7382	49.5	11	1
MR22-06C St.5 Sediment2	MR22-06C St.5 A1-3	St. 5	2022	08	25	16:14:25	67.4931	-168.7374	49.6	15.5	3
MR22-06C St.7 Sediment	MR22-06C St.7 Sediment	St. 7	2022	08	26	7:05:16	68.5092	-168.7608	53.8	15.5	1
MR22-06C St.8 Sediment	MR22-06C St.8 Sediment	St. 8	2022	08	26	17:07:02	69.0016	-168.7239	53.2	17	1
MR22-06C St.11 Sediment	MR22-06C St.11 Sediment	St. 11	2022	08	27	3:16:07	70.4996	-168.7557	39	11	1
MR22-06C PC01	MR22-06C MT1 PC01	MT1	2022	09	01	18:14:13	69.9748	-137.2464	59	672	7
MR22-06C GC01	MR22-06C MT1 GC01	MT1	2022	09	01	20:24:28	69.9749	-137.2462	62	390	4+CC
MR22-06C BC01	MR22-06C MT1 B1-6	MT1	2022	09	01	22:48:29	69.9756	-137.2445	57	33	1
MR22-06C MC01	MR22-06C MT1 M1-8	MT1	2022	09	01	23:30:38	69.9756	-137.2444	57	34	8
MR22-06C GC02	MR22-06C MT1 GC02	MT1	2022	09	02	1:48:00	69.9755	-137.2445	57	378	4+CC
MR22-06C PL01	MR22-06C MT1 A1-2	MT1	2022	09	02	1:48:00	69.9755	-137.2445	57	36	2
MR22-06C GC03	MR22-06C MT1 GC03	MT1	2022	09	03	17:52:50	69.9764	-137.2447	59	424	4+CC
MR22-06C PL02	MR22-06C MT1 A3-5	MT1	2022	09	03	17:52:50	69.9764	-137.2447	59	36	3
MR22-06C GC04	MR22-06C MT1 GC04	MT1	2022	09	03	22:39:25	69.9756	-137.2445	58	429	4+CC
MR22-06C PL03	MR22-06C MT1 A6-8	MT1	2022	09	03	22:39:25	69.9756	-137.2445	58	38	3
MR22-06C GC05	MR22-06C MT2 GC05	MT2	2022	09	04	17:54:17	69.7189	-138.1491	153	424	4+CC
MR22-06C PL04	MR22-06C MT2 A1-3	MT2	2022	09	04	17:54:17	69.7189	-138.1491	153	39	3
MR22-06C BC02	MR22-06C MT2 B1-9	MT2	2022	09	04	19:32:43	69.7191	-138.1490	152	39	1
MR22-06C MC02	MR22-06C MT2 M1-8	MT2	2022	09	04	23:26:32	69.7192	-138.1485	152	26	8
MR22-06C GC06	MR22-06C MT2 GC06	MT2	2022	09	05	0:32:20	69.7193	-138.1486	159	476	4+CC
MR22-06C GC07	MR22-06C BC2 GC07	BC2	2022	09	07	17:55:40	71.9099	-154.1578	227	491	5+CC
MR22-06C PL05	MR22-06C BC2 A1-3	BC2	2022	09	07	17:55:40	71.9099	-154.1578	227	30	3
MR22-06C BC03	MR22-06C BC2 B1-8	BC2	2022	09	07	20:10:12	71.9099	-154.1577	224	27	1
MR22-06C MC03	MR22-06C BC2 M1-8	BC2	2022	09	07	22:30:00	71.9099	-154.1590	226	26	8
MR22-06C GC08	MR22-06C BC2 GC08	BC2	2022	09	08	0:11:35	71.9102	-154.1604	223	475	5+CC
MR22-06C PL06	MR22-06C BC2 A4-6	BC2	2022	09	08	0:11:35	71.9102	-154.1604	223	24	3
MR22-06C GC09	MR22-06C BC2-2 GC09	BC2-2	2022	09	13	17:53:39	71.9244	-154.1164	268	500	5+CC
MR22-06C PL07	MR22-06C BC2-2 A1-3	BC2-2	2022	09	13	17:53:39	71.9244	-154.1164	268	26	3
MR22-06C MC04	MR22-06C BC2-2 M1-8	BC2-2	2022	09	13	19:19:38	71.9245	-154.1165	268	24	8
MR22-06C BC04	MR22-06C BC2-2 B1-9	BC2-2	2022	09	13	20:04:47	71.9245	-154.1159	268	24	1
MR22-06C GC10	MR22-06C BC2-2 GC10	BC2-2	2022	09	13	23:48:54	71.9244	-154.1165	275	476	5+CC
MR22-06C PL08	MR22-06C BC2-2 A4-6	BC2-2	2022	09	13	23:48:54	71.9244	-154.1165	275	36	3

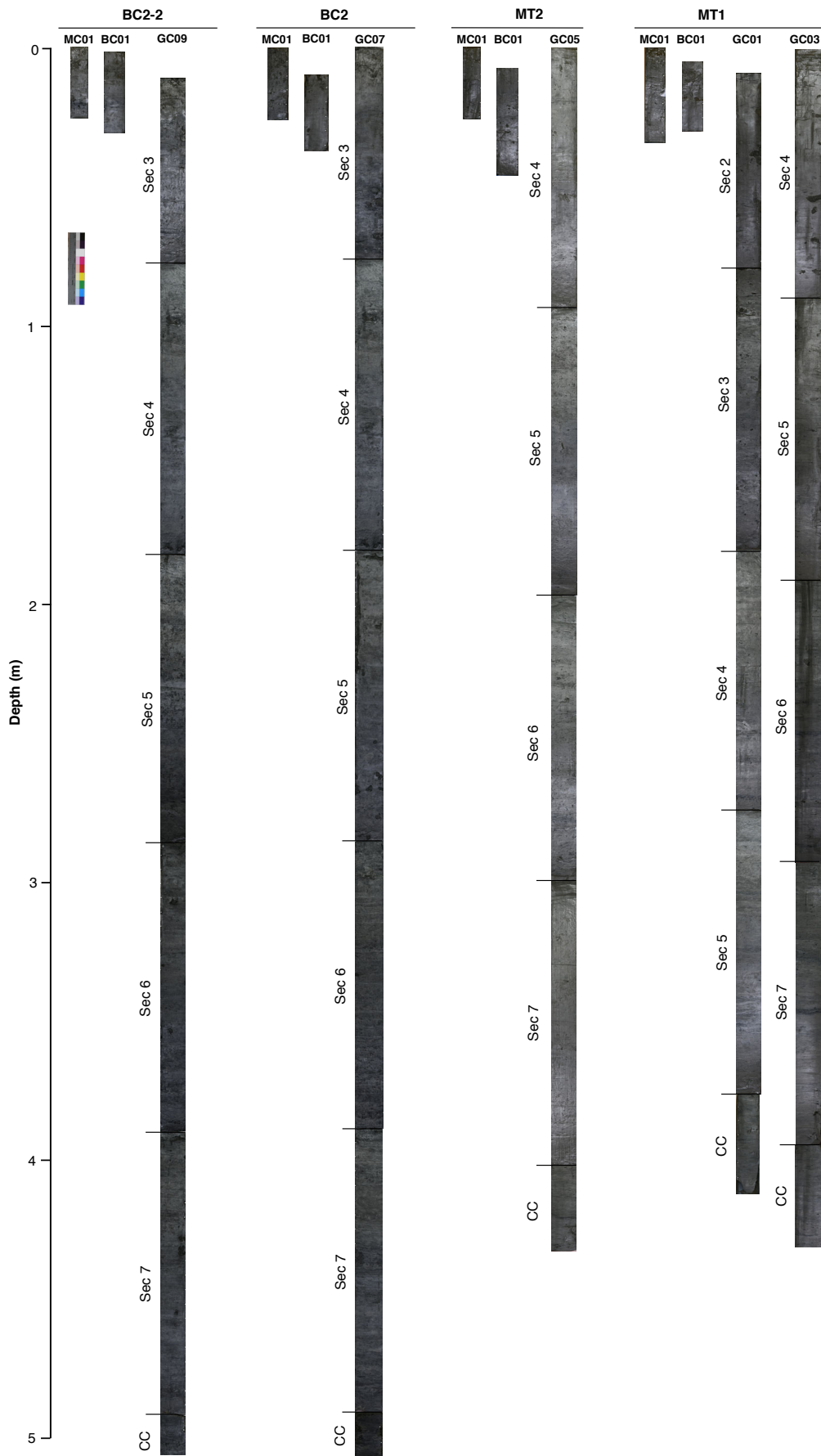


Figure 6.1-3: Stratigraphic columns of cores from the MT1, MT2, BC2, and BC2-2 sites.

(6) Preliminary results

Site MT1

This site is ~130 km north of the Mackenzie River mouth at water depths of ~60 m in the northeastern shelf of the Mackenzie Trough (Figure 6.1-2) and was selected to retrieve sediment cores with a high sedimentation rate to reconstruct changes in the Mackenzie River inflow to the Arctic Ocean, permafrost thawing in the catchment area, summer sea ice cover, primary productivity, and biological communities over the past 2000 years.

The study area is called the “Garry Knolls,” characterized by multiple pingo-like seafloor structures identified in earlier data (Figure 6.1-4) (Paull et al., 2007). Moat deposits accumulated adjacent to the pingo structures constitute depocenters of well-stratified sediments suitable for collecting high-resolution sediment-core records, as demonstrated in a prior study (Gemery et al., 2023). The coring site MT1 was chosen in one of these local depocenters, nearby core HLY1302 from the above study.

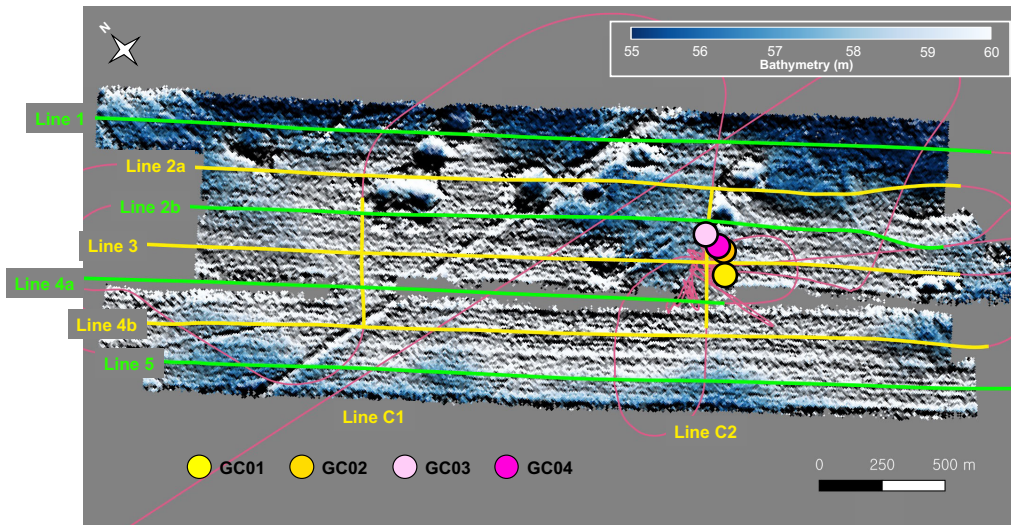
We retrieved a piston, four gravity, three pilot Asyura, a multiple, and a box cores at this site. The first two gravity cores using a five-meter-long barrel were over-penetrated, and the mudline was missing. Therefore we retrieved two additional cores using a seven-meter-long barrel. This further coring was successful, and we recognized the mudline (the water-sediment contact surface) at the core top. The long Asyura did not work correctly due to unknown reasons, and thus, we used the conventional Asyura as a pilot corer.

GC01, GC03, MC01, and BC01 were half split, described, photographed, and color measured by MSCL. The sediments consist of dark olive gray (5Y 3/2 to 3/1) sticky silty clay with a slight change in color and appearance of mm-scale dark and blackish, fine interlayers and speckles throughout the cores (Figures 6.1-5 and 6.1-6). Cm-scale prominent black bands were intercalated. The surface of the box core sample was covered with muddy sediments with a few individuals of brittle stars.

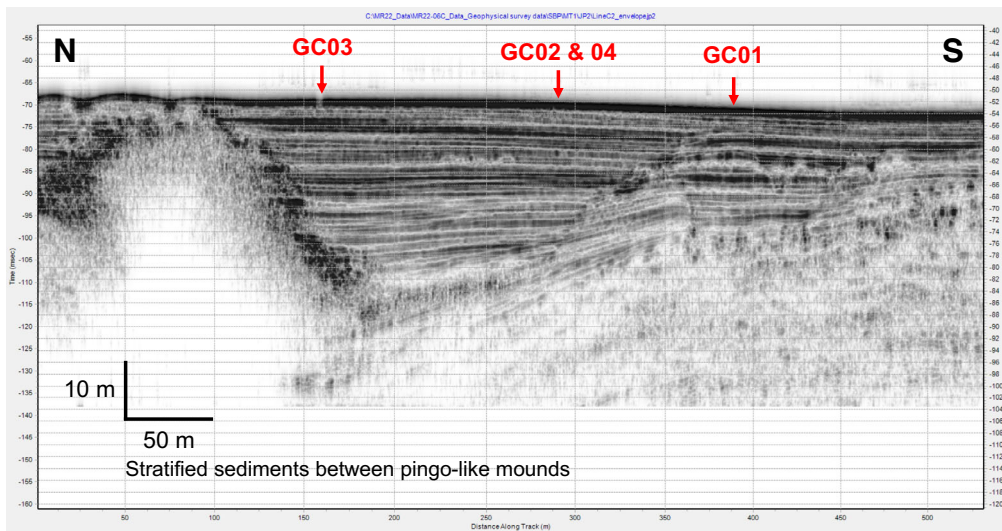
Color indices and magnetic susceptibility show significant variations throughout the cores (Figure 6.1-7). The correlations between GC01, GC03, MC01, and BC01 suggest the core-top of GC01, GC03, and BC01 correspond to the depths of 9 cm, 0.5 cm, and 5 cm, respectively, of MC01.

Onboard microscopic observation of box core (BC01; MT1 B6) samples indicated that foraminifera and ostracod were well preserved (Table 6.1-3). There were no obvious visual signs of carbonate dissolution or compromise.

MT1 MBES including coring sites



MT1 SBP_coring sites (line C2)



MT1 SBP_coring sites (line 3)

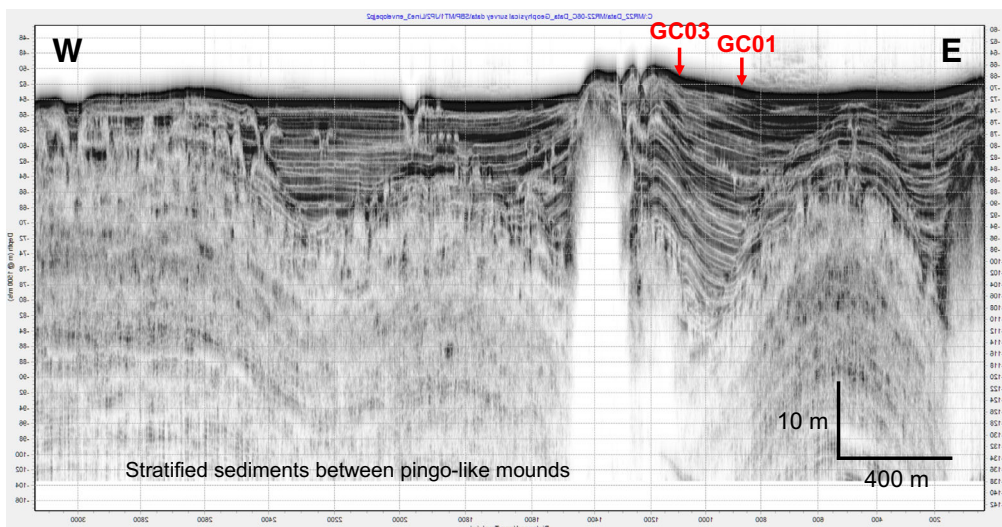


Figure 6.1-4: Site survey MBES and SBP data from the MT1 area. Coring sites are shown by circles and arrows on the MBES and SBP images, respectively.

Holocene Arctic Palaeoclimatology and Palaeoceanography Investigation (HAPPI) 2022

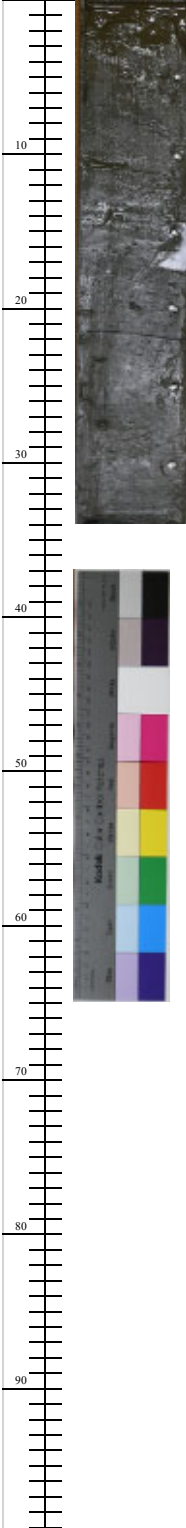
Site name: MT1	Core type: MC	Core number: 1	Section number: 1
Section length 34 cm	Described by Polyak	Core name: MR02-06C MT1 M1	
cm	Column	Description	
0		0-7 cm Very soft, dark olive gray (5Y 3/2), fine-grained, silty mud, waterly at the top. Boundary by a slight change in color and appearance of dark, fine laminations.	
10		7-17 cm Very soft, dark olive gray (5Y 3/2), fine-grained mud with indistinct mm-scale, blackish interlayers, overall slightly darker than unit on top. Boundary by further darkening of sediment.	
20		17-34 cm Very soft, dark olive gray (5Y 3/1), fine-grained mud with blackish interlayers.	
30			
40			
50			
60			
70			
80			
90			
100			

Figure 6.1-5: Lithologic columns of cores at the MT1 sites.

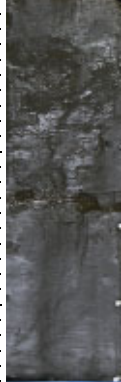
Holocene Arctic Palaeoclimatology and Palaeoceanography Investigation (HAPPI) 2022			
	Site name: MT1	Core type: BC	Core number: 1 Section number: 1
cm	Section length 25 cm	Described by Polyak	Core name: MR02-06C MT1 B1
	Column	Description	
0		0-11 cm Very soft, dark olive gray (5Y 3/2), fine-grained, slightly silty mud. Boundary by slight change to overall darker color. Corresponds to 0-12 cm in the cohole box-core sample.	
10		11-25 cm Soft, sticky, dark olive gray (5Y 3/2 to 3/1), fine-grained, slightly silty mud. Indistinct mm-scale, blackish interlayers.	
20			
30			
40			
50			
60			
70			
80			
90			
100			

Figure 6.1-5: Lithologic columns of cores at the MT1 sites (Continued).

Holocene Arctic Palaeoclimatology and Palaeoceanography Investigation (HAPPI) 2022

	Site name: MT1	Core type: BC	Core number: 1	Section number: 6
cm	Section length 32.5 cm	Described by Polyak	Core name: MR02-06C MT1 B6 Bento	
	Column	Description		
0		0-4 cm Very soft, waterly, dark olive gray (5Y 3/2), fine-grained, slightly silty mud. Boundary gradual by appearance of blackish layers.		
10		4-12 cm Very soft, dark olive gray (5Y 3/2), fine-grained mud with thin (mm-scale) blackish interlayers. Boundary by a slight change to overall darker color.		
20		12-32.5 cm Soft, sticky, dark olive gray (5Y 3/1), fine-grained, slightly silty mud. Indistinct thin (mm-scale) blackish interlayers (difficult to see due to due to a darker background color).		
30				
40				
50				
60				
70				
80				
90				
100				

Figure 6.1-5: Lithologic columns of cores at the MT1 sites (Continued).

Holocene Arctic Palaeoclimatology and Palaeoceanography Investigation (HAPPI) 2022

	Site name: MT1	Core type: GC	Core number: 1	Section number: 2
cm	Section length 68 cm	Described by Polyak	Core name: MR02-06C MT1 GC01 Section 2	
	Column	Description		
0		0-68 cm Very soft, dark olive gray (5Y 3/2), fine-grained, slightly silty, sticky mud with scattered blackish interlayers and speckles.		
10		No surface layer due to overpenetration.		
20				
30				
40				
50				
60				
70				
80				
90				
100				

Figure 6.1-5: Lithologic columns of cores at the MT1 sites (Continued).

Holocene Arctic Palaeoclimatology and Palaeoceanography Investigation (HAPPI) 2022

	Site name: MT1	Core type: GC	Core number: 1	Section number: 2
cm	Section length 68 cm	Described by Polyak	Core name: MR02-06C MT1 GC01 Section 2	
	Column	Description		
0		0-68 cm Very soft, dark olive gray (5Y 3/2), fine-grained, slightly silty, sticky mud with scattered blackish interlayers and speckles.		
10		No surface layer due to overpenetration.		
20				
30				
40				
50				
60				
70				
80				
90				
100				

Figure 6.1-5: Lithologic columns of cores at the MT1 sites (Continued).

Holocene Arctic Palaeoclimatology and Palaeoceanography Investigation (HAPPI) 2022

	Site name: MT1	Core type: GC	Core number: 1	Section number: 3
cm	Section length 99 cm	Described by Polyak	Core name: MR02-06C MT1 GC01 Section 3	
	Column	Description		
0		0-99 cm Very soft, sticky, dark olive-gray (5Y 3/2), fine-grained, slightly silty mud with scattered blackish, mm-scale interlayers and speckles. Small mollusc picked at ~86 cm.		
10				
20				
30				
40				
50				
60				
70				
80				
90				
100				

Figure 6.1-5: Lithologic columns of cores at the MT1 sites (Continued).

Holocene Arctic Palaeoclimatology and Palaeoceanography Investigation (HAPPI) 2022

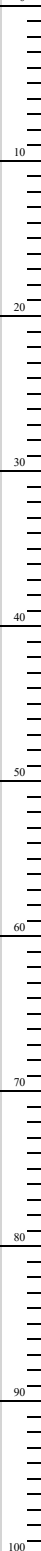
	Site name: MT1	Core type: GC	Core number: 1	Section number: 2
cm	Section length 68 cm	Described by Polyak	Core name: MR02-06C MT1 GC01 Section 2	
	Column	Description		
<p>0</p>  <p>10</p> <p>20</p> <p>30</p> <p>40</p> <p>50</p> <p>60</p> <p>70</p> <p>80</p> <p>90</p> <p>100</p>		<p>0-68 cm Very soft, dark olive gray (5Y 3/2), fine-grained, slightly silty, sticky mud with scattered blackish interlayers and speckles.</p> <p>No surface layer due to overpenetration.</p>		

Figure 6.1-5: Lithologic columns of cores at the MT1 sites (Continued).

Holocene Arctic Palaeoclimatology and Palaeoceanography Investigation (HAPPI) 2022

	Site name: MT1	Core type: GC	Core number: 1	Section number: 4
cm	Section length 99 cm	Described by Polyak	Core name: MR02-06C MT1 GC01 Section 4	
	Column	Description		
0		0-99 cm Soft, stiky, dark olive gray (5Y 3/2), fine-grained, slightly silty mud with scattered blackish, mm-scale interlayers and speckles. A prominent black band at 86-87 cm.		
1				
2				
3				
4				
5				
6				
7				
8				
9				
10				
11				
12				
13				
14				
15				
16				
17				
18				
19				
20				
21				
22				
23				
24				
25				
26				
27				
28				
29				
30				
31				
32				
33				
34				
35				
36				
37				
38				
39				
40				
41				
42				
43				
44				
45				
46				
47				
48				
49				
50				
51				
52				
53				
54				
55				
56				
57				
58				
59				
60				
61				
62				
63				
64				
65				
66				
67				
68				
69				
70				
71				
72				
73				
74				
75				
76				
77				
78				
79				
80				
81				
82				
83				
84				
85				
86				
87				
88				
89				
90				
91				
92				
93				
94				
95				
96				
97				
98				
99				
100				

Figure 6.1-5: Lithologic columns of cores at the MT1 sites (Continued).

Holocene Arctic Palaeoclimatology and Palaeoceanography Investigation (HAPPI) 2022

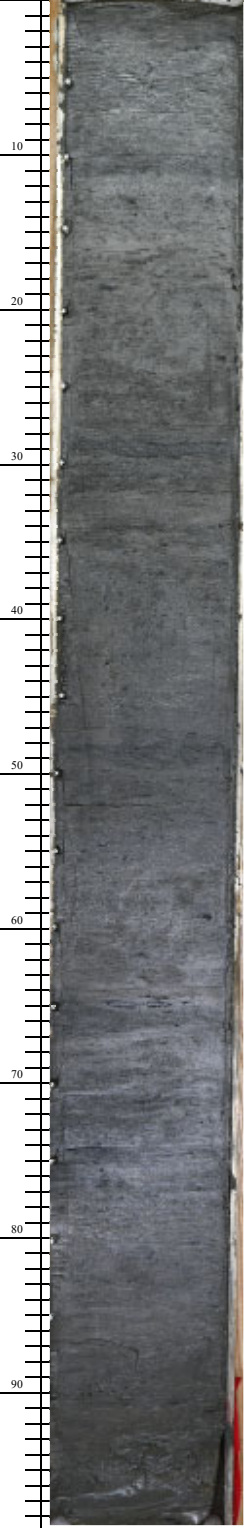
	Site name: MT1	Core type: GC	Core number: 1	Section number: 5
cm	Section length 99 cm	Described by Polyak	Core name: MR02-06C MT1 GC01 Section 5	
	Column	Description		
0		0-99 cm Soft, sticky dark olive-gray (5Y 3/2), fine-grained, slightly silty mud with scattered blackish, mm-scale interlayers and speckles. A prominent black band at 28-29 cm.		
10				
20				
30				
40				
50				
60				
70				
80				
90				
100				

Figure 6.1-5: Lithologic columns of cores at the MT1 sites (Continued).

Holocene Arctic Palaeoclimatology and Palaeoceanography Investigation (HAPPI) 2022

	Site name: MT1	Core type: GC	Core number: 1	Section number: CC
cm	Section length 36 cm	Described by Polyak	Core name: MR02-06C MT1 GC01 CC	
	Column	Description		
0		0-36 cm Soft, sticky, dark olive-gray (5Y 3/2 to 3/1), fine-grained, slightly silty mud with diffuse mm-scale, blackish interlayers and speckles.		
10				
20				
30				
40				
50				
60				
70				
80				
90				
100				

Figure 6.1-5: Lithologic columns of cores at the MT1 sites (Continued).

	Site name: MT1	Core type: GC	Core number: 2	Section number: CC
cm	Section length 25 cm	Described by Polyak	Core name: MR02-06C MT1 GC02 CC	
	Column	Description		
0		0-25 cm Soft, sticky, dark olive-gray (5Y 3/2 to 3/1), fine-grained, slightly silty mud with diffuse mm-scale, blackish interlayers and speckles.		
10				
20				
30				
40				
50				
60				
70				
80				
90				
100				

Figure 6.1-5: Lithologic columns of cores at the MT1 sites (Continued).

Holocene Arctic Palaeoclimatology and Palaeoceanography Investigation (HAPPI) 2022

	Site name: MT1	Core type: GC	Core number: 3	Section number: 4
cm	Section length 88 cm	Described by Polyak	Core name: MR02-06C MT1 GC03 Section 4	
	Column	Description		
0		0-3 cm Very soft, grayish olive (5Y 4/2), fine-grained, slightly silty, homogenous mud. Boundary by change in color and appearance of blackish patches.		
10		3-88 cm Soft, sticky, dark olive gray (5Y 3/2 to 3/1), fine-grained, slightly silty mud with blackish interlayers and speckles, especially numerous below ~28 cm.		
20		A small mollusc shell picked at 79 cm.		
30				
40				
50				
60				
70				
80				
90				
100				

Figure 6.1-5: Lithologic columns of cores at the MT1 sites (Continued).

Holocene Arctic Palaeoclimatology and Palaeoceanography Investigation (HAPPI) 2022

	Site name: MT1	Core type: GC	Core number: 3	Section number: 5
cm	Section length 100 cm	Described by Polyak	Core name: MR02-06C MT1 GC03 Section 5	
	Column	Description		
0		<p>0-100 cm Soft, dark olive-gray (5Y 3/2 to 3/1), fine-grained, slightly silty, sticky mud with numerous blackish interlayers and speckles. Bands of blackish materials spaced at cm scale. Pronouced blackish bands at 55-56, 72-73, 75-76, and 88-89 cm.</p>		
10				
20				
30				
40				
50				
60				
70				
80				
90				
100				

Figure 6.1-5: Lithologic columns of cores at the MT1 sites (Continued).

Holocene Arctic Palaeoclimatology and Palaeoceanography Investigation (HAPPI) 2022				
	Site name: MT1	Core type: GC	Core number: 3	Section number: 6
cm	Section length 100 cm	Described by Polyak	Core name: MR02-06C MT1 GC03 Section 6	
	Column	Description		
0		0-100 cm Soft, dark olive-gray (5Y 3/2 to 3/1), fine-grained, slightly silty, sticky mud with numerous blackish interlayers and speckles. Bands of blackish materials spaced at cm scale. Pronounced blackish bands at 53-54 (most pronounced) and 92-93 cm.		
10				
20				
30				
40				
50				
60				
70				
80				
90				
100				

Figure 6.1-5: Lithologic columns of cores at the MT1 sites (Continued).

Holocene Arctic Palaeoclimatology and Palaeoceanography Investigation (HAPPI) 2022

	Site name: MT1	Core type: GC	Core number: 3	Section number: 5
cm	Section length 100 cm	Described by Polyak	Core name: MR02-06C MT1 GC03 Section 5	
	Column	Description		
0		<p>0-100 cm Soft, dark olive-gray (5Y 3/2 to 3/1), fine-grained, slightly silty, sticky mud with numerous blackish interlayers and speckles. Bands of blackish materials spaced at cm scale. Pronouced blackish bands at 55-56, 72-73, 75-76, and 88-89 cm.</p>		
10				
20				
30				
40				
50				
60				
70				
80				
90				
100				

Figure 6.1-5: Lithologic columns of cores at the MT1 sites (Continued).

Holocene Arctic Palaeoclimatology and Palaeoceanography Investigation (HAPPI) 2022

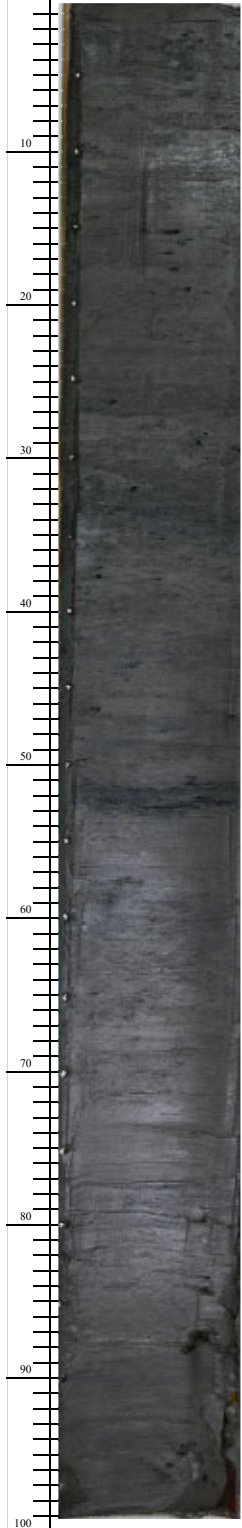
Site name: MT1	Core type: GC	Core number: 3	Section number: 7
Section length 100 cm	Described by Polyak	Core name: MR02-06C MT1 GC03 Section 7	
Column	Description		
	<p>0-100 cm Soft, dark olive-gray (5Y 3/2 to 3/1), fine-grained, slightly silty, sticky mud with numerous blackish interlayers and speckles. Bands of blackish materials spaced at cm scale. Most pronounced blackish bands at 33-34, ~52, and ~53 cm.</p>		

Figure 6.1-5: Lithologic columns of cores at the MT1 sites (Continued).

Holocene Arctic Palaeoclimatology and Palaeoceanography Investigation (HAPPI) 2022

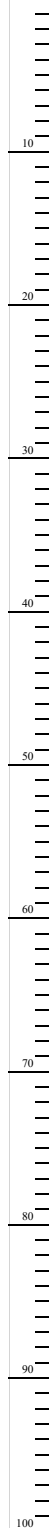
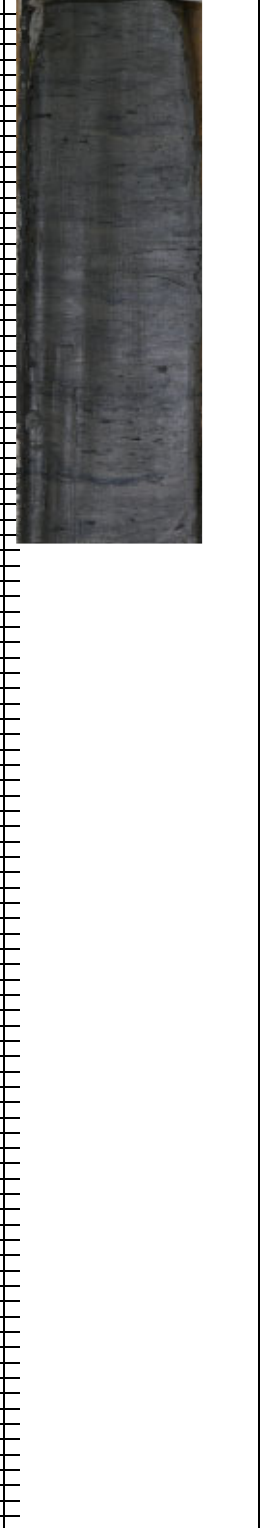
	Site name: MT1	Core type: GC	Core number: 3	Section number: CC
cm	Section length 35.5 cm	Described by Polyak	Core name: MR02-06C MT1 GC03 CC	
	Column	Description		
<p>0</p> 		<p>0-35.5cm Soft, dark olive-gray (5Y 3/2 to 3/1), sticky, fine-grained, slightly silty mud with numerous mm-scale, blackish interlayers and speckles. Pronounced 1-2 cm bands of blackish material occur at ~2-5 cm spacing.</p>		

Figure 6.1-5: Lithologic columns of cores at the MT1 sites (Continued).

	Site name: MT1	Core type: GC	Core number: 4	Section number: CC
cm	Section length 36 cm	Described by Polyak	Core name: MR02-06C MT1 GC04 CC	
	Column	Description		
0		0- 3 cm Soft, dark olive-gray (5Y 3/2), fine-grained, slightly silty mud with scattered small (mm-scale), blackish speckles. Boundary by increase in the amount of blackish inclusions.		
10		3-36 cm Soft, dark olive gray (5Y 3/1), fine-grained, slightly silty mud with numerous mm-scale, blackish interlayers and speckles. Pronounced 1-2 cm thick bands of blackish material occur at ~2-5 cm spacing (notably at ~4, 6, 9, 12, 15, 17, 20, 23, 25, 27, 30, 32, 34 cm). Note: by the time of description blackish color has partly faded away (after ~5-6 hours).		
20				
30				
40				
50				
60				
70				
80				
90				
100				

Figure 6.1-5: Lithologic columns of cores at the MT1 sites.

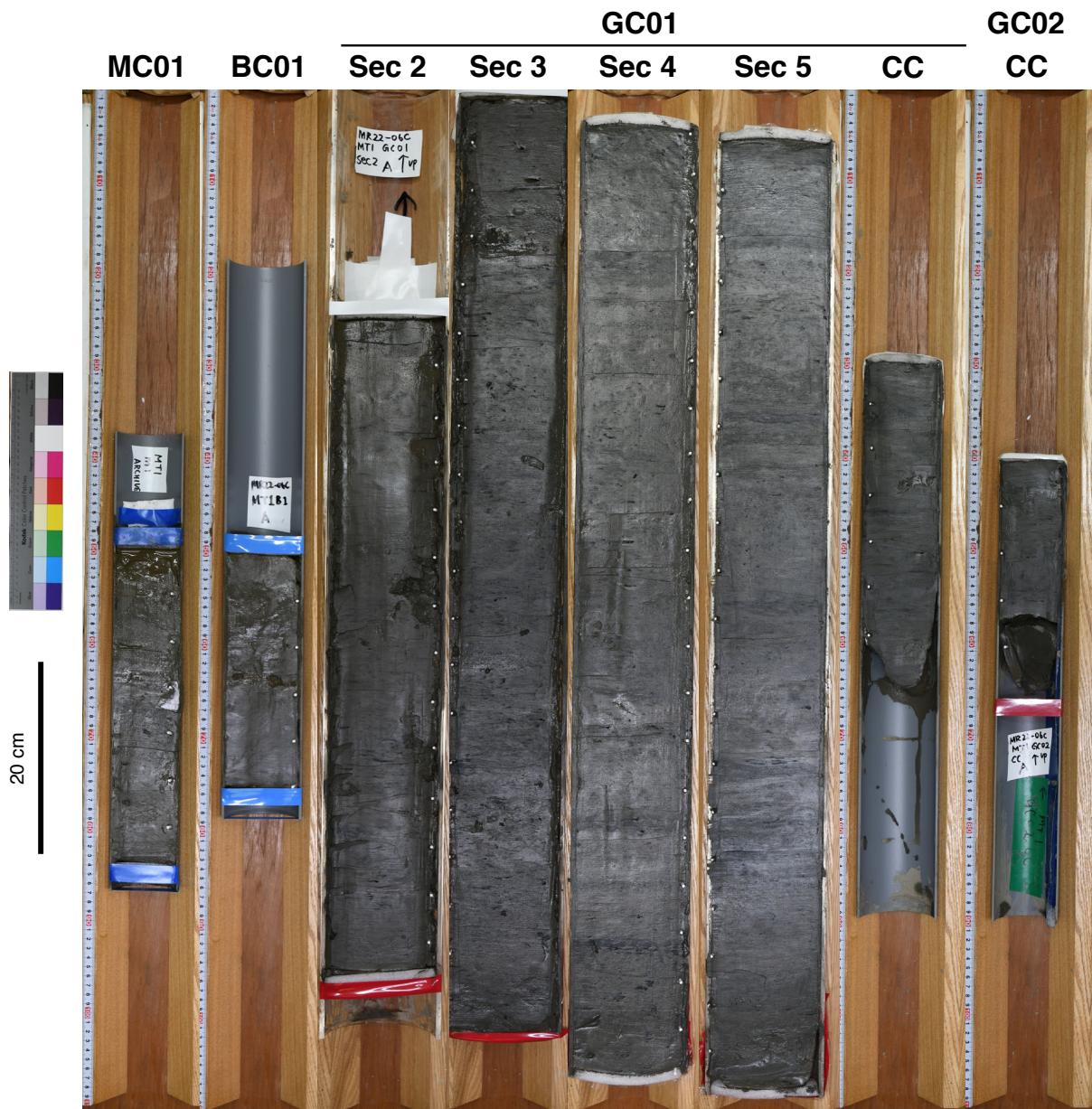


Figure 6.1-6: (1) Photographs of MT1 cores (1/2).



Figure 6.1-6: (2) Photographs of MT1 cores (2/2).

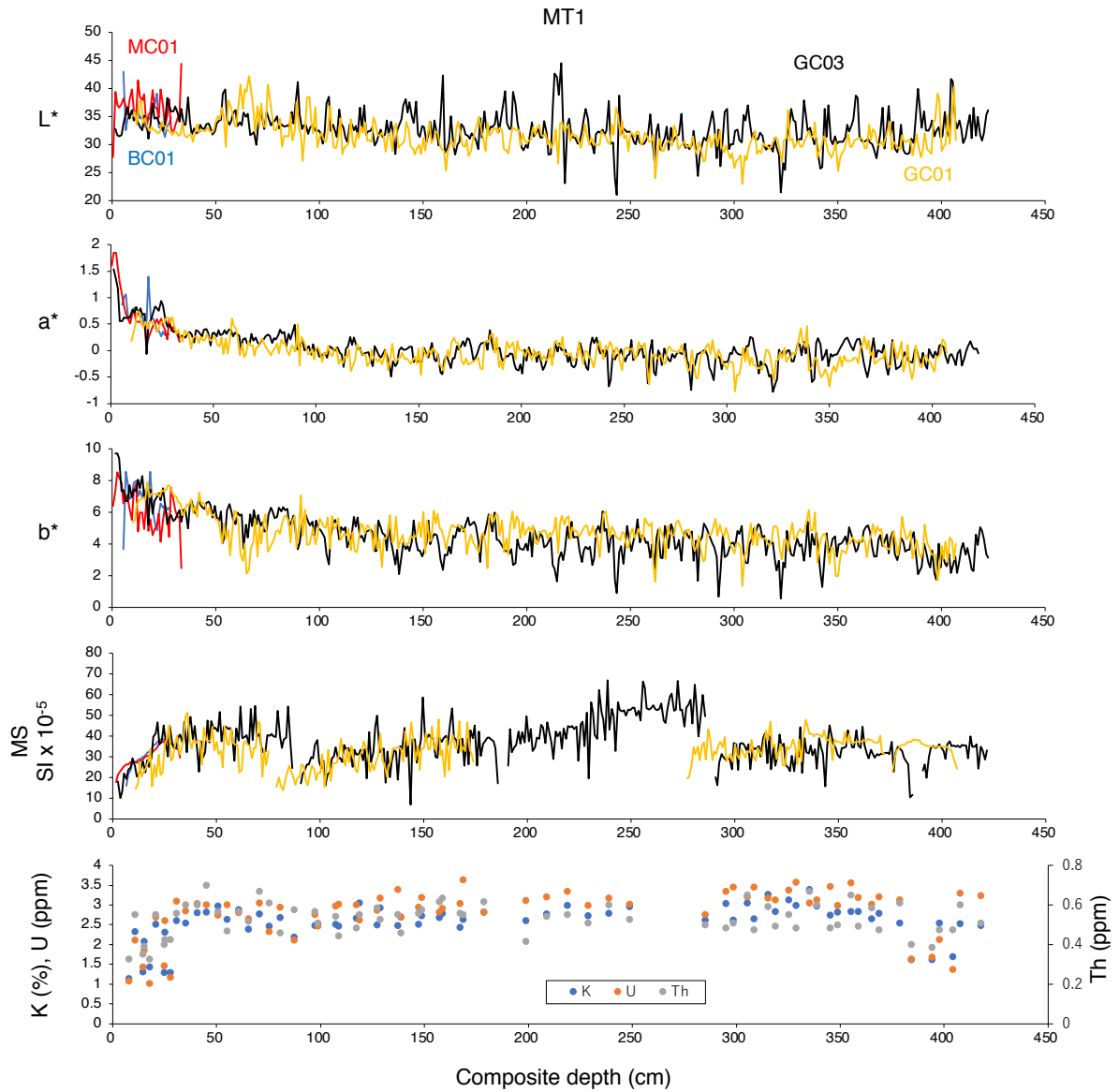


Figure 6.1-7: Variations in color indices, Magnetic Susceptibility (MS), K, U, and Th contents in cores at Site MT1.

Table 6.1-3: Abundance of foraminifera and ostracods in MT1 Box samples

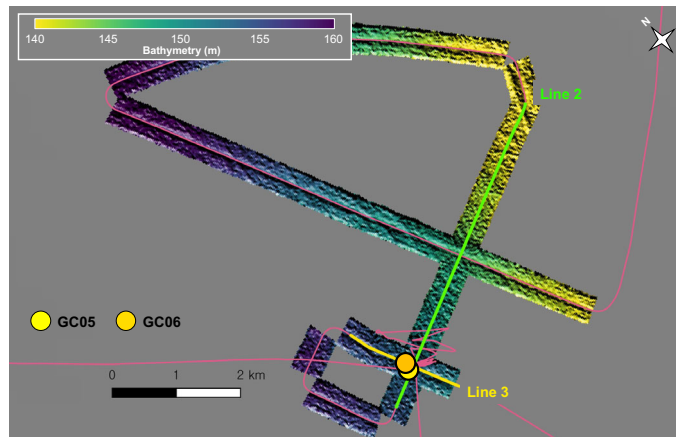
Top depth (cm)	Bottom depth (cm)	Benthic foraminifera	Agglutinated foraminifera	Ostracods
0	1	A	A	A
1	2	A	A	P
2	3	A	A	P
3	4	A	A	P
4	5	A	A	P
5	6	A	A	P
6	7	A	A	P
7	8	A	A	P
8	9	A	A	P
9	10	P	P	P
10	11	A	P	P
11	12	A	P	P
12	13	A	A	P
13	14	A	A	P
14	15	A	A	P
15	16	A	P	P
16	17	A	P	P
17	18	A	P	A
18	19	A	P	A
19	20	A	P	A
20	21	A	P	P
21	22	A	P	P
22	23	A	A	A
23	24	A	A	A
24	25	A	A	A
25	26	A	A	A
26	27	A	A	A
27	28	A	A	A
28	29	A	A	A

A=Abundant (>100 forams, >30 ostracods), P=Present but fewer (<30 ostracods), B=Barren

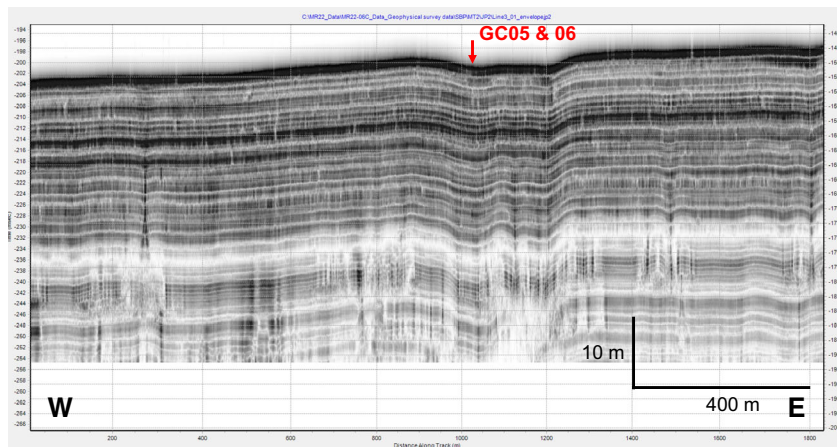
Site MT2

The MT2 area is located at the axis of the Mackenzie Trough (Figure 6.1-2) at a water depth of ~150 m (Figure 6.1-8). The coring site is located between cores PC2 and PC3 collected from the R/V Mirai in 2002 (MR02-K05 Leg1). Sedimentation rates at this location are expected to be lower than at the MT1 site due to a larger water depth, although the distance from the Mackenzie River (~130 km) is similar.

MT2 MBES including coring sites



MT2 SBP_coring sites (line 3)



MT2 SBP_coring sites (line 2)

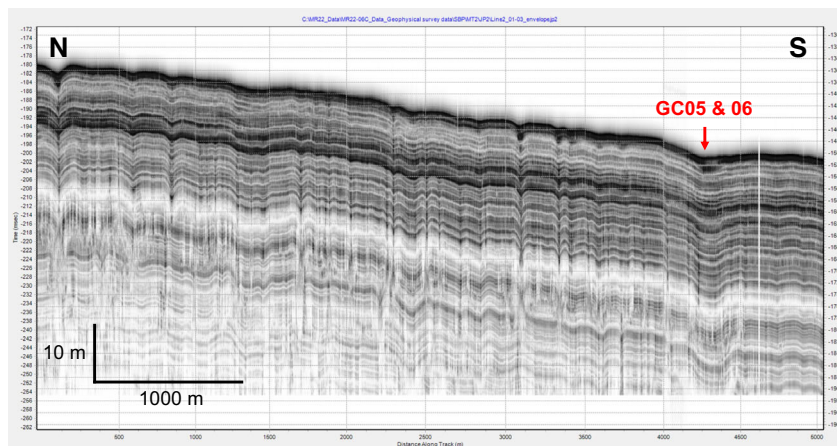


Figure 6.1-8: Site survey MBES and SBP data from the MT2 area. The yellow circle shows coring site MT2.

The underwater photograph shows abundant brittle stars on the seafloor surface (82 individuals/m²; Figure 6.1-9). The box core sample lacks seafloor surface because the sampler was over-penetrated the seafloor.

We retrieved two gravity, two pilot Asyura, a multiple, and a box cores at this site. GC05, MC02, and BC02 were half split, described, photographed, color measured, and measured by MSCL. The sediments consist of dark olive gray (5Y 3/2 to 3/1) silty clay with a slight change in color and appearance of mm-scale dark and blackish, fine interlayers and speckles throughout the cores (Figures 6.1-10 and 6.1-11).

Color indices and magnetic susceptibility show significant variations throughout the cores (Figure 6.1-12). The correlations between GC05, MC02, and BC02 suggest the core-top of GC05 and BC02 correspond to the depths of 0 cm and 7.5 cm, respectively, of MC02.

Onboard microscopic observation of box core (BC02; MT2 B8) samples indicated that foraminifera and ostracod are well preserved (Table 6.1-4). There are no obvious visual signs of carbonate dissolution or compromise.

MT2 seafloor photo

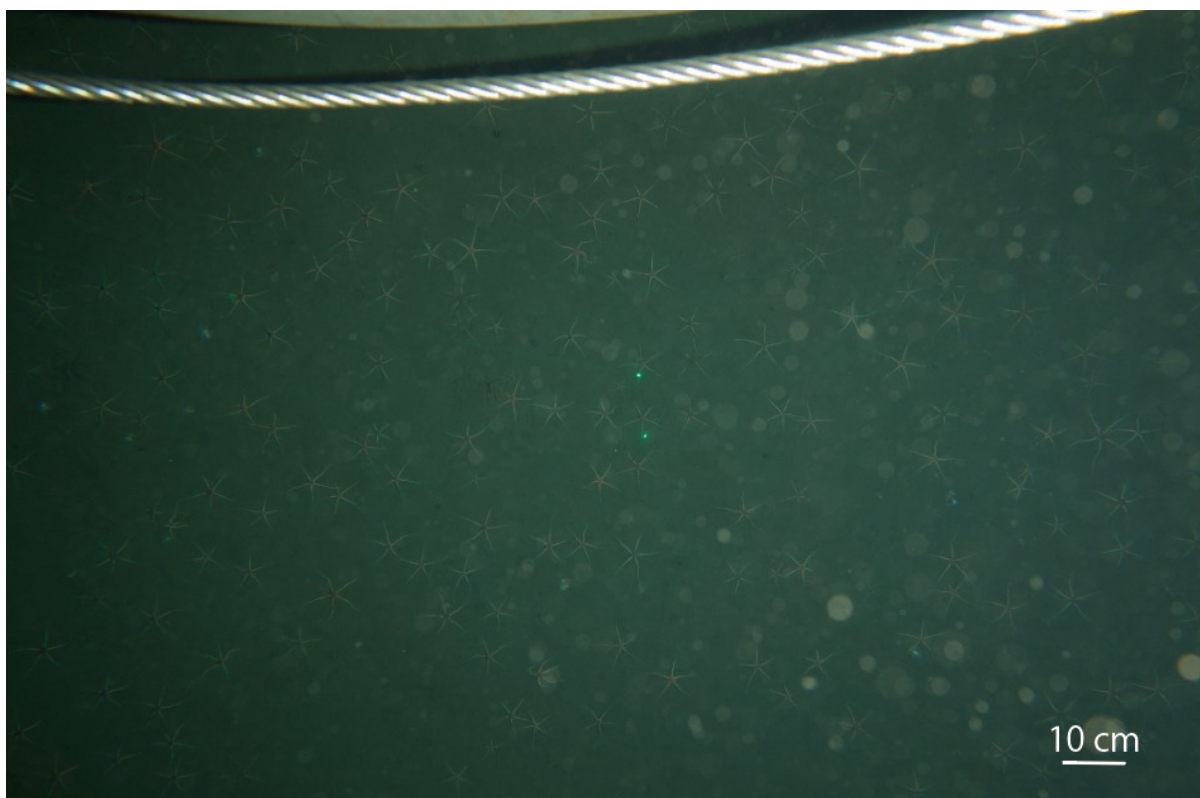


Figure 6.1-9: Photograph of sediment surface at site MT2.

Holocene Arctic Palaeoclimatology and Palaeoceanography Investigation (HAPPI) 2022

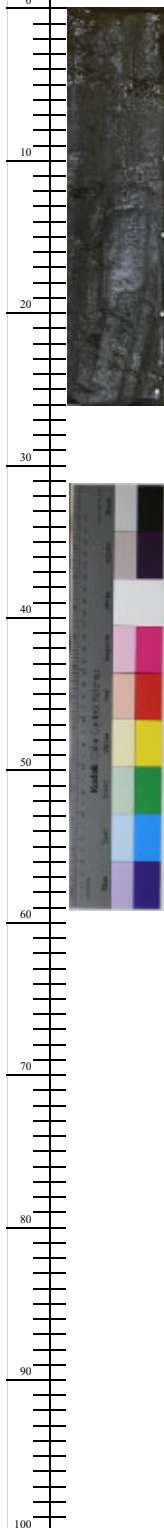
Site name: MT2	Core type: MC	Core number: 2	Section number: 1
Section length 26 cm	Described by Polyak	Core name: MR02-06C MT2 M1	
Column		Description	
		<p>0-12 cm Very soft, dark olive gray (5Y 3/2), fine-grained, silty mud. Boundary by a slight change in color.</p> <p>12-26 cm Soft, olive gray (5Y 3/1), fine-grained, silty mud with indistinct mm-scale, blackish interlayers and speckles. Intense blackish color at 12-14 cm.</p>	

Figure 6.1-10: Lithologic columns of cores at the MT2 site.

Holocene Arctic Palaeoclimatology and Palaeoceanography Investigation (HAPPI) 2022

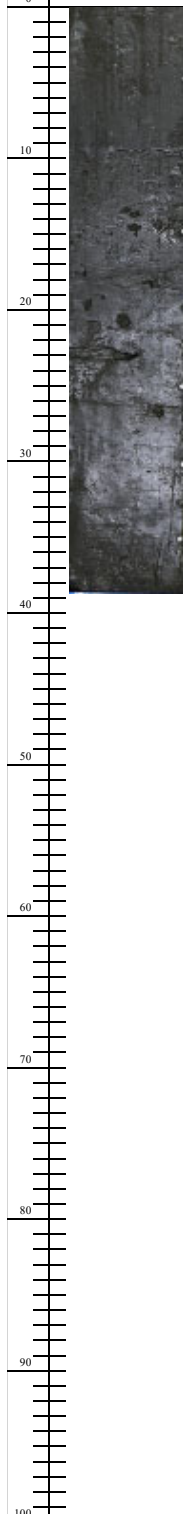
	Site name: MT2	Core type: Box	Core number: 2	Section number: 1
cm	Section length 38.5 cm	Described by Polyak	Core name: MR02-06C MT2 B1	
	Column	Description		
0		0-11 cm Very soft, dark olive gray (5Y 3/2), fine-grained, slightly silty mud. Boundary by slight change in color.		
10		10-38.5 cm Soft, dark olive gray (5Y 3/1), fine-grained, silty mud with some indistinct, mm-scale, blackish laminations and speckles.		
20				
30				
40				
50				
60				
70				
80				
90				
100				

Figure 6.1-10: Lithologic columns of cores at the MT2 site (Continued).

Holocene Arctic Palaeoclimatology and Palaeoceanography Investigation (HAPPI) 2022			
	Site name: MT2	Core type: GC	Core number: 5 Section number: 4
cm	Section length 90 cm	Described by Polyak	Core name: MR02-06C MT2 GC05 Section 4
	Column	Description	
0		0-12 cm Very soft, dark olive-gray (5Y 3/2), fine-grained, somewhat silty mud, homogenous. Boundary uneven, by change in color hue and appearance of blackish interlayers /specles.	
10		12-90 cm Soft, dark olive gray (5Y 3/2 to 3/1), fine-grained, somewhat silty mud with blackish, mm-scale interlayers and speckles.	
20			
30			
40			
50			
60			
70			
80			
90			
100			

Figure 6.1-10: Lithologic columns of cores at the MT2 site (Continued).

Holocene Arctic Palaeoclimatology and Palaeoceanography Investigation (HAPPI) 2022

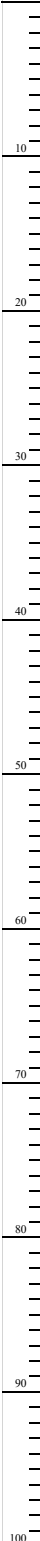
	Site name: MT2	Core type: GC	Core number: 5	Section number: 5
cm	Section length 100 cm	Described by Polyak		Core name: MR02-06C MT2 GC05 Section 5
	Column	Description		
		<p>0-100 cm Soft, dark olive-gray (5Y 3/2 to 3/1), fine-grained, somewhat silty mud, with numerous blackish, mm-scale interlayers and speckles, especially well expressed below ~35 cm.</p>		

Figure 6.1-10: Lithologic columns of cores at the MT2 site (Continued).

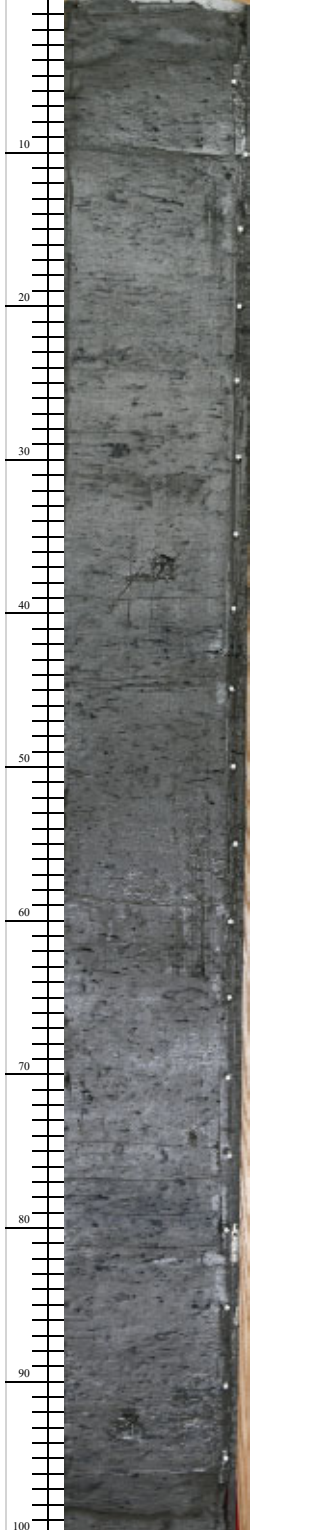
Holocene Arctic Palaeoclimatology and Palaeoceanography Investigation (HAPPI) 2022				
	Site name: MT2	Core type: GC	Core number: 5	Section number: 6
cm	Section length 100 cm	Described by Polyak	Core name: MR02-06C MT2 GC05 Section 6	
	Column	Description		
0		0-100 cm Soft, dark olive-gray (5Y 3/2 to 3/1), fine-grained, somewhat silty mud, with numerous blackish, mm-scale interlayers and speckles, apparently randomly distributed.		
10				
20				
30				
40				
50				
60				
70				
80				
90				
100				

Figure 6.1-10: Lithologic columns of cores at the MT2 site (Continued).

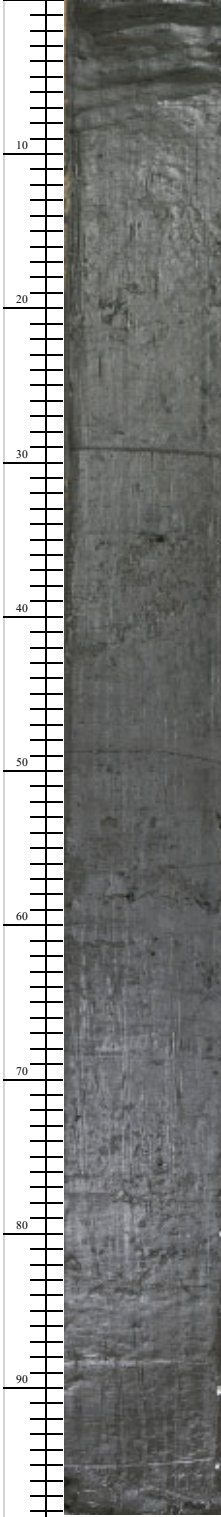
Holocene Arctic Palaeoclimatology and Palaeoceanography Investigation (HAPPI) 2022			
	Site name: MT2	Core type: GC	Core number: 5 Section number: 7
cm	Section length 98 cm	Described by Polyak	Core name: MR02-06C MT1 GC05 Section 7
	Column	Description	
0		0-98 cm Soft, dark olive-gray (5Y 3/2 to 3/1), fine-grained, somewhat slightly silty mud with scattered interlayers and speckles of black material, especially clearly seen at ~0-5, 26-30, and 33-35 cm. Almost no blackish material seen below ~65 cm.	
10			
20			
30			
40			
50			
60			
70			
80			
90			
100			

Figure 6.1-10: Lithologic columns of cores at the MT2 site (Continued).

Holocene Arctic Palaeoclimatology and Palaeoceanography Investigation (HAPPI) 2022			
	Site name: MT2	Core type: GC	Core number: 5 Section number: CC
cm	Section length 30.5 cm	Described by Polyak	Core name: MR02-06C MT1 GC05 CC
	Column	Description	
0		0-30.5cm Soft, dark olive-gray (5Y 3/2 to 3/1), fine-grained, somewhat silty mud with mm-scale, blackish interlayers and speckles.	
10			
20			
30			
40			
50			
60			
70			
80			
90			
100			

Figure 6.1-10: Lithologic columns of cores at the MT2 site (Continued).



Figure 6.1-11: Photographs of MT2 cores.

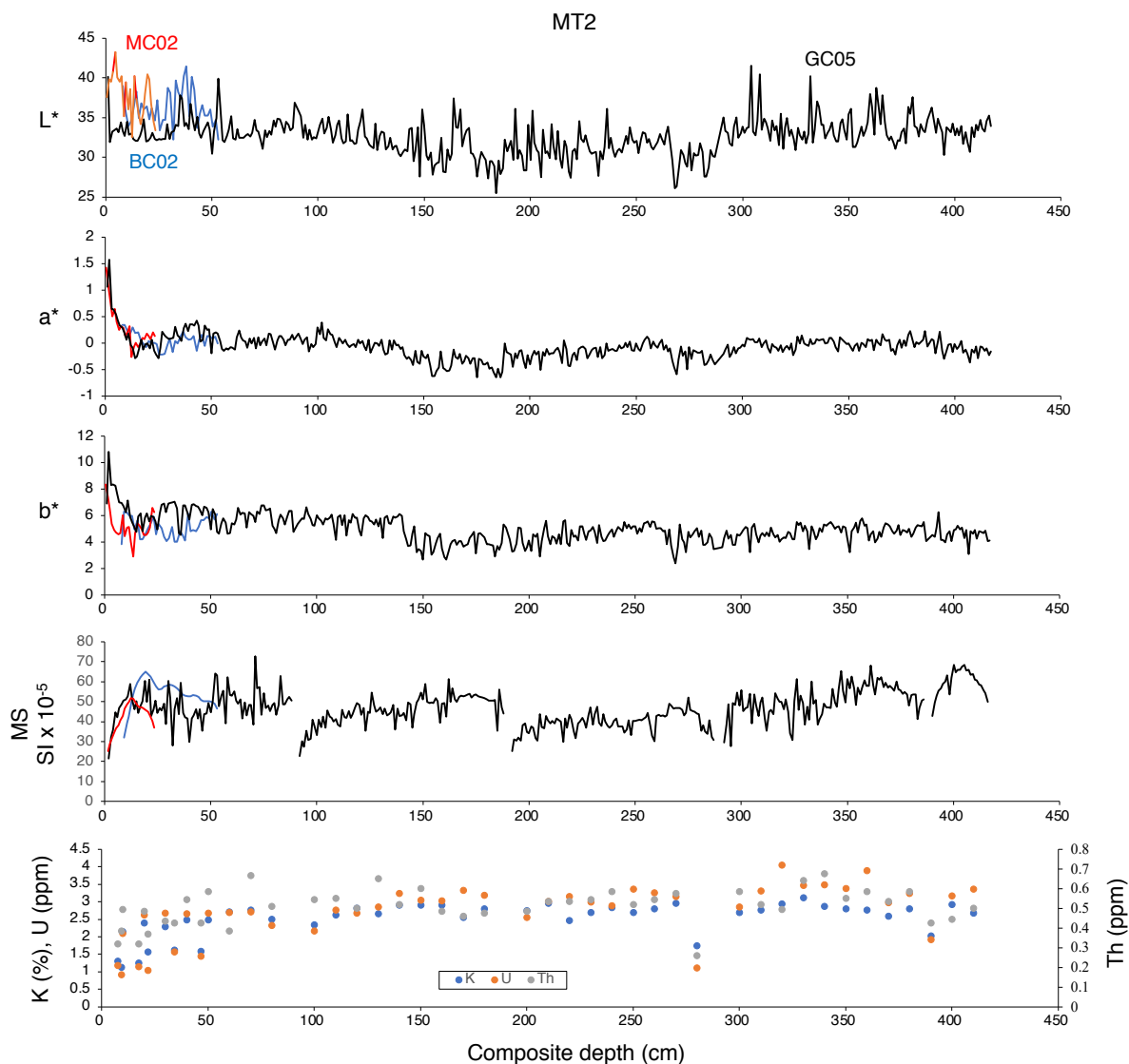


Figure 6.1-12: Variations in color indices in cores at site MT2.

Table 6.1-4: Abundance of foraminifera and ostracods in MT2 box samples

Top depth (cm)	Bottom depth (cm)	Planktic foraminifera	Benthic foraminifera	Agglutinated foraminifera	Ostracods
surface		P	A	B	A
0	1	A	A	P	P
1	2				
2	3				
3	4				
4	5				
5	6	A	A	A	A
6	7				
7	8				
8	9				
9	10				

10	11	P	A	P	P
11	12				
12	13				
13	14				
14	15				
15	16	P	A	P	P
16	17				
17	18				
18	19				
19	20				
20	21	P	A	P	P
21	22				
22	23				
23	24				
24	25				
25	26	P	A	B	P
26	27				
27	28				
28	29				
29	30				
30	31	P	A	B	P
31	32				
32	33				
33	34				
34	35				
35	36	P	A	P	P
36	37				
37	38				
38	39				
39	40				
40	41	P	A	P	P
41	42				
42	43				
43	44	P	A	B	P

A=Abundant (>100 forams, >30 ostracods), P=Present but fewer (<30 ostracods), B=Barren

Site BC2

The Barrow Canyon (BC) area is located on the Alaska Beaufort shelf, slightly east of the Barrow Canyon (Figure 6.1-2). The BC2 site was selected to retrieve sediment cores with a high sedimentation rate to reconstruct changes in the Bering Strait inflow (the Alaskan Coastal Current) to the Arctic Ocean, the strength of the Beaufort gyre circulation, summer sea ice cover, primary productivity, and biological communities over the past 2000 years.

Sedimentation in this area is affected by the Alaska Coastal Current, which likely causes sediment winnowing and redeposition. The ARA04 data indicate that the sea floor on the outer shelf features multiple, generally W-E trending furrows. We have augmented the ARA04 lines with an MBES mosaic that provides more insight into these features (Figure 6.1-13). The deeper part of the survey area (~250-300 mwd) is covered by more extensive, sparser, and more NW-SE trending furrows, whereas, at shallower depths, this pattern is complicated by smaller, denser, W-E furrows. While the detailed interpretation of these features is yet to be developed, we presume that they represent a development of the current system during the Holocene sea-level rise.

The practical aspects of this seafloor morphology/seismostratigraphy involve the choice of the coring sites (BC2 and BC2-2) in between the furrows on the ridges representing proximal deposition of the winnowed sediment (Figure 6.1-13). Coring site BC2-2 was selected from the deeper part of the survey area, where sedimentation rates may be lower due to a somewhat longer distal transportation.

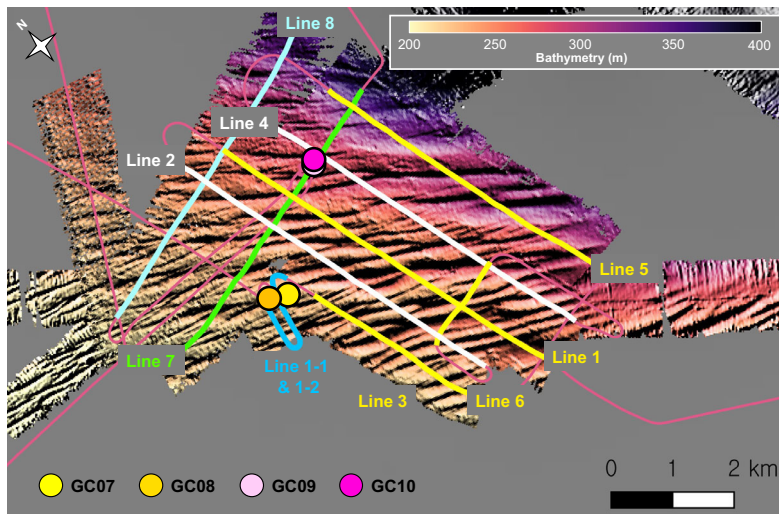
The underwater photograph shows a dense occurrence of brittle stars on the seafloor surface (216 individuals/m²; Figure 6.1-14). Numerous burrows produced by polychaete worms were developed on the sediment surface. Box core sample contained 33 individuals of the brittle star (206.25 individuals/m²) on the surface.

We retrieved two gravity, two pilot Asyura, a multiple, and a box cores at this site. GC07, MC03, and BC03 were half split, described, photographed, color measured, and measured by MSCL. The sediments consist of dark olive gray (5Y 3/2 to 3/1), slightly sandy mud with abundant blackish (iron sulfide) interlayers and lenses on mm-scale traces of bioturbation (Figures 6.1-15 and 6.1-16). The upper 8 cm contains abundant polychaete tubes.

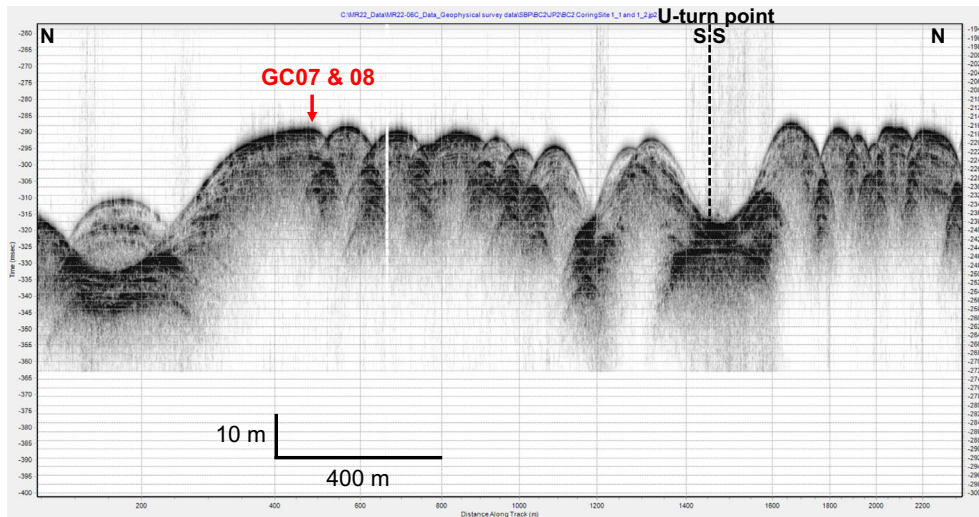
Color indices and magnetic susceptibility show significant variations throughout the cores (Figure 6.1-15). The correlations between GC07, MC03, and BC03 suggest the core-top of GC07 and BC03 correspond to the depths of 1 cm and 2 cm, respectively, of MC03.

Onboard microscopic observation of box core (BC03; BC2 B4) samples indicated that foraminifera and ostracod are well preserved. There are no obvious visual signs of carbonate dissolution or compromise.

BC2 and BC2-2 MBES including coring sites



BC2 coring sites (Line 1-1 and 1-2)



BC2-2 GC09 & 10 and ARA04B/3GC (Line 7)

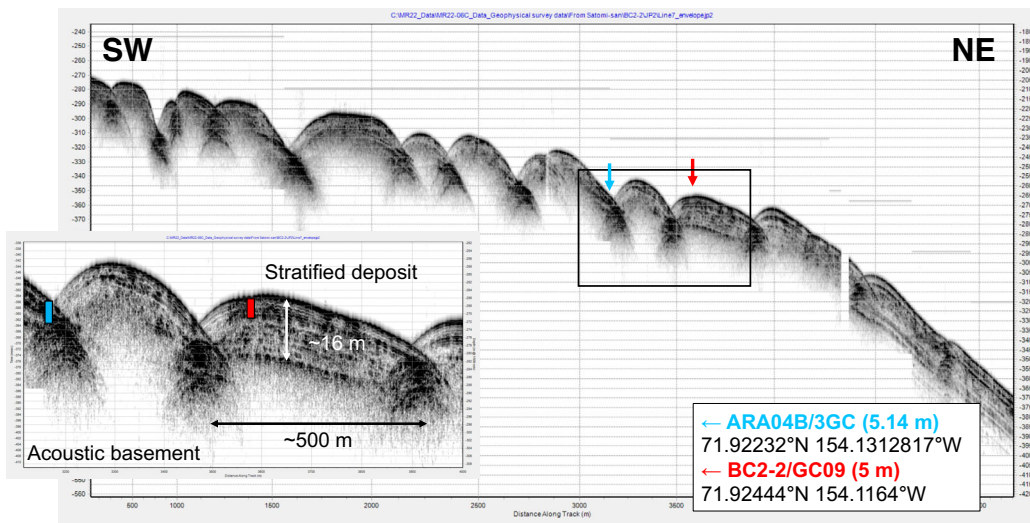
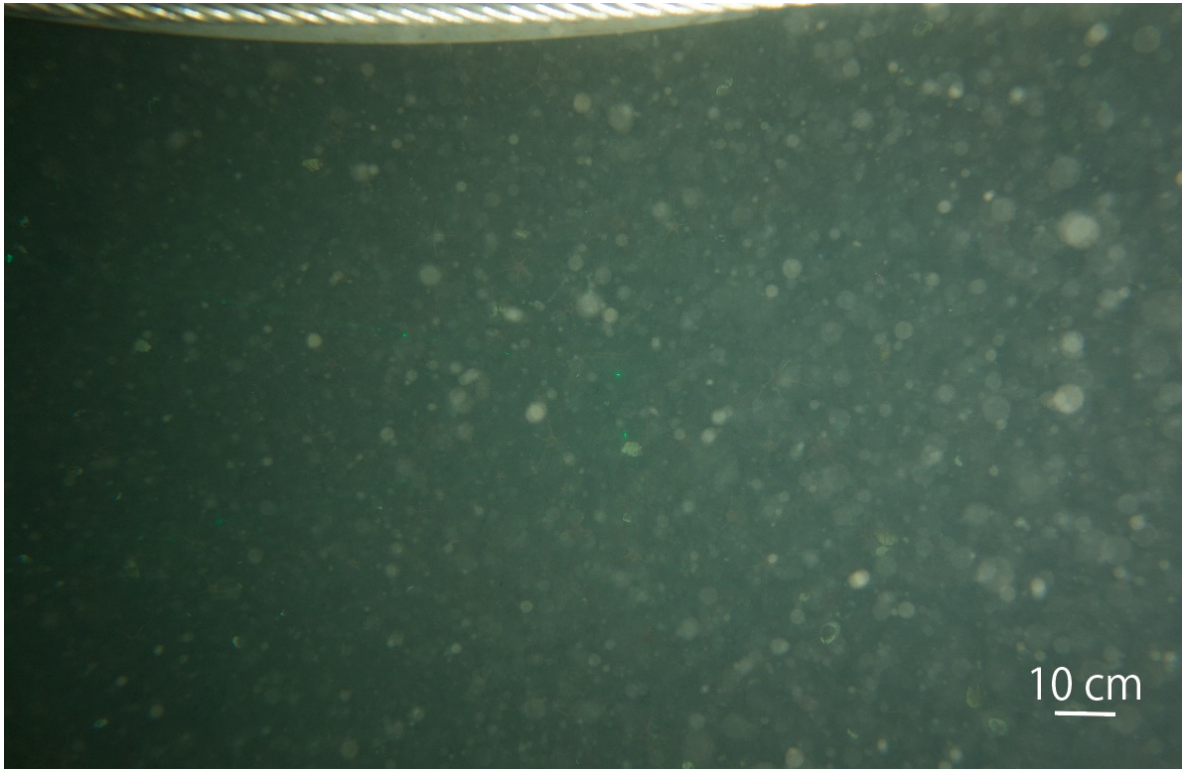


Figure 6.1-13: Site survey MBES and SBP data from the BC-2 and BC2-2 coring areas.

BC2 seafloor photo



BC2 box core surface



Figure 6.1-14: Photographs of sediment surface at BC2.

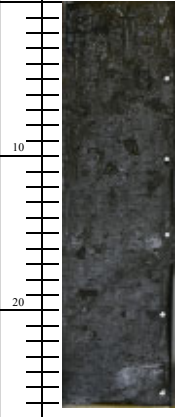
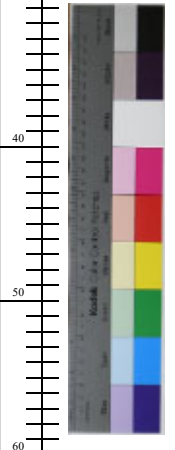
Holocene Arctic Palaeoclimatology and Palaeoceanography Investigation (HAPPI) 2022			
	Site name: BC2	Core type: MC	Core number: 3 Section number: 1
cm	Section length 26 cm	Described by Polyak	Core name: MR02-06C BC2 M1
	Column	Description	
0		0-25.5 cm Soft, dark olive gray (5Y 3/2), fine-grained, slightly sandy mud with indistinct blackish patches, especially large at 0-3 cm.	
10			
20			
30			
40			
50			
60			
70			
80			
90			
100			

Figure 6.1-15: Lithologic columns of BC2 cores.

Holocene Arctic Palaeoclimatology and Palaeoceanography Investigation (HAPPI) 2022

	Site name: BC2	Core type: BC	Core number: 3	Section number: 4
cm	Section length 27 cm	Described by Polyak	Core name: MR02-06C BC2 B4	
	Column	Description		
0		0-27 cm Soft, dark olive gray (5Y 3/2), fine-grained, slightly sandy mud with a few vague, indistinct blackish patches. The upper ~4cm contain some polychete tubes and mollusc shells.		
10				
20				
30				
40				
50				
60				
70				
80				
90				
100				

Figure 6.1-15: Lithologic columns of BC2 cores (Continued).

Holocene Arctic Palaeoclimatology and Palaeoceanography Investigation (HAPPI) 2022			
	Site name: BC2	Core type: BC	Core number: 3 Section number: 4
cm	Section length 27 cm	Described by Polyak	Core name: MR02-06C BC2 B 4 bento
	Column	Description	
0		0-4 cm Soft, dark olive gray (5Y 3/2), fine-grained, slightly sandy mud with a dense mat of polychaete tubes on top. Boundary by a change in color and appearance of blackish patches.	
10		4-26 cm Soft, dark olive-gray (5Y 3/2 to 3/1), fine-grained, slightly sandy mud with diffuse patches of blackish material.	
20			
30			
40			
50			
60			
70			
80			
90			
100			

Figure 6.1-15: Lithologic columns of BC2 cores (Continued).

Holocene Arctic Palaeoclimatology and Palaeoceanography Investigation (HAPPI) 2022

		Site name: BC2	Core type: GC	Core number: 7	Section number: 3
cm	Section length 73 cm	Described by Polyak		Core name: MR02-06C BC2 GC07 Section 3	
	Column	Description			
0		0-40 cm Soft, dark olive-gray (5Y 3/2 to 3/1), fine-grained, slightly sandy mud with rare diffuse blackish patches. Top 2-3 cm, very soft somewhat with blackish patches and some polychaete tubes. Boundary by appearance of distinct blackish interlayers and overall change in color.			
10		40-73 cm Soft to relatively compact, very dark olive-gray to black (5Y 3/1 to 2/1), fine-grained, slightly sandy mud with abundant blackish interlayers and lenses on mm-scale; traces of bioturbation. Mollusc shell fragments picked at 23 cm.			
20					
30					
40					
50					
60					
70					
80					
90					
100					

Figure 6.1-15: Lithologic columns of BC2 cores (Continued).

Holocene Arctic Palaeoclimatology and Palaeoceanography Investigation (HAPPI) 2022

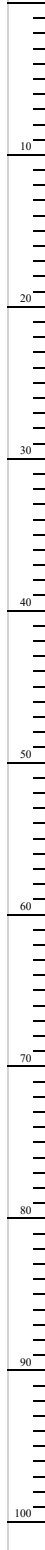
	Site name: BC2	Core type: GC	Core number: 7	Section number: 4
cm	Section length 101 cm	Described by Polyak	Core name: MR02-06C BC2 GC07 Section 4	
0	Column	Description		
		<p>0-101 cm Soft to relatively compact, very dark olive-gray (5Y 3/1 to 2/1), fine-grained, slightly sandy mud with blackish patches (interlayers and lenses) throughout the section.</p>		

Figure 6.1-15: Lithologic columns of BC2 cores (Continued).

Holocene Arctic Palaeoclimatology and Palaeoceanography Investigation (HAPPI) 2022

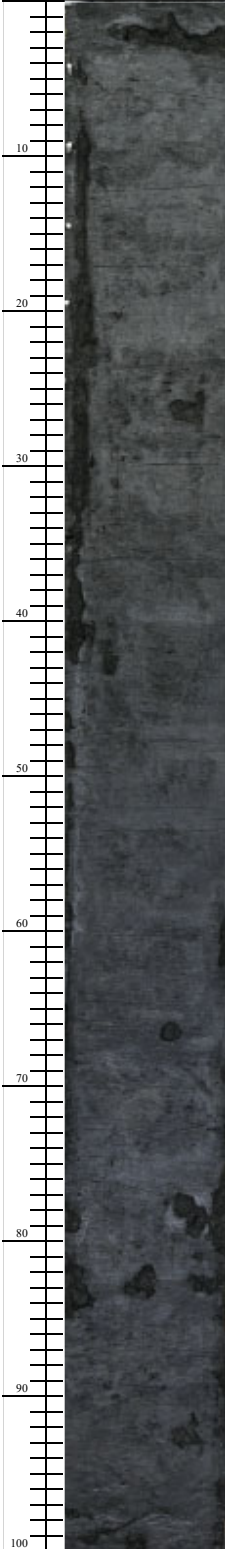
	Site name: BC2	Core type: GC	Core number: 7	Section number: 5
cm	Section length 101 cm	Described by Polyak	Core name: MR02-06C BC2 GC07 Section 5	
	Column	Description		
0		0-101 cm Soft to relatively compact, very dark olive-gray to black (5Y 3/2 to 2/1), silty, slightly sandy mud with diffuse interlayers and lenses of black (iron sulfide) material and tace mottles.		
10				
20				
30				
40				
50				
60				
70				
80				
90				
100				

Figure 6.1-15: Lithologic columns of BC2 cores (Continued).

Holocene Arctic Palaeoclimatology and Palaeoceanography Investigation (HAPPI) 2022

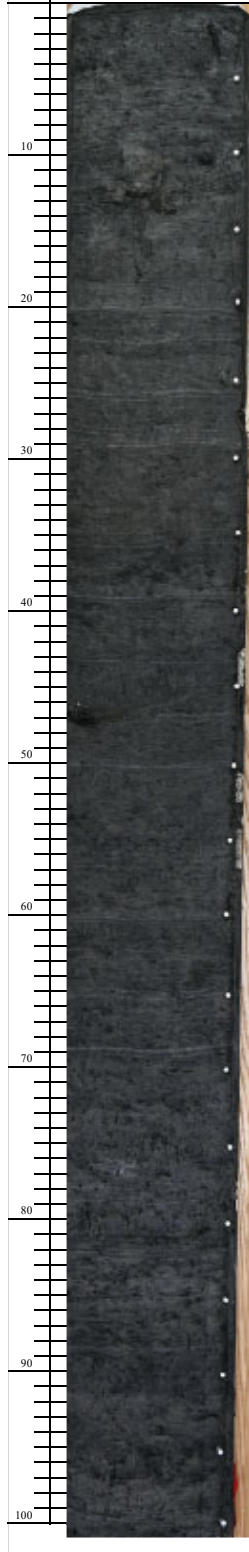
	Site name: BC2	Core type: GC	Core number: 7	Section number: 6
cm	Section length 100 cm	Described by Polyak	Core name: MR02-06C BC2 GC07 Section 6	
0	Column	Description		
		<p>0-102 cm Soft to relatively compact, very dark olive-gray to black (5Y 3/1 to 2/1), silty, slightly sandy mud. Diffuse, mottled (bioturbated) interlayers and lenses of black (iron sulfide) material. Pervasive trace mottles. Some with remnants of polychaete tubes. Small, dense aggregates of black material, especillay abundant below ~60 cm. Mollusc shell for dating at ~47 cm.</p>		

Figure 6.1-15: Lithologic columns of BC2 cores (Continued).

Holocene Arctic Palaeoclimatology and Palaeoceanography Investigation (HAPPI) 2022

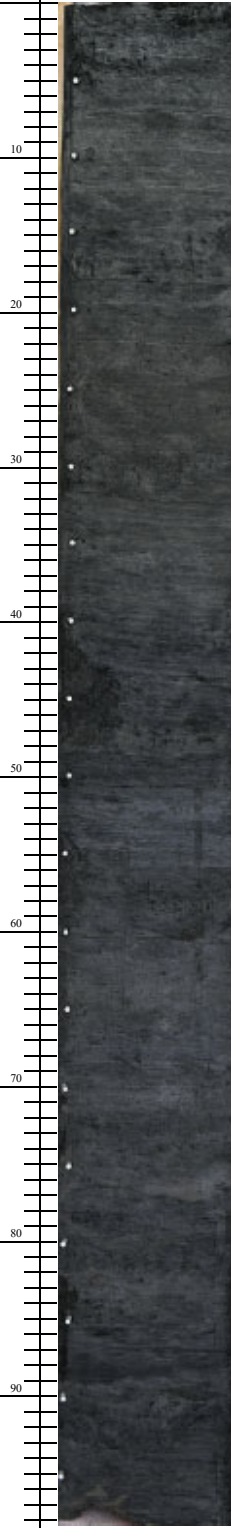
	Site name: BC2	Core type: GC	Core number: 7	Section number: 7
cm	Section length 98 cm	Described by Polyak	Core name: MR02-06C BC2 GC07 Section 7	
	Column	Description		
0		<p>0-98 cm Soft to relatively compacted, very dark olive-gray to black (5Y 3/1 to 2/1), silty, slightly sandy mud. Diffuse, mottled interlayers and speckles of black material (iron sulfide) arranged in mm-scale laminae and cm-/dm-scale bands. Prominent blackish bands at 1-5, 13-17, 40-45, 53-55, 67-69, 77-82, and 86-89 cm.</p>		
10				
20				
30				
40				
50				
60				
70				
80				
90				
100				

Figure 6.1-15: Lithologic columns of BC2 cores (Continued).

Holocene Arctic Palaeoclimatology and Palaeoceanography Investigation (HAPPI) 2022

	Site name: BC2	Core type: GC	Core number: 7	Section number: CC
cm	Section length 16 cm	Described by Polyak	Core name: MR02-06C BC2 GC07 CC	
	Column	Description		
0		0-16 cm Relatively compacted, very dark olive-gray to black (5Y 3/1 to 2/1), silty, slightly sandy mud. Diffuse blackish material interlayers and lenses throughout the section.		
1				
2				
3				
4				
5				
6				
7				
8				
9				
10				
11				
12				
13				
14				
15				
16				
17				
18				
19				
20				
21				
22				
23				
24				
25				
26				
27				
28				
29				
30				
31				
32				
33				
34				
35				
36				
37				
38				
39				
40				
41				
42				
43				
44				
45				
46				
47				
48				
49				
50				
51				
52				
53				
54				
55				
56				
57				
58				
59				
60				
61				
62				
63				
64				
65				
66				
67				
68				
69				
70				
71				
72				
73				
74				
75				
76				
77				
78				
79				
80				
81				
82				
83				
84				
85				
86				
87				
88				
89				
90				
91				
92				
93				
94				
95				
96				
97				
98				
99				
100				

Figure 6.1-15: Lithologic columns of BC2 cores (Continued).

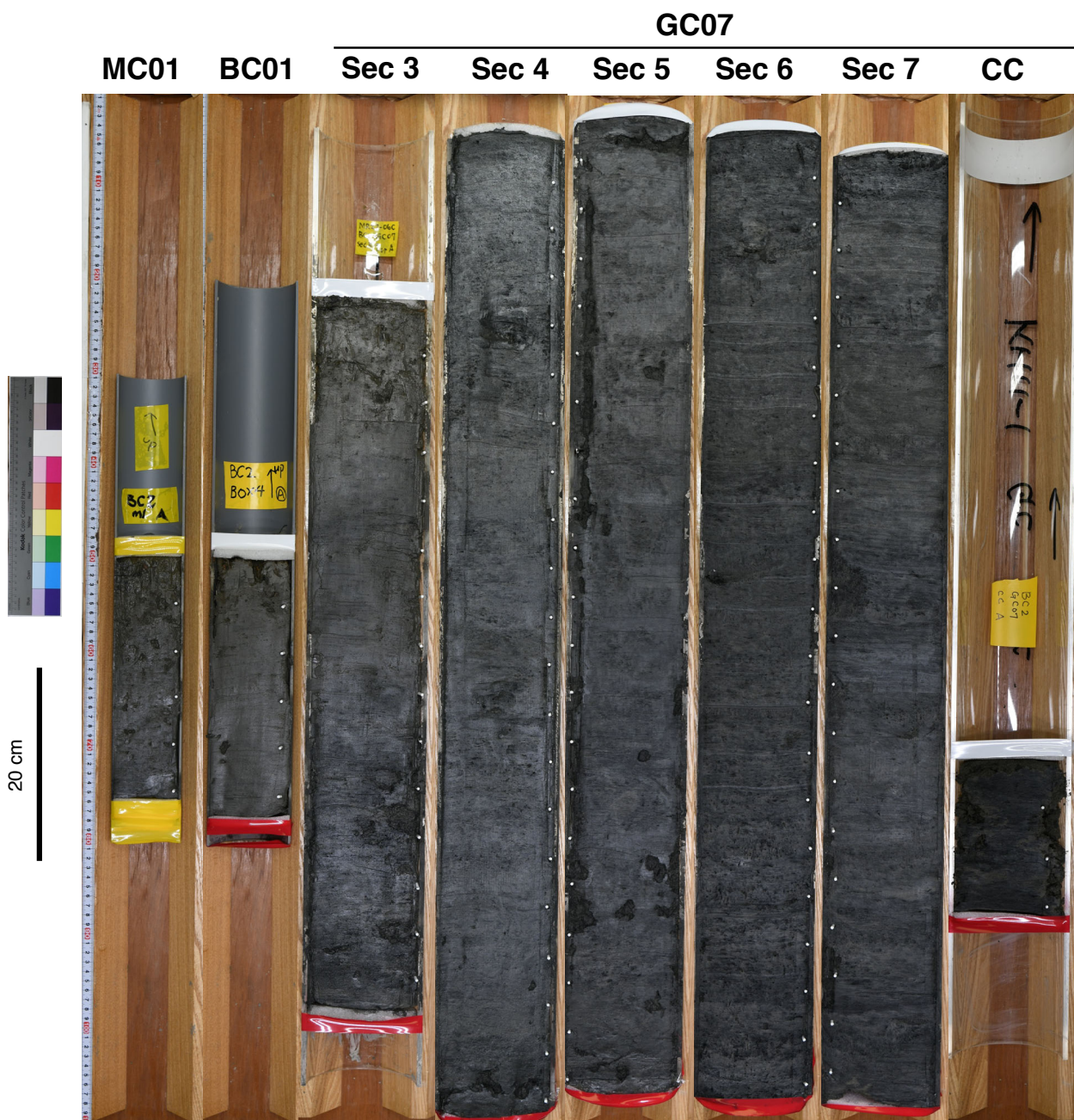


Figure 6.1-16: Photographs of BC2 cores.

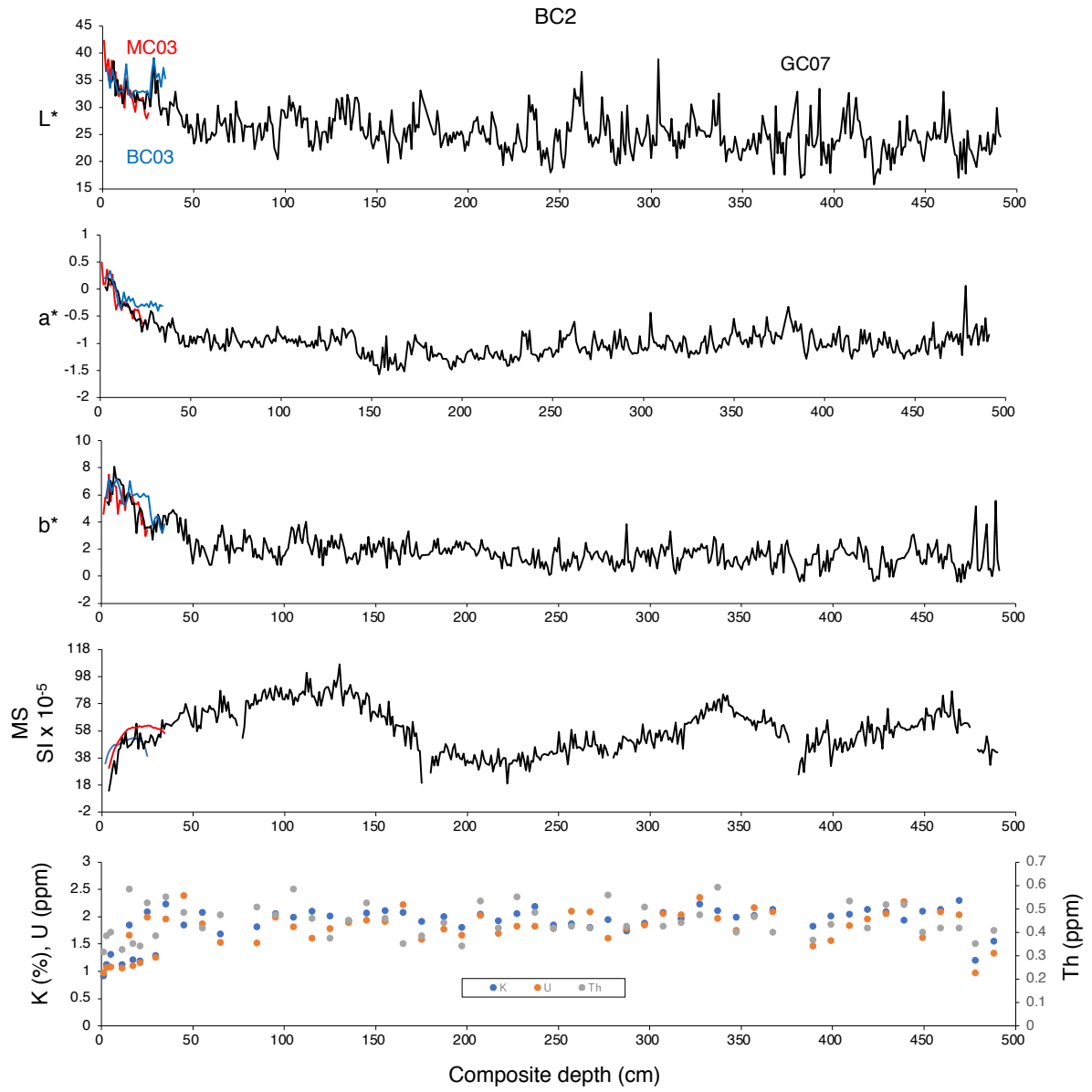


Figure 6.1-17: Variations in color indices in site BC2.

Table 6.1-5: Abundance of foraminifera and ostracods in BC2 box samples

Top depth (cm)	Bottom depth (cm)	Planktic foraminifera	Benthic foraminifera	Agglutinated foraminifera	Ostracods
0	1	P	A	A	P
1	2				
2	3				
3	4				
4	5				
5	6	P	A	P	P
6	7				
7	8				
8	9				
9	10				
10	11	P	P	P	P
11	12				
12	13				
13	14				
14	15				
15	16	P	P	P	P
16	17				
17	18				
18	19				
19	20				
20	21	B	P	P	P
21	22				
22	23				
23	24				
24	25				
25	26	B	P	P	P

A=Abundant (>100 forams, >30 ostracods), P=Present but fewer (<30 ostracods), B=Barren

Site BC2-2

This site is located ~3km north of the BC2-2 site at the northern edge of the eastern shelf of the Barrow Canyon (Figure 6.1-2) and was selected to retrieve sediment cores with a high sedimentation rate.

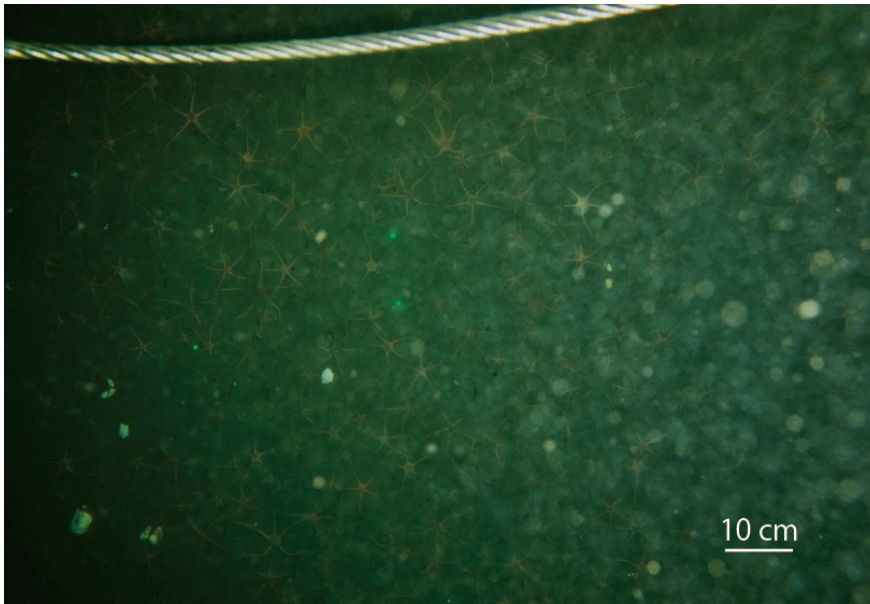
The underwater photograph shows brittle stars abundantly occurred on the seafloor surface (>176 individuals/m²; Figure 6.1-18), although precise population density estimation was impossible due to the high turbidity of the overlying water. The surface of the box core sample was covered with numerous burrows produced by a polychaete worm and contained 19 individuals of the brittle star (118.75 individuals m⁻²) on the surface.

We retrieved two gravity, two pilot Asyura, a multiple, and a box core at this site. GC09, MC04, and BC04 were half split, described, photographed, color measured, and measured by MSCL. The sediments consist of dark olive gray (5Y 3/2, 3/1, and 2/1), slightly sandy mud with abundant blackish (iron sulfide) interlayers and lenses on mm-scale traces of bioturbation (Figures 6.1-19 and 6.1-20). Blackish material focuses on cm-scale bands. The upper 9 cm contains abundant polychaete tubes.

Color indices and magnetic susceptibility show significant variations throughout the cores (Figure 6.1-21). The correlations between GC09, MC04, and BC04 suggest that the core-top of GC07 and BC03 correspond to the depths of 11 cm and 1.5 cm, respectively, of MC04.

Onboard microscopic observation of box core samples was not conducted due to time constrain.

BC2-2 seafloor photo



BC2-2 box core surface

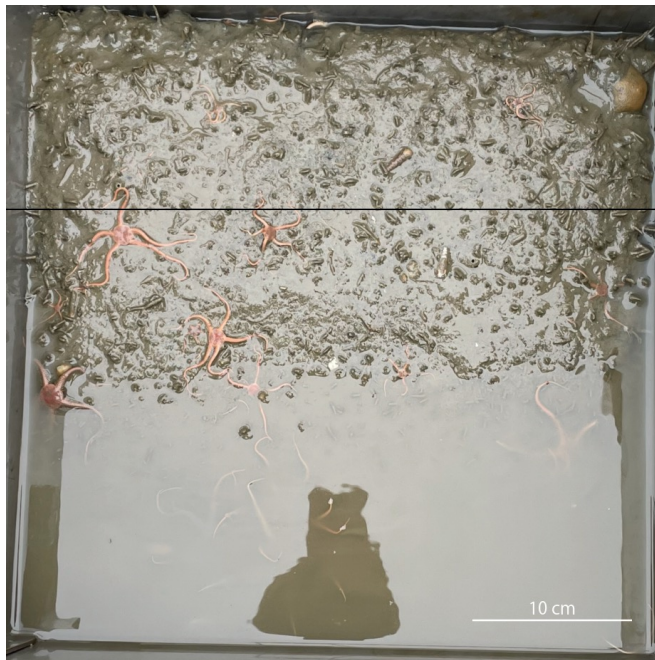


Figure 6.1-18: Photographs of sediment surface at site BC2-2.

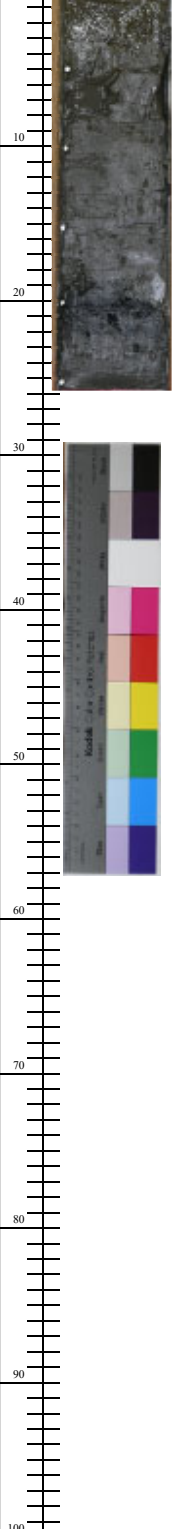
Holocene Arctic Palaeoclimatology and Palaeoceanography Investigation (HAPPI) 2022			
	Site name: BC2-2	Core type: MC	Core number: 4 Section number: 1
cm	Section length 25 cm	Described by Polyak	Core name: MR02-06C BC2-2 M1
	Column	Description	
0		0-15.5 cm Soft, dark olive gray (5Y 3/2), somewhat sandy mud with a few vague, indistinct blackish patches and a prominent black band at 19-21.5 cm. The upper ~8 cm are waterly and contain some polychaete tubes.	
100			

Figure 6.1-19: The lithology of sediments in BC2-2.

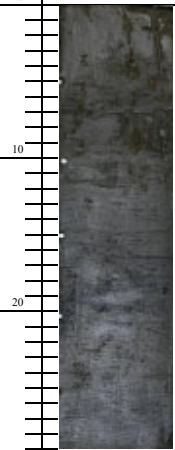
Holocene Arctic Palaeoclimatology and Palaeoceanography Investigation (HAPPI) 2022			
	Site name: BC2-2	Core type: BC	Core number: 4 Section number: 1
cm	Section length 29 cm	Described by Polyak	Core name: MR02-06C BC2-2 B1
	Column	Description	
0		0-29 cm Soft, dark olive gray (5Y 3/2), somewhat sandy mud. Vague diffuse blackish patches can be seen below ~9 cm; a prominent blackish band at ~17-21 cm. Polychete tubes in the upper ~9 cm.	
10			
20			
30			
40			
50			
60			
70			
80			
90			
100			

Figure 6.1-19: The lithology of sediments in BC2-2 (Continued).

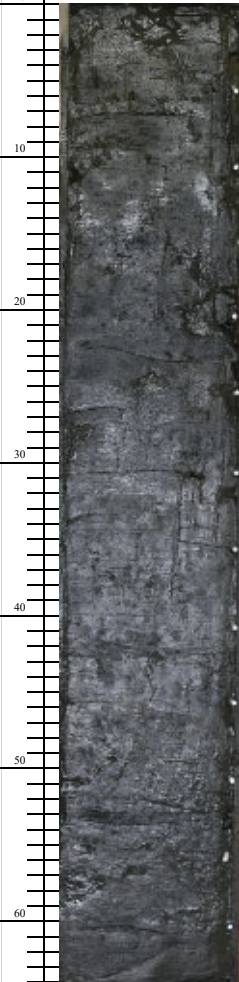
Holocene Arctic Palaeoclimatology and Palaeoceanography Investigation (HAPPI) 2022			
	Site name: BC2-2	Core type: GC	Core number: 9 Section number: 3
cm	Section length 64 cm	Described by Polyak	Core name: MR02-06C BC2-2 GC09 Section 3
	Column	Description	
0		0-4 cm Very soft, dark dark olive gray (5Y 3/2 to 3/1), fine-grained, slightly sandy mud with some diffuse blackish patches. Boundary by appearance of blackish material. Some polychaete tubes.	
10		4-64 cm Soft, dark olive-gray to black (5Y 3/2 to 3/1), fine-grained, slightly sandy mud with blackish interlayers and lenses, especially below ~14 cm.	
20			
30			
40			
50			
60			
70			
80			
90			
100			

Figure 6.1-19: The lithology of sediments in BC2-2 (Continued).

Holocene Arctic Palaeoclimatology and Palaeoceanography Investigation (HAPPI) 2022

	Site name: BC2-2	Core type: GC	Core number: 9	Section number: 4
cm	Section length 100 cm	Described by Polyak	Core name: MR02-06C BC2-2 GC07 Section 4	
0	Column	Description		
		<p>0-100 cm Soft to relatively compacted, very dark olive gray to black (5Y 3/1 to 2/1), fine-grained, slightly sandy mud with blackish mm-scale interlayers and lenses. Blackish material focuses in cm-scale bands, notably at ~2-4, 8-10, 14-16, 23-25, 33-35, 37-39, 40-42, 45-47, 48-50, 67-69, 75-80, 86-88, and 91-96 cm. Interval between ~51-65 cm has less black material than above and below. Sediment becomes more compacted down the section.</p>		

Figure 6.1-19: The lithology of sediments in BC2-2 (Continued).

Holocene Arctic Palaeoclimatology and Palaeoceanography Investigation (HAPPI) 2022

	Site name: BC2-2	Core type: GC	Core number: 9	Section number: 5
cm	Section length 101 cm	Described by Polyak	Core name: MR02-06C BC2-2 GC09 Section 5	
0	Column	Description		
	<p>0-101 cm Soft to relatively compacted, very dark olive-gray to black (5Y 3/2 to 2/1), fine-grained, slightly sandy mud with blackish, mm-scale interlayers and lenses focused in cm-scale bands, notably at 2-4, 9-12, 14-17, 22-27, 33-37, 40-44, 48-51, 54-56, 57-59, 64-67, 71-74, 77-80, 83-86, 91-94 cm. Black bands are especially vivid above ~50 cm.</p>			

Figure 6.1-19: The lithology of sediments in BC2-2 (Continued).

Holocene Arctic Palaeoclimatology and Palaeoceanography Investigation (HAPPI) 2022

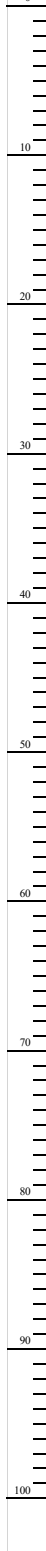
	Site name: BC2-2	Core type: GC	Core number: 9	Section number: 6
cm	Section length 102 cm	Described by Polyak	Core name: MR02-06C BC2-2 GC09 Section 6	
0	Column	Description		
		<p>0-102 cm Soft to relatively compacted, very dark olive-gray to black (5Y 3/1 to 2/1), fine-grained, slightly sandy mud with widespread blackish patches (interlayers, lenses, and broader bands), especially prominent above ~31 cm and below ~63 cm. .</p>		

Figure 6.1-19: The lithology of sediments in BC2-2 (Continued).

Holocene Arctic Palaeoclimatology and Palaeoceanography Investigation (HAPPI) 2022			
	Site name: BC2-2	Core type: GC	Core number: 9 Section number: 7
cm	Section length 99 cm	Described by Polyak	Core name: MR02-06C BC2-2 GC09 Section 7
	Column	Description	
0		0-99 cm Soft to relatively compacted, very dark olive-gray to black (5Y 3/1 to 2/1), fine-grained, slightly sandy mud with widespread blackish patches (interlayers, lenses, and broader bands). Mollusc shell collected at 90-91 cm.	
10			
20			
30			
40			
50			
60			
70			
80			
90			
100			

Figure 6.1-19: The lithology of sediments in BC2-2 (Continued).

Holocene Arctic Palaeoclimatology and Palaeoceanography Investigation (HAPPI) 2022

	Site name: BC2-2	Core type: GC	Core number: 9	Section number: CC
cm	Section length 14 cm	Described by Polyak	Core name: MR02-06C BC2-2 GC09 CC	
	Column	Description		
0		0-14 cm Relatively compacted, very dark olive-gray to black (5Y 3/1 to 2/1), fine-grained, slightly sandy mud with widespread blackish patches (interlayers and lenses).		
1				
2				
3				
4				
5				
6				
7				
8				
9				
10				
11				
12				
13				
14				
15				
16				
17				
18				
19				
20				
21				
22				
23				
24				
25				
26				
27				
28				
29				
30				
31				
32				
33				
34				
35				
36				
37				
38				
39				
40				
41				
42				
43				
44				
45				
46				
47				
48				
49				
50				
51				
52				
53				
54				
55				
56				
57				
58				
59				
60				
61				
62				
63				
64				
65				
66				
67				
68				
69				
70				
71				
72				
73				
74				
75				
76				
77				
78				
79				
80				
81				
82				
83				
84				
85				
86				
87				
88				
89				
90				
91				
92				
93				
94				
95				
96				
97				
98				
99				
100				

Figure 6.1-19. The lithology of sediments in BC2-2 (Continued).

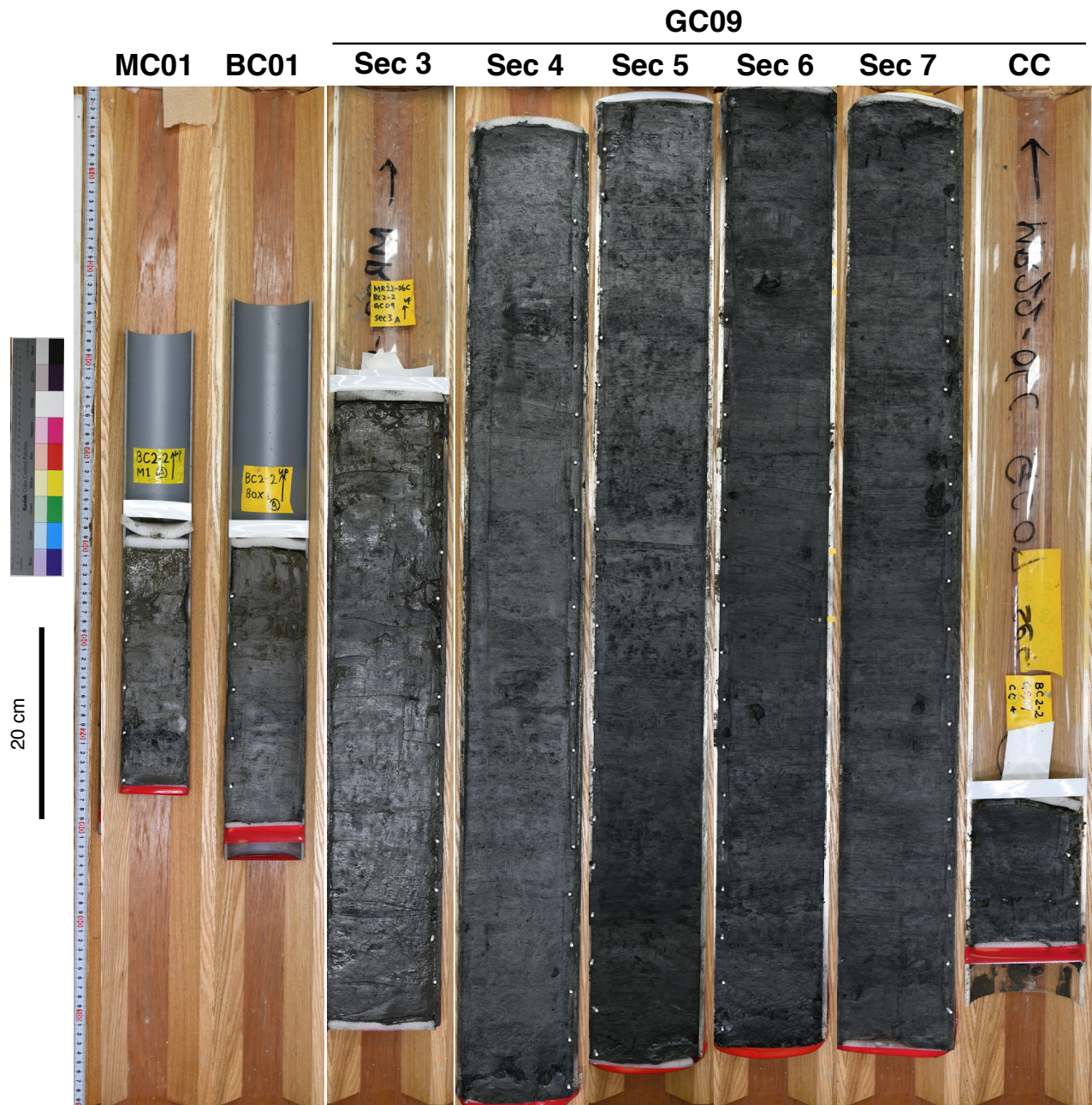


Figure 6.1-20: Photographs of BC2-2 cores.

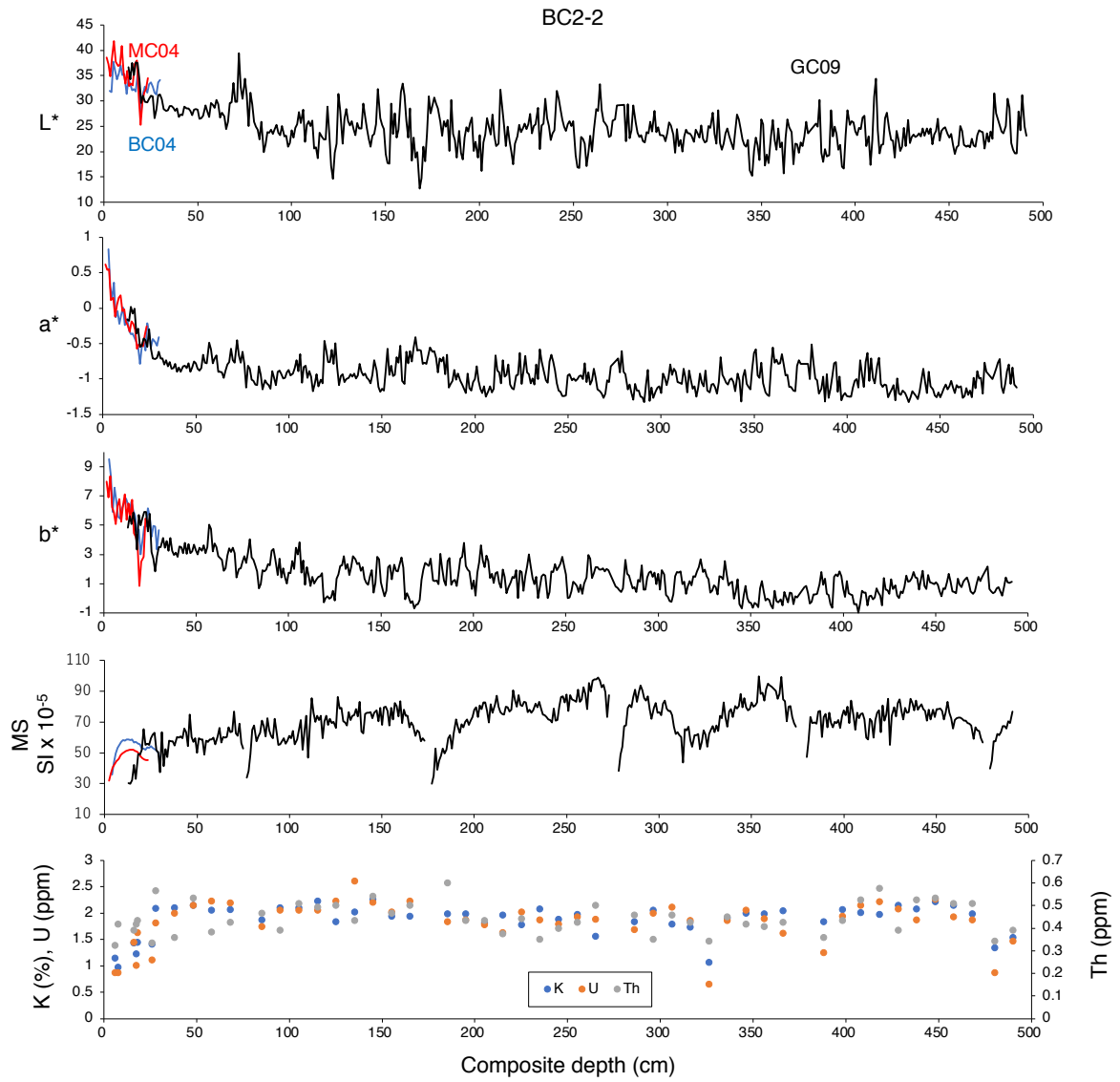


Figure 6.1-21: Variations in color indices in site BC2-2.

Microplastic study sites

Station 5

This site is located in the southern Chukchi shelf and was selected for microplastic study (See Chapter 4.18). Two Asyura cores were retrieved at this site. Sediments consist of dark olive gray (5Y 3/2 to 3/1), sandy mud with intense bioturbation, and scattered bivalve shells (Figures 6.1-22(1) and 6.1-23). The color indices are shown in Figure 6.1-24.

Station 7

This site is located in the southern Chukchi shelf and was selected for microplastic study (See Chapter 4.18). Two Asyura cores were retrieved at this site. Sediments consist of dark olive gray (5Y 3/2 to 3/1), sandy mud. Indistinct lamination appears in color due to variation in iron sulfides. A distinct darker (more iron sulfides) band appears at 7.5-9 cm (Figures 6.1-22(2) and 6.1-23). The color indices are shown in Figure 6.1-24.

Station 8

This site is located in the southern Chukchi shelf and was selected for microplastic study (See Chapter 4.18). Two Asyura cores were retrieved at this site. Sediments consist of dark olive gray (5Y 3/2 to 3/1) and sandy mud (Figures 6.1-22(3) and 6.1-23). The color indices are shown in Figure 6.1-24.

Station 11

This site is located on the central Chukchi shelf and was selected for microplastic study (See Chapter 4.18). Two Asyura cores were retrieved at this site. Sediments consist of olive gray-dark gray (5Y 3/2 to 4/2) and sandy mud and are visually homogenous. Sediment grades to slightly darker color towards the below. A large (~1.5 x 2 cm) pebble was collected at the core bottom (Figures 6.1-22(4) and 6.1-23). The color indices are shown in Figure 6.1-24.

Holocene Arctic Palaeoclimatology and Palaeoceanography Investigation (HAPPI) 2022

	Site name: Station 5	Core type: Asyura	Core number: A1	Section number: 1
cm	Section length 15.5 cm	Described by Polyak	Core name: MR02-06C St. 5 A1	
0	Column	Description		
10		0-9 cm Very soft, dark olive gray (5Y 3/2), sandy mud, waterly at the surface. Intense bioturbation, scattered bivalve shells. Sand content seems to decrease to the bottom. Contact uneven, indistinct, by color change.		
20		9-15.5 cm Soft olive black (5Y 3/1), slightly sandy mud. Blackish iron sulfide stain.		
30				
40				
50				
60				
70				
80				
90				
100				

Figure 6.1-22(1): Lithologic columns of cores at Station 5

Holocene Arctic Palaeoclimatology and Palaeoceanography Investigation (HAPPI) 2022			
	Site name: Station 7	Core type: Asyura	Core number: Hand C
cm	Section length 15.5 cm	Described by Polyak	Core name: MR02-06C St. 7 Sediment C
	Column	Description	
0		0-5.5 cm Very soft, dark olive gray (5Y 3/2), sandy mud, waterly at the surface. Bioturbated. Sand content seems to decrease to the bottom. Contact uneven, indistinct by slight color change.	
10		5.5-10.5 cm Soft, dark olive gray to black (5Y 3/2 to 3/1), silty-fine sandy mud. Indistinct lamination in color due to variation in iron sulfides. A distinct darker (more iron sulfides) band at 7.5-9 cm. Distinct even contact.	
20		10.5-15.5 cm Soft olive black (5Y 3/1), silty mud, homogeneous visually.	
30			
40			
50			
60			
70			
80			
90			
100			

Figure 6.1-22(2): Lithologic columns of cores at Station 7

Holocene Arctic Palaeoclimatology and Palaeoceanography Investigation (HAPPI) 2022

	Site name: Station 8	Core type: Asyura	Core number: Hand C	Section number: 1
cm	Section length 17 cm	Described by Polyak	Core name: MR02-06C St. 8 Sediment C	
	Column	Description		
0		0-7 cm Very soft, dark olive gray (5Y 3/2), sandy mud, waterly at the surface, visually homogenous. Contact slightly uneven, relatively distinct by color change.		
10		7-17 cm Soft, dark olive gray to black (5Y 3/2 to 3/1), silty mud. Some fine sand at 7-10 cm. Finer grained, darker (5Y 3/1 to 2/1) sediment below.		
20				
30				
40				
50				
60				
70				
80				
90				
100				

Figure 6.1-22(3): Lithologic columns of cores at Station 8

Holocene Arctic Palaeoclimatology and Palaeoceanography Investigation (HAPPI) 2022

	Site name: Station 11	Core type: Asyura	Core number: Hand C	Section number: 1
cm	Section length 11 cm	Described by Polyak	Core name: MR02-06C St. 11 Sediment C	
	Column	Description		
0		0-10.5 cm Soft, olive gray-dark gray (5Y 3/2 to 4/2), sandy mud, visually homogenous. Sediment grades to slightly darker color towards the below. A large (~1.5 x 2 cm) pebble collected at the core bottom.		
1				
2				
3				
4				
5				
6				
7				
8				
9				
10				
11				
12				
13				
14				
15				
16				
17				
18				
19				
20				
21				
22				
23				
24				
25				
26				
27				
28				
29				
30				
31				
32				
33				
34				
35				
36				
37				
38				
39				
40				
41				
42				
43				
44				
45				
46				
47				
48				
49				
50				
51				
52				
53				
54				
55				
56				
57				
58				
59				
60				
61				
62				
63				
64				
65				
66				
67				
68				
69				
70				
71				
72				
73				
74				
75				
76				
77				
78				
79				
80				
81				
82				
83				
84				
85				
86				
87				
88				
89				
90				
91				
92				
93				
94				
95				
96				
97				
98				
99				
100				

Figure 6.1-22(4): Lithologic columns of cores at Station 11.



Figure 6.1-23: Photographs of Asyura cores from Stations 5, 7, 8, and 11.

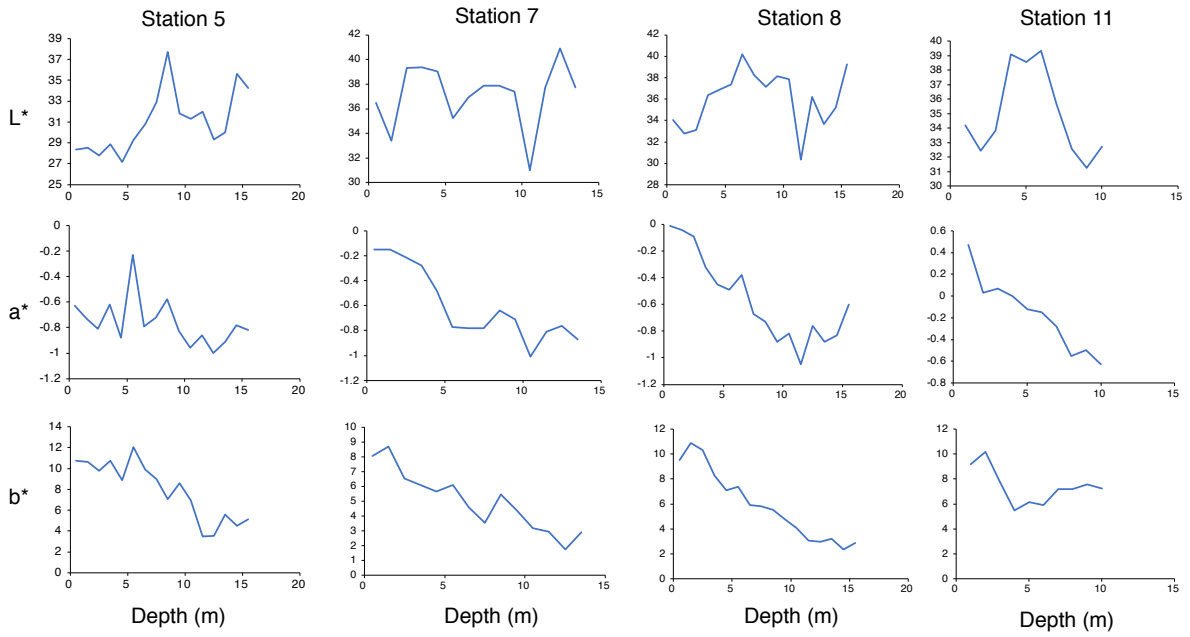


Figure 6.1-24: Variations in color indices in Stations 5, 7, 8, and 11 sediments.

(7) Data archive

These data obtained in this cruise will be submitted to the Data Management Group of JAMSTEC. They will be opened to the public via “Data Research System for Whole Cruise Information in JAMSTEC (DARWIN)” on the JAMSTEC website.

<<http://www.godac.jamstec.go.jp/darwin/e>>

6.2. Porewater sampling

(1) Personnel

Mariko Hatta JAMSTEC

(2) Objectives

The goals of this study are following:

- 1) Collect the porewater from the box corer and determine chemical parameters to understand the geochemical process in the sediments.
- 2) Determine the aluminum and silicate concentrations and compositions to investigate the aluminum distributions in the Arctic Ocean.

(3) Parameters

- Physical observation of the sediments
- Nutrients (NH_4 , NO_3 , NO_2 , PO_4 , SiO_2)
- Dissolved trace metals (Fe, Al etc.)
- Silicate isotopes
- Barium concentrations
- Major ions (Cl^- , SO_4^{2-} etc.)

(4) Instruments and methods

(4-1) Porewater sampling by the Rhizon samplers

In order to obtain the porewater from the sedimental core, we use the Rhizon sampler (Figure 6.2-1).



Figure 6.2-1: The Rhizon samplers, after they were used for the sampling during MR22-06C.

Details of the Rhizon sampler was described by Gerald R. Dickens et al. Progress report: Rhizon Sampling of Pore Waters on Scientific Drilling Expeditions: An example from the IODP Expedition 302, Arctic Coring Expedition (ACEX),

doi:10.2204/lodp.sd.4.08.2007. “The Rhizon samplers are thin tubes of hydrophilic porous polymer designed to extract water from porous sediment using a vacuum. Unlike the aforementioned squeezing or some other common porewater collection methods (e.g., centrifuging, pressurized gas) that “push” water from discrete sediment samples, Rhizon samplers “pull” water from intact sediment, thereby preserving the sedimentary record. They are also inexpensive and disposable, which eliminates the intensive cleaning steps associated with squeezers. Several studies have been successfully used Rhizon samplers to obtain porewaters from marine sediment collected in a gravity core or below a benthic chamber (Seeberg-Elverfeldt et al., 2005).”

The Rhizon sampler consists of four parts: (1) a thin tube comprised of hydrophilic polymer, (2) a wire to support the tube, (3) a flexible hose to pass water from the tube, and (4) a connector (Figure 6.2-2).

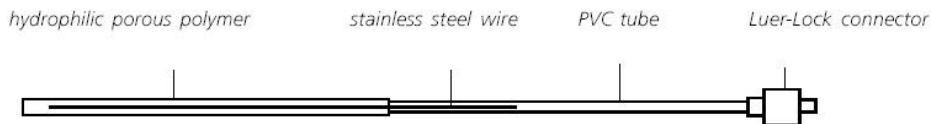


Figure 6.2-2: Sketch of a Rhizon sampler (from “Rhizon soil moisture sampler: operating instructions”. www.eijkelkamp.nl).

“The porous tube is inserted into the sediment, and an evacuated container is attached to the connector. Pore water then passes from sediment through the porous tube and flexible hose into the collection chamber. Given a sufficiently small tube pore size (0.1 μm), the Rhizon sampler also serves as a filter, removing microbial and colloidal contamination (Knight et al., 1998).”

The sampling intervals were selected in generally 1, 2, 3, 4, 5 cm from the surface and then 3-5cm intervals depending on the total length of the core samples we obtained. The initial 1-mL in each syringe was discarded, while the rest was retained. In total, 10 Rhizon samples were taken from sediment cores for each site.

For these intervals, a small hole into the Acryl pipe (diameter 89mm) were drilled through the core liner 1 cm apart before the sediment samples from the box corer were collected. The Acryl pipe were soaked with a weak acid (HCl, pH <2) overnight, and then rinsed with milliQ waters (18.2) well and dried well in the clean bench. Each hole was carefully sealed with a black vinyl tape and a white tape was used every 10 cm to identify the length. Once the intervals were decided, the tape was carefully removed and the tube of the Rhizon sampler was inserted into the target depths.

The new Rhizon samplers were inserted through the holes so the porous tube was just

buried. A tube connector with double luer-locks was connected to each Rhizon sampler, and then a 20-mL syringe was attached to each tube connector, pulled to generate a vacuum, and held open with a wooden spacer. Cores were remained as a “standing position” on the rack (Figure 6.2-3).

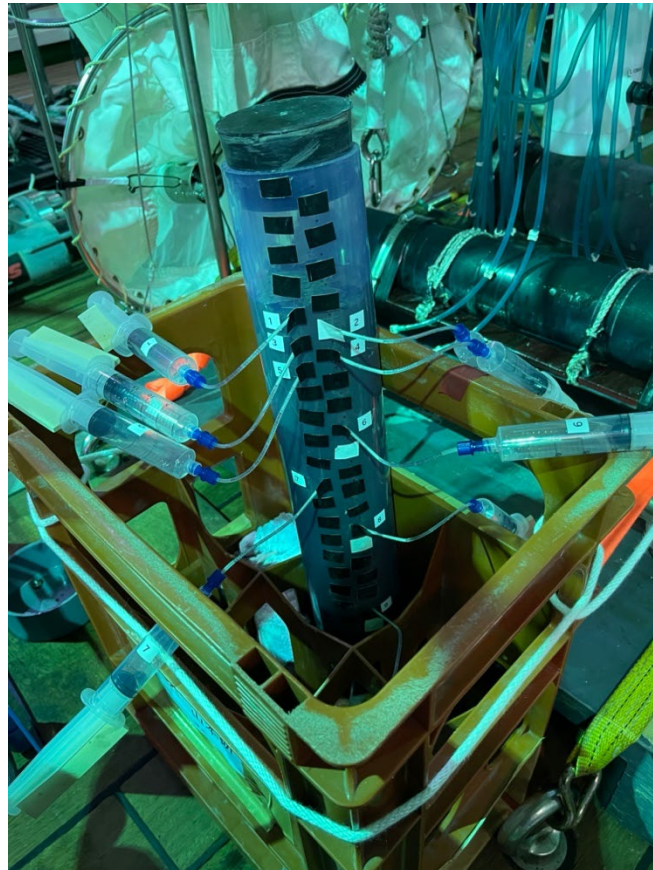


Figure 6.2-3: The photo of the pore water sampling using the Rhizon samplers.

After collection of the pore water samples, aliquots were divided into individual containers for various chemical analyses.

(4-2) Sub-sampling:

The following samples were drained from each syringe:

<u>Parameter</u>	<u>Analysis on the board[y/n]</u>	<u>Stored samples[y/n]</u>
Nutrients	y	n
Dissolved		
Metal (Fe, Al)	n	y
Si isotope	n	y
Ba	n	y
Major Ions	n	y

Each sample was directly injected into the individual sub-sampling bottles. Each bottle was pre-cleaned by the acid solution (10% HCl), rinsed with milliQ water thoughtfully, and then dried inside the clean bench. Each syringe is also pre-cleaned with a weak acid (HCl, pH <2), rinsed with milliQ water, and then dried inside the clean bench. Samples for nutrient analysis were diluted 20 times or 10 times with Low Nutrient Sea Water (LNSW), and stored in the refrigerator, and then determined on R/V MIRAI using the shipboard protocol by MWJ.

(4-3) Data:

Nutrients: The nutrient analysis was carried out on R/V MIRAI during the cruise of MR22-06C using the QuAAtro 5. The details of the analysis were reported in Chapter 4.2.

(5) Station list or Observation log

The porewater samplings were carried out at the coring sites, shown in the following Table 6.2-1. Total 40 samples were collected, and addition to the two bottom water sampling.

Table 6.2-1: List of the sampling locations for porewater sampling.

#	ID	Type	Sampling method	Year	Month	Date	Time	UTC	Lat	N	Long	W	Water Depth
1	MT1-#001-1cm	Porewater	Box corer	2022	09	01	1:48	UTC	69	58.5304	N 137	14.668	W 57
2	MT1-#002-2cm	Porewater	Box corer	2022	09	01	1:48	UTC	69	58.5304	N 137	14.668	W 57
3	MT1-#003-3cm	Porewater	Box corer	2022	09	01	1:48	UTC	69	58.5304	N 137	14.668	W 57
4	MT1-#004-4cm	Porewater	Box corer	2022	09	01	1:48	UTC	69	58.5304	N 137	14.668	W 57
5	MT1-#005-5cm	Porewater	Box corer	2022	09	01	1:48	UTC	69	58.5304	N 137	14.668	W 57
6	MT1-#006-7cm	Porewater	Box corer	2022	09	01	1:48	UTC	69	58.5304	N 137	14.668	W 57
7	MT1-#007-9cm	Porewater	Box corer	2022	09	01	1:48	UTC	69	58.5304	N 137	14.668	W 57
8	MT1-#008-13cm	Porewater	Box corer	2022	09	01	1:48	UTC	69	58.5304	N 137	14.668	W 57
9	MT1-#009-17cm	Porewater	Box corer	2022	09	01	1:48	UTC	69	58.5304	N 137	14.668	W 57
10	MT1-#010-20cm	Porewater	Box corer	2022	09	01	1:48	UTC	69	58.5304	N 137	14.668	W 57
11	MT1-bottom	Seawater	Multiple corer	2022	09	01	23:30	UTC	69	58.5341	N 137	14.6646	W 57
12	MT2-#011-1cm	Porewater	Box corer	2022	09	04	19:32	UTC	69	43.147	N 138	8.9378	W 152
13	MT2-#012-2cm	Porewater	Box corer	2022	09	04	19:32	UTC	69	43.147	N 138	8.9378	W 152
14	MT2-#013-3cm	Porewater	Box corer	2022	09	04	19:32	UTC	69	43.147	N 138	8.9378	W 152
15	MT2-#014-4cm	Porewater	Box corer	2022	09	04	19:32	UTC	69	43.147	N 138	8.9378	W 152
16	MT2-#015-5cm	Porewater	Box corer	2022	09	04	19:32	UTC	69	43.147	N 138	8.9378	W 152
17	MT2-#016-10cm	Porewater	Box corer	2022	09	04	19:32	UTC	69	43.147	N 138	8.9378	W 152
18	MT2-#017-15cm	Porewater	Box corer	2022	09	04	19:32	UTC	69	43.147	N 138	8.9378	W 152
19	MT2-#018-20cm	Porewater	Box corer	2022	09	04	19:32	UTC	69	43.147	N 138	8.9378	W 152
20	MT2-#019-30cm	Porewater	Box corer	2022	09	04	19:32	UTC	69	43.147	N 138	8.9378	W 152
21	MT2-#020-38cm	Porewater	Box corer	2022	09	04	19:32	UTC	69	43.147	N 138	8.9378	W 152
22	BC2-bottom	Seawater	Asyura	2022	09	07	17:55	UTC	71	54.5913	N 154	9.4669	W 224
23	BC2-#021-1cm	Porewater	Box corer	2022	09	07	20:10	UTC	71	54.5913	N 154	9.4637	W 224
24	BC2-#022-2cm	Porewater	Box corer	2022	09	07	20:10	UTC	71	54.5913	N 154	9.4637	W 224
25	BC2-#023-3cm	Porewater	Box corer	2022	09	07	20:10	UTC	71	54.5913	N 154	9.4637	W 224
26	BC2-#024-4cm	Porewater	Box corer	2022	09	07	20:10	UTC	71	54.5913	N 154	9.4637	W 224
27	BC2-#025-5cm	Porewater	Box corer	2022	09	07	20:10	UTC	71	54.5913	N 154	9.4637	W 224
28	BC2-#026-7cm	Porewater	Box corer	2022	09	07	20:10	UTC	71	54.5913	N 154	9.4637	W 224
29	BC2-#027-10cm	Porewater	Box corer	2022	09	07	20:10	UTC	71	54.5913	N 154	9.4637	W 224
30	BC2-#028-15cm	Porewater	Box corer	2022	09	07	20:10	UTC	71	54.5913	N 154	9.4637	W 224
31	BC2-#029-20cm	Porewater	Box corer	2022	09	07	20:10	UTC	71	54.5913	N 154	9.4637	W 224
32	BC2-#030-25cm	Porewater	Box corer	2022	09	07	20:10	UTC	71	54.5913	N 154	9.4637	W 224
33	BC2-2-#031-1cm	Porewater	Box corer	2022	09	13	20:04	UTC	71	55.4682	N 154	6.9537	W 268
34	BC2-2-#032-2cm	Porewater	Box corer	2022	09	13	20:04	UTC	71	55.4682	N 154	6.9537	W 268
35	BC2-2-#033-3cm	Porewater	Box corer	2022	09	13	20:04	UTC	71	55.4682	N 154	6.9537	W 268
36	BC2-2-#034-4cm	Porewater	Box corer	2022	09	13	20:04	UTC	71	55.4682	N 154	6.9537	W 268
37	BC2-2-#035-5cm	Porewater	Box corer	2022	09	13	20:04	UTC	71	55.4682	N 154	6.9537	W 268
38	BC2-2-#036-7cm	Porewater	Box corer	2022	09	13	20:04	UTC	71	55.4682	N 154	6.9537	W 268
39	BC2-2-#037-10cm	Porewater	Box corer	2022	09	13	20:04	UTC	71	55.4682	N 154	6.9537	W 268
40	BC2-2-#038-15cm	Porewater	Box corer	2022	09	13	20:04	UTC	71	55.4682	N 154	6.9537	W 268
41	BC2-2-#039-20cm	Porewater	Box corer	2022	09	13	20:04	UTC	71	55.4682	N 154	6.9537	W 268
42	BC2-2-#040-25cm	Porewater	Box corer	2022	09	13	20:04	UTC	71	55.4682	N 154	6.9537	W 268

(6)Preliminary results

(6-1) Water characteristics of the coring site:

There are 4 coring sites which were carefully selected. At each sampling site, there were several different techniques to collect the sediment samples. The pore water samples were collected from the box corer. The RINKO profiler was attached with the core sampler, and the data was reported by elsewhere. The preliminary results of the vertical profiles of each station were shown in Figure 6.2-4.

On the Mackenzie trough, a strong riverine influence were shown at the shallow depth at Stations MT1 and MT2. Below the low-warm surface waters, the cold saline water was observed on the trough. This water looked like the local winter waters. Near the Barrow Canyon, the PWW and AW were observed. The BC2-2 showed the strong PSW influence but there is no such the water mass at BC2.

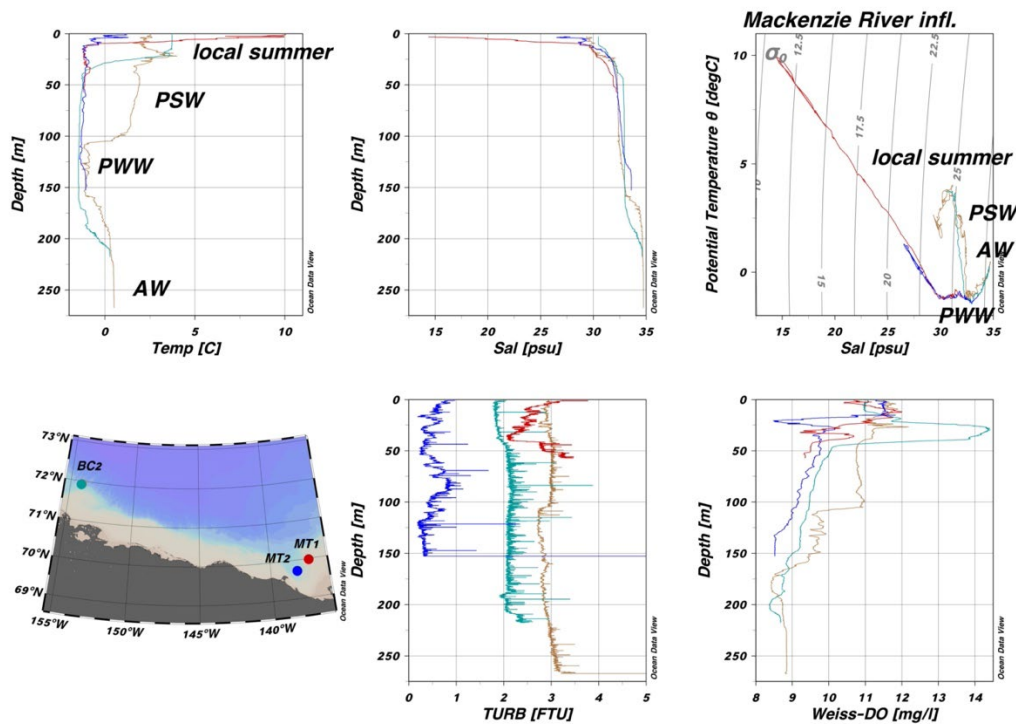


Figure 6.2-4: Vertical profiles of temperature, salinity, turbidity, and dissolved oxygen at each station obtained by the RINKO profiler. T-S diagram indicates that there are 4 water masses in those stations. AW: Atlantic Water, PWW: Pacific Winter Water, PSW: Pacific Summer Water, local summer water.

(6-2) The sediment samples:

The four core samples were obtained from the box corer, operated by Dr. Seike and the core team. The length of each core was measured before and after the pore water sampling (Figure 6.2-5).

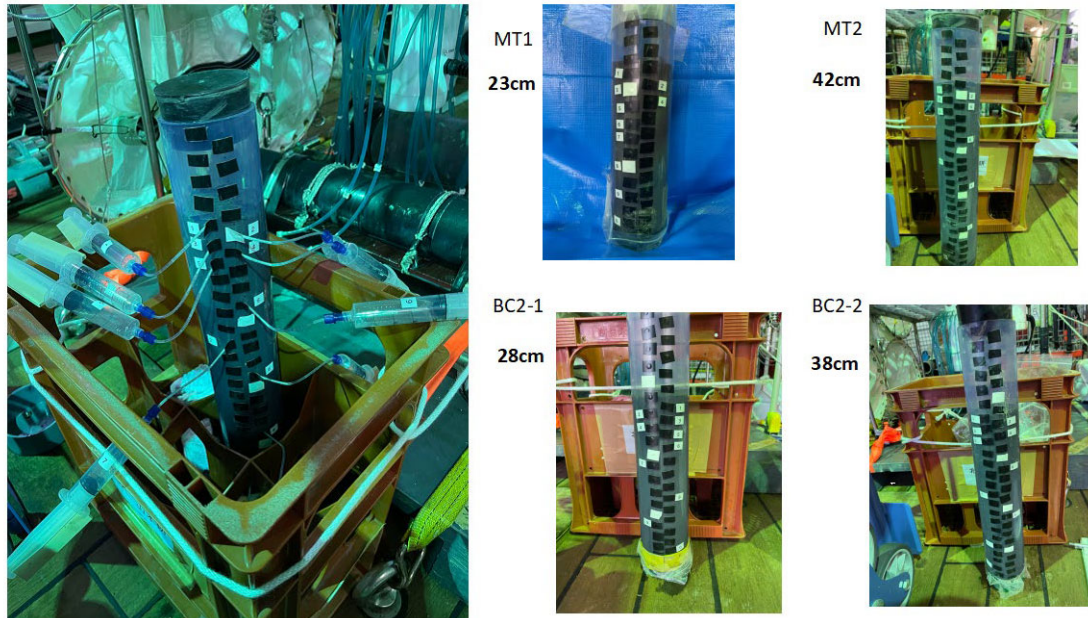


Figure 6.2-5: Each sediment core samples before sampling. There were 4 sample cores provided from the box corer at stations MT1, MT2, BC2, and BC2-2.

(7) Data archive

These data obtained in this cruise will be submitted to the Data Management Group of JAMSTEC, and will be opened to the public via “Data Research System for Whole Cruise Information in JAMSTEC (DARWIN)” in JAMSTEC web site.

<<http://www.godac.jamstec.go.jp/darwin/e>>

6.3. Sea bottom topography measurements

(1) Personnel

Masanobu Yamamoto	Hokkaido University	-PI
Leonid Polyak	Hokkaido University	
Young-Jin Joe	Korea Polar Research Institute	
Masakazu Fujii	NIPR (National Institute of Polar Research) (not on board)	
Kazuho Yoshida	NME (Nippon Marine Enterprises, Ltd.)	
Satomi Ogawa	NME	
Fumine Okada	NME	
Ryo Kimura	NME	
Yoichi Inoue	MIRAI Crew	

(2) Objectives

R/V MIRAI is equipped with the Multi Beam Echo Sounding system (MBES; SEABEAM 3012 (L3 Communications ELAC Nautik, Germany)) and Sub-Bottom Profiler (SBP), Bathy 2010 (SyQwest). The objective of MBES and SBP is to collect continuous bathymetric data and sub-bottom profiling data along ship track especially for geological and geophysical studies.

(3) Parameters

MBES: Depth [m]
SBP: Sub-bottom profiling [m]

(4) Instruments and methods

The “SEABEAM 3012” on R/V MIRAI was used for bathymetry mapping during this cruise. To get accurate sound velocity of water column for ray-path correction of acoustic beams, we determined sound velocities at the depth of 6.62m, the bottom of the ship, by the surface sound velocimeter. We made sound velocity profiles based on the observations of CTD, XCTD and Argo float conducted in this cruise by the equation in Del Grosso (1974).

The “Bathy 2010” system was used for determining physical properties of the sea floor and for imaging and characterizing geological information several tens of meters below the sea floor. Its sound velocity was fixed 1,500m/s during operations. In the site surveys of MT1, MT2 and BC2, Bathy 2010 and SEABEAM 3012 were operated in 3kt vessel speed over ground. In the geophysical wide area survey around Barrow Canyon, these instruments were operated in 8kt over ground. During operations, settings of these instruments were changed according to the water depth, bottom type and condition of the bottom and sediment layers detection.

Table 6.3-1 and 6.3-2 show system configuration and performance of SEABEAM

3012 and Bathy2010 system.

Table 6.3-1: SEABEAM 3012 System configuration and performance

Frequency:	12 kHz
Transmit beam width:	2.0 degree
Transmit power:	4 kW
Transmit pulse length:	2 to 20 msec.
Receive beam width:	1.6 degree
Depth range:	50 to 11,000 m
Number of beams:	301 beams (Spacing mode: Equi-angle)
Beam spacing:	1.5 % of water depth (Spacing mode: Equi-distance)
Swath width:	60 to 150 degrees
Depth accuracy:	< 1 % of water depth (average across the swath)

Table 6.3-2: Bathy2010 System configuration and performance

Frequency:	3.5 kHz (FM sweep)
Transmit beam width:	30 degree
Transmit pulse length:	0.5 to 50 msec
Strata resolution:	Up to 8 cm with 300 m of bottom penetration according to bottom type
Depth resolution:	0.1 feet, 0.1 m
Depth accuracy:	±10 cm to 100 m, ± 0.3% to 6,000 m
Sound velocity:	1,500 m/s (fix)

(5) Observation log

MBES: 12 Aug. 2022 - 26 Sep. 2022 (UTC)

SBP: 30 Aug. 2022 - 14 Sep.2022 (UTC)

(6) Preliminary results

The results will be published after primary processing.

(7) Data archive

These data obtained in this cruise will be submitted to the Data Management Group of JAMSTEC, and will be opened to the public via “Data Research System for Whole Cruise Information in JAMSTEC (DARWIN)” in JAMSTEC web site.

<<http://www.godac.jamstec.go.jp/darwin/e>>

(8) Remarks

- i) Geophysical wide area survey around Barrow Canyon
 - 02:53UTC 08 Sep. 2022 - 10:32UTC 08 Sep. 2022
 - 04:12UTC 09 Sep. 2022 - 10:49UTC 09 Sep. 2022

- ii) The following periods, MBES data acquisition was suspended due to sending acoustic commands of ANS.
 - 20:30UTC 19 Aug. 2022 - 21:26UTC 19 Aug. 2022
 - 15:13UTC 28 Aug. 2022 - 15:55UTC 28 Aug. 2022
 - 16:55UTC 28 Aug. 2022 - 16:58UTC 28 Aug. 2022
 - 18:25UTC 28 Aug. 2022 - 18:34UTC 28 Aug. 2022
 - 21:57UTC 28 Aug. 2022 - 22:04UTC 28 Aug. 2022
 - 18:02UTC 29 Aug. 2022 - 18:12UTC 29 Aug. 2022
 - 23:11UTC 29 Aug. 2022 - 23:39UTC 29 Aug. 2022
 - 01:08UTC 30 Aug. 2022 - 01:35UTC 30 Aug. 2022
 - 14:50UTC 08 Sep. 2022 - 17:58UTC 08 Sep. 2022
 - 00:36UTC 09 Sep. 2022 - 01:29UTC 09 Sep. 2022

- iii) The following periods, MBES data acquisition was suspended due to the shallow water area.
 - 00:25UTC 21 Aug. 2022 - 03:00UTC 22 Aug. 2022 (including the period of calling at Dutch Harbor)
 - 16:51UTC 22 Aug. 2022 - 09:47UTC 28 Aug. 2022
 - 02:28UTC 29 Aug. 2022 - 03:59UTC 29 Aug. 2022
 - 01:54UTC 30 Aug. 2022 - 17:05UTC 30 Aug. 2022
 - 02:47UTC 02 Sep. 2022 - 05:28UTC 02 Sep. 2022
 - 07:36UTC 03 Sep. 2022 - 10:40UTC 03 Sep. 2022
 - 11:52UTC 03 Sep. 2022 - 13:38UTC 03 Sep. 2022
 - 04:30UTC 05 Sep. 2022 - 06:20UTC 05 Sep. 2022
 - 18:21UTC 05 Sep. 2022 - 19:08UTC 05 Sep. 2022
 - 12:29UTC 10 Sep. 2022 - 19:18UTC 10 Sep. 2022
 - 02:49UTC 11 Sep. 2022 - 08:47UTC 11 Sep. 2022
 - 10:10UTC 11 Sep. 2022 - 01:00UTC 12 Sep. 2022
 - 03:40UTC 14 Sep. 2022 - 21:39UTC 14 Sep. 2022
 - 02:35UTC 16 Sep. 2022 - 03:08UTC 19 Sep. 2022

- iv) The following period, MBES data was invalid due to Surface Sound Velocity sensor trouble.
 - 20:25UTC 13 Sep. 2022 - 00:03UTC 14 Sep. 2022

- v) The following periods, MBES data acquisition was stopped due to system trouble.
 - 00:03UTC 14 Sep. 2022 - 00:35UTC 14 Sep. 2022
 - 15:25UTC 15 Sep. 2022 - 15:29UTC 15 Sep. 2022

- vi) The following period, SSV data were calculated from the SST and SSS due to SSV sensor trouble.
 - 00:35UTC 14 Sep. 2022 - 03:40UTC 14 Sep. 2022

- vii) The following period, SSV data were invalid due to rough sea condition.
 - 00:25UTC 14 Sep. 2022 - 01:42UTC 14 Sep. 2022
 - 00:19UTC 22 Sep. 2022 - 00:45UTC 22 Sep. 2022

- viii) The following day, the SSV data had some spike values due to rough sea condition.
 - 22 Sep. 2022

- ix) The following period, the SBP observation was carried out.
 - 17:17UTC 30 Aug. 2022 - 04:33UTC 31 Aug. 2022
 - 01:22UTC 01 Sep. 2022 - 15:26UTC 01 Sep. 2022
 - 17:03UTC 01 Sep. 2022 - 10:00UTC 02 Sep. 2022
 - 02:09UTC 03 Sep. 2022 - 00:02UTC 04 Sep. 2022
 - 02:22UTC 04 Sep. 2022 - 09:34UTC 04 Sep. 2022
 - 16:52UTC 04 Sep. 2022 - 12:30UTC 05 Sep. 2022
 - 07:05UTC 07 Sep. 2022 - 10:32UTC 08 Sep. 2022
 - 03:55UTC 09 Sep. 2022 - 10:53UTC 09 Sep. 2022
 - 19:28UTC 10 Sep. 2022 - 03:23UTC 11 Sep. 2022
 - 06:40UTC 13 Sep. 2022 - 10:17UTC 13 Sep. 2022
 - 16:50UTC 13 Sep. 2022 - 03:40UTC 14 Sep. 2022

6.4. Sea surface gravity measurements

(1) Personnel

Masanobu Yamamoto	Hokkaido University	-PI
Masakazu Fujii	NIPR (National Institute of Polar Research)	(not on board)
Kazuho Yoshida	NME (Nippon Marine Enterprises, Ltd.)	
Satomi Ogawa	NME	
Fumine Okada	NME	
Ryo Kimura	NME	
Yoichi Inoue	MIRAI Crew	

(2) Objectives

The local gravity is an important parameter in geophysics and geodesy. The gravity data were collected during this cruise.

(3) Parameters

Relative Gravity [CU: Counter Unit]
[mGal] = (coefl: 0.9946) * [CU]

(4) Instruments and methods

The relative gravity was measured by using LaCoste and Romberg air-sea gravity meter S-116 (Micro-g LaCoste, LLC) during the cruise. To convert the relative gravity to absolute one, we measured gravity, by using the portable gravity meter (Scintrex gravity meter CG-5), at Shimizu port as a reference point.

(5) Observation log

11 Aug. 2022 - 30 Sep. 2022

(6) Preliminary results

Absolute gravity table is shown in Table 6.4-1.

Table 6.4-1: Absolute gravity table of the MR22-06C cruise

No.	Date	UTC	Port	Absolute Gravity [mGal]	Sea Level [cm]	Ship Draft [cm]	Gravity at Sensor *1 [mGal]	S-116 Gravity [mGal]
#1	8/11	23:19	Shimizu(Hinode)	979728.87	203	657	979729.78	12002.12
#2	9/30	08:39	Shimizu(Sodeshi)	979728.95	145	628	979729.62	12001.64

*1: Gravity at Sensor = Absolute Gravity + Sea Level*0.3086/100 + (Draft-530)/100*0.2222

(7) Data archives

These data obtained in this cruise will be submitted to the Data Management Group of JAMSTEC, and will be opened to the public via “Data Research System for Whole Cruise Information in JAMSTEC (DARWIN)” in JAMSTEC web site.

<<http://www.godac.jamstec.go.jp/darwin/e>>

(8) Remarks

- i) Geophysical wide area survey around Barrow Canyon
 - 02:53UTC 08 Sep. 2022 - 10:32UTC 08 Sep. 2022
 - 04:12UTC 09 Sep. 2022 - 10:49UTC 09 Sep. 2022

6.5. Surface magnetic field measurement

(1) Personnel

Masanobu Yamamoto	Hokkaido University	-PI
Masakazu Fujii	NIPR (National Institute of Polar Research) (not on board)	
Kazuho Yoshida	NME (Nippon Marine Enterprises, Ltd.)	
Satomi Ogawa	NME	
Fumine Okada	NME	
Ryo Kimura	NME	
Yoichi Inoue	MIRAI Crew	

(2) Objectives

Measurement of magnetic force on the sea is required for the geophysical investigations of marine magnetic anomaly caused by magnetization in upper crustal structure. We measured geomagnetic field using a three-component magnetometer during this cruise.

(3) Parameters

Three components of a magnetic field vector on-board, H_x , H_y , H_z [nT]

H_x : A magnetic field component in the bow/stern direction on the vessel horizontal plane. “To bow” is positive.

H_y : A magnetic field component in the port/starboard direction on the vessel horizontal plane. “To starboard” is positive.

H_z : A perpendicular magnetic field component to the vessel horizontal plane. “upward” is positive.

(4) Instruments and methods

A shipboard three-components magnetometer system (SFG2018, Tierra Tecnica) is equipped on-board R/V MIRAI. Three-axes flux-gate sensors with ring-cored coils are fixed on the fore mast. Outputs from the sensors are digitized by a 20-bit A/D converter (1 nT/LSB) and sampled 8 times per second. Yaw (heading), Pitch and Roll are measured by the Inertial Navigation Unit (INU) for controlling attitude of a Doppler radar. Ship's position, speed over ground (Differential GNSS) and gyro data are taken from LAN every second.

The relation between a magnetic-field vector observed on-board, \mathbf{H}_{ob} , (in the ship's fixed coordinate system) and the geomagnetic field vector, \mathbf{F} , (in the Earth's fixed coordinate system) is expressed as:

$$\mathbf{H}_{ob} = \tilde{\mathbf{A}} \tilde{\mathbf{R}} \tilde{\mathbf{P}} \tilde{\mathbf{Y}} \mathbf{F} + \mathbf{H}_p \quad (\text{a})$$

where $\tilde{\mathbf{R}}$, $\tilde{\mathbf{P}}$ and $\tilde{\mathbf{Y}}$ are the matrices of rotation due to roll, pitch and heading of a

ship, respectively. $\tilde{\mathbf{A}}$ is a 3 x 3 matrix which represents magnetic susceptibility of the ship, and \mathbf{H}_p is a magnetic field vector produced by a permanent magnetic moment of the ship's body. Rearrangement of Eq. (a) makes

$$\tilde{\mathbf{B}} \mathbf{H}_{ob} + \mathbf{H}_{bp} = \tilde{\mathbf{R}} \tilde{\mathbf{P}} \tilde{\mathbf{Y}} \mathbf{F} \quad (\text{b})$$

where $\tilde{\mathbf{B}} = \tilde{\mathbf{A}}^{-1}$, and $\mathbf{H}_{bp} = -\tilde{\mathbf{B}} \mathbf{H}_p$. The magnetic field, \mathbf{F} , can be obtained by measuring $\tilde{\mathbf{R}}$, $\tilde{\mathbf{P}}$, $\tilde{\mathbf{Y}}$ and \mathbf{H}_{ob} , if $\tilde{\mathbf{B}}$ and \mathbf{H}_{bp} are known. Twelve constants in $\tilde{\mathbf{B}}$ and \mathbf{H}_{bp} can be determined by measuring variation of \mathbf{H}_{ob} with $\tilde{\mathbf{R}}$, $\tilde{\mathbf{P}}$, and $\tilde{\mathbf{Y}}$ at a place where the geomagnetic field, \mathbf{F} , is known.

(5) Observation log

31 Aug. 2021 - 28 Sep. 2022

(6) Preliminary results

The results will be published after the primary processing.

(7) Data archive

These data obtained in this cruise will be submitted to the Data Management Group of JAMSTEC, and will be opened to the public via “Data Research System for Whole Cruise Information in JAMSTEC (DARWIN)” in JAMSTEC web site.

<<http://www.godac.jamstec.go.jp/darwin/e>>

(8) Remarks

- i) For calibration of the ship's magnetic effect, “figure-eight” turns (a pair of clockwise and anti-clockwise rotation) were held at the following periods and positions.

02:28UTC 06 Sep. 2022 - 02:50UTC 06 Sep. 2022 (70-46N, 142-27W)

01:47UTC 09 Sep. 2022 - 02:11UTC 09 Sep. 2022 (72-28N, 155-22W)

02:32UTC 26 Sep. 2022 - 02:53UTC 26 Sep. 2022 (40-20N, 150-18E)

- ii) Geophysical wide area survey around Barrow Canyon

02:53UTC 08 Sep. 2022 - 10:32UTC 08 Sep. 2022

04:12UTC 09 Sep. 2022 - 10:49UTC 09 Sep. 2022

7. Notice on using

This cruise report represents final documentation as of the end of the cruise. This report might not be corrected even if changes regarding its content (e.g., taxonomic classifications) are found after its publication. Moreover, this report might also be changed without notice. Data in this cruise report might be raw or unprocessed. If you intend to use or to refer to the data presented in this report, please ask the Chief Scientist for the latest information.

Users of information on this report are requested to submit Publication Report to JAMSTEC.

https://www.godac.jamstec.go.jp/darwin_tmp/explain/81/e/

E-mail: dmo@jamstec.go.jp